Oklahoma Department of Transportation
200 NE 21st Street, Oklahoma City, OK 73105-3204

FINAL REPORT ~ FHWA-OK-22-02

A SYSTEMS APPROACH FOR DESIGN, CONSTRUCTION, AND MAINTENANCE OF BRIDGES AND ADJACENT ROADWAYS

Tommy Bounds, Ph.D., P.E.
K.K. Muraleetharan, Ph.D., P.E., G.E.
Jeffery Volz, Ph.D., P.E., S.E.
Gerald Miller, Ph.D., P.E.
Royce Floyd, Ph.D., P.E., S.E.

School of Civil Engineering and Environmental Science (CEES)
The University of Oklahoma
Norman, Oklahoma

January 2022

OKLAHOMA
Transportation

The Oklahoma Department of Transportation (ODOT) ensures that no person or groups of persons shall, on the grounds of race, color, sex, religion, national origin, age, disability, retaliation or genetic information, be excluded from participation in, be denied the benefits of, or be otherwise subjected to discrimination under any and all programs, services, or activities administered by ODOT, its recipients, sub-recipients, and contractors. To request an accommodation please contact the ADA Coordinator at 405-521-4140 or the Oklahoma Relay Service at 1-800-722-0353. If you have any ADA or Title VI questions email ODOT-ada-titlevi@odot.org.

A SYSTEMS APPROACH FOR DESIGN, CONSTRUCTION, AND MAINTENANCE OF BRIDGES AND ADJACENT ROADWAYS

FINAL REPORT ~ FHWA-OK-22-02

ODOT SPR ITEM NUMBER 2307

Submitted to:

Office of Research and Implementation
Oklahoma Department of Transportation

Submitted by:

Tommy Bounds, Ph.D., P.E.
K.K. Muraleetharan, Ph.D., P.E., G.E.
Jeffery Volz, Ph.D., P.E., S.E.
Gerald Miller, Ph.D., P.E.
Royce Floyd, Ph.D., P.E., S.E.
School of Civil Engineering and Environmental Science (CEES)
The University of Oklahoma

OKLAHOMA
Transportation

January 2022

TECHNICAL REPORT DOCUMENTATION PAGE

1. REPORT NO.	2. GOVERNMENT ACCESSION NO.	3. RECIPIENT'S CATALOG NO.
FHWA-OK-22-02		

4. TITLE AND SUBTITLE	5. REPORT DATE
A Systems Approach for Design, Construction, and Maintenance of Bridges and Adjacent Roadways	January 2022
	6. PERFORMING ORGANIZATION CODE
7. AUTHOR(S)	8. PERFORMING ORGANIZATION REPORT
Tommy Bounds, K.K. Muraleetharan, Jeffery Volz, Gerald Miller, Royce Floyd	Click here to enter text.
9. PERFORMING ORGANIZATION NAME AND ADDRESS	10. WORK UNIT NO.
University of Oklahoma, School of Civil Engineering and Environmental Science, 202 West Boyd Street, Room 334 Norman, OK 73012	
	11. CONTRACT OR GRANT NO.
	ODOT SPR Item Number 2307
12. SPONSORING AGENCY NAME AND ADDRESS	13. TYPE OF REPORT AND PERIOD COVERED
Oklahoma Department of Transportation Office of Research and Implementation 200 N.E. 21st Street, Room G18 Oklahoma City, OK 73105	Final Report Oct 2019 - Dec 2021
	14. SPONSORING AGENCY CODE

15. SUPPLEMENTARY NOTES

Click here to enter text.

16. ABSTRACT

Previous research projects funded by the Oklahoma Department of Transportation, Federal Highway Administration, and other agencies have revealed that many problems faced by bridges, such as expansion joints closing, are related to how the interfaces between a bridge and the adjacent roadway are designed, constructed, and maintained. Design, construction, repair, and maintenance guidelines to alleviate some of the problems related to the interactions between bridges and adjacent roadways are developed. The recommendations are based on published literature, adopted regional practices, field observations, field monitoring, and computer simulations. Pressure relief joints for excessive pavement pressure were installed and monitored at three bridges. The efficacy of ultra-high performance concrete (UHPC) as a possible solution for bridge expansion joint headers was also studied. To better understand the behavior of tall bridge approach embankments constructed on soft soils, computer simulations were performed using the finite element software PLAXIS 2D. To ensure satisfactory bridge performance, it is necessary to put pressure relief joints in rigid pavements leading up to bridges. When bridge embankments are built on soft foundation soils, and especially for taller embankments, the potential for lateral deformation of the embankment should be considered. A water barrier should be incorporated in the abutment backfill design to keep infiltrated water from short circuiting the backfill drainage system. UHPC is a viable alternative for joint headers and has excellent durability. Additional recommendations for conventional, semi-integral, and integral bridges are also presented.

17. KEY WORDS	18. DISTRIBUTION STATEMENT
bridge-roadway interactions, pavement pressure, embankment lateral displacement, ultra-high performance concrete, integral bridges, semi-integral bridges, abutment backfill drainage	No restrictions. This publication is available from the Office of Research and Implementation, Oklahoma DOT.

19. SECURITY CLASSIF. (OF THIS REPORT)	20. SECURITY CLASSIF. (OF THIS PAGE)	21. NO. OF PAGES	22. PRICE
Unclassified	Unclassified	250	N/A

Form DOT F 1700.7 (08/72)

SI* (MODERN METRIC) CONVERSION FACTORS

APPROXIMATE CONVERSIONS TO SI UNITS

SYMBOL	WHEN YOU KNOW	MULTIPLY BY	TO FIND	SYMBOL
		LENGTH		
in	inches	25.4	millimeters	mm
ft	feet	0.305	meters	m
yd	yards	0.914	meters	m
mi	miles	1.61	kilometers	km
		AREA		
in^2	square inches	645.2	square millimeters	mm^2
ft^2	square feet	0.093	square meters	m^2
yd^2	square yard	0.836	square meters	m^2
ac	acres	0.405	hectares	ha
mi^2	square miles	2.59	square kilometers	km^2
		VOLUME		
fl oz	fluid ounces	29.57	milliliters	mL
gal	gallons	3.785	liters	L
ft^3	cubic feet	0.028	cubic meters	m^3
yd^3	cubic yards	0.765	cubic meters	m^3
		NOTE: volumes greater than 1000 L shall be shown in m^3		
		MASS		
oz	ounces	28.35	grams	g
lb	pounds	0.454	kilograms	kg
T	short tons (2000 lb)	0.907	megagrams (or "metric ton")	Mg (or "t")
		TEMPERATURE (exact degrees)		
°F	Fahrenheit	5 (F-32)/9 or (F-32)/1.8	Celsius	°C
		ILLUMINATION		
fc	foot-candles	10.76	lux	lx
fl	foot-Lamberts	3.426	candela/m^2	cd/m^2
		FORCE and PRESSURE or STRESS		
lbf	poundforce	4.45	newtons	N
lbf/in^2	poundforce per square inch	6.89	kilopascals	kPa

APPROXIMATE CONVERSIONS FROM SI UNITS

SYMBOL	WHEN YOU KNOW	MULTIPLY BY	TO FIND	SYMBOL
		LENGTH		
mm	millimeters	0.039	inches	in
m	meters	3.28	feet	ft
m	meters	1.09	yards	yd
km	kilometers	0.621	miles	mi
		AREA		
mm^2	square millimeters	0.0016	square inches	in^2
m^2	square meters	10.764	square feet	ft^2
m^2	square meters	1.195	square yards	yd^2
ha	hectares	2.47	acres	ac
km^2	square kilometers	0.386	square miles	mi^2
		VOLUME		
mL	milliliters	0.034	fluid ounces	fl oz
L	liters	0.264	gallons	gal
m^3	cubic meters	35.314	cubic feet	ft^3
m^3	cubic meters	1.307	cubic yards	yd^3
		MASS		
g	grams	0.035	ounces	oz
kg	kilograms	2.202	pounds	lb
Mg (or "t")	megagrams (or "metric ton")	1.103	short tons (2000 lb)	T
		TEMPERATURE (exact degrees)		
°C	Celsius	1.8C+32	Fahrenheit	°F
		ILLUMINATION		
lx	lux	0.0929	foot-candles	fc
cd/m^2	candela/m^2	0.2919	foot-Lamberts	fl
		FORCE and PRESSURE or STRESS		
N	newtons	0.225	poundforce	lbf
kPa	kilopascals	0.145	poundforce per square inch	lbf/in^2

*SI is the symbol for the International System of Units. Appropriate rounding should be made to comply with Section 4 of ASTM E380. (Revised March 2003)

Table of Contents

1.0 General 1

2.0 Review of Design and Construction Practices 2

2.1 Conventional Bridge Joints 2

2.2 Abutment Backfill 4

2.2.1 Backfill Drainage 4

2.2.2 Approach Slab Settlement 6

2.2.3 Low Density Cellular Concrete (LDCC) as Backfill Material 9

2.3 Pavement Pressure Relief Joints 13

2.4 Pavement Lugs 15

2.5 Integral Bridges 16

3.0 Results of the State DOT Survey 20

3.1 Bridge Approach Roadway and Excessive Pavement Pressure 21

3.2 Tall Embankment Performance 25

3.3 Conventional Bridges with Expansion Joints 27

3.4 Integral and Semi-Integral Bridges 30

3.5 Abutment Backfill Material 38

4.0 Implementation, Monitoring, and Modeling 41

4.1 Pressure Relief Joint Retrofit - Asphalt 41

4.1.1 Site Investigation 45

4.1.2 Remediation 47

4.1.3 Monitoring 48

4.2 Pressure Relief Joint Retrofit – 4-inch BEJS Joint 52
4.2.1 Remediation 54
4.2.2 Monitoring 55
4.3 Pressure Relief Joint Retrofit – Series of 2-inch BEJS Joints 58
4.3.1 Site Investigation 62
4.3.2 Remediation 65
4.3.2.1 Foam Injection 65
4.3.2.2 Pressure Relief Joints 67
4.3.3 Monitoring 74
4.3.3.1 Instrumentation 74
4.3.3.2 Monitoring Results 80
4.4 Joint Replacements Using Ultra-High Performance Concrete 86
4.4.1 SH-3E Bridge Over the N. Canadian River 87
4.4.2 U.S. 183/412 over Wolf Creek in Woodward County 103
4.4.3.1 Load Test Procedure 106
4.4.3.2 Continuity Joint Instrumentation and Repair 109
4.4.3.3 UHPC Joint Construction Data 115
4.4.3.4 Load Test Results 117
4.5 Tall Embankments on Soft Soils 121
4.5.1 Site Investigation 124
4.5.2 Numerical Analysis 126

4.5.2.1 Bounding Surface Plasticity Model; Dafalias and Herrmann (1986) 127
4.5.2.2 Model Parameters 128
4.5.2.3 Finite Element Model 131
4.5.2.4 Simulation Results 132
4.6 Observations of Oklahoma Bridge Drainage Systems 136
5.0 Recommended Practices 146
5.1 General Recommendations for Design and Construction 146
5.1.1 Pressure Relief Joints 146
5.1.2 Tall Approach Embankments on Soft Soil 150
5.1.3 Drainage Systems 152
5.1.4 Abutment Backfill 155
5.1.5 Wingwalls 156
5.1.6 Joint Retrofits 157
5.1.6.1 Expansion Joint Rehabilitation 158
5.1.6.2 Expansion Joint Removal 160
5.1.6.3 UHPC Connections of Precast Girders for Live Load Continuity 163
5.2 Conventional Bridges 164
5.3 Integral Abutment Bridges 166
5.4 Semi-Integral Abutment Bridges 172
5.5 Bridge Retrofit – Integral and Semi-Integral Conversions 175
6.0 Conclusions 181

7.0 Acknowledgements 185

References 186

Appendix A – State Dot Standard Plans Referenced 192

Appendix B – Bridge Systems Survey 195

Appendix C – SH-3 over BNSF Boring Logs 202

Appendix D – SH-3 over BNSF Lab Test Results 207

D.1 One Dimensional Consolidation Results 207

D.2 Triaxial Compression Results 221

Table of Figures

Figure 1. Elastomeric Concrete Plug Joint (Balakumaran et al. 2018) 3

Figure 2. Backfill Drainage Systems a) Geosynthetic Vertical Drain; b) Tire Chips; c) Porous Backfill; d) Laboratory Model for the Porous Backfill System (from Mekkawy et al. 2005) 5

Figure 3. Kansas DOT Backfill Drain with Geofoam Spacer 6

Figure 4. Texas DOT Approach Slab Details: Section B-B Approach Slab/Approach Pavement Interface, Section D-D Abutment/Approach Slab Interface 8

Figure 5. New York DOT Approach Slab Sleeper Slab Detail 9

Figure 6. Passive Force Deflection Curves Obtained by Rollins et al. (2019) (from Rollins et. al 2019) 11

Figure 7. Backfill Construction with LDCC (from Loewen et al. 2012) 12

Figure 8. Louisiana DOT Pavement Pressure Relief Joint (Louisiana DOT Standard Drawings) 14

Figure 9. Arizona DOT Pavement Lug (Arizona DOT Standard Drawings) 16

Figure 10. Proposed IAB Design Alternatives (Horvath 2005) 17

Figure 11. Moment Break at Pile Top (from Sherafati and Azizinami 2014) 18

Figure 12. States Responding to the Survey 21

Figure 13. Pressure Relief Joint Width - New Construction 22

Figure 14. Pressure Relief Joint Spacing - New Construction 23

Figure 15. Prevalence of Excessive Pavement Pressure Problems 23

Figure 16. Pressure Relief Joint Width – Rehabilitation 25

Figure 17. Embankment Height that is Considered Tall 26

Figure 18. Prevalence of Conventional Bridges - New Construction 28
Figure 19. Performance of Conventional Bridges 28
Figure 20. Performance of Integral Bridges 31
Figure 21. Performance of Semi-Integral Bridges 31
Figure 22. Backfill Distribution: (a) Conventional Bridges, (b) Integral Bridges, and (c) Semi-Integral Bridges 39
Figure 23. Shields Boulevard over I-40, Oklahoma City 43
Figure 24. Shields Boulevard over I-40: (a) deck uplift, (b) deck movement, (c) uncompressed relief joint, (d) rotated bearings 44
Figure 25. Shields Boulevard over the Oklahoma River: North Abutment 45
Figure 26. Shields Boulevard over I-40: Expansion joint pavement core 46
Figure 27. Shields Boulevard over I-40: Full depth asphalt pressure relief joint 48
Figure 28. Shields Boulevard over I-40: Measurement reference points (a) west (b) east 49
Figure 29. Shields Boulevard over I-40: West measurement reference point 50
Figure 30. Shields Boulevard over I-40: Monitoring results - east side 51
Figure 31. Shields Boulevard over I-40: Monitoring results - West side 51
Figure 32. I-40 over SH-81, El Reno 52
Figure 33. I-40 over SH-81: (a) closed expansion joint, (b) deck shoving, (c) rotated bearing, (d) pedestal damage 53
Figure 34. EMSEAL® BEJS, courtesy of EMSEAL® 54

Figure 35. I-40 over SH-81 Joint Installation: (a) Westbound bridge – east approach, (b) Westbound bridge – west approach, (c) Eastbound bridge – east approach, (d) Eastbound bridge – west approach 55
Figure 36. I-40 over SH-81: Joint width WB-east approach 56
Figure 37 I-40 over SH-81: Joint width WB-west approach 56
Figure 38 I-40 over SH-81: Joint width EB-east approach 57
Figure 39 I-40 over SH-81: Joint width EB-west approach 57
Figure 40. 19th Street over I-35: Pressure relief joint installed in 2016 60
Figure 41. 19th Street over I-35: Pressure relief joint in 2019 61
Figure 42. 19th Street over I-35: CPT-1 results 63
Figure 43. 19th Street over I-35: CPT-2 results 64
Figure 44. 19th Street over I-35: Foam injection 66
Figure 45. 19th Street over I-35: Locations of pressure relief joints 67
Figure 46. 19th Street over I-35: Approach roadway replacement (a) facing approach roadway, (b) facing approach slab 69
Figure 47. 19th Street over I-35: New approach roadway panels (a) west side of bridge, (b) east side of bridge 70
Figure 48. 19th Street over I-35: Pressure relief joint installation (a) epoxy application, (b) joint installation 72
Figure 49. 19th Street over I-35: Installed pressure relief joints (a) west approach (b) east approach 73
Figure 50. Geokon model 8021 Micro-1000 data logger and multiplexer (Geokon 2017) 75

Figure 51. Geokon model 4200 vibrating wire strain gauge (Geokon 2019) 76
Figure 52. Mounting bracket with Geokon strain gauge 77
Figure 53. Geokon model 4420 crackmeter shown with mounting brackets (Geokon 2020) 78
Figure 54. 19th Street over I-35 instrument locations 79
Figure 55. 19th Street over I-35 concrete strain: East approach roadway south lane ... 80
Figure 56. 19th Street over I-35 concrete strain: East approach roadway north lane 81
Figure 57. 19th Street over I-35 concrete strain: West approach roadway north lane ... 81
Figure 58. 19th Street over I-35 pressure relief joint width: East approach south non-doweled joint 82
Figure 59. 19th Street over I-35 pressure relief joint width: 83
Figure 60. 19th Street over I-35 pressure relief joint width: East approach north non-doweled joint 83
Figure 61. 19th Street over I-35 pressure relief joint width: East approach north doweled joint 84
Figure 62. 19th Street over I-35 pressure relief joint width: West approach south non-doweled joint 84
Figure 63. 19th Street over I-35 pressure relief joint width: West approach south doweled joint 85
Figure 64. 19th Street over I-35 pressure relief joint width: West approach north non-doweled joint 85
Figure 65. 19th Street over I-35 pressure relief joint width: West approach north doweled joint 86

Figure 66. SH-3 bridge over N. Canadian River (left) and expansion joint to be replaced (right) 88
Figure 67. Underside of the SH-3 bridge over N. Canadian River at the candidate joint showing concrete deterioration 88
Figure 68. Details of the UHPC expansion joint headers including formwork 90
Figure 69. High shear mixers used for mixing UHPC 91
Figure 70. Joint after removal of existing concrete and before placement of the top form 92
Figure 71. Strain gages within the joint header 93
Figure 72. UHPC temperature over the first week after casting 95
Figure 73. UHPC joint before (left) and after (right) grinding 96
Figure 74. Entire Joint after grinding 97
Figure 75. Installation of BEJS material by SSI Highway Products personnel 98
Figure 76. End of BEJS stick prepared for splicing 98
Figure 77. UHPC joint headers on SH-3E bridge immediately after BEJS material was placed 99
Figure 78. UHPC joint headers on SH-3E bridge before joint sealant was placed and showing hairline cracks 100
Figure 79. UHPC joint headers on SH-3E bridge before joint sealant was placed and showing surface rusting of the exposed steel fibers 101
Figure 80. Photos of the UHPC joint on the SH-3E bridge over the North Canadian River (a) immediately after BEJS placement, on March 29, 2018 3 months after casting,

(b) 7 months after casting, (c) 14 months after casting, (d) 21 months after casting, (e) 29 months after casting, (f) 33 months after casting, and (g) 45 months after casting 102
Figure 81. Strain measured in the UHPC material for approximately seven months after placement 103
Figure 82. Example of positive moment cracking in a continuity joint of the U.S. 183/412 bridge over Wolf Creek 104
Figure 83. Plan view of U.S. 183/412 over Wolf Creek bridge 105
Figure 84. Cross-section view of U.S. 183/412 over Wolf Creek bridge 105
Figure 85. U.S. 183/412 over Wolf Creek continuity joint details from original drawings 106
Figure 86. Laser measurer and plumb bob setup (left), clamp on the girder bottom (middle), and method used for measurement with the plumb bob (right) 107
Figure 87. Truck locations for each load stage 108
Figure 88. Trucks located for Load Stage 6 108
Figure 89. Strain gauge placement in the joint 109
Figure 90. High shear pan mixer in place on the bridge deck (left) and placement of UHPC materials in the mixer (right) 110
Figure 91. Pour holes for UHPC joints on the Wolf Creek bridge 111
Figure 92. Placement of UHPC into fill hole in the bridge deck 112
Figure 93. UHPC from failed formwork 113
Figure 94. Final joint forms after adding bracing 114
Figure 95. Completed UHPC continuity joint after form removal 115
Figure 96. UHPC heat evolution for center and exterior joint on pier 3 117

Figure 97. Span 4 midspan deflections during each of the six load stages 118
Figure 98. Foil strain gauge data for post-repair load test 120
Figure 99. Collected average strain gauge readings 121
Figure 100. SH-3 over BNSF Railroad; aerial overview 122
Figure 101. SH-3 over BNSF: Bridge distress (a) closed expansion joint, (b) buckled slope wall, (c) cracked backwall, (d) sheared anchor bolt 123
Figure 102. SH-3 over BNSF: Boring locations 125
Figure 103. Schematic illustration of bounding surface model, from Dafalias and Herrmann (1986) 127
Figure 104. SH-3 over BNSF Railroad: Finite element mesh (a) east embankment, (b) west embankment 132
Figure 105. SH-3 over BNSF Railway: simulated settlement (a) east embankment, (b) west embankment 133
Figure 106. SH-3 over BNSF Railway: simulated lateral displacement (a) east embankment, (b) west embankment 133
Figure 107. SH-3 over BNSF Railroad: Settlement isochrones – east embankment .. 134
Figure 108. SH-3 over BNSF Railroad: Settlement isochrones – west embankment .. 134
Figure 109. SH-3 over BNSF Railroad: Lateral deformation isochrones – east embankment 135
Figure 110. SH-3 over BNSF Railroad: lateral deformation isochrones – west embankment 136

Figure 111. Void beneath approach slab and possible path for water flow (black arrow) at bridge over Sadler Creek (left photo), and another under the approach slab at SH59A over Big Creek (right photo) 137
Figure 112. Erosion observed under abutment at Bridge B on US177 over the Salt Fork River (left photo) and at the bridge on SH152 over Willow Creek (right photo) 138
Figure 113. Underdrain design, after ODOT Proposed Plan for S.H. 3W over Big Creek 139
Figure 114. Underdrain Design, after ODOT Proposed Plan for S.H. 6 over West Elk Creek..... 139
Figure 115. Underdrain Design, after ODOT Proposed Plan US 177 over Salt Fork, Bridge A 139
Figure 116. Underdrain Design, After ODOT Proposed Plan for Shields Boulevard over I-35 141
Figure 117. Underdrain Design, After ODOT Proposed Plan for Tecumseh Road over I-35 142
Figure 118. Schematic Cross-Section View of Hydraulic Short Circuit that Can Develop in the Abutment Drainage System (from Miller et al. 2013) 142
Figure 119. Proposed Abutment Backfill Drainage System with Geomembrane and Geotextile Filter (units in mm: 300 mm≈12 inches) (from Miller et al. 2013)..... 143
Figure 120. Proposed Abutment Backfill Drainage System, Depressed with Geomembrane and Geotextile Filter (units in mm: 300 mm≈12 inches) (from Miller et al. 2013) 143
Figure 121. Soil flowing out of underdrain outlet. 144

Figure 122. Water flowing from underdrain outlets onto slope wall, Tecumseh Rd. over I-35. (note large void under slope wall) 145
Figure 123. Michigan DOT pressure relief joint spacing standard drawing (from MDOT) 147
Figure 124. Louisiana DOTD pressure relief joint retrofit standard (from Louisiana DOTD) 149
Figure 125. Backfill drainage system for SPUI bridge on Main Street over I-35 in Norman 155
Figure 126. Retrofit of bridge deck expansion joint using conventional concrete (a) before retrofit, (b) after demolition, and (c) after retrofit completion 158
Figure 127. Recommended general detail for UHPC expansion joint headers 160
Figure 128. Full-depth (left) and half-depth (right) UHPC connections intended for removal of expansion joints in bridge deck slabs 161
Figure 129. Typical detail for retrofit of an existing expansion joint using a UHPC link slab (NYSDOT) 162
Figure 130. Conventional concrete link slab detail for full-depth deck replacement (NYSDOT) 162
Figure 131 UHPC link slab detail for new construction (NYSDOT) 163
Figure 132. Integral Stub-Type Abutment Detail (Burke 2009) 168
Figure 133. I-44 Bridge Over Medicine Bluff Creek (ODOT 2008) 171
Figure 134. Semi-Integral Abutment Detail (Burke 2009) 173
Figure 135 Integral Abutment Conversion: Before (l) and After (r) (Burke 2009) 176

Figure 136. Semi-Integral Abutment Conversion: Before (l) and After (r) (Burke 2009) 177
Figure 137. I-44 Bridge Over Southwest 15th Street, Oklahoma City, Oklahoma (ODOT 1975) 179

Table of Tables

Table 1. UHPC compressive strength for SH-3E joint 95
Table 2. Truck Information 107
Table 3. Compressive strength test results for the UHPC used on Wolf Creek bridge 117
Table 4. Adopted Soil Parameters 129
Table 5. Parameter Values for Abutment Piles 130
Table 6. Parameter Values for Abutment Plates 130

1.0 General

Previous research projects funded by the Oklahoma Department of Transportation (ODOT), Federal Highway Administration (FHWA), and other agencies have revealed that many problems faced by bridges, such as expansion joints closing, are related to how the interfaces between a bridge and the adjacent roadway are designed, constructed, and maintained. The current design practice views the bridge and the adjacent roadway as separate components. Therefore, a systems-based approach is needed that considers the important interactions of the bridge and adjacent roadways in a holistic manner. The current project utilizes the knowledge gained from previous studies and develops implementable strategies for improving design, construction, and maintenance of bridges and adjacent roadways.

2.0 Review of Design and Construction Practices

A comprehensive review of details, specifications, and repair practices used by ODOT and other state DOTs and the published research literature with a specific focus on expansion joints for conventional bridges, abutment backfill, pavement pressure relief joints, pavement lugs, and integral abutment bridges was conducted. Some of the design and construction practices identified are still in the early stages and have only been implemented in a limited scope while others have been incorporated into bridge and roadway design standards within various state DOTs. The following sections present some of the more notable design and construction practices identified.

2.1 Conventional Bridge Joints

Conventional bridge joints are necessary to allow for movement associated with thermal expansion and contraction that bridges experience. The joints are typically sealed with a neoprene gland or foam compression joint to prevent water and deicing chemical infiltration. Water and deicing chemical infiltration in the joint can damage the girder ends and pier caps (Enright and Frangopol 2000).

The joint headers, pavement corners adjacent to the joint, can either be armored or armorless. Strip seal joints, such as neoprene glands, are mechanically locked to a steel rail that is attached to the concrete. These types of joints are considered armored. Compression foam joints are held into place using compression and are not attached to a steel rail. The joint headers for compression foam joints are not required to be armored. Armorless joints can be prone to spalling when traffic volume is high. Elastomeric (polymer) concrete headers have been used to increase the toughness of the concrete and reduce spalling (Connecticut DOT 2003; New York State DOT 2019).

Multiple iterations for the expansion joint design have been proposed over the years emphasizing the continued need for a durable expansion joint. More recently Balakumaran et al. (2018) proposed a new durable expansion joint. The joint consists of a debonded steel plate that is covered with elastomeric concrete. The details of this joint are shown in Figure 1.

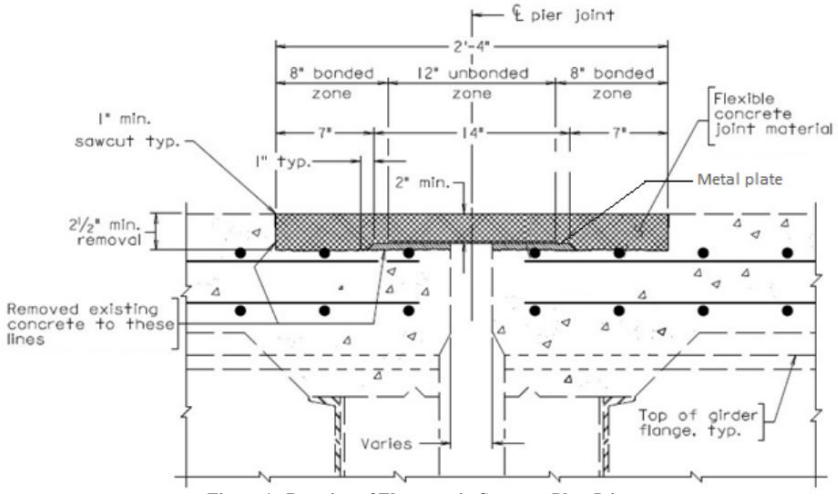

Figure 1. Elastomeric Concrete Plug Joint (Balakumaran et al. 2018)

After monitoring the joint at a bridge in Virginia for one year, the authors reported satisfactory performance considering the weather conditions the joint was exposed to. There were issues with the installation of the joint and there were concerns that the elastomeric concrete could be damaged from snowplows.

All expansion joints will eventually leak if not properly cared for. A proactive maintenance program is vital to ensure joint performance (Purvis and Burke 2003). A proactive maintenance program should include keeping joints clean of debris, washing bridge decks, and repairing any small problems in the joints before they result in failure. Purvis and Burke (2003) suggests that for a proactive maintenance program to be

successful it must be incorporated into agency policy. The program must also be supported and promoted by top management for benefits to be fully realized.

2.2 Abutment Backfill

Abutment backfill can be a cause of distress in the event of backfill washout or settlement that will cause the downward movement of the approach slab. There have been several efforts to reduce backfill washout and settlement of the approach slab, including using non-traditional backfill materials and geogrids as described in the following sections.

2.2.1 Backfill Drainage

Mekkawy et al. (2005) performed research for the Iowa DOT to address erosion problems that were commonplace in Iowa. The research looked at examples in the field and involved a ¼ scale model of the Iowa DOT's bridge abutment. The model was then subjected to water infiltration through an unsealed expansion joint for a period of 4 hours under steady state conditions. Based on the results of the tests, the researchers suggested 3 backfill systems: porous backfill, geogrid reinforced granular backfill with a vertical drain, and tire chips with foam board separating the tire chips from the granular backfill. The details for these systems and a photograph of the laboratory setup are shown in

Figure **2**.

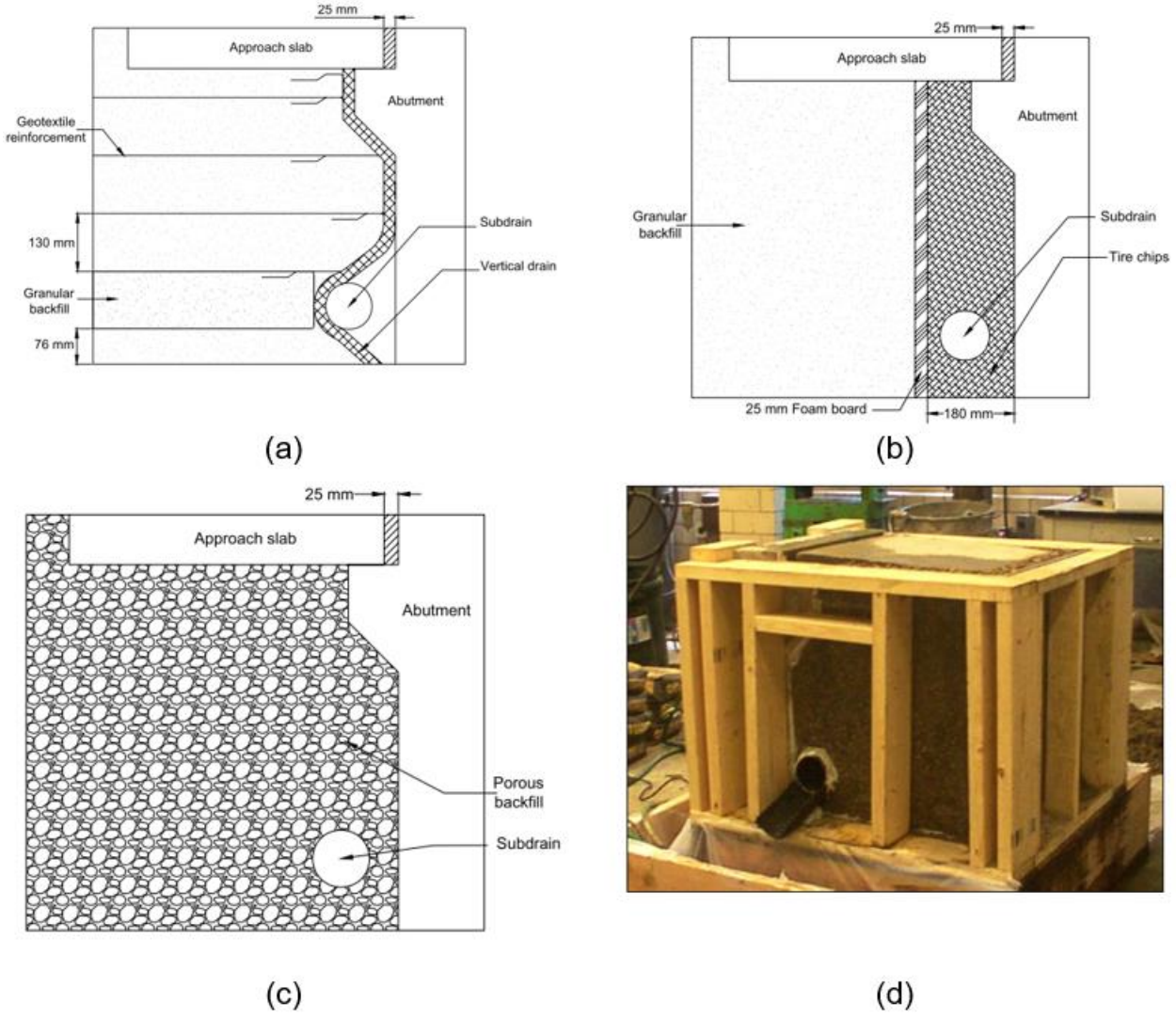

Figure 2. Backfill Drainage Systems a) Geosynthetic Vertical Drain; b) Tire Chips; c) Porous Backfill; d) Laboratory Model for the Porous Backfill System (from Mekkawy et al. 2005)

Based on available online standard drawings it does not appear that Iowa DOT has adopted the recommendations presented by Mekkawy et al. (2005), however the Kansas DOT has a backfill system that incorporates some of the same elements suggested by the researchers. The standard for the Kansas DOT integral bridges is to place a layer of geofoam adjacent to the abutment followed by a geosynthetic reinforced aggregate backfill. Furthermore, there is a cohesive soil wedge at the bottom of the stub abutment to direct water away from the bridge and into a 4” drainage pipe. Details of

this backfill system are shown in Figure 3. It should be noted that most, if not all, of the available design standards for the Kansas DOT are for integral bridges so the geofoam is likely intended to help relieve buildup of passive pressure on the backfill due to thermal expansion of the bridge and to allow for proper rebound during thermal contraction.

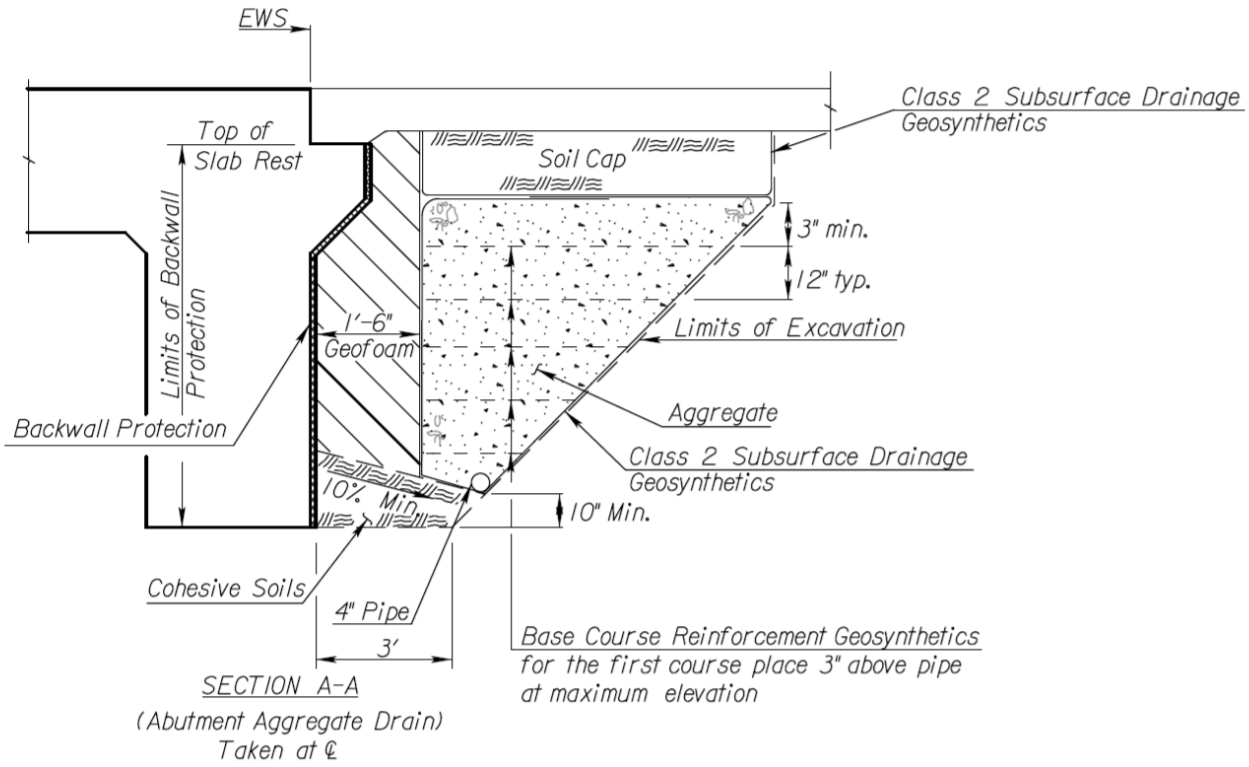

Figure 3. Kansas DOT Backfill Drain with Geofoam Spacer

Other DOT's, such as the North Carolina DOT, have moved the backfill drainage pipe away from the abutment and placed a wedge of soil that positions the drain at the lowest point within the backfill to avoid the issue of a hydraulic short circuit as presented by Miller et al. (2013).

2.2.2 Approach Slab Settlement

Approach slab settlement is a major issue due to the hazards to vehicles associated with the rough transition between the roadway and the bridge. Researchers

have proposed various methods to deal with the approach slab settlement. Cai et al. (2005), for example, proposed determining the anticipated settlement for the soil under the approach slab and then increasing the approach slab thickness and rebar or reducing the anticipated settlement. To assist with this method the researchers developed design aids using finite element analysis, however, for this method to be of used in an economical manner, the settlement under the approach slab had to be accurately estimated. Other methods to decrease approach slab settlement involve mechanical stabilized base course such as the geosynthetic reinforced aggregate used by the Kansas DOT (see Figure 3).

Several states have proposed standards to limit or eliminate approach slab settlement. For example, the Louisiana DOT places a sleeper slab between the approach roadway and the approach slab on an aggregate bedding with drains in it to prevent pumping in the event of a leak in the joint. The Arkansas DOT places two footings under their approach slab, one of the footings is located at the half length of the approach slab and the other is located at the end of the approach slab. The footings are monolithically constructed with the approach slab, when the approach pavement is concrete the approach pavement will rest on the footing otherwise the footing ends at the edge of the approach slab. At the bridge side, the approach slab rest on a paving notch that is part of the abutment. The Texas DOT has a standard like that of Arkansas, but without the footing at the half length. The details for the Texas DOT standard are shown in Figure 4.

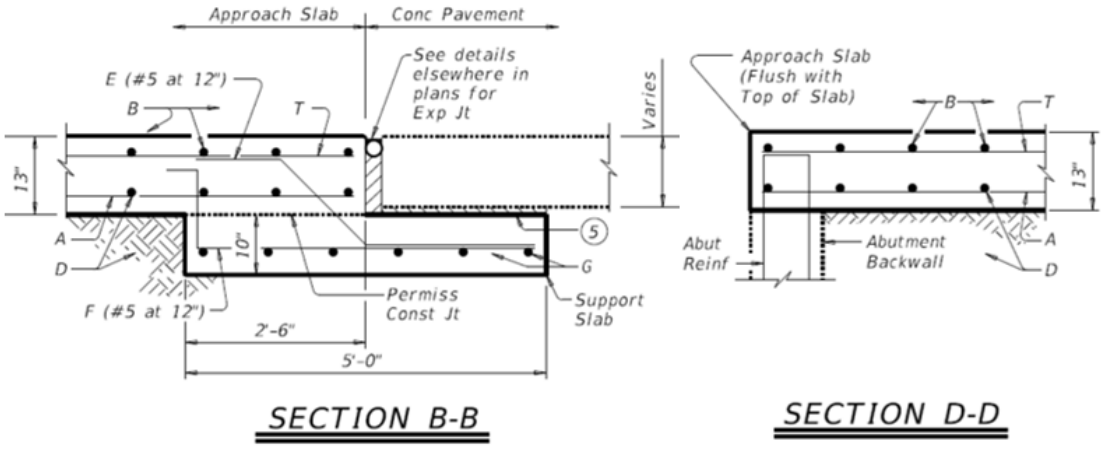

Figure 4. Texas DOT Approach Slab Details: Section B-B Approach Slab/Approach Pavement Interface, Section D-D Abutment/Approach Slab Interface

New York DOT uses a T shaped sleeper slab to minimize settlement of the approach slab. A detail of the T shaped sleeper slab used by the New York DOT is shown in Figure 5. The detail shown does not apply to integral bridges with concrete approach pavement. For those bridges an asphalt pressure relief joint is required in lieu of the compressible foam joint.

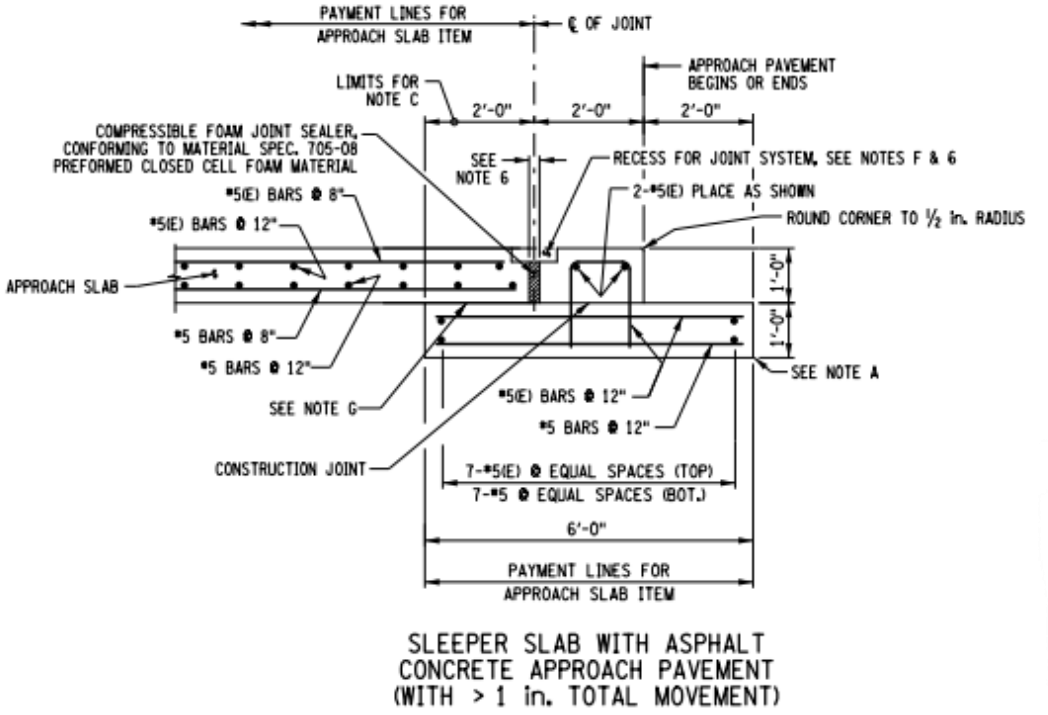

Figure 5. New York DOT Approach Slab Sleeper Slab Detail

2.2.3 Low Density Cellular Concrete (LDCC) as Backfill Material

ODOT has expressed an interest in using LDCC as a flowable backfill material behind bridge abutments. LDCC is considered a special Controlled Low Strength Material (CLSM) that has entrained air. LDCC can be formulated to allow for drainage and has the advantage of density reduction without sacrificing strength according to manufacturers. For the remainder of this report LDCC will refer to CLSM that has entrained air, CLSM will refer to materials without an air entraining agent or without much air purposely added. In general, ODOT uses CLSM (without an air entrainer) as a backfill material and has restrictions on the lift height leading to longer installation and curing times. LDCC on the other hand is marketed as being able to be placed in a single lift making it an attractive option for the construction industry. A few researchers have

begun to study the engineering properties as they relate to bridge abutment backfill, but this research is limited. In addition, a few case studies involving the use of LDCC as abutment backfill have been located.

Rollins et al. (2019) measured passive force deflection curves for CLSM and LDCC, or lightweight cellular concrete (LCC) as denoted in that publication. The researchers evaluated the material properties using large scale lab tests. Granular backfill, a dense sand compacted to 98% modified Proctor maximum density, was also evaluated for comparison. The LCC and CLSM produced a larger passive force than the granular backfill. The CLSM was about 10 times stiffer than the granular backfill while the LCC was about twice as stiff as the granular backfill. The post peak strength of the LCC tested behaved more like the granular backfill. The CLSM had a massive reduction in strength post peak. Passive force deflection curves developed as part of the research are included in Figure 6.

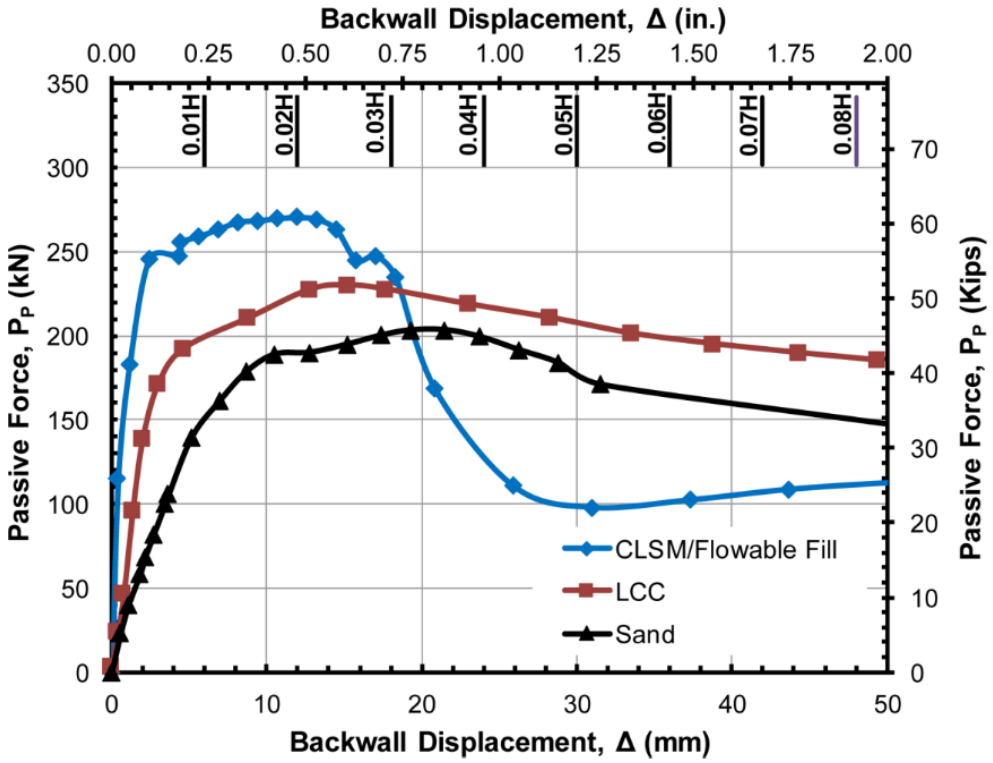

Figure 6. Passive Force Deflection Curves Obtained by Rollins et al. (2019) (from Rollins et. al 2019)

A case study involving LDCC as abutment backfill was presented by Loewen et al. (2012). The project involved an integral abutment bridge located over low strength soils with an embankment bound by MSE walls due to horizontal restrictions. The designers used LDCC as the embankment and backfill material. The piles were placed in corrugated plastic pipes filled with Styrofoam pellets to isolate the backfill from the thermal lateral movements of the bridge. The authors reported good performance of the bridge and abutment system one year after construction, an image of LDCC placement at the bridge is shown in Figure 7.

Figure 7. Backfill Construction with LDCC (from Loewen et al. 2012)

The case study from Loewen et al. (2012) is representative of available case studies on LDCC. The bridges where LDCC is used as abutment backfill typically have MSE retaining walls leading up the bridge. The LDCC is also typically placed for the full depth embankment height. A case study presenting a stub type abutment with an earthen embankment has not been located. LDCC has the added advantage of limiting settlement on soft soils due to its lightweight characteristics. This is likely why it has been used primarily to replace the embankment fill material as well.

While research on LDCC is limited, several states have listed it as an approved backfill material. These states include Colorado, Florida, Minnesota, New York, and Rhode Island (Colorado DOT 2021; Florida DOT 2021; Minnesota DOT 2021; New York State DOT 2021; Rhode Island DOT 2018). In many of the standard specifications, the LDCC is labeled by different names such as lightweight concrete fill, flowable fill with cellular foam and cellular concrete. The New York DOT has reportedly used lightweight foamed concrete as backfill since 1981. Harbuck (1993) reported that at that time there were no apparent lateral movements of abutments using lightweight foamed concrete,

however, at the time of the publication the New York DOT had only used the material on 7 projects. Harbuck (1993) also noted that at one project site, the foamed concrete was left open over the winter and showed no signs of deterioration.

The California Nevada Cement Association has published a technical resource on the use of LDCC or LCC materials for geotechnical applications which includes a small section on bridge applications (Tiwari et al. 2020). The publication references the backfilling of bridge abutments as a use for LCC. However, no case studies other than those which involve MSE walls (similar to Loewen et al. 2012) are presented.

2.3 Pavement Pressure Relief Joints

Burke (2009) outlined pavement pressure phenomena, which he called pavement growth. During contraction of rigid pavements (cooling) the joints fill with debris and then when the pavement expands the joint is no longer wide enough to accommodate the movement. This process continues over and over and can cause the pavement to push into objects such as bridges. One solution to avoid this phenomenon is to have pavement pressure relief joints. Ideally the joints would be included in the construction plans to mitigate the potential for bridge damage, however, the joints can also be added later as necessary. Many DOT's have adopted pavement pressure relief joints to deal with excessive pavement pressure buildup. Some of the standards located include varying joint thickness based on the temperature during construction and the maximum and minimum anticipated temperature.

For example, the Kansas DOT places two pressure relief joints, one at the approach slab – approach pavement interface and one 20 feet beyond the approach slab in the approach pavement. The joint widths are contingent on the temperature during construction. The Kansas DOT pressure relief joint is also placed on a sleeper

slab that has a smooth trowel finish to allow for lateral movement of the slabs and proper joint transfer. The Louisiana DOT also places their pressure relief joint over a sleeper slab, however, they use an elastomeric bearing pad between the sleeper slab and the pavement. The Louisiana DOT also places a drain under the sleeper slab and reinforces the soil with 5 layers of geosynthetic reinforcement to reduce settlement potential, the Louisiana DOT standard details for a pavement pressure relief joint is shown in Figure 8.

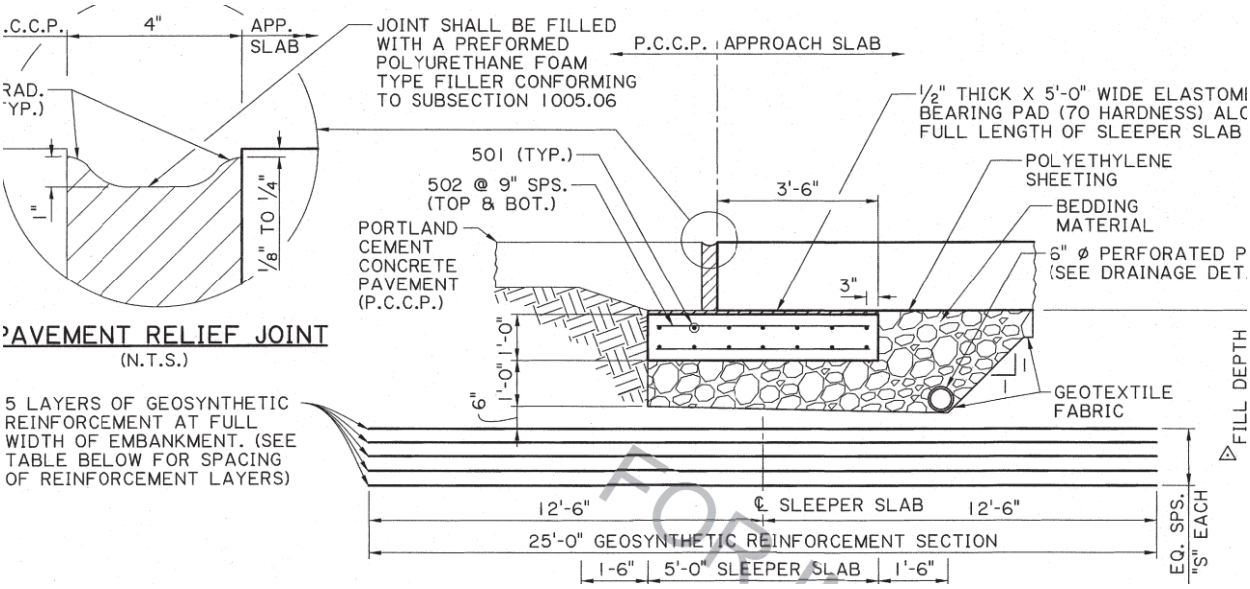

Figure 8. Louisiana DOT Pavement Pressure Relief Joint (Louisiana DOT Standard Drawings)

The Pennsylvania DOT has a pavement pressure relief joint standard, but their joint is 1 foot wide and is filled with Superpave asphalt. Like many of the other pavement pressure relief joints, the Pennsylvania DOT also supports the joint over a sleeper slab. Other states with pavement pressure relief joints similar to the ones already described include Tennessee and South Carolina.

The pavement pressure relief joint standards located in the literature review, generally, only addressed pavement pressure relief joints at the end of the approach

slab. The location of adjacent structures or the length of rigid pavement adjacent to a bridge will influence the need for additional pavement pressure relief joints. Michigan DOT has a standard for the placement of pavement pressure relief joints when there are adjacent structures. All the pavement pressure relief joints in the Michigan DOT standard are 1 inch wide. When the structure spacing is less than 185 feet a single expansion joint is placed at the end of the structure approach slab. For a spacing ranging from 185 to 485 feet an expansion joint is placed at the end of the approach slab with an additional expansion joint 20 feet past the approach slab. For structures spaced 485 to 810 feet an additional expansion joint is added in the pavement. The spacing to the additional expansion joint is based on the pavement thickness and ranges from 12 to 16 feet. For greater lengths an expansion joint is placed at the end of the approach slab followed by a series of three expansion joints in the pavement. The first expansion joint is 20 feet beyond the approach slab. The remaining expansion joints are based on the pavement thickness with spacing ranging between 12 and 16 feet.

2.4 Pavement Lugs

As discussed in the previous section, excessive pavement pressure can be a serious problem for bridges. As described in the previous section, one solution to dealing with the pavement pressure is to provide pavement pressure relief joints. Another solution is to include mechanisms to prevent the pavement from excessively moving in the direction of the bridge. Several DOTs use what are called pavement lugs to accomplish this. Pavement lugs are basically a rectangular footing cast monolithically with the approach pavement that extends into the subgrade. The Alabama and Arizona DOTs that had pavement lug details also included an expansion joint between the

approach slab and the approach pavement to isolate the thermal movements of the approach roadway from the bridge. The details for the Arizona DOT pavement lugs are shown in Figure 9. The performance and effectiveness of pavement lugs are not known.

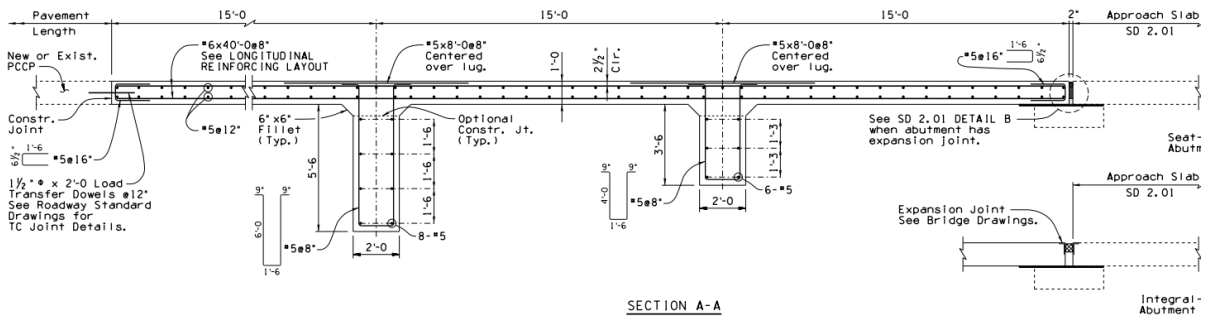

Figure 9. Arizona DOT Pavement Lug (Arizona DOT Standard Drawings)

2.5 Integral Bridges

Integral abutment bridges are standard practice in many states, including Oklahoma. While performance of integral abutment bridges is generally considered to be good there are typically length and skew restrictions due to the complexity with the soil structure interactions at the abutment. Additional problems can arise due to approach slab settlement in these bridges. A survey of 30 road and bridge agencies in the United States and Canada found that the most common problem was the approach slab settlement likely due to the cyclical thermal movements of the abutment and the associated backfill settlements (Kunin and Alampalli 2000). Research has been carried out to limit the lateral earth pressures on the abutment from the backfill and hence limit the backfill settlement and the lateral loads transferred to the abutment piles.

Horvath (2005) studied the effect of using resilient expanded polystyrene (EPS) geofoam as an abutment backfill alternative. There were 2 promising designs, one included a rectangular section of geofoam that extended the depth of the stub abutment and the other resembled traditional abutment backfill in the shape of a wedge. The

details for these designs are shown in Figure 10. Geofoam within the backfill was only located in the standard drawings from the Kansas DOT (see Figure 3).

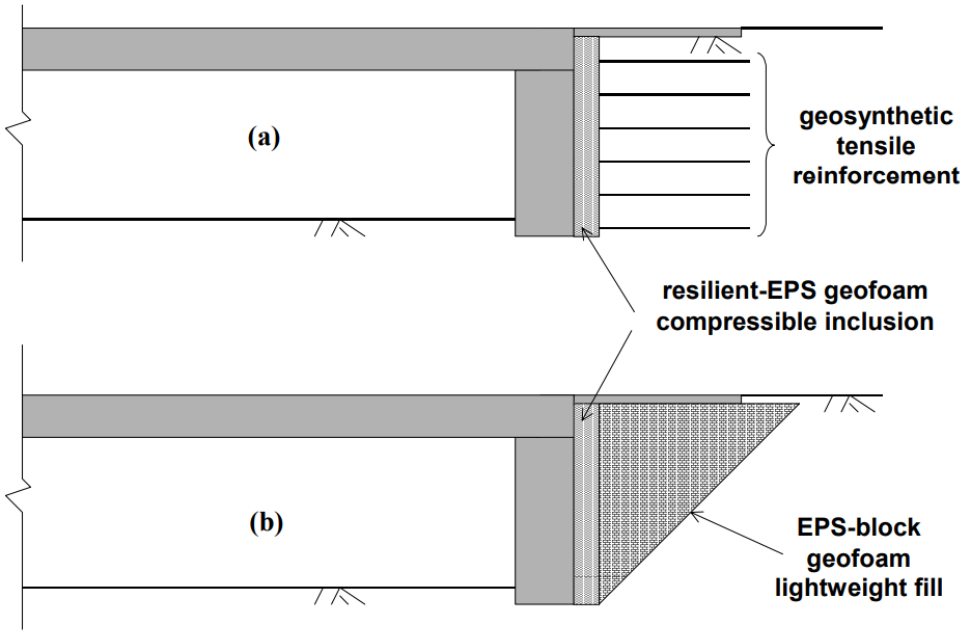

Figure 10. Proposed IAB Design Alternatives (Horvath 2005)

In an attempt to reduce the lateral movements of the top of the piles, Sherafati and Azizinamini (2015) sought to develop a moment break between the integral bridge abutment and supporting piles. They built and tested a pile top encased in elastomeric material that was then embedded in concrete. An image of the tested pile is shown in Figure 11. The elastomeric material ultimately failed during the later load testing that was equivalent to 100 years of cyclical thermal loading. The researchers suggested improvements in detailing could improve the performance. This method of moment break at the pile top, nor any other moment break, was not found in the approved standard details provided by state DOTs.

Figure 11. Moment Break at Pile Top (from Sherafati and Azizinami 2014)

Additional comprehensive studies have been completed on integral abutment bridges to understand the behavior and determine the best practices for these bridges. Oesterle et al. (1999) for example, completed a large research project that included experimental and analytical work regarding integral bridges. Some of the conclusions of this study are as follows:

- Based on testing of piles under integral abutments, yielding of the piles will occur with a horizontal movement of about 0.5"
- As lengths of the jointless integral abutment bridge increase, the abutment movement will cause yielding of the steel pile at the pile cap
- Plastic hinge formation resulted in local distortion (buckling), but did not result in major damage or loss of axial strength
- Vertical load capacities decrease when horizontal displacements increase
- According to computer analysis, passive pressure can be decreased significantly by using relatively less compacted backfill and/or increasing the horizontal length of the backfill zone. Increasing the length of the backfill will require a longer approach and could increase the settlement of the approach slab.

- When the approach slab is not tied to the abutment, the cyclic expansion and contraction from thermal movement allowed a gap to form at the abutment – approach slab interface
- Voids under the approach slab develop from bridge contraction beyond the initial point, even when the backfill was compacted to 97% relative density.

A literature review revealed that integral bridges are used in many states and almost exclusively in some states with reported good performance (Kunin and Alampalli 2000). It appears that the length limits are still in place for many states with regard to standard bridge details.

Muraleetharan et al. (2012) monitored and modeled a skewed integral bridge over Medicine Bluff Creek north of Lawton, OK. Their study found that abutment pile biaxial bending occurs in skewed integral abutment bridges. The bending moments in both directions will increase as the skew angle increases. They recommended that integral abutment bridges with large skew angles be carefully designed. It was also recommended to consider the effects of biaxial bending carefully. When the skew angle is very large the bending moment in the transverse direction will exceed the bending moment in the longitudinal direction. They also presented recommendations for all integral abutment bridges. Their recommendations and findings are as follows:

- The upper portion of abutment piles should be in pre-bored holes. The pre-bored holes should be backfilled with a material with low strength (ex. bentonite or loose sand).
- Abutment piles should be placed in weak axis bending.
- Short spans with shallow girders perform better than long spans with deep girders.

- The temperature gradient along the cross section of the bridge is not uniform. This uniformity needs to be considered during the design of integral bridges.

3.0 Results of the State DOT Survey

A survey was distributed throughout the United States to gain a better understanding of the design, maintenance, and performance of bridge systems. The survey link was distributed through the AASHTO Committee on Bridges and Structures (COBS) for each state department via email. The recipients were encouraged to complete the survey or forward the link to the most appropriate individual within their transportation department to complete the survey. The survey included 35 questions covering the following topics:

1. Bridge approach roadway and excessive pavement pressure,
2. Tall embankment performance,
3. Conventional bridges with expansion joints,
4. Integral and semi-integral bridges,
5. Abutment backfill material.

Responses were received from 22 state agencies (see Figure 12) from May 20, 2021 to June 18, 2021.

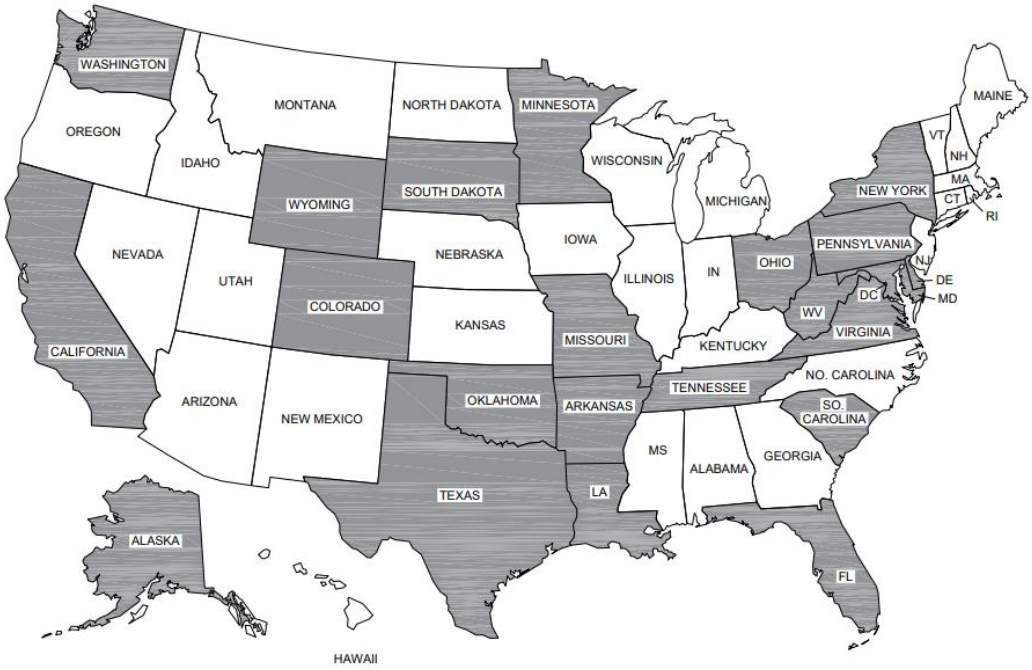

Figure 12. States Responding to the Survey

A summary of the responses is presented and discussed in the following sections. Some questions were skipped or did not apply, therefore, there are less than 22 responses for some of the questions. A full list of the survey questions is shown in Appendix B. The survey results are kept anonymous, so a full tabulated list of the results is not provided.

3.1 Bridge Approach Roadway and Excessive Pavement Pressure

The first section of the survey focused on the interactions of approach pavements and the bridge abutments. The respondents were asked about pressure relief joints, excessive pavement pressure, and repair and retrofit procedures as it pertains to excessive pavement pressure. The pavement pressure phenomena has been discussed extensively by Burke (2009) and is summarized in Section 2.3 of this report.

The respondents were initially asked if expansion joints, or pressure relief joints were installed in new pavements leading up to bridges. Installing expansion or pavement pressure relief joints in new pavements can be an effective prevention strategy. Of the responding agencies 16 responded yes and 6 responded no. The standard pressure relief joint for new construction ranged from 0.5 inches to 12 inches. The distribution of responses is shown in Figure 13.

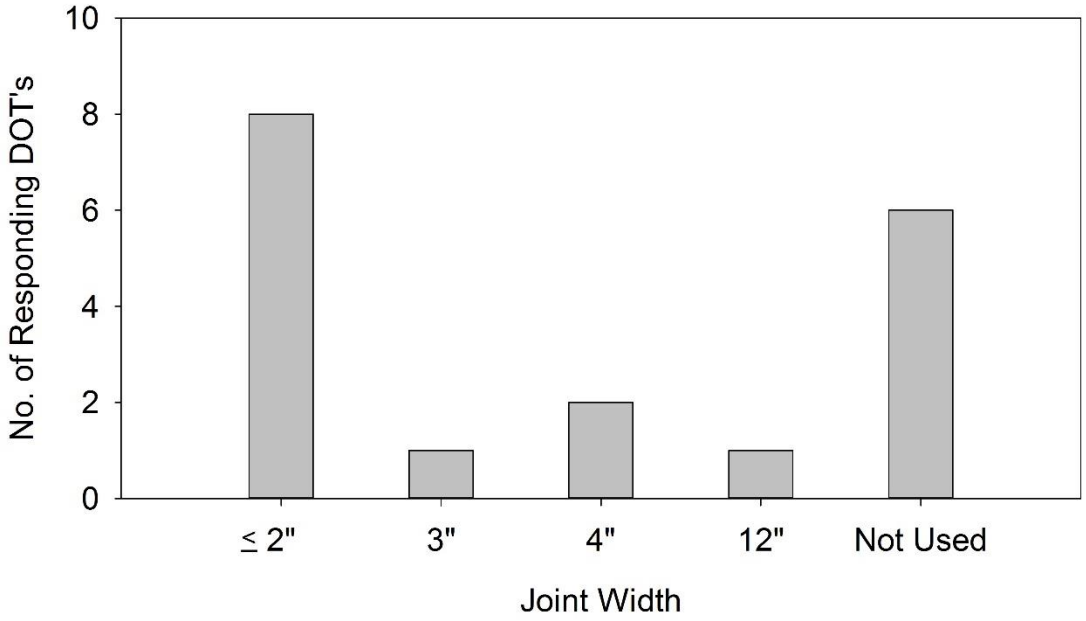

Figure 13. Pressure Relief Joint Width - New Construction

The joint material used was reported as poured silicone sealant for smaller joints and neoprene strip seal or standard compression fit joints for joints with larger movement.

The standard pressure relief joint spacing reported ranged from adjacent to the bridge up to intervals of 900 feet. The most common response was only adjacent to the bridge. The distribution of responses is shown in Figure 14.

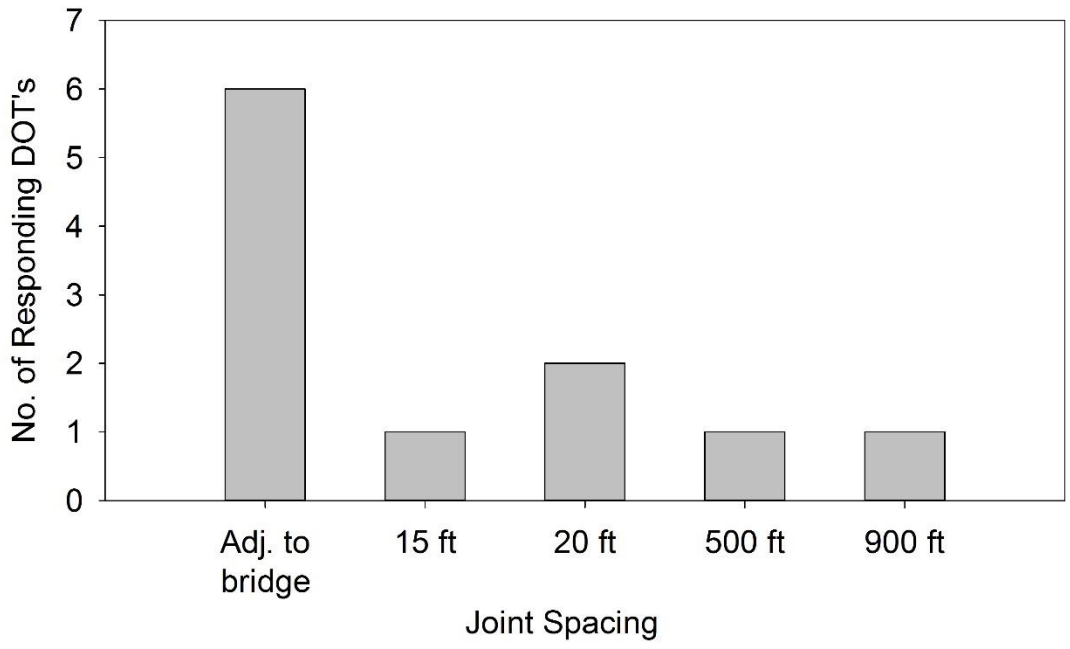

Figure 14. Pressure Relief Joint Spacing - New Construction

The respondents were asked about the prevalence of excessive pavement pressure on bridge abutments in their states. Of the responding states only five reported no problems. The most common response was yes at a few locations. The distribution of responses is shown in Figure 15.

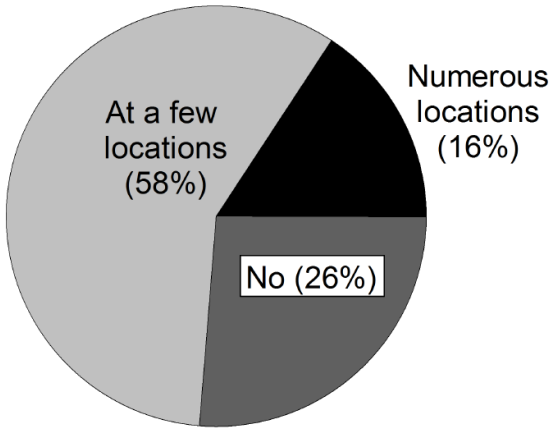

Figure 15. Prevalence of Excessive Pavement Pressure Problems

Of the respondents that have dealt with excessive pavement pressure problems, 12 reported that their agency retrofits or repairs the problem with expansion or pressure relief joints. Two respondents reported that their agency did not use pressure relief joints to mitigate damage from excessive pavement pressure. Nine of the respondents elaborated on the repair process. The responses are shown below. Some of the responses have been edited for clarity.

1. Install one 4-inch pressure relief joint consisting of foam sealant with a silicone topping or install multiple 2-inch pressure relief joints.
2. Repair and/or replace existing pressure relief joint and possibly widen the existing joint. The repair will vary depending on the circumstances of the bridge and pavement.
3. Install pressure relief joints at the end of bridge above the sleeper slabs.
4. Remove 5 feet of pavement for the full width of the roadway. Then install a sleeper slab. The thickness of the new sleeper slab is 1 foot. Dowel #5 bars to both sides of existing pavement. Install #4 rebar and pour new roadway section leaving a 4-inch gap above the sleeper slab for the new pavement pressure relief joint. Install polyurethane foam joint filler.
5. Replace bridge approach slabs and adjacent approach roadway pavement. Construct sleeper slabs. Install new approach slabs and approach roadway pavement leaving gap for joint above the sleeper slab. Install pavement pressure relief joint above the sleeper slab.
6. Remove 50 feet of pavement and replace with hot mix asphalt.
7. Install a sleeper slab with a pressure relief joint.
8. Repair any damaged concrete and add pressure relief joints, if needed.
9. Add pressure relief joint at the end of the bridge deck

Of the state agencies that install pressure relief joints as a rehabilitation or mitigation measure the joint width used varied from 0.5 inch to 12 inches. The most common range reported with was 2 to 4 inches. The distribution is shown in Figure 16.

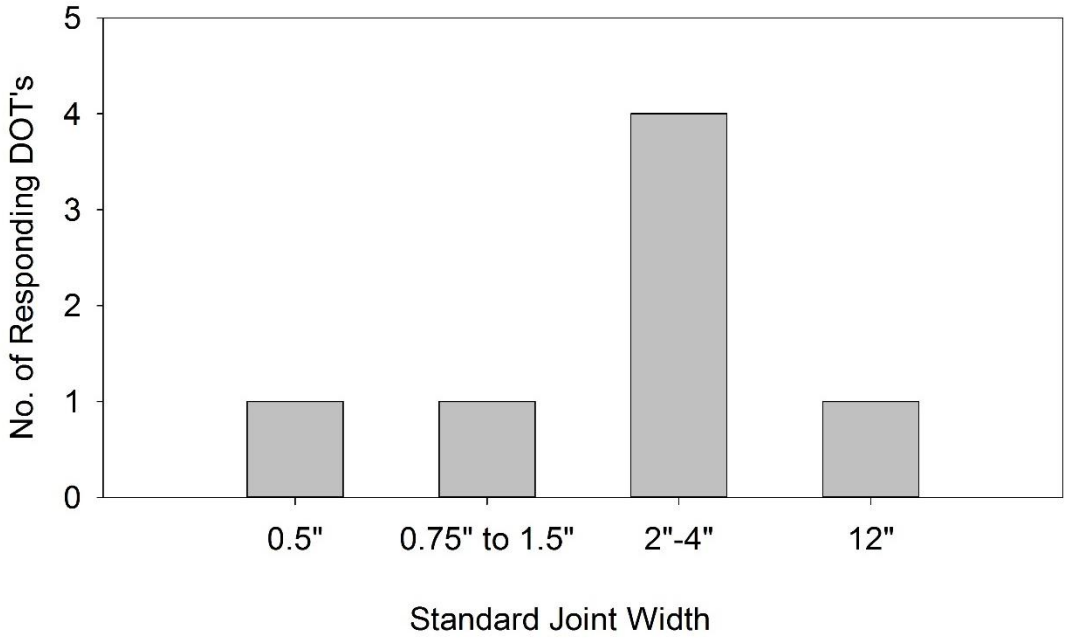

Figure 16. Pressure Relief Joint Width – Rehabilitation

Three state agencies reported using a series of joints for the rehabilitation. The spacing of the joints varied from 10 to 500 feet. The spacing reported did not appear to be standard lengths. Instead, the ranges reported suggest that the spacing length is largely project specific.

3.2 Tall Embankment Performance

The second section of the survey focused on the performance of tall bridge embankments. The respondents were asked the height at which an embankment was considered tall and any performance issues when the embankments are tall.

Of the responding agencies nine reported performance problems with tall embankments and ten reported no problems with tall embankments. Three respondents did not submit a response. Of those that reported problems the range of height that is

considered tall was from 10 to 60 feet. The most common response was 10 feet. The distribution of responses to this question is shown in Figure 17.

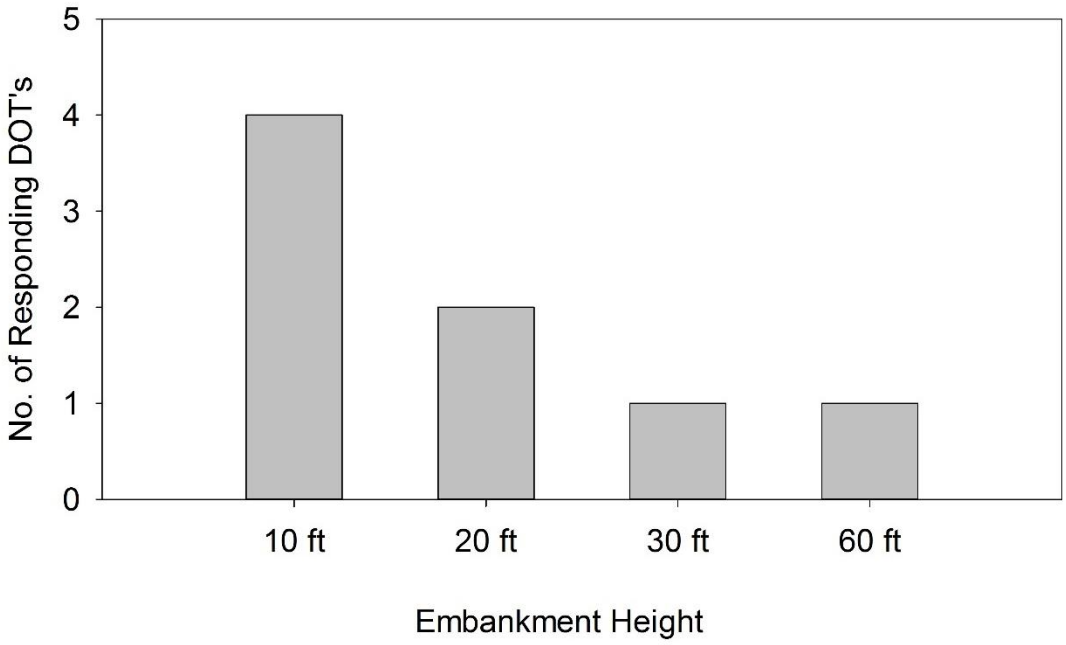

Figure 17. Embankment Height that is Considered Tall

The respondents were also asked about specific performance issues for tall embankments. The responses are shown below. Some of the responses have been edited for clarity.

1. Lateral spreading and/or pavement pushing on the bridge deck.
2. Excessive settlement of the embankment. The settlement can expose the piling supporting the abutments. Abutment backwall rotation has also been noted.
3. Long term settlement resulting in problems with the approach slab.
4. Pavement settlement causing a rough ride onto the bridges.
5. Embankment settlement. The taller embankments experience non-uniform settlement. Drainage problems with the backfill causing the wingwalls to pushout at the interface with the abutment backwall.

6. Settlement of approach fill and approach slab.
7. Drainage issues and erosion of backfill material. Wingwall rotation due to the failing drainage.
8. Lateral movement of the embankment. Settlement of the embankment. When MSE retaining walls are present there is an issue with the migration of fines.
9. Long term creep settlement of the embankment.

3.3 Conventional Bridges with Expansion Joints

The third section of the survey focused on the amount and performance of conventional bridges. The survey specifically requested information about conventional bridges with expansion joints.

Based on the survey conventional bridge construction is still widespread. Many states have put an emphasis on constructing integral type bridges when feasible. However, that trend is not happening everywhere. Approximately 18% of respondents reported that 90 to 100% of bridges constructed within their state are conventional bridges with expansion joints. The distribution of conventional bridge construction is shown in Figure 18.

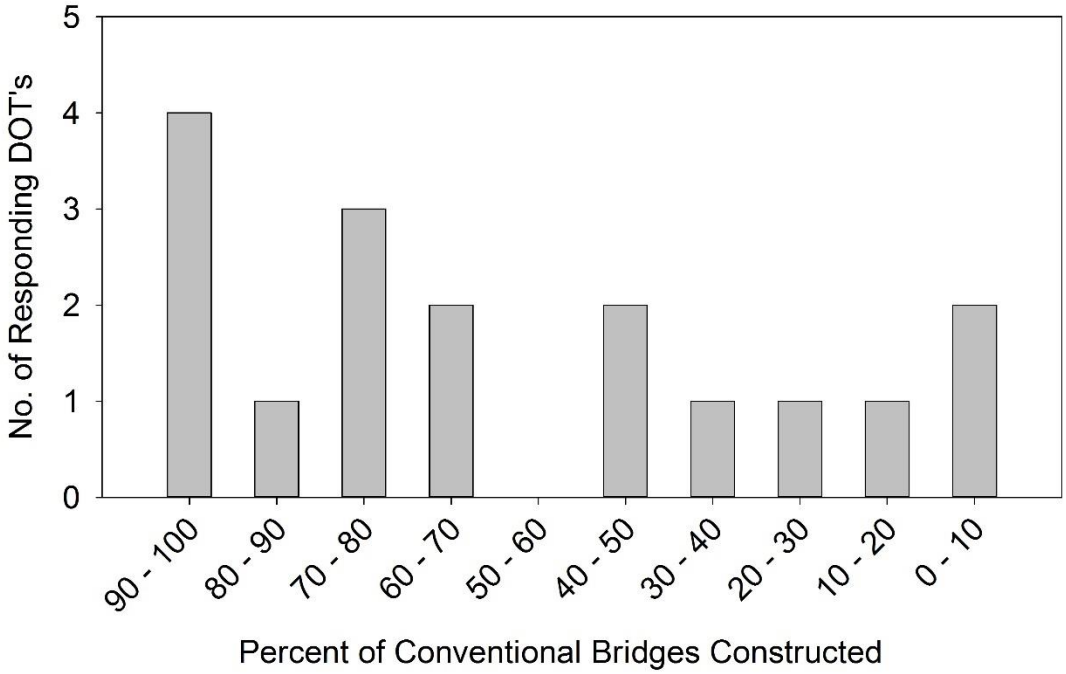

Figure 18. Prevalence of Conventional Bridges - New Construction

The respondents were also asked about the performance of conventional bridges within their state. Most of the bridge performance was categorized as good or fair. Poor and severe rated bridges only made up about 10% of the bridges on average. The distribution of the performance categories is shown in Figure 19. Figure 19 represents the average of the responses received for 15 state agencies. The remaining respondents skipped the questions pertaining to conventional bridges.

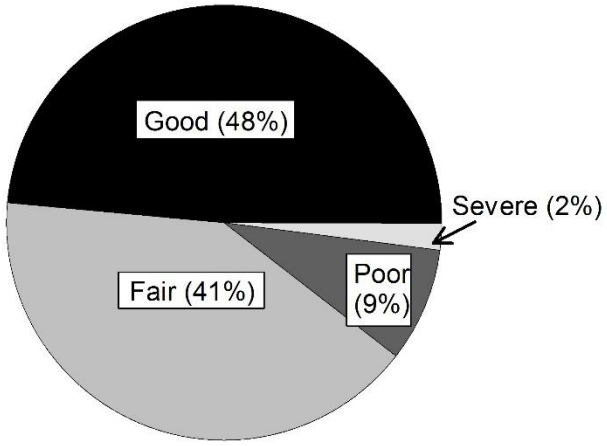

Figure 19. Performance of Conventional Bridges

The respondents were asked to list any common performance problems related to conventional bridges. The recorded responses are presented below. Some of the responses have been edited for clarity.

1. Bumps at the end of the bridge, embankment settlement, approach slab cracking, moisture leaking through backwall, sheared anchor bolts, closed expansion joints, severe cracks in wing resulting from lateral spreading, movement in the slope walls, misaligned parapet walls especially on skewed bridges, and expansion joint failures.
2. Corrosion of steel at bridge joint locations (due to water seepage and joint failure), premature cracking of concrete bridge decks, concrete spalling allowing reinforcing steel to be exposed to the elements.
3. Corrosion.
4. Issues with deteriorating deck joints.
5. Poorly performing deck joints.
6. Leaking deck joints and abutment backwalls rotating into girder ends.
7. Joint damage and deterioration. Joints closing up. Deterioration of bearing pads. Bearing pads “walking” over time.
8. Leaking and failed expansion joints. Leaking joints cause deterioration of the superstructure adjacent to the joints and the substructure under the joints.
9. Leaking joints, corrosion and spalling under the joints, and deteriorating decks.
10. Joints leaking and beam end deterioration.

11. Chloride induced corrosion, deck deterioration, steel coating failure, and leaking joints.
12. Beam end deterioration, bearing area deterioration, and box beams filling with water and rusting internally.

Several issues were reported with conventional bridges; however, the most prevalent issues appear to be the result of expansion joints failing.

3.4 Integral and Semi-Integral Bridges

The fourth section of the survey focused on Integral and semi-integral bridges. Questions related to the performance, design restrictions, and special design details pertaining to integral and semi-integral bridges were included in this section of the survey. Of the respondents, 17 states allow the construction of integral and/or semi-integral bridges.

The respondents were asked about the performance of integral and semi-integral bridges. The respondents were asked to enter the percentage of bridges which fall into the following categories: good, fair, poor, and severe. Most of the reported performance fell into the good category for integral and semi-integral bridges. The distribution of performance for integral bridges is shown in Figure 20 and the distribution for semi-integral bridges is shown in Figure 21. Both Figures represent the average performance from all the responses received.

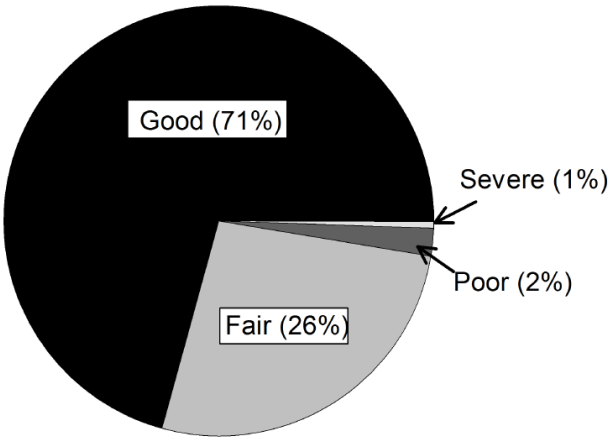

Figure 20. Performance of Integral Bridges

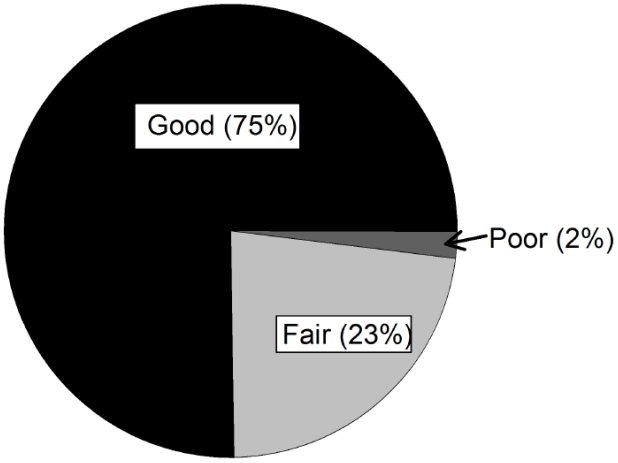

Figure 21. Performance of Semi-Integral Bridges

The respondents were asked to list any common performance problems related to integral bridges. The recorded responses are presented below. Some of the responses have been edited for clarity.

1. Distress such as cracking and spalling where beam meets abutment. Wing walls moving outward, this may be a result of excess water in the backfill.
2. Settlement of the approach asphalt pavement requiring additional asphalt later to smooth out bump.

3. Settlement of approach fill and pavement. Settlement of embankment causing the abutment piles to be exposed.
4. Cracking in the end diaphragms. Cracking of the bridge deck near the end of the deck.
5. Small thermal cracks in the abutment walls.

Several of the agencies reported no problems with integral bridges. A few of the agencies noted that their integral bridge program was still in the early or pilot phases and no common issues have been noted yet. The respondents were also asked about common performance problems with semi-integral bridges. Less responses were received, likely due to semi-integral bridges being less common. Of those that responded the common performance problems for semi-integral bridges were like those for integral bridges.

The respondents were asked about restrictions such as length, skew, and curvature for integral and semi-integral bridges. A summary of the responses is shown below. All non-applicable answers have been omitted from the summary.

Length Restriction – Integral Bridges

1. 400 feet
2. 250 feet
3. 300 feet for steel girder bridges with no skew, 150 feet for steel girder bridges with a 30 degree skew, 500 feet for concrete girder bridges with no skew, and 250 feet for concrete girder bridges with a 30 degree skew.
4. 500 feet for steel girder bridges and 600 feet for concrete girder bridges.
5. 350 feet for steel girder bridges and 700 feet for concrete girder bridges.
6. Based on anticipated thermal movement. Thermal movement limit is set at 2 inches.

7. 400 feet for steel girder bridges and 800 feet for concrete girder bridges.
8. 300 feet for bridges with a skew of 20 degrees and up to 100 feet for bridges with a skew of 45 degrees. The length is interpolated for skews between 20 and 45 degrees.
9. 400 feet for standard designed bridges. For bridges longer than 400 feet refined analysis is required.

Length Restriction – Semi-Integral Bridges

1. 600 feet
2. 250 feet
3. 450 feet for steel girder bridges with a skew up to 30 degrees and 750 feet for concrete girder bridges and a skew up to 30 degrees.
4. Based on anticipated thermal movement. Thermal movement limit is set at 2 inches.
5. 300 feet for bridges with a skew of 20 degrees and up to 100 feet for bridges with a skew of 30 degrees. The length is interpolated for skews between 20 and 30 degrees.
6. 230 feet.

Skew Restriction – Integral Bridges

1. Project specific not to exceed 10 degrees.
2. 25 degrees.
3. 30 degrees (3 respondents listed 30 degrees as the restriction)
4. 55 degrees.
5. 45 degrees

Skew Restriction – Semi-Integral Bridges

1. 30 degrees – limit in place due to seismic concerns

2. 45 degrees.
3. 25 degrees.
4. 30 degrees
5. 30 degrees max skew for bridges lengths up to 120 feet. 20 degrees max skew for bridges with a length greater than 120 feet.

Curvature Restriction – Integral Bridges

1. No standard restrictions listed

Curvature Restriction – Semi-Integral Bridges

1. 6 degrees.

The respondents were asked about the distribution of steel girder and concrete girder bridges within their state for integral and semi-integral bridges. The responses were averaged to gain a better representation. It was reported that 68% of integral bridges are constructed with concrete girders while 32% are constructed with steel girders. A similar trend was reported for semi-integral bridges; 53% are constructed with concrete girders and 47% are constructed with steel girders.

The respondents were asked about special substructure or superstructure details that are specific to integral or semi-integral bridges in their state. A summary of the responses is shown below. All non-applicable responses have been omitted. Duplicate responses are indicated using parenthesis.

Special Substructure Details – Integral Bridges

1. Abutment piles oriented in weak axis bending. (7)
2. Expanded Polystyrene (EPS) is required behind the backwall. Dowels are required between the backwall and pile cap. Abutment pile size is limited
3. Abutment piles oriented in weak axis bending for skews less than 45 degrees. Abutment piles oriented in strong axis bending for skews greater than 45

degrees. Wingwalls are integral up to 22 feet in length. Wingwalls are typically turned back parallel to the roadway.

4. Joint is placed at the end of the approach slab.
5. Abutment piles were placed in oversized augured holes. Rubber fenders were used near the tops of the piles adjacent to the web to slightly increase the stiffness in this region and move the point of fixity downward. The fenders helped reduce the maximum moment in the piles.
6. Geosynthetic backfill is used. U shaped wingwalls limited to a maximum length of 12 feet. Straight wingwalls limited to a maximum length of 6 feet unless isolated from the bridge and on a separate foundation. When anticipated thermal movement exceeds 0.5 inches a non-compacted select material is used for backfilling.
7. Joints between abutment and wingwalls.
8. Abutment piles oriented in strong axis bending. Abutment piles placed in single row without batter.
9. U shaped or straight wingwalls more than 13 feet in length must be isolated from the abutment and supported on a separate foundation. Stem deflection during construction is considered during design.

Special Substructure Details – Semi-Integral Bridges

1. Weak axis pile orientation.
2. For skewed semi-integral bridges stainless steel rub plates are placed at the acute corner and shear blocks are used to restrain rotations.
3. 1 inch joint filler is used between concrete end diaphragm and backwall.
4. Joint required between abutment end diaphragm and wingwalls. A seal is required between the abutment seat and cap to maintain backfill waterproofing.

Full length curb is added to the top of the semi-integral stem to help retain the backfill when bearing height exceeds 1.5 inches.

Special Superstructure Details – Integral Bridges

1. Closure pours over piers are done last. To prevent cracks over the piers a bond breaker (neoprene pads) is placed on top of the beams to limit rotation in the bridge deck such as to prevent cracking from negative deck moments.
2. Provide additional reinforcement over the abutment. Tie the approach slab to the bridge deck.
3. Pour the pile cap separately from the integral backwall. Backfill material for integral bridges shall be placed such that the differential in the height of fill at each abutment does not exceed 6 inches. Use special backfill material.
4. Prestressed Girders - Use Bent-up P/s strands for positive moment restraint. Concrete diaphragm is poured 30 minutes to 2 hours prior slab pouring. Coil Ties are used to anchor girder to diaphragms. Steel Girders - Web holes are used to thread concrete diaphragm reinforcing steel. Construction joints are used between the concrete diaphragm and slab at end bents. Structure is only integral at end bents.
5. Additional #5 reinforcement in the top of the deck at the bents. Pouring sequence: "A" segments are the spans. "B" segments are 12 feet wide section centered at each bent. "C" segments are the end blocks and 4 feet deck slab closures. The contractor is allowed to select from the following options. 1. Segments "A" may be poured first followed by "B". 2. Adjacent segments "A" and "B" may be poured together beginning and ending with an "A". Beginning with a "B" may be allowed only if a segment "A" was poured previously. 3. Segments "A" and "B" may be poured in one continuous pour. 4. Continuity diaphragms

must be poured at the same time as segments "B". Other diaphragms must be poured prior to the deck pour. 5. Segments "C" are poured a minimum of 7 days after the rest of the deck is poured. The 4 feet deck closure pours are made a minimum of 2 hours after pouring the respective end blocks.

6. Expansion joints provided for utilities, sidewalks, concrete barriers, guardrail, or other features that pass over integral abutments onto the approach roadway. Deck closure pour of 0.5 feet + effective slab length measured from front face of abutment required as final pour at each abutment. Additional reinforcing required in end zones.
7. Deck Pour Guidance is provided for concrete and steel beams. Continuity reinforcing is placed over the piers. Continuity diaphragms are used on concrete beams.
8. The ends of the superstructure slab shall be reinforced for negative flexure. This reinforcement shall extend for a distance of 20% of the span for single span bridges and 20% of the positive moment zone for multi-span bridges.

Special Superstructure Details – Semi-Integral Bridges

1. Provide additional reinforcement over the abutment. Tie the approach slab to the bridge deck.
2. Pour the integral backwall before deck. Backfill material for semi-integral bridges shall be placed such that the differential in the height of fill at each abutment does not exceed 6 inches. Use special backfill material.
3. Designer must account for uplift and buoyancy. Additional reinforcement is placed in the end zones.

4. The ends of the superstructure slab shall be reinforced for negative flexure. The reinforcement shall extend for a distance of 20% of the span for single span bridges and 20% of the positive moment zone for multi-span bridges.

The respondents were also asked about converting conventional bridges to integral or semi-integral bridges through elimination of the bridge expansion joints. Six responding agencies eliminate the expansion joints converting the bridges while eight agencies do not. The remaining respondents did not provide a response. Of the agencies that allow conversions, the performance was rated as good to excellent. The conversions do not appear to be very common based on the comments received. However, it was noted that the conversions are a cost-effective solution to extend the life of a bridge.

3.5 Abutment Backfill Material

The final section of the survey focused on abutment backfill material. Additional questions were asked about low-density cellular concrete (LDCC) as backfill material. Based on the responses received granular backfill is what is primarily used for all bridge types followed by controlled low strength material (CLSM) and then LDCC. The distribution of backfill material for each bridge type is shown in Figure 22.

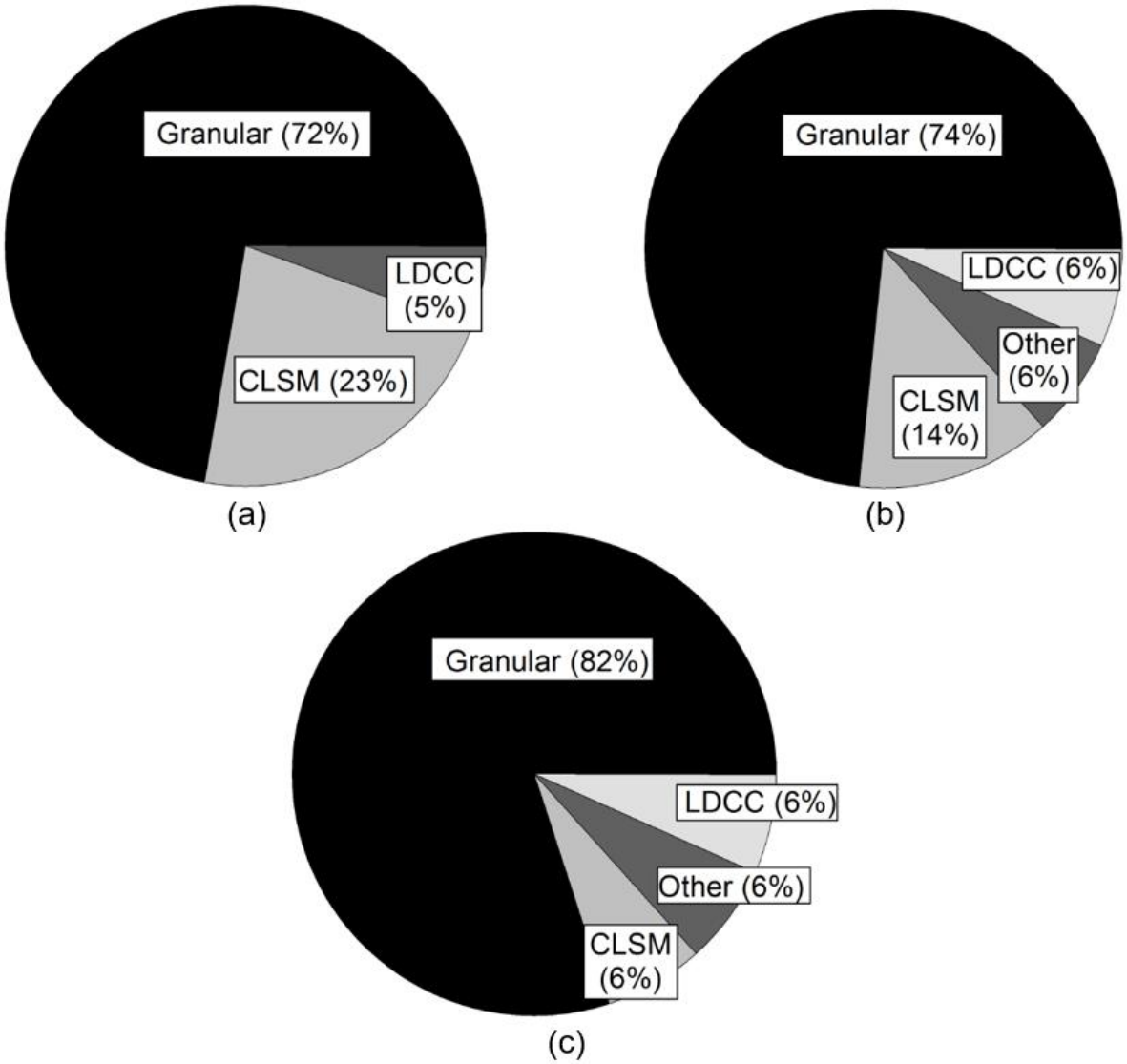

Figure 22. Backfill Distribution: (a) Conventional Bridges, (b) Integral Bridges, and (c) Semi-Integral Bridges

LDCC was rated as having average to good performance as a backfill material. However, it should be noted that only five of the responding agencies use LDCC as backfill material. The main comments received regarding LDCC emphasized that it is very expensive when compared to other backfill materials. One respondent reported that LDCC was pulverized due to rigid pavement flexure at the joints for one of their

early projects utilizing LDCC. The respondent attributed the behavior to the subbase thickness being inadequate.

4.0 Implementation, Monitoring, and Modeling

Three bridges were monitored during a portion or throughout this project. The bridges were monitored to evaluate the effectiveness of various repairs. The bridges monitored were:

1. Shields Boulevard over I-40 in Oklahoma City
2. I-40 over SH- 81 in El Reno
3. 19th Street over I-35 in Moore

Monitoring results for two bridges, SH-3E over the North Canadian River and U.S. 183/412 over Wolf Creek, that used ultra-high performance concrete (UHPC) during the bridge rehabilitation are also presented. These two bridges were part of two other ODOT funded projects. The geotechnical aspects of the SH-3 bridge over Burlington Northern Santa Fe (BNSF) railroad in Ada were also numerically modeled. The numerical modeling provided insight into the behavior of tall embankments on soft soils. Finally, observations from abutment backfill drainage systems are presented. These observations were part of another ODOT funded project.

A brief history of each bridge, rehabilitation steps taken, monitoring protocol, monitoring results, and discussion of results are presented in the following sections.

4.1 Pressure Relief Joint Retrofit - Asphalt

The Shields Boulevard over I-40 bridge is a ten-span bridge oriented north-south. The span lengths starting from the south side of the bridge are 43 ft – 100 ft – 128 ft – 128 ft – 53 ft – 72 ft – 67 ft – 147 ft* - 90 ft* - 90 ft*. The asterisk indicates that the span length is approximate. Originally the bridge only contained six spans and crossed the Union Pacific railroad and Southwest 7th Street. During the relocation of I-40 a portion of the bridge was demolished while the northernmost three spans were left in place. Seven

additional spans were added to cross the new alignment of I-40. An aerial view of the bridge is shown in Figure 23. The new spans were less than 15 years old at the time of this report. The age of the original spans is not known.

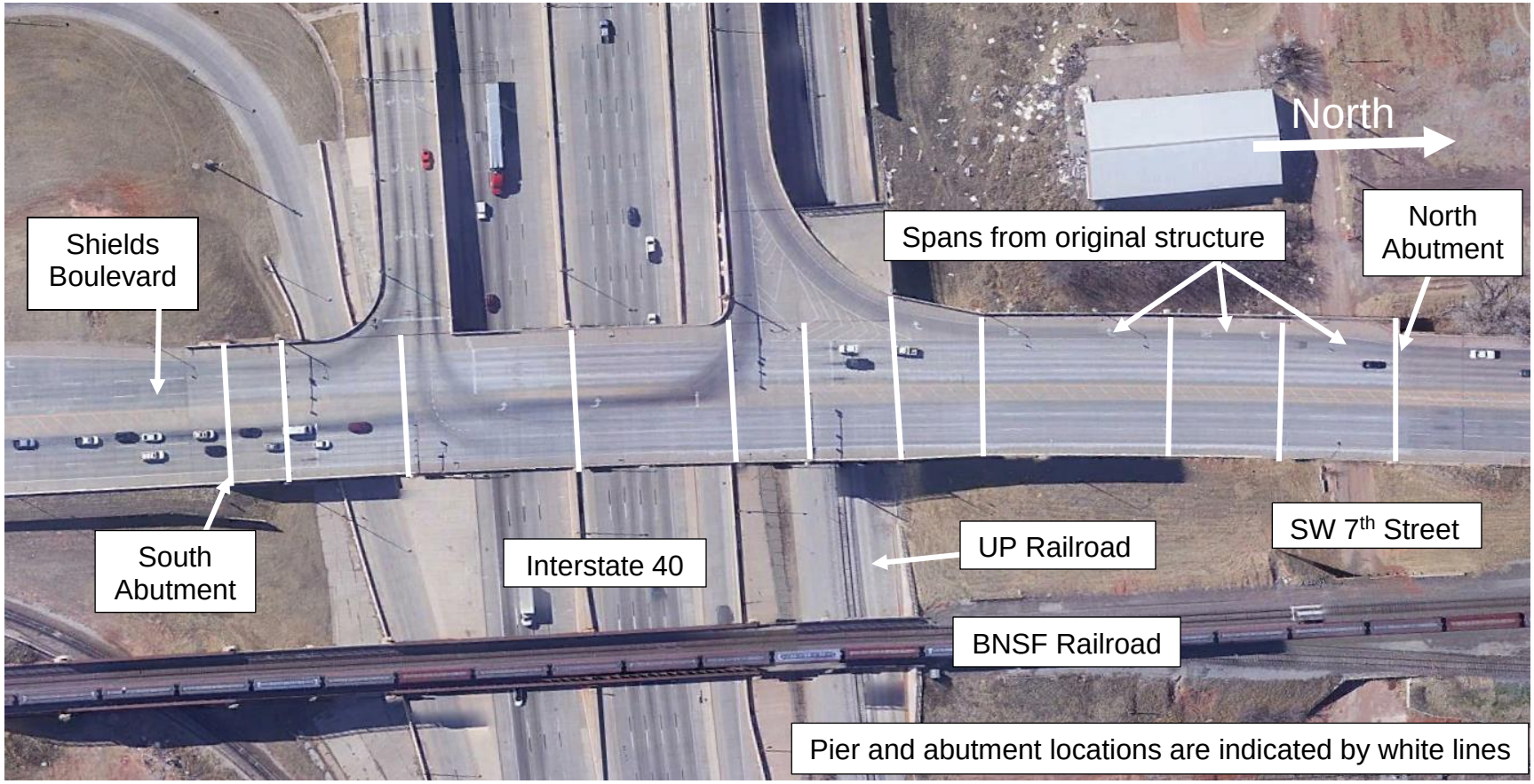

Figure 23. Shields Boulevard over I-40, Oklahoma City

Sometime prior to 2019 it was discovered that the southernmost bridge span had moved north by approximately 3 inches. Interestingly the pressure relief joint located at the end of the south approach slab had not compressed. In addition, the span had lifted approximately 1 inch at the abutment. It appears the span was being compressed by the pavement south of the bridge. Photographs provided by ODOT showing the deck movement at the abutment, the uncompressed pressure relief joint, and the rotated bearings are shown in Figure 24.

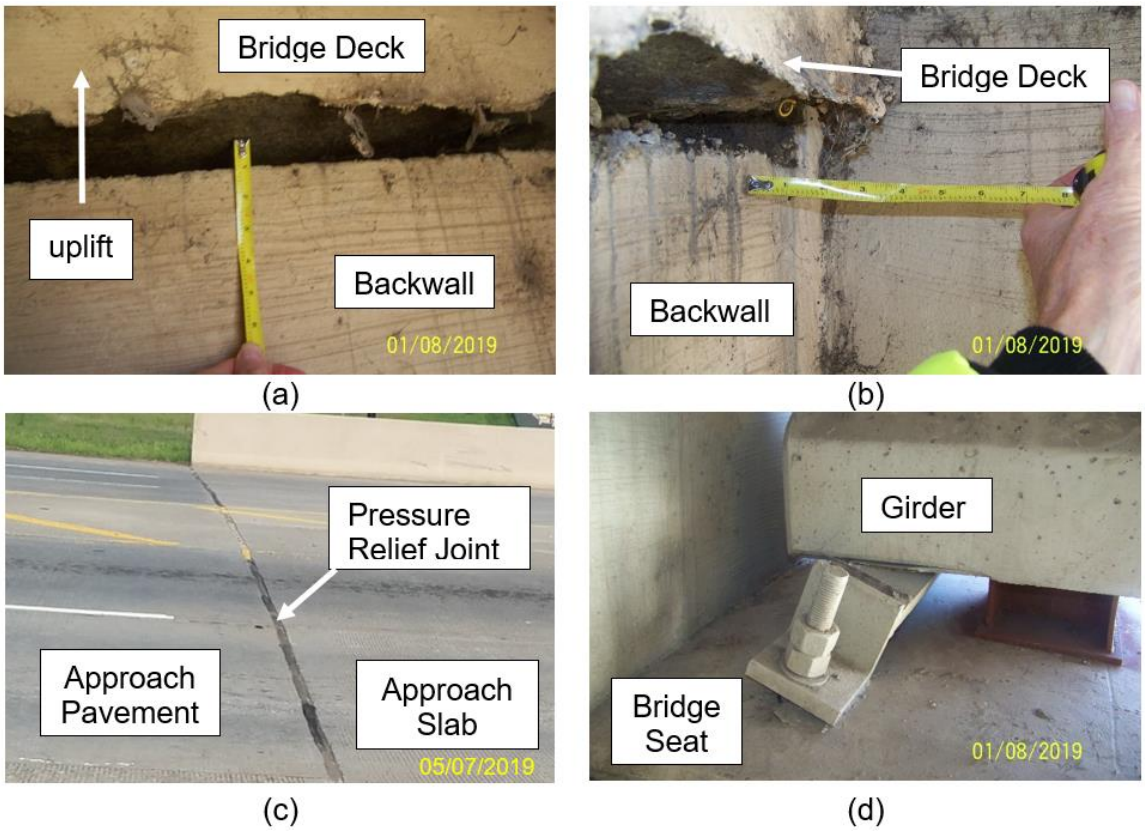

Figure 24. Shields Boulevard over I-40: (a) deck uplift, (b) deck movement, (c) uncompressed relief joint, (d) rotated bearings

There is approximately 2,000 feet of rigid pavement located south of the Shields Boulevard bridge. Beyond that is another bridge that crosses the Oklahoma River. The Oklahoma River bridge is owned and maintained by the City of Oklahoma City. The Oklahoma River bridge was visited to see if similar problems were also occurring at that

bridge. Due to the full height abutments the bridge abutment was not able to be inspected up close. However, from the roadway elevation it was observed that the Oklahoma River bridge is experiencing similar types of distress. A photograph taken in September of 2019 is shown in Figure 25. The image shows that the anchor bolts are angled away from the abutment backwall indicating that the pavement was pushing on the bridge deck.

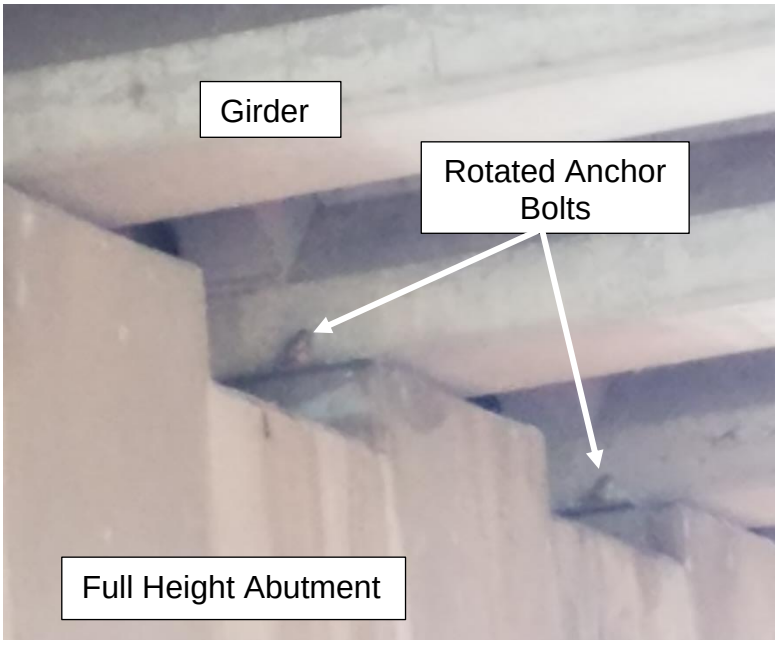

Figure 25. Shields Boulevard over the Oklahoma River: North Abutment

There are two additional expansion joints in the 2,000 feet of rigid pavement between the bridges not including the pressure relief joint at the I-40 bridge. The first joint is located approximately 770 feet south of the I-40 approach slab. The second joint is located at the Oklahoma River bridge approach slab. The two additional expansion joints appeared to be closed. These expansion joints are maintained by the City of Oklahoma City. It is not known what the width of the joints were when constructed.

4.1.1 Site Investigation

A site investigation was performed by the geotechnical branch of ODOT. Initially a pavement core was taken along the I-40 bridge pressure relief joint. The joint was expected to contract under the observed conditions at the bridge. A photograph of the pavement core through the pressure relief joint is shown in Figure 26.

Figure 26. Shields Boulevard over I-40: Expansion joint pavement core

The expansion joint shown in the pavement core is not compressed. This indicated that the pavement pressure was being transferred to the bridge despite the pressure relief joint. It is suspected that the pavement pressure is being transferred across the joint through the asphalt base layer. The design anticipated that the rigid pavement would expand and contract independent of the asphalt pavement. However, it appears that the asphalt pavement is moving along with the rigid pavement.

Four soil borings were also drilled at the bridge site. The purpose of the borings was to determine if any soft or unstable areas are present in the embankment. The pavement was cored and then the soil borings were advanced 15 feet below the pavement. Testing in the borings was competed using the Standard Penetration Test

(SPT) (ASTM-D1586 2011). Originally Cone Penetration Testing (CPT) (ASTM-D3441 2016) was planned as part of the site investigation. However, CPT was abandoned due to the stiffness of the embankment soils encountered. The SPT N values ranged from 30 to 70 in the borings. The embankment was visually classified as sand based on samples collected using a split spoon sampler. Weak layers or spots in the embankment were ruled out based on the high SPT N values from the site investigation.

4.1.2 Remediation

Since excessive pavement pressure was determined to be the cause of the approach slab shoving into the bridge, a full depth joint was placed adjacent to the approach slab. A single 12-inch full depth asphalt joint was placed at the end of the approach slab. The joint was installed in April 2020 by ODOT. A photograph of the completed joint is shown in Figure 27. The photograph was taken in December 2020.

Figure 27. Shields Boulevard over I-40: Full depth asphalt pressure relief joint

4.1.3 Monitoring

The bridge was monitored monthly beginning in December 2020. During the monitoring visits the movement of the bridge deck relative to the wingwall was

measured. The temperature of the pavement near the asphalt pressure relief joint was also measured and recorded. The pressure relief joint was not measured due to the varying width of the asphalt sides as seen in Figure 27. Photographs showing the locations where the bridge movement was measured are shown in Figure 28. The photographs were taken from above the wingwall. The reference lines used for the measurement are also shown in the photographs. The north edge of the wingwall was used as one reference point and was assumed to be stationary. Between the wingwall and parapet there is a section of concrete that is attached to the approach slab and deck. Beyond the wingwall the “filler” section of concrete is terminated. The north edge of this section of concrete was used as the reference point for the bridge. For clarity a photograph showing the side of the west reference area is shown in Figure 29.

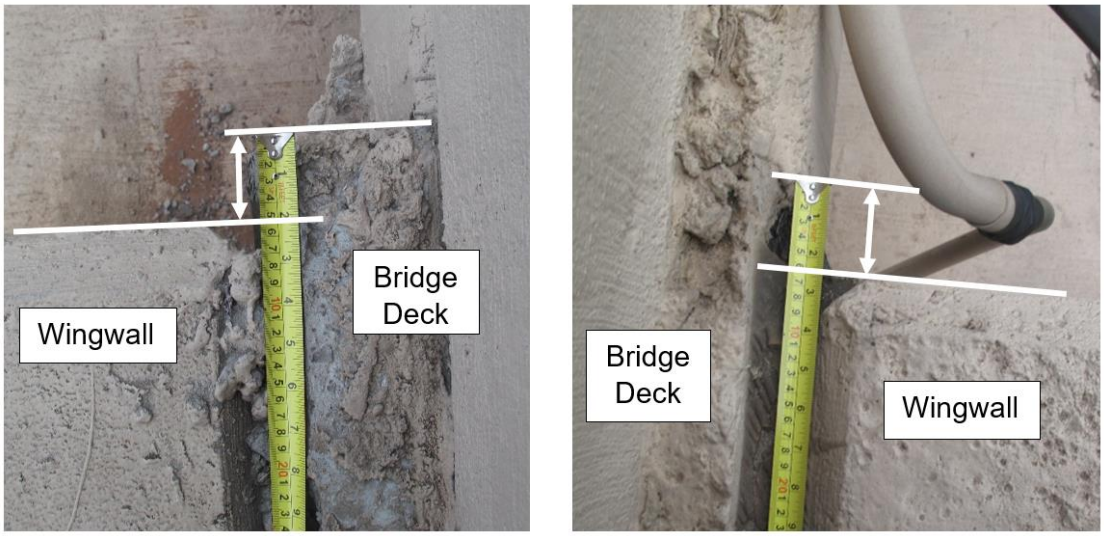

Figure 28. Shields Boulevard over I-40: Measurement reference points (a) west (b) east

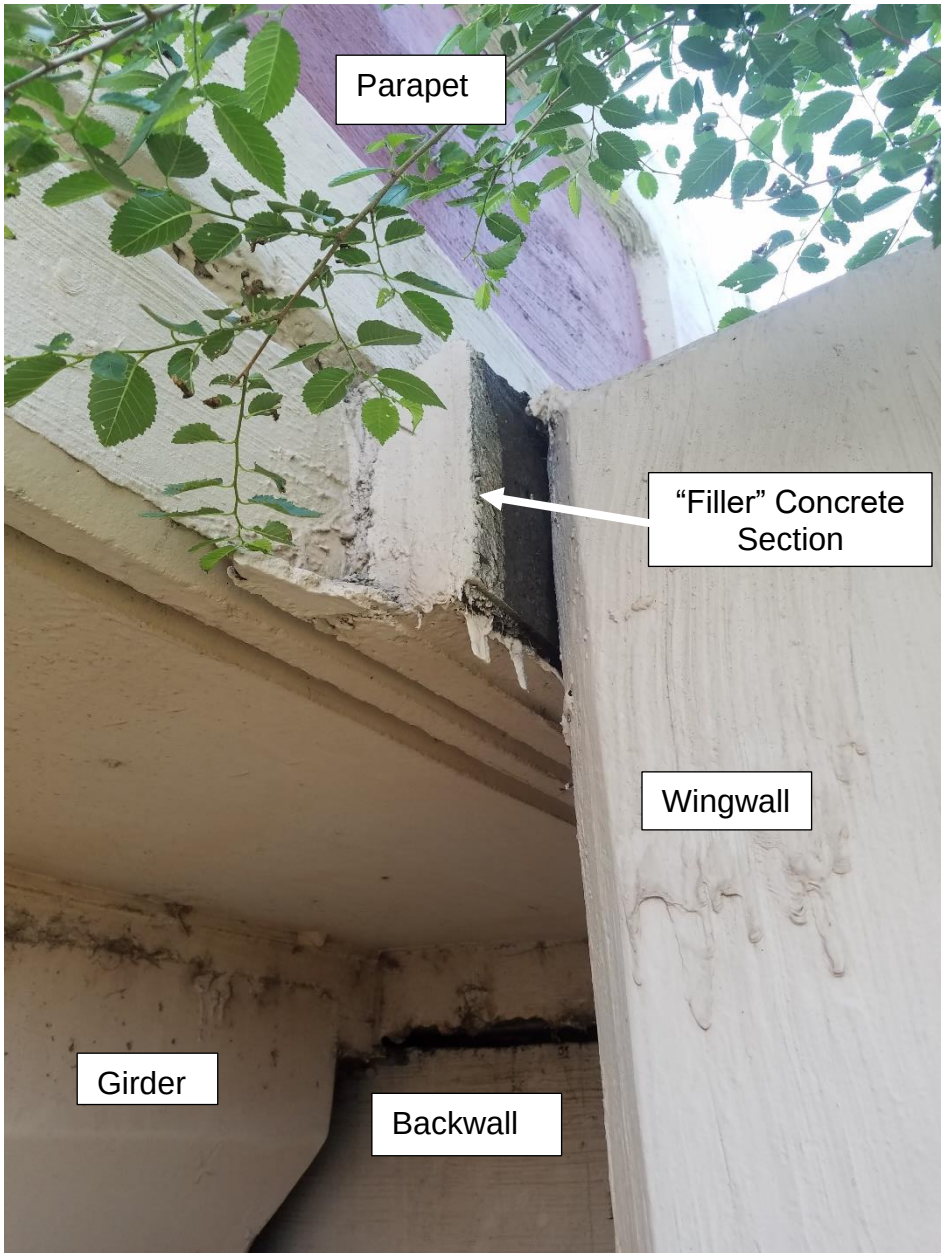

Figure 29. Shields Boulevard over I-40: West measurement reference point

The displacement as measured at the wingwall and the temperature are shown in Figure 30 and Figure 31 for the east and west sides of the abutment, respectively. The measured movement is relative to the initial measurement which was set to zero.

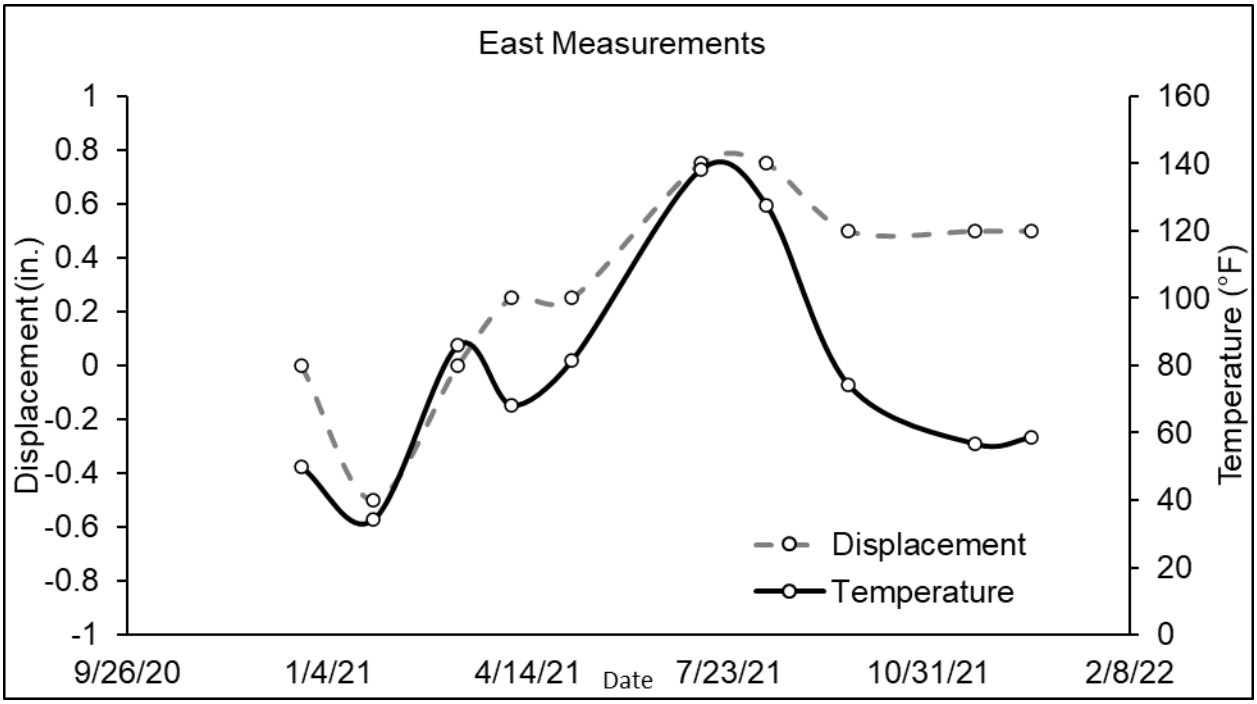

Figure 30. Shields Boulevard over I-40: Monitoring results - east side

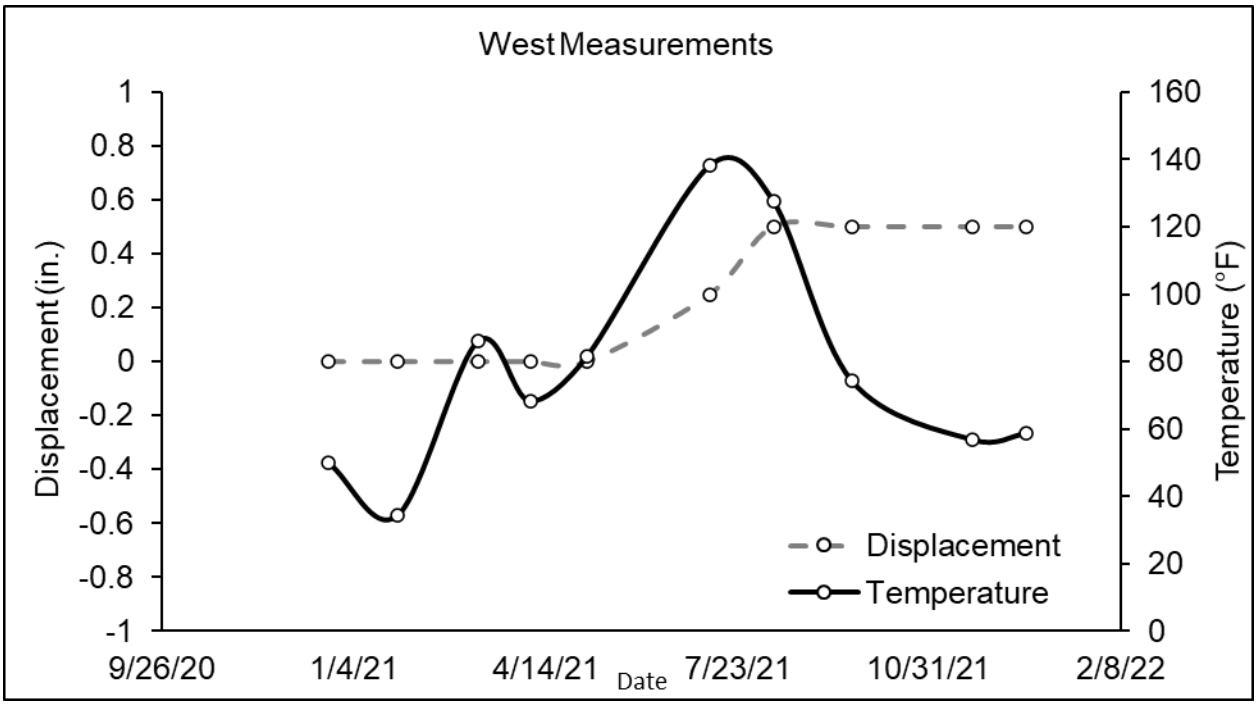

Figure 31. Shields Boulevard over I-40: Monitoring results - West side

Throughout the monitoring period the recorded temperature of the pavement ranged from 34.4 °F to 138.2°F. The maximum movement in the direction of the south bridge pier throughout the monitoring period was 0.75 inch for the east side and 0.5 inch

for the west side. The east side appears to relax a little as the temperature drops whereas a decrease in the displacement was not measured on the west side. The east side also responds more to variations in temperature than the west side does. Based on the results of the monitoring it appears that the pavement is still shoving the bridge deck. It is not known how the amount of shoving compares before and after the installation of the asphalt pressure relief joint. Continued monitoring and remedial measures may be required if the movement becomes unacceptable.

4.2 Pressure Relief Joint Retrofit – 4-inch BEJS Joint

I-40 is carried by twin four span bridges over SH-81 in El Reno. The span lengths are approximately 30 ft – 65 ft – 65 ft – 30 ft. An aerial view of the bridges is shown in Figure 32.

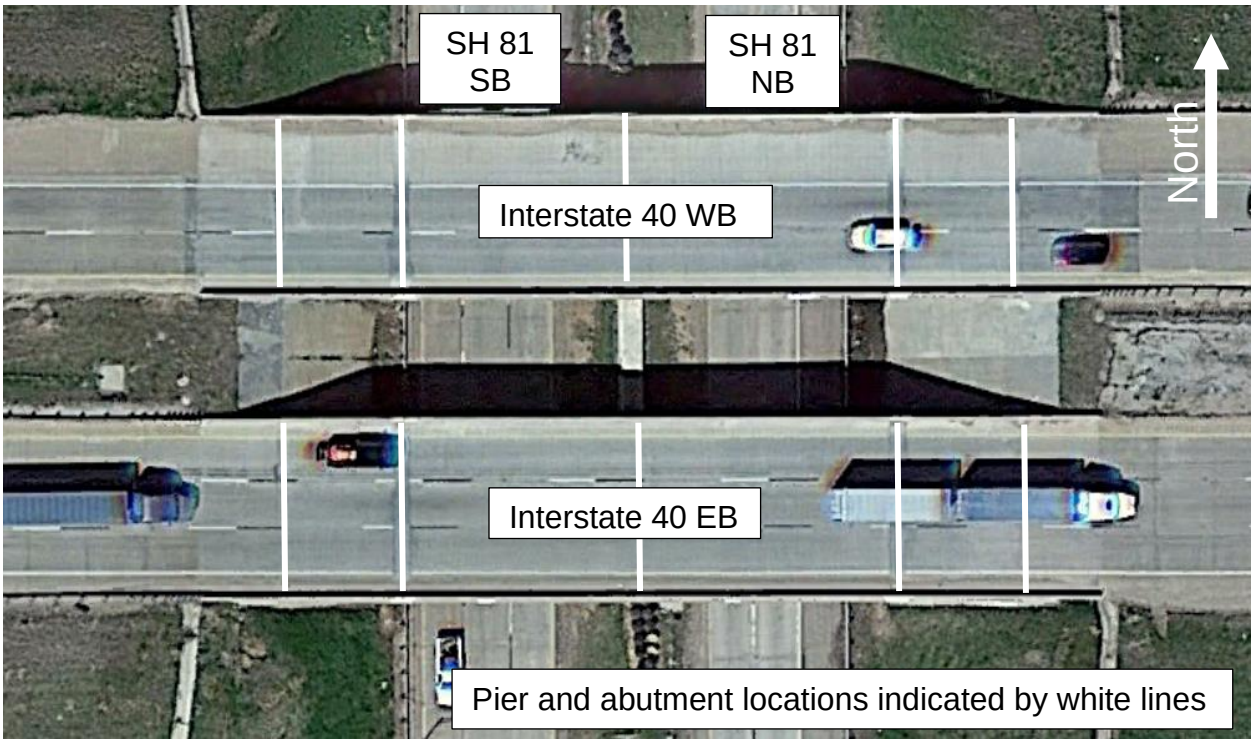

Figure 32. I-40 over SH-81, El Reno

The rigid concrete approach pavement was pushing on the approach slab and bridge deck. The pressure was enough to cause the steel girder ends to touch under

the bridge expansion joints. The beam ends were shortened to allow the bridge room for thermal movement. Following the shortening of the beam ends the bridge relaxed into the bridge expansion joints. When this happened the roller bearings supporting the shortened beams rotated. Photographs of the observed bridge distress are shown in Figure 33. The photographs were taken in May 2019.

Figure 33. I-40 over SH-81: (a) closed expansion joint, (b) deck shoving, (c) rotated bearing, (d) pedestal damage

4.2.1 Remediation

To prevent further damage to the bridge from excessive pavement pressure, four pressure relief joints were installed. One pressure relief joint was installed adjacent to each abutment. The joint was approximately 4 inches wide at the time of installation. The Bridge Expansion Joint System (BEJS) from EMSEAL® was used as the pressure relief joint. The BEJS joint is a compression joint made from foam that is covered in a layer of silicone for the surface exposed to the elements (EMSEAL 2021). The joint is attached to the concrete bridge deck ends using epoxy. A bead of silicone is then used to seal the top edge of the joint to the bridge deck. The BEJS joints used for this project was in 5 feet sticks. Silicone was used to seal the top of the joint at the stick connections. A photograph of the joint used for this project from the EMSEAL product sheet is included in Figure 34.

Figure 34. EMSEAL® BEJS, courtesy of EMSEAL®

The pressure relief joints were installed on June 6, 2019. Photographs of the joints during and immediately after the installations are shown in Figure 35. The photographs were provided by ODOT.

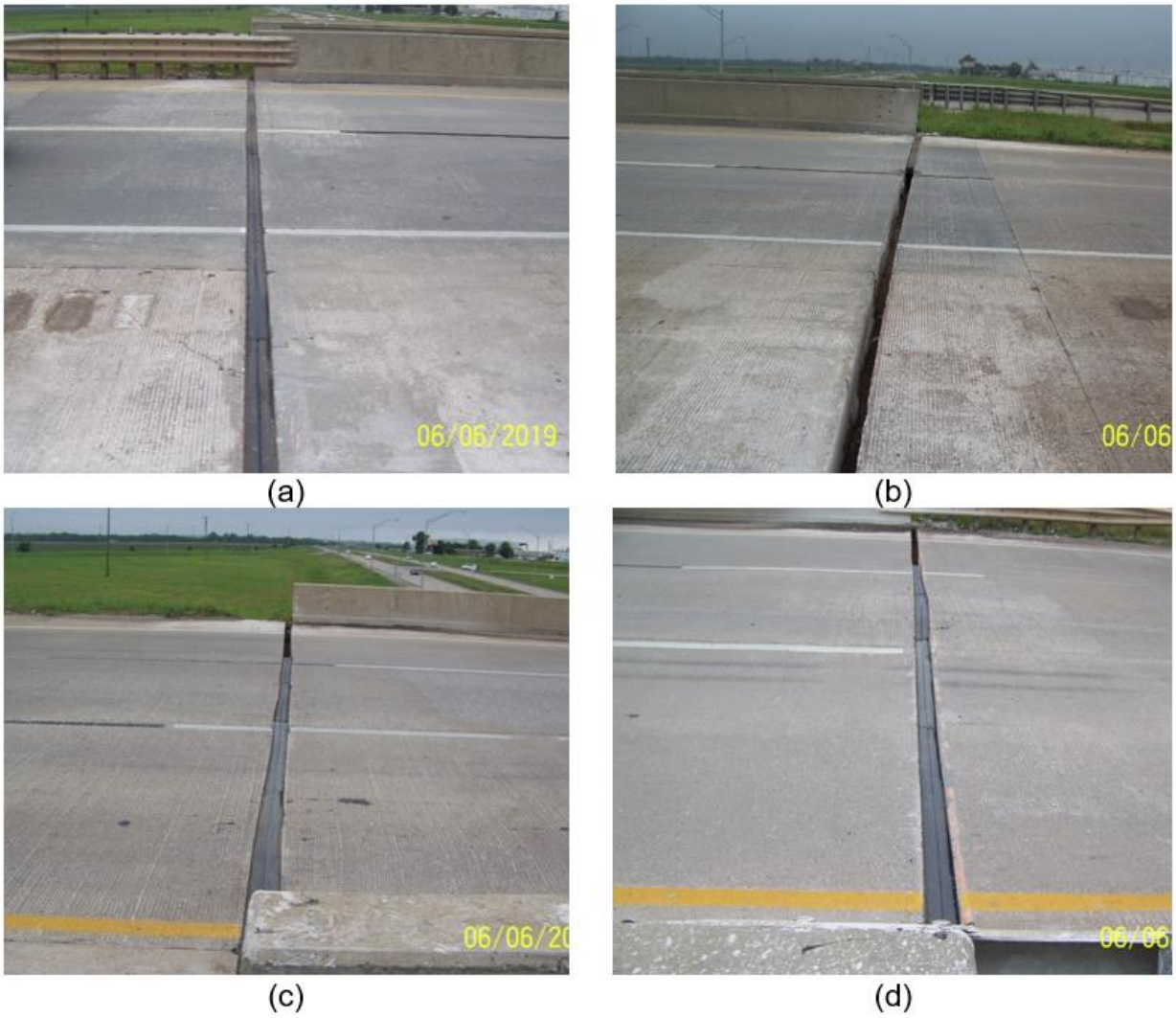

Figure 35. I-40 over SH-81 Joint Installation: (a) Westbound bridge – east approach, (b) Westbound bridge – west approach, (c) Eastbound bridge – east approach, (d) Eastbound bridge – west approach

4.2.2 Monitoring

The bridge was monitored monthly beginning in December 2020. The width of each pavement pressure relief joint was measured during the monitoring visits. The width was measured in the outside shoulders of I-40. The pavement temperature was also measured during the visits. The joint width and the pavement temperature are shown in Figure 36 through Figure 39. The initial joint widths shown in the figures are approximate.

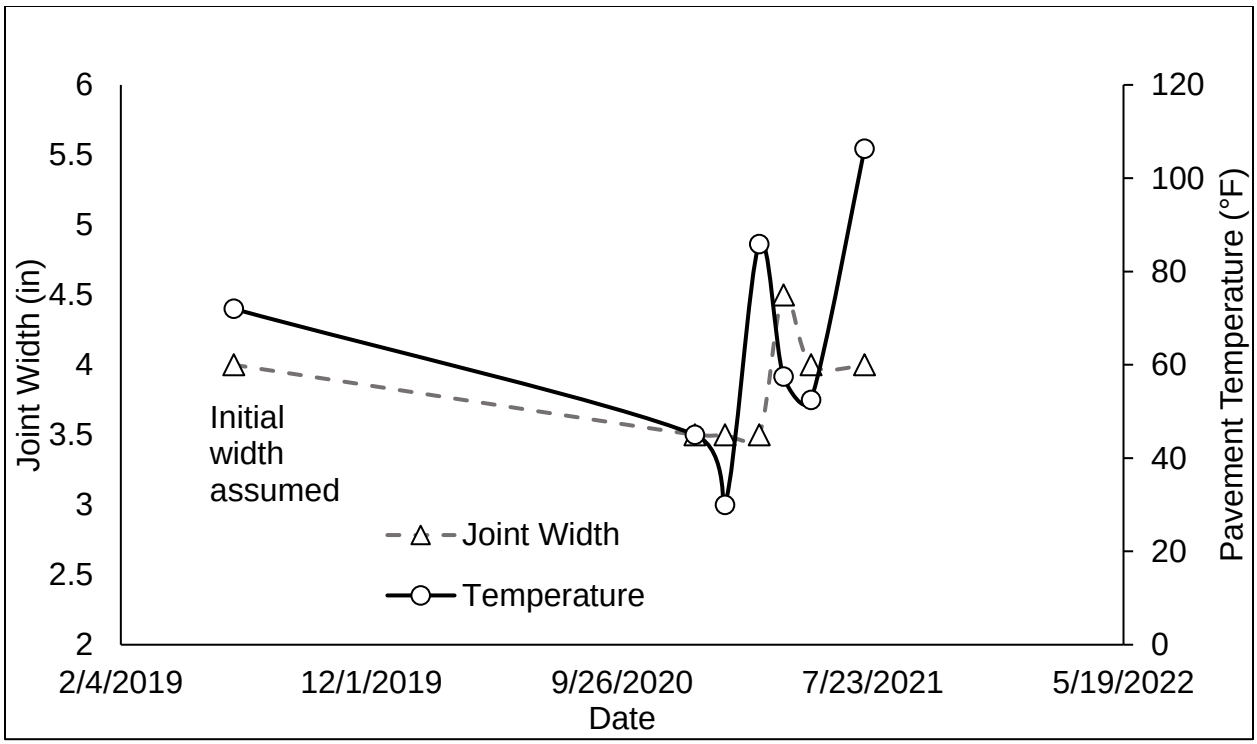

Figure 36. I-40 over SH-81: Joint width WB-east approach

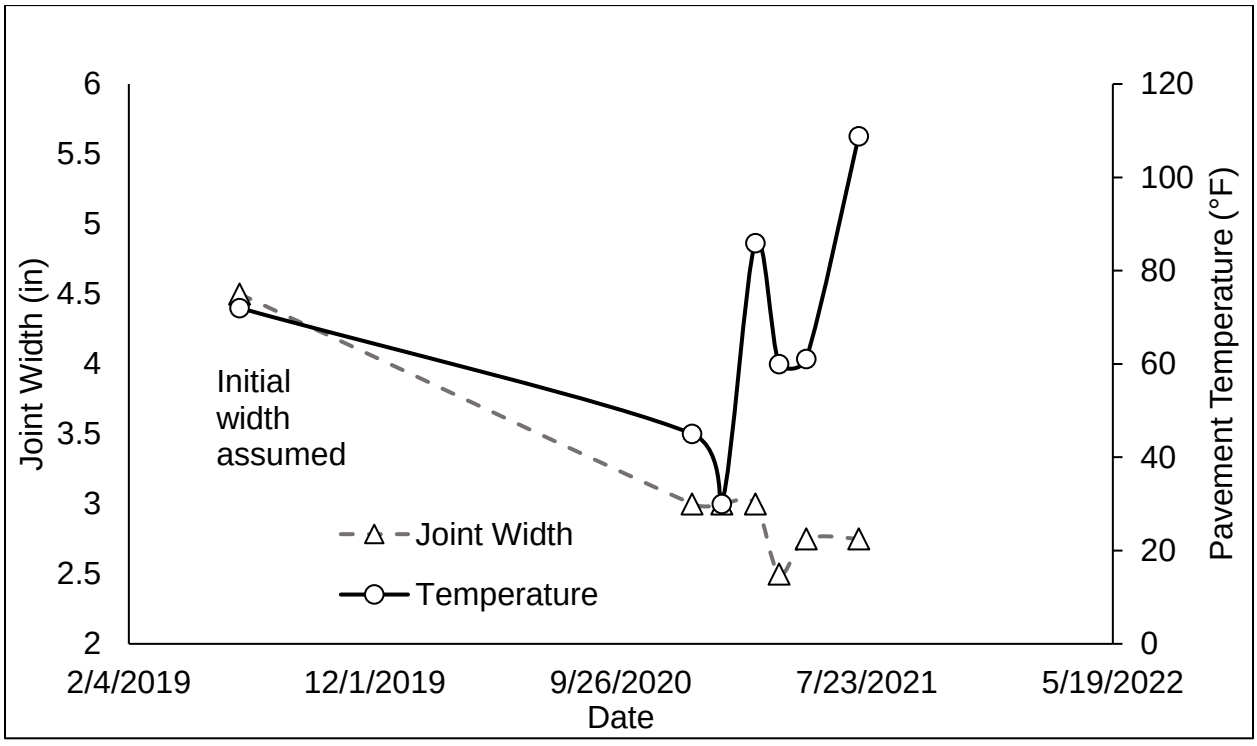

Figure 37 I-40 over SH-81: Joint width WB-west approach

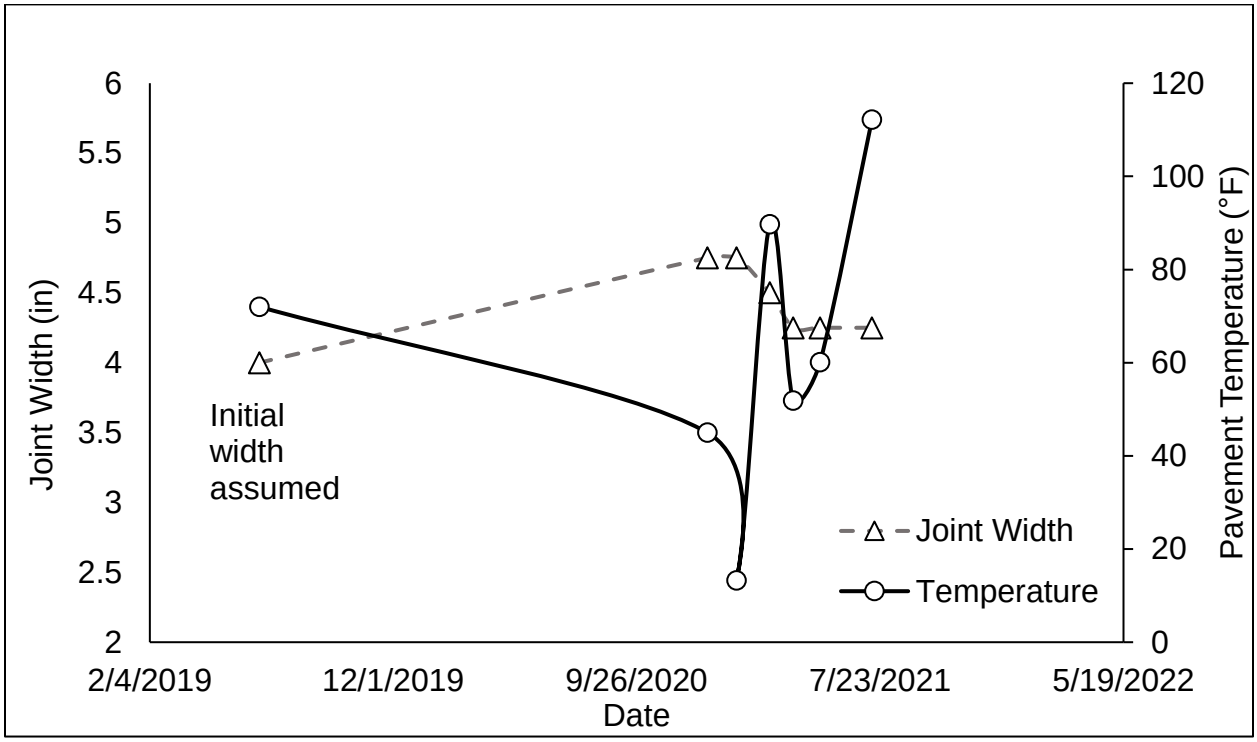

Figure 38 I-40 over SH-81: Joint width EB-east approach

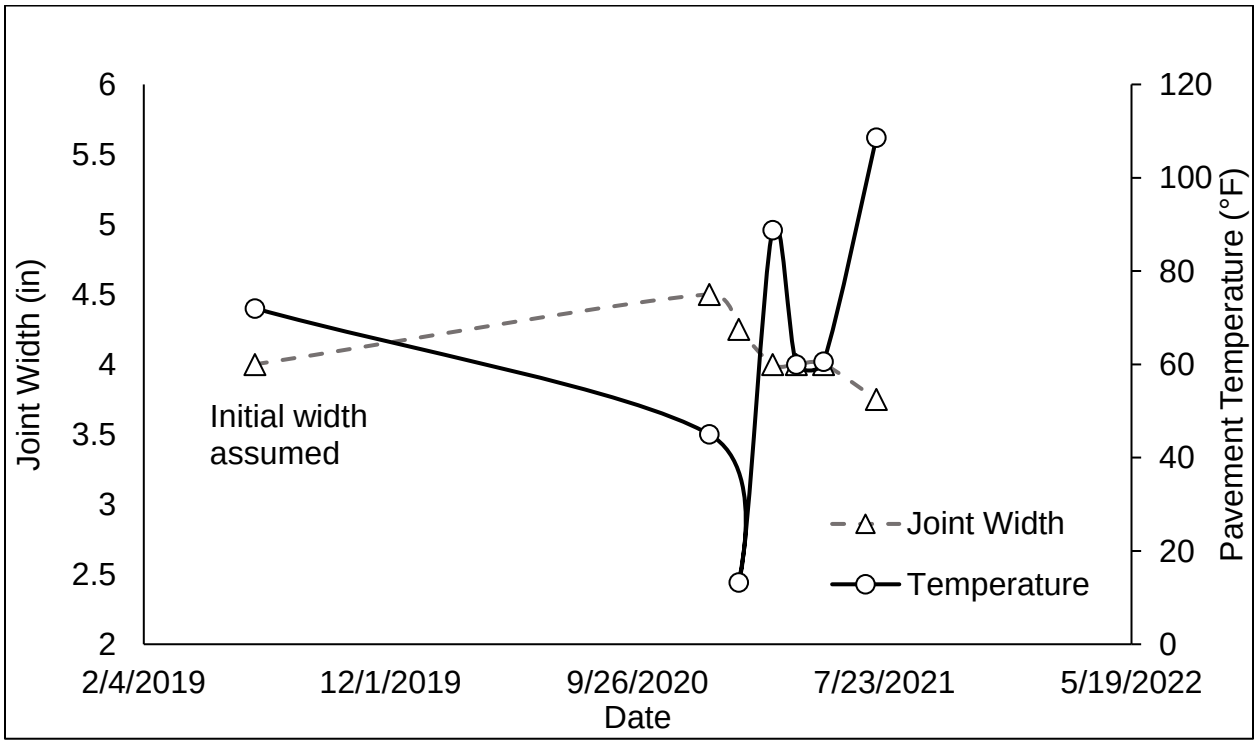

Figure 39 I-40 over SH-81: Joint width EB-west approach

The pavement pressure relief joints appear to be functioning correctly. However, the west approach joint on the westbound bridge is currently closing (Figure 37). The joint is currently about half the original width. The expansion joint does not appear to be rebounding for the 2021-2022 cooling season. The temperatures thus far have been mild, the joint may still relax as the temperature decreases for longer periods of time. It is not known why the west approach joint on the westbound bridge closed more than the other joints. There is approximately 3,600 feet of straight rigid pavement west of the bridge before another structure is encountered. In the east direction there is a mile or more of straight rigid pavement before the roadway begins to curve. The presence or absence of joints in the adjacent pavement is not known.

Maintenance of the joint is crucial to ensure continued performance of the joint. The joints should also be monitored routinely. Based on the nominal size of the joint (4 inches) the minimum width for the joints is 1.625 inches according to the joint manufacturer. The west approach joint on the westbound bridge can handle approximately one additional inch of compression before the pavement joint should be widened and a new joint installed.

4.3 Pressure Relief Joint Retrofit – Series of 2-inch BEJS Joints

19th Street crosses I-35 in Moore on a two-span bridge. Each span is approximately 82 feet long. Originally the east and westbound lanes were carried by separate bridges. However, in 2009 a center turn lane was added and the bridges were joined. The bridge has experienced problems with excessive pavement pressure as early as 2003 when the bridges were still separated. After 2005 but before 2009 a 4-inch pressure relief joint was placed on both sides of the bridges. The pressure relief joint was an asphalt filled joint. The pressure relief joints are located approximately 150

feet away from the end of the approach slab. When the bridges were joined in 2009 the bridge expansion joint above the center pier was eliminated.

Due to the noted pavement pressure problems, the University of Oklahoma (OU) has been monitoring the bridge since 2012. The bridge monitoring was funded through ODOT under the project number SP&R 2228. During the initial monitoring period (2012-2017) a BEJS pressure relief joint was installed on the east side of the bridge. The pressure relief joint was installed by the City of Moore and ODOT on May 12, 2016. In addition, 7.5 feet of approach pavement directly adjacent to the east approach slab was replaced. The BEJS pressure relief joint was placed in the middle of this new pavement section. A photograph of the pressure relief joint as installed in 2016 is shown in Figure 40.

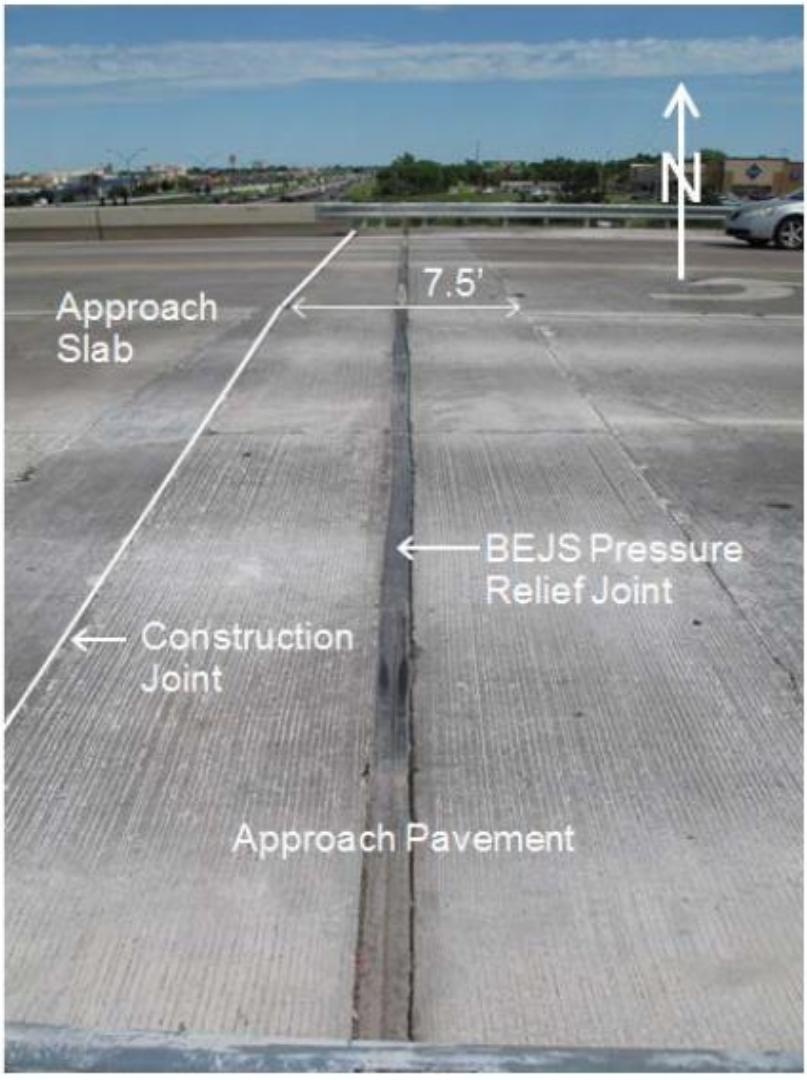

Figure 40. 19th Street over I-35: Pressure relief joint installed in 2016

The bridge and pavement expanded into the pressure relief joint during the hotter seasons. Unfortunately, the new pavement section separated from the approach slab during the cooler seasons. As a result, the pressure relief joint stayed compressed while it was cold and a gap was left between the new pavement section and the approach slab. The gap opened up as early as 2018. Later in 2019 the new pavement section began to crack and suffer from subgrade failure in the south lane. A photograph showing the new pavement section in 2019 is shown in Figure 41. Since there was not any load transfer mechanism for the pressure relief joint the new pavement section also

tilted into the area where the subgrade failed. As a result, the approach pavement was left with a large bump.

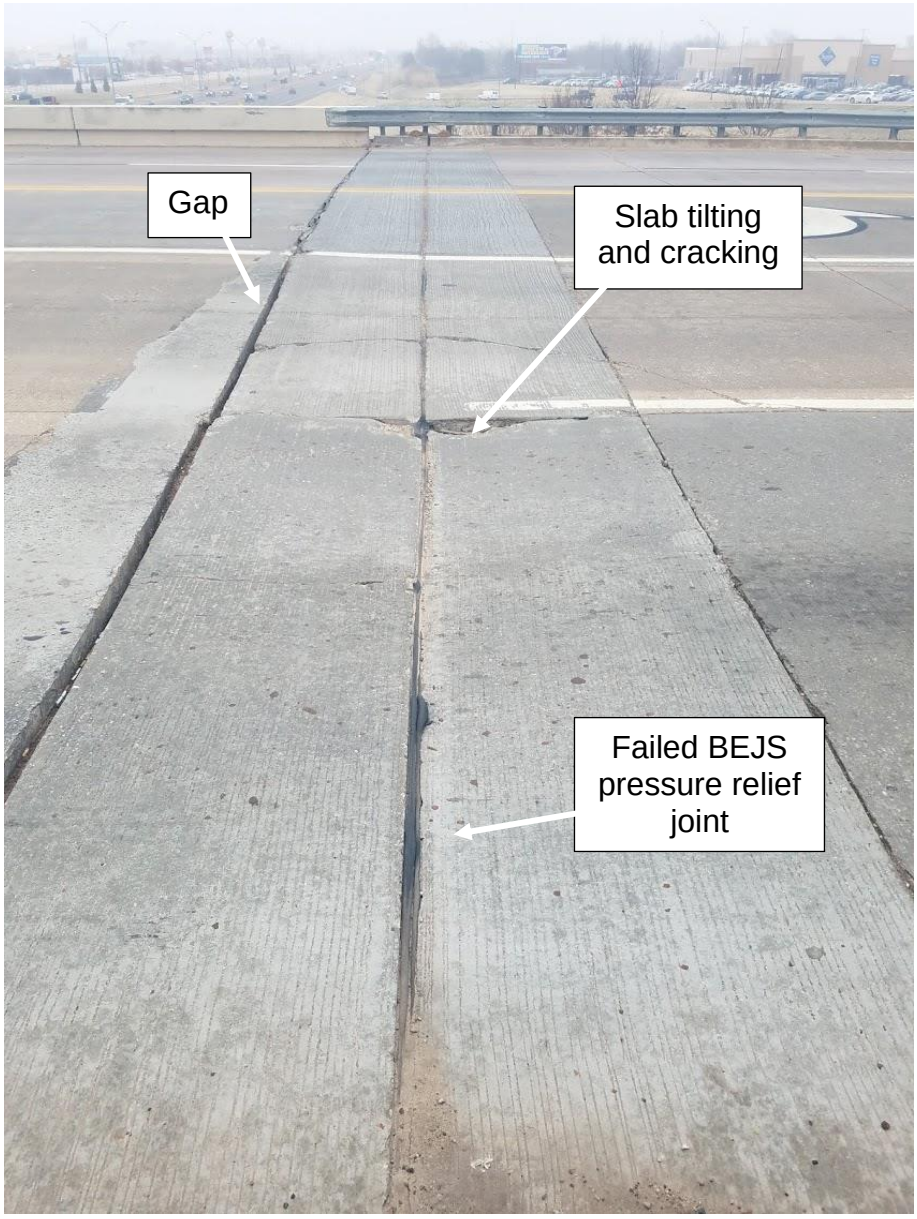

Figure 41. 19th Street over I-35: Pressure relief joint in 2019

During the planning phase of the BEJS pressure relief joint it was not realized that a sleeper slab was present at the end of the approach slab. Otherwise, the pressure relief joint would have been placed adjacent to the approach slab and the sleeper slab. Water may have entered through the gap at the end of the approach slab and softened the roadway subgrade causing the subgrade failure that was observed.

The west side of the bridge was not fixed during this remediation. Sensors were used to gather hourly measurements of temperature, joint width, abutment backwall tilt, pavement strain at various locations on both sides of the bridge as a part of SP&R 2228.

4.3.1 Site Investigation

A site investigation was conducted as a part of the current project to determine whether the embankment contained any soft spots prior to remediation of the pavement and pressure relief joint. Two CPTs (ASTM-D3441 2016) were completed at the site by the ODOT Geotechnical Branch. The investigation occurred on September 9, 2019. The CPTs were both located in the south driving lane near the pressure relief joint. CPT-1 was located approximately 2 feet east of the pressure relief joint. CPT-2 was located approximately 15 feet east of the pressure relief joint. The CPTs were advanced to 25 and 28 feet before refusal was achieved in CPT-1 and CPT-2, respectively. The CPT results including tip resistance, sleeve friction, porewater pressure, and friction ratio are shown in Figure 42 and Figure 43.

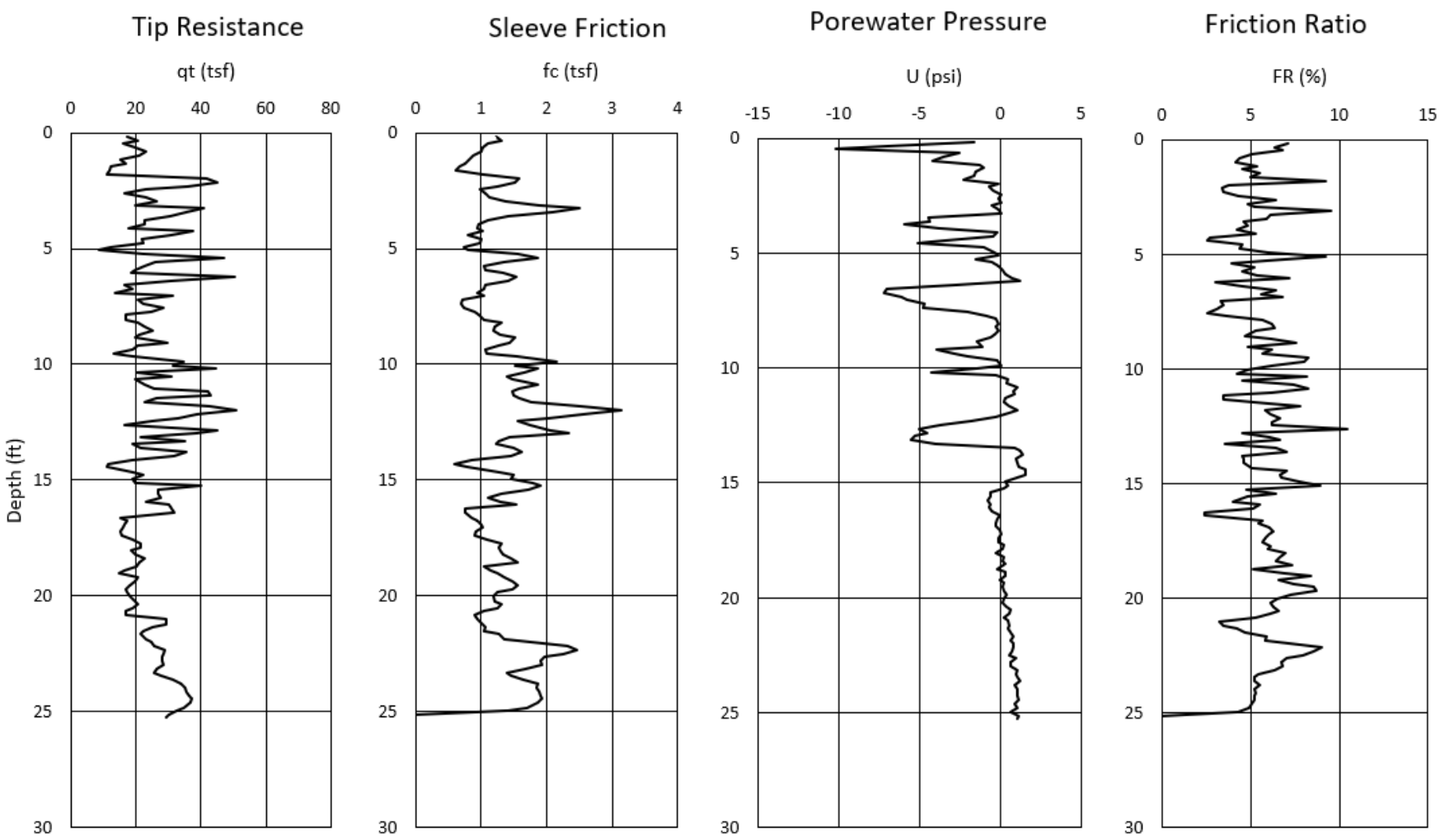

Figure 42. 19th Street over I-35: CPT-1 results

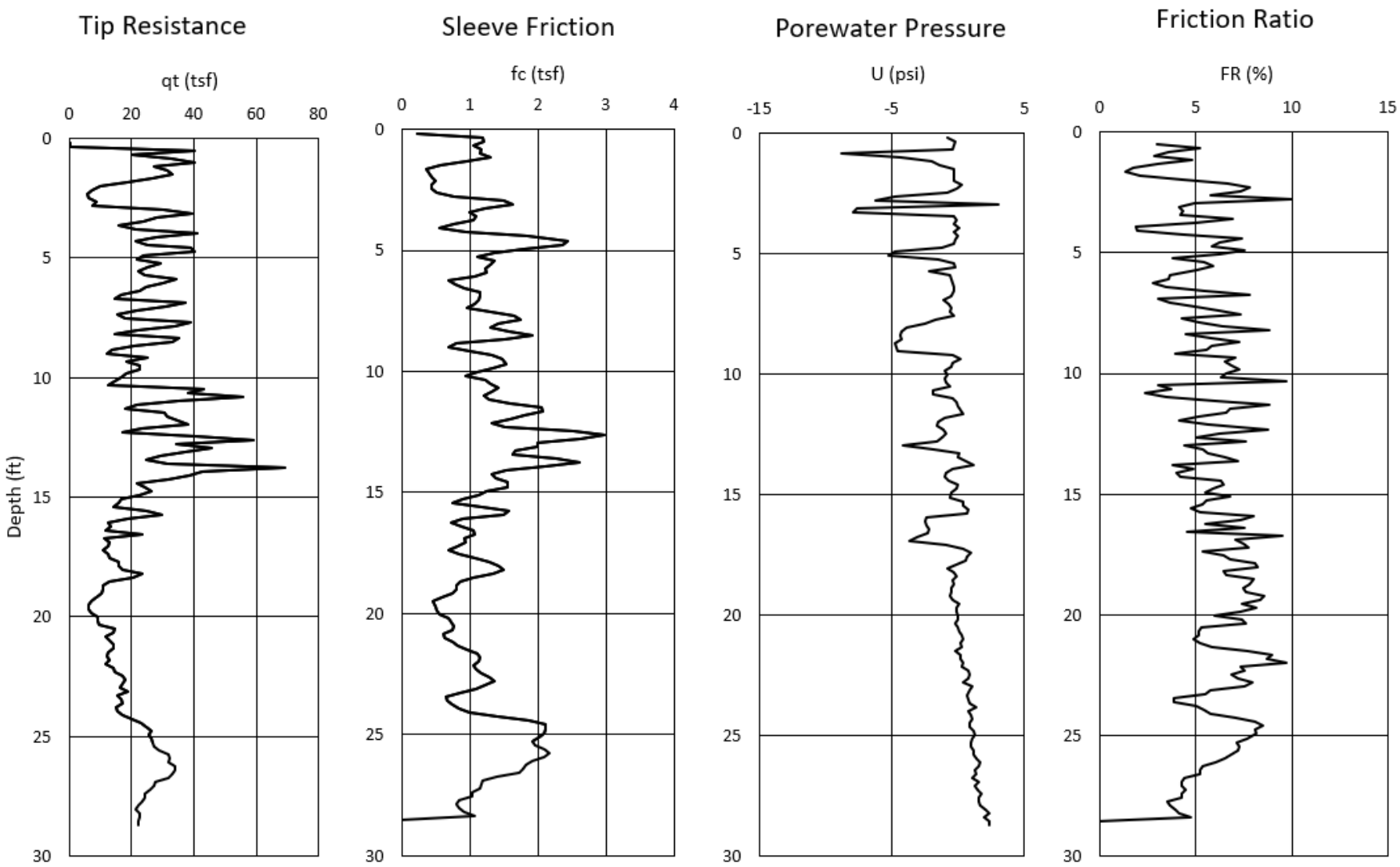

Figure 43. 19th Street over I-35: CPT-2 results

4.3.2 Remediation

The remediation planned for this bridge involved two parts. First, the subgrade and backfill located beneath the approach slabs was injected with polyurethan foam to fill any voids and densify the soil and backfill. Once this was completed a section of approach pavement was replaced adjacent to both the east and west approach slabs. During the replacement a gap was left for a pressure relief joint between the approach slab and approach pavement. Later the pressure relief joint was installed.

4.3.2.1 Foam Injection

The abutment backfill and subgrade below the approach slab and approach roadway was densified using foam injection. Foam injection was completed on the nights of November 17, 18, and 19, 2019. Nortex Concrete Lift and Stabilization, Inc. was the company contracted for foam injection. A representative from OU was present the first night of foam injection. The polyurethan foam was injected through holes drilled in the approach slab and approach roadway. Foam was injected at depths of 5 and 10 feet below the top of the pavement slabs. In addition, foam was injected directly below the pavement slabs to fill any voids that had developed. The foam was injected in a grid pattern resulting in approximately 10 injection locations per panel. Each approach slab panel is approximately 20 feet long and 12 feet wide. Each approach roadway panel is approximately 15 feet long and 12 feet wide.

For the purpose of stabilization, 5040 lbs. of foam were injected in the backfill and soil on the east side of the bridge. An additional 1723 lbs. of foam were injected directly below the pavement panels for the purpose of void filling on the east side of the bridge. On the west side of the bridge 4491 lbs. of foam were injected into the backfill

and soil for stabilization. An additional 1560 lbs. of foam was used for void filling beneath the pavement panels on the west side of the bridge. The amount of foam injected per driving lane or per panel was not tracked. During void filling foam was injected until the panels started to rise. The panels were not jacked up using foam injection. Photographs taken during foam injection are shown in Figure 44.

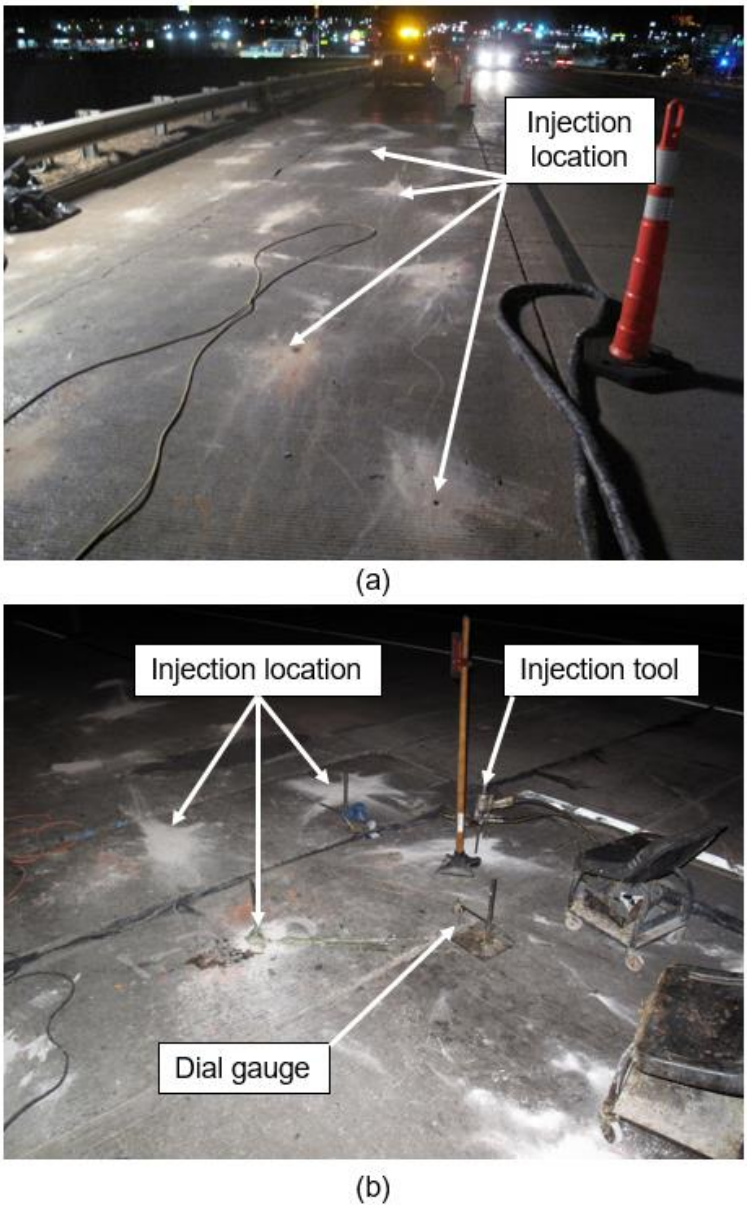

Figure 44. 19th Street over I-35: Foam injection

4.3.2.2 Pressure Relief Joints

Prior to the installation of pressure relief joints, approximately 15 feet of the approach pavement was replaced for all lanes on both sides of the bridge. Dowel holes were drilled into the adjacent approach pavement. A gap for the pressure relief joint was left on each side of the new panel. The dowels provided load transfer on the approach roadway side of the new panel. A schematic showing the locations of pressure relief joints is shown in Figure 45.

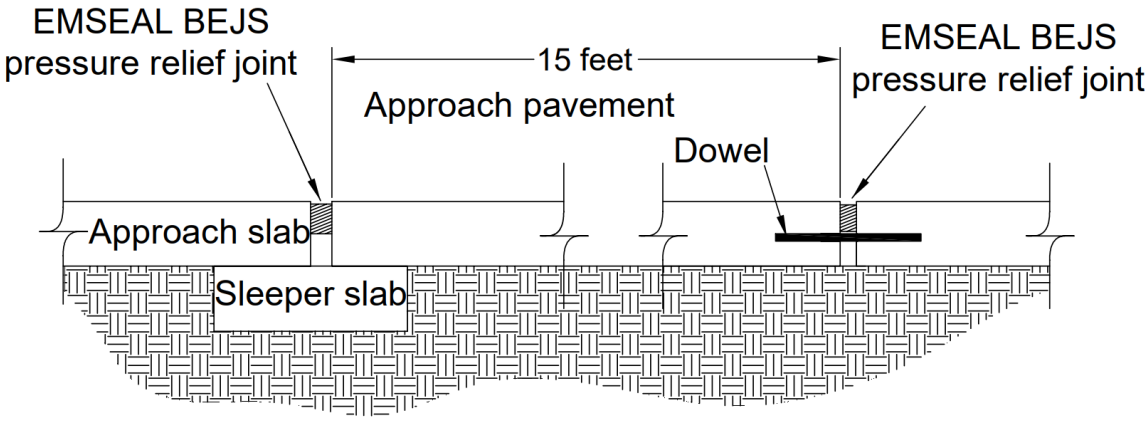

Figure 45. 19th Street over I-35: Locations of pressure relief joints

In December 2019 the planned construction started on the east side of the bridge. An additional 30 ft of pavement was replaced in the south driving lane. The additional approach pavement was replaced due to deterioration of the panels. Communication errors caused this initial attempt at the repair to be constructed incorrectly. A gap was not left open for the doweled expansion joint. Instead, a rubber expansion joint material was placed in the gap. Furthermore, the COVID-19 pandemic delayed the installation of the pressure relief joints. This delay caused the gap for pressure relief to close about halfway for the non-doweled joint. The amount of concrete to be sawed off so the joint

could be installed was too thin. The concrete would break rather than cut away from the edge of the panel. This would leave a rough edge to attach the joint to. Since the joint is glued into place a smooth edge is required. For these reasons it was decided to redo the panels.

The east and west side panels were replaced on the nights of September 21, 22, 23, and 24, 2020. A 2-inch gap was left on each side of the new panels for a pressure relief joint to later be installed. The gap was temporarily filled with foam board and sealed with silicone. A representative from OU was onsite during the construction on the nights of September 21 and 24, 2020. A strain gauge was embedded in the concrete of the outside driving lane in each direction on both sides of the bridge for a total of four concrete embedded strain gauges. Photographs showing the construction and placement of the strain gauges are shown in Figure 46. A portion of the new panels are underlain by an existing layer of Econocrete. The Econocrete, shown in Figure 46, was used as a leveling pad when the bridge was originally constructed. Photographs showing the panels completed are shown in Figure 47.

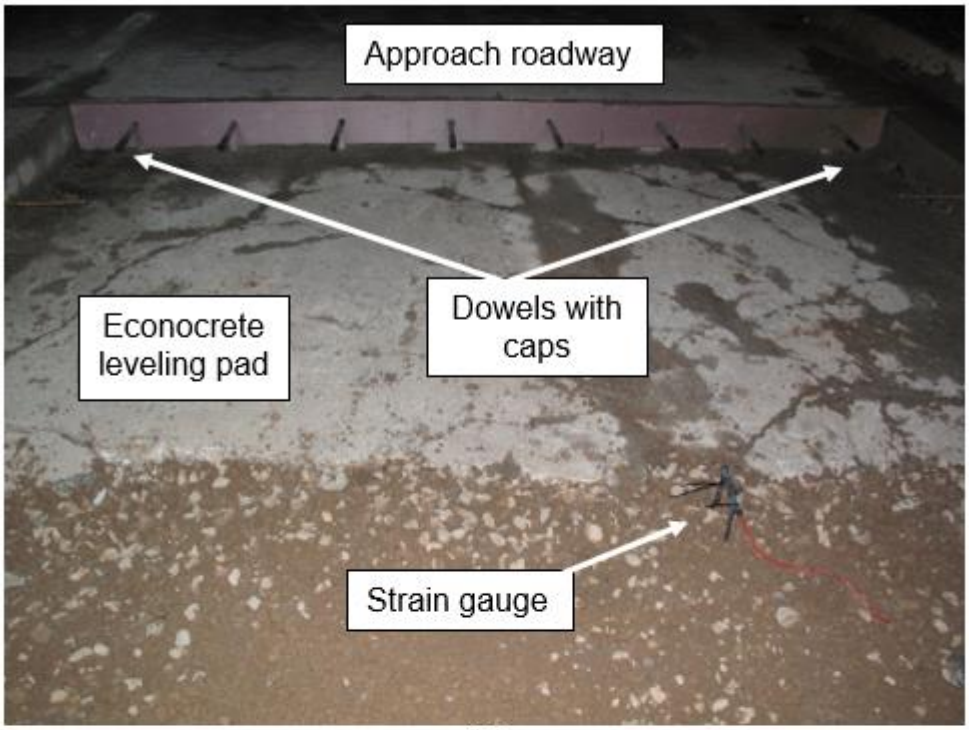

(a)

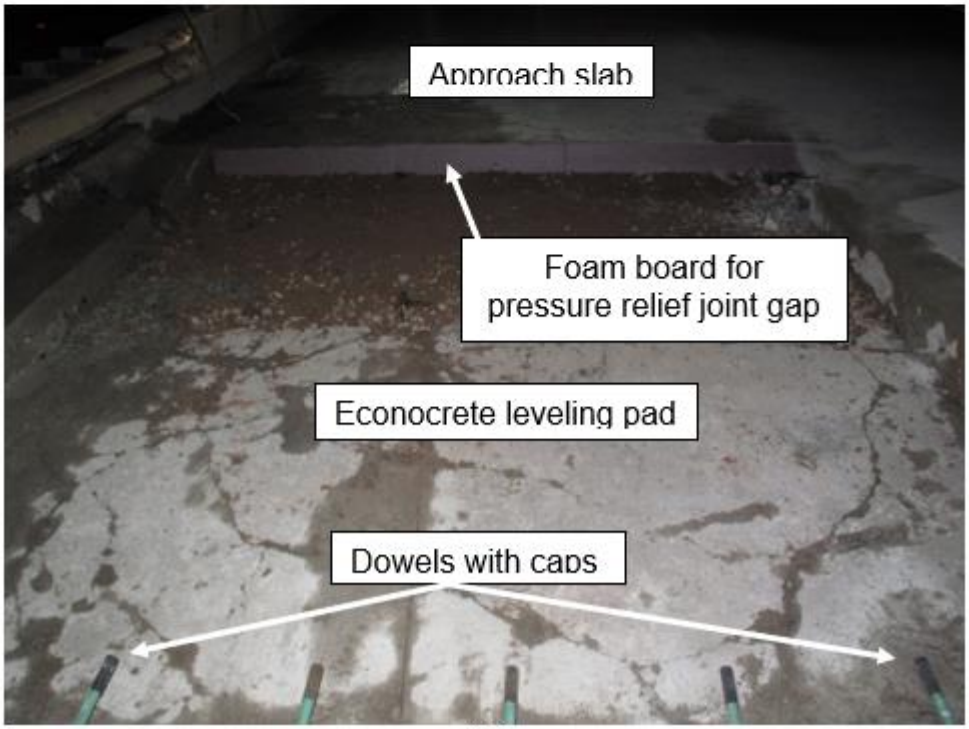

(b)

Figure 46. 19th Street over I-35: Approach roadway replacement (a) facing approach roadway, (b) facing approach slab

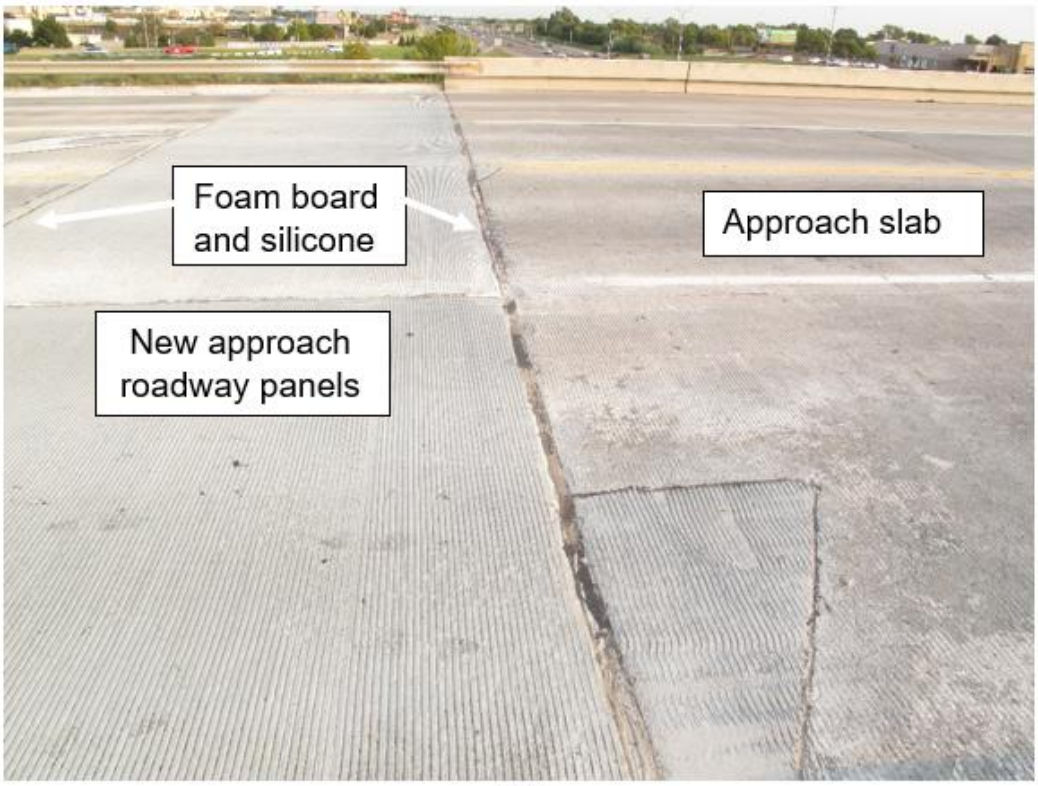

(a)

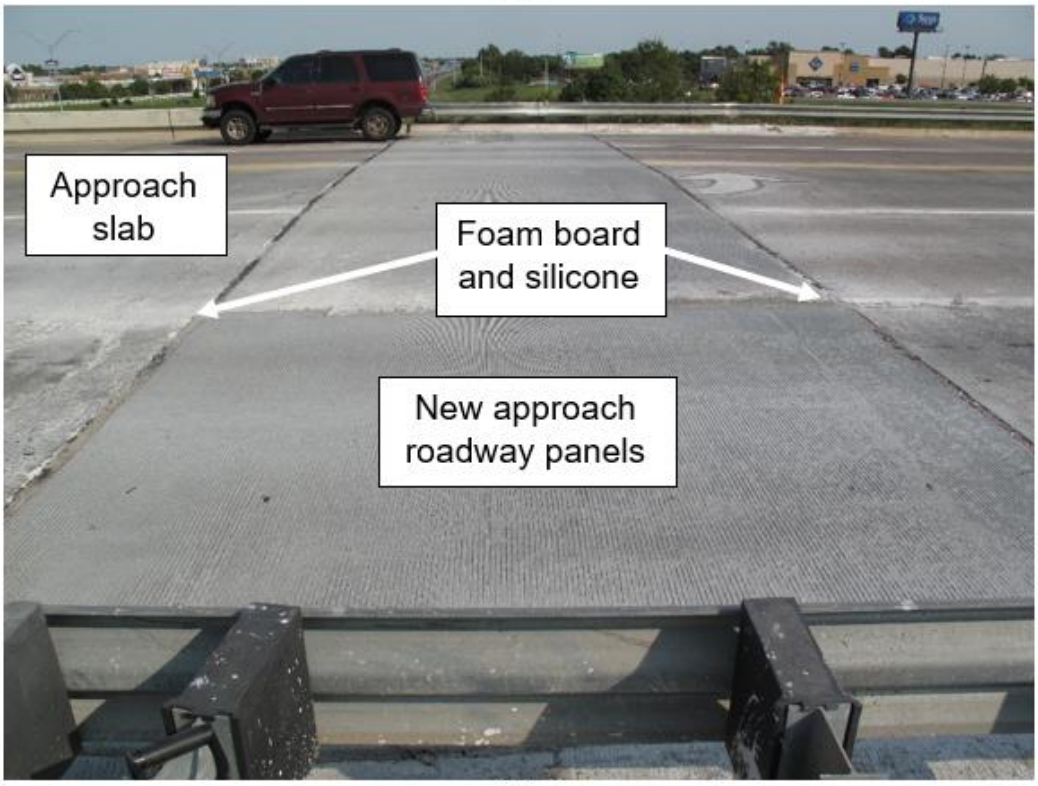

(b)

Figure 47. 19th Street over I-35: New approach roadway panels (a) west side of bridge, (b) east side of bridge

EMSEAL® BEJS was used for the pressure relief joints on this bridge. Each joint had a nominal width of 2 inches resulting in 4 inches of expansion width on each side of the bridge. The installation of expansion joints was delayed due to the COVID-19 pandemic. The pressure relief joint for the center three lanes on each side of the bridge was installed on the night of March 24, 2021. The pressure relief joint for the outer lanes on both sides of the bridge was installed on the night of June 16, 2021. The delay between the center and outer lanes was attributed to the pandemic and stored location of the joint material. One box, approximately 50 feet, of joint material was stored separately and could not be located. Photographs of the joint installation are shown in Figure 48. Photographs showing the completed joints are shown in Figure 49. The photographs of the competed joints were taken in July 2021 once all lanes had been installed.

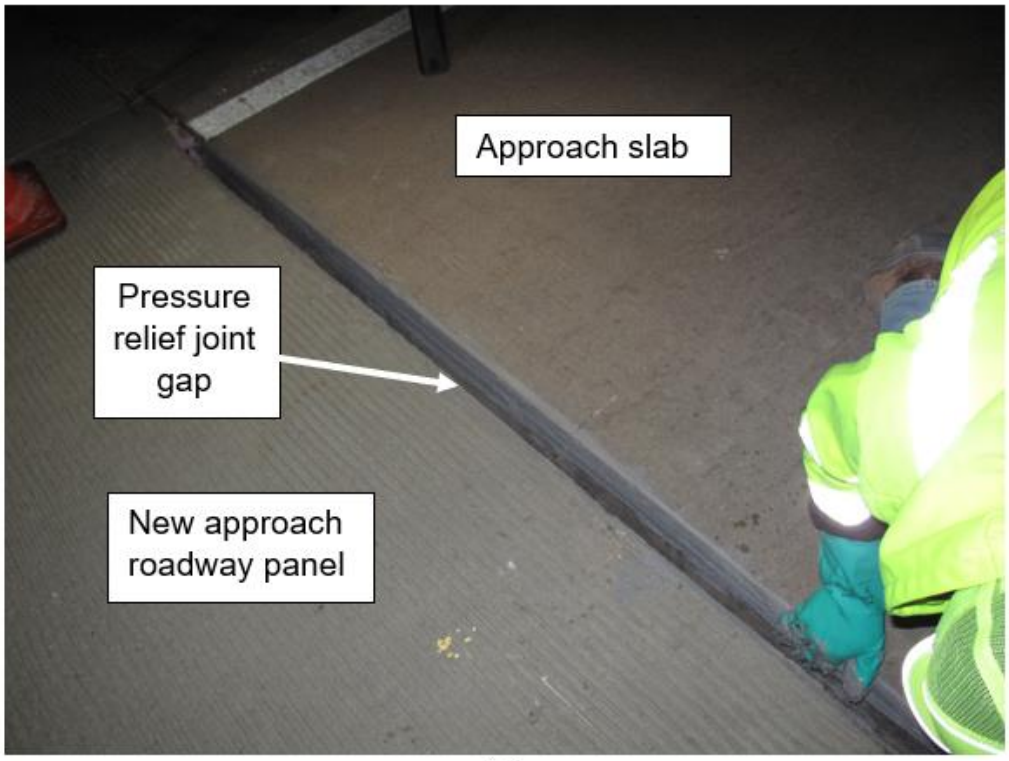

(a)

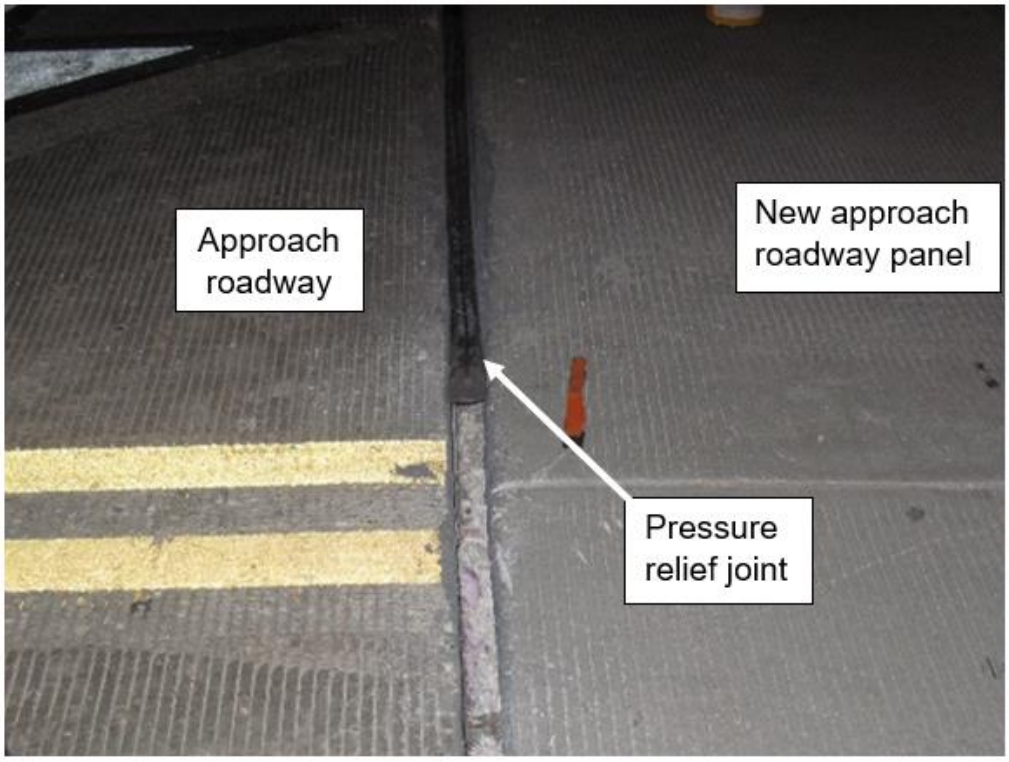

(b)

Figure 48. 19th Street over I-35: Pressure relief joint installation (a) epoxy application, (b) joint installation

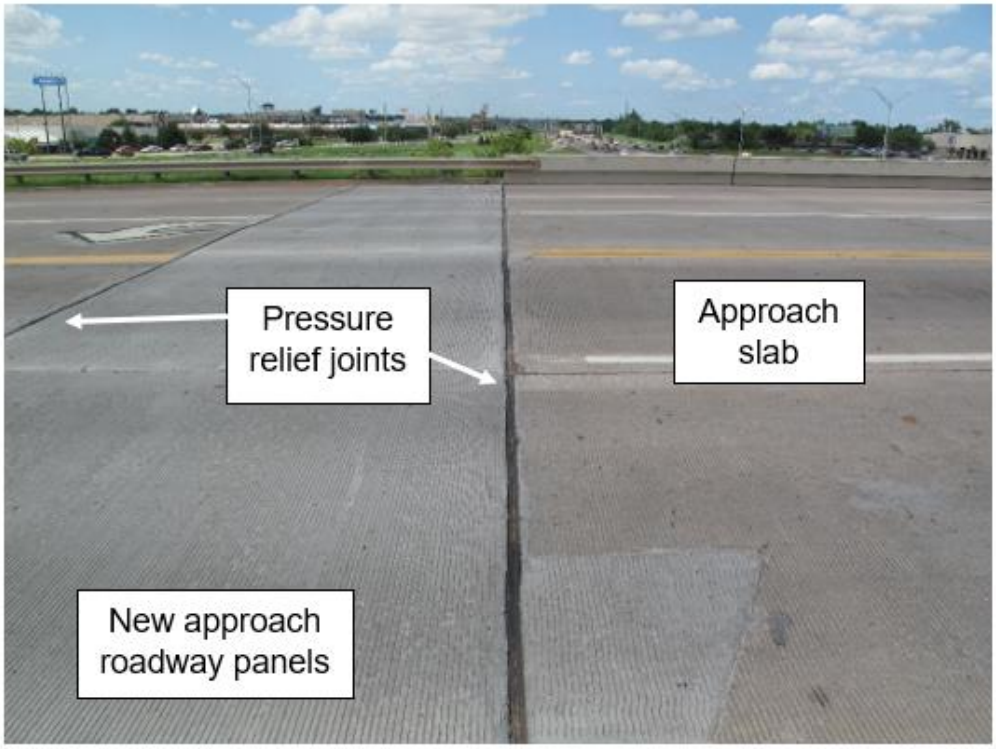

(a)

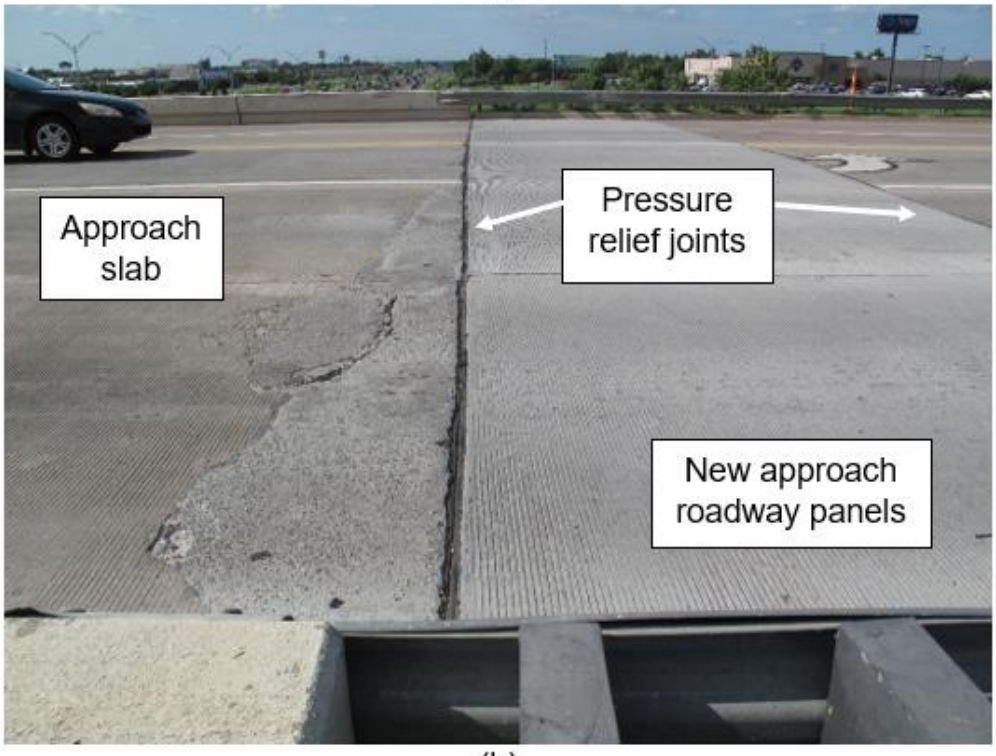

(b)

Figure 49. 19th Street over I-35: Installed pressure relief joints (a) west approach (b) east approach

4.3.3 Monitoring

The strains in the new approach panel concrete and the widths of the new pressure relief joints were monitored using vibrating wire strain gauges and crackmeters. Instrumented monitoring utilized data loggers and supporting equipment that were installed as a part of SP&R 2228. The sensors used in that monitoring project had all failed except four crackmeters. The crackmeters were reused as part of this project. During monitoring the bridge was visited monthly. During the visits, the pressure relief joints were observed, and the stored data was collected. The battery for the data logger was also replaced in these visits. Details of the monitoring equipment and the monitoring results are presented in the following sections.

4.3.3.1 Instrumentation

Vibrating wire transducers were used for monitoring of this bridge. The instruments were connected to an existing data logger powered by batteries. The data logger was stored in a heavy-duty lockbox underneath the bridge deck near the abutment. The data logger and instruments were produced by Geokon.

Data Logging System

The data logger reused from SP&R 2228 was a Geokon Model 8021 Micro-1000 data logger (Geokon 2017). A data logger was located on each side of the bridge; east and west. The data logger can support up to six multiplexers allowing more instruments to be connected to the logger. For this project two multiplexers were attached to each data logger. Each multiplexer correlated to either the north or south side of the bridge. The data logger and multiplexers are contained in a weatherproof enclosure as shown in Figure 50.

Figure 50. Geokon model 8021 Micro-1000 data logger and multiplexer (Geokon 2017)

The data logger is powered by an internal 12 Volt DC lead acid battery. However, the internal battery was used as a backup in the field. The main power source in the field was a large deep cycle marine battery. The data logger provides an excitation by plucking the vibrating wires embedded in each instrument. The instrument then returns a reading to the data logger. The logger recorded readings hourly.

Strain Gauge

Geokon Model 4200 (Geokon 2019) strain gauges were embedded in the new concrete panels. The vibrating wire strain gauge is well suited to measure small incremental strains over time. The gauge has a range of 3000 microstrain and a

resolution of 1 microstrain. The strain gauges consist of a coil assembly and a plucking wire suspended between two blocks (Figure 51). The blocks are in contact with the concrete when installed. The strain gauges can be mounted to rebars in reinforced concrete as long as proper isolation measures are taken, such as foam mounting blocks. Since the concrete in the approach pavement is not continuously reinforced, simple mounting brackets were made using rebar. The mounting bracket was essentially a piece of rebar that was bent into a U shape. The rebar was then hammered into the subgrade soil during the installation. The strain gauge was then attached to the mounting bracket using zip ties (Figure 52). The zip ties were attached to the vibrating wire housing. The circular ends or “blocks” are allowed to move freely as the concrete expands or contracts. The strain gauge was positioned to be approximately at the mid depth of the panel. The gauge was placed approximately in the center of panel with respect to width and length.

Figure 51. Geokon model 4200 vibrating wire strain gauge (Geokon 2019)

Figure 52. Mounting bracket with Geokon strain gauge

Crackmeter

Geokon model 4420 vibrating wire crackmeters (Geokon 2020) were used to measure the widths of the pressure relief joints (Figure 53). The crackmeters are available in displacement ranges from 0.125 inches to 12 inches. Two ranges of crackmeters were used on this project. Crackmeters with a range of 2 inches were placed on the doweled pressure relief joints. Crackmeters with a range of 4 inches were placed on the non-doweled pressure relief joints. It was anticipated that the non-doweled pressure relief joints adjacent to the bridge approach slab would experience more seasonal movement than the doweled joints. The crackmeters with a 2-inch range were reused from SP&R 2228. The crackmeters are mounted using mounting brackets which are embedded in the concrete on either side of the joint. The mounting brackets are attached to the concrete using epoxy.

Figure 53. Geokon model 4420 crackmeter shown with mounting brackets (Geokon 2020)

In total, the bridge was instrumented with eight crackmeters and four strain gauges. The strain gauge in the south lane on the west side of the bridge was damaged during installation. A diagram showing the approximate location of the instruments is included in Figure 54. The labeling scheme used during the results presentation is also included in the figure.

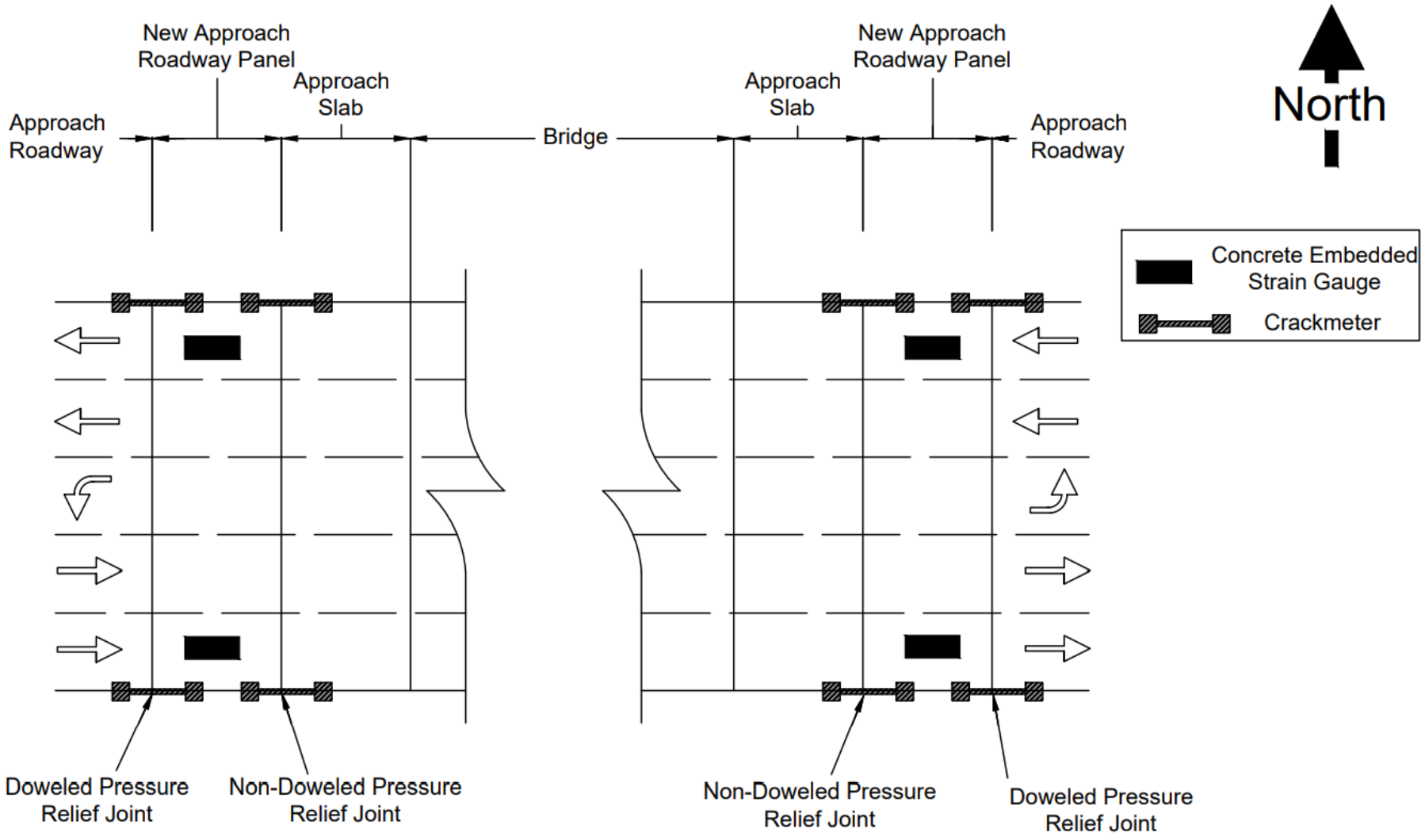

Figure 54. 19th Street over I-35 instrument locations

4.3.3.2 Monitoring Results

Concrete Strain

The recorded data from the embedded concrete strain gauges are shown in Figure 55, Figure 56, and Figure 57. The strain gauge in the south approach roadway lane on the east side of the bridge failed on December 12, 2020. The strain gauge in the north approach roadway lane on the east side of the bridge failed on August 17, 2021. The remaining strain gauge, north lane on the west side of the bridge, continues to collect data hourly.

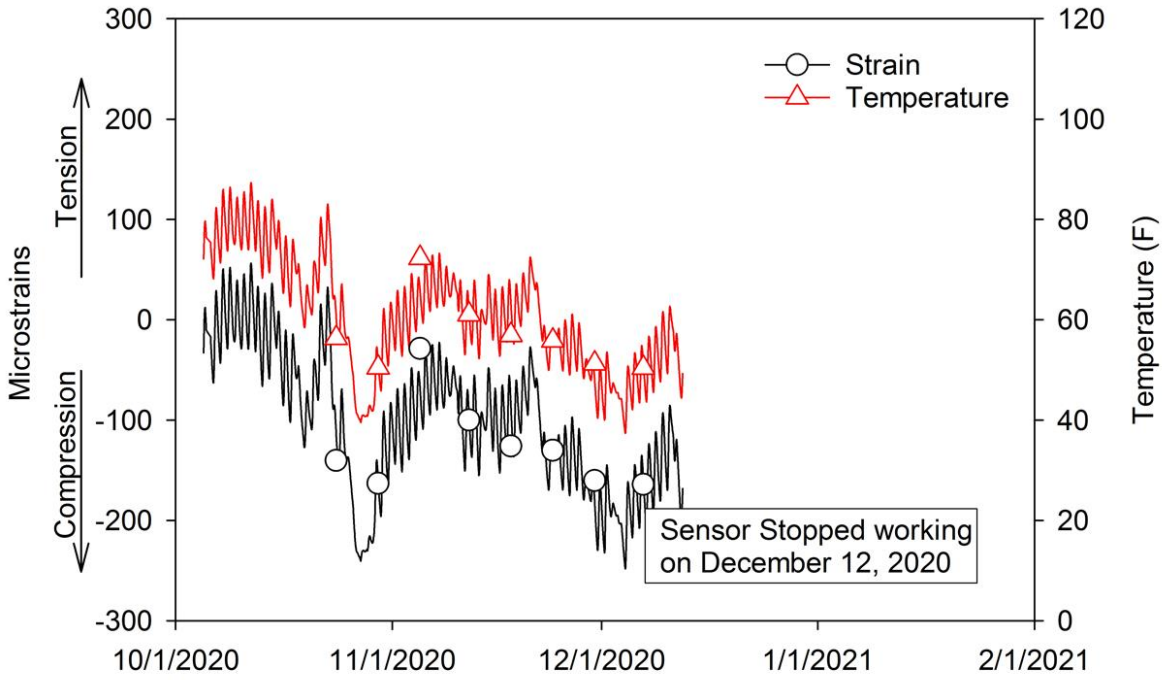

Figure 55. 19th Street over I-35 concrete strain:
East approach roadway south lane

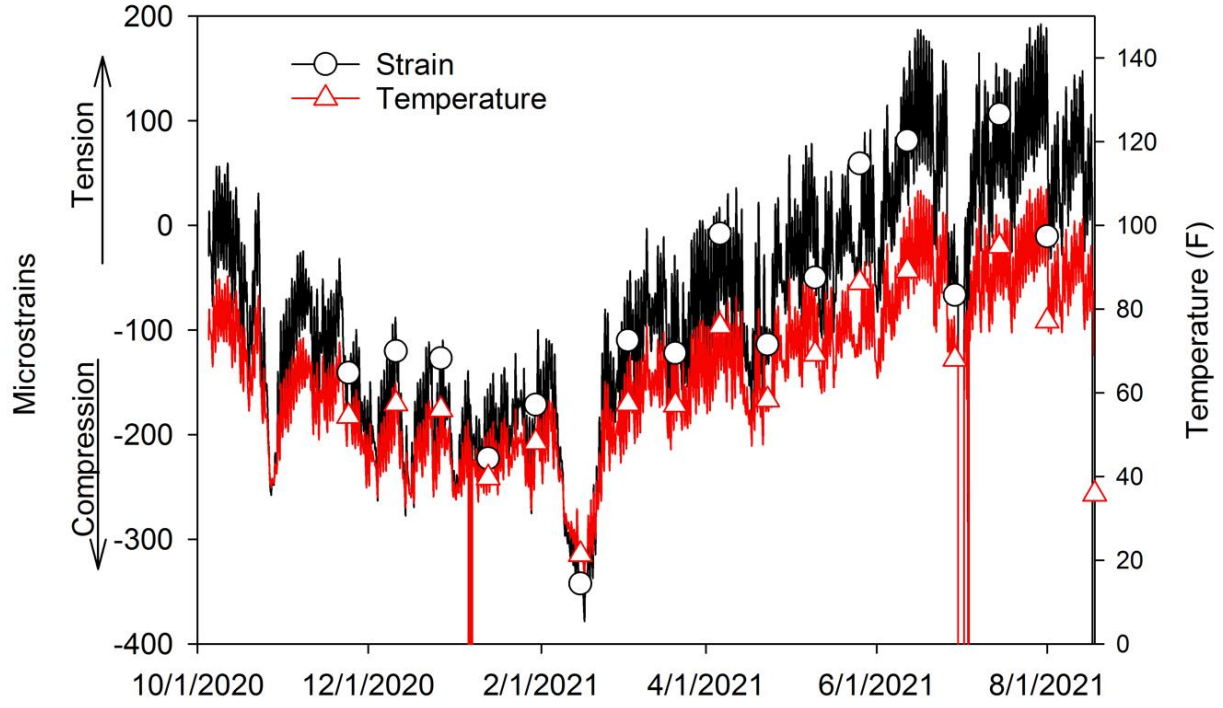

Figure 56. 19th Street over I-35 concrete strain:

East approach roadway north lane

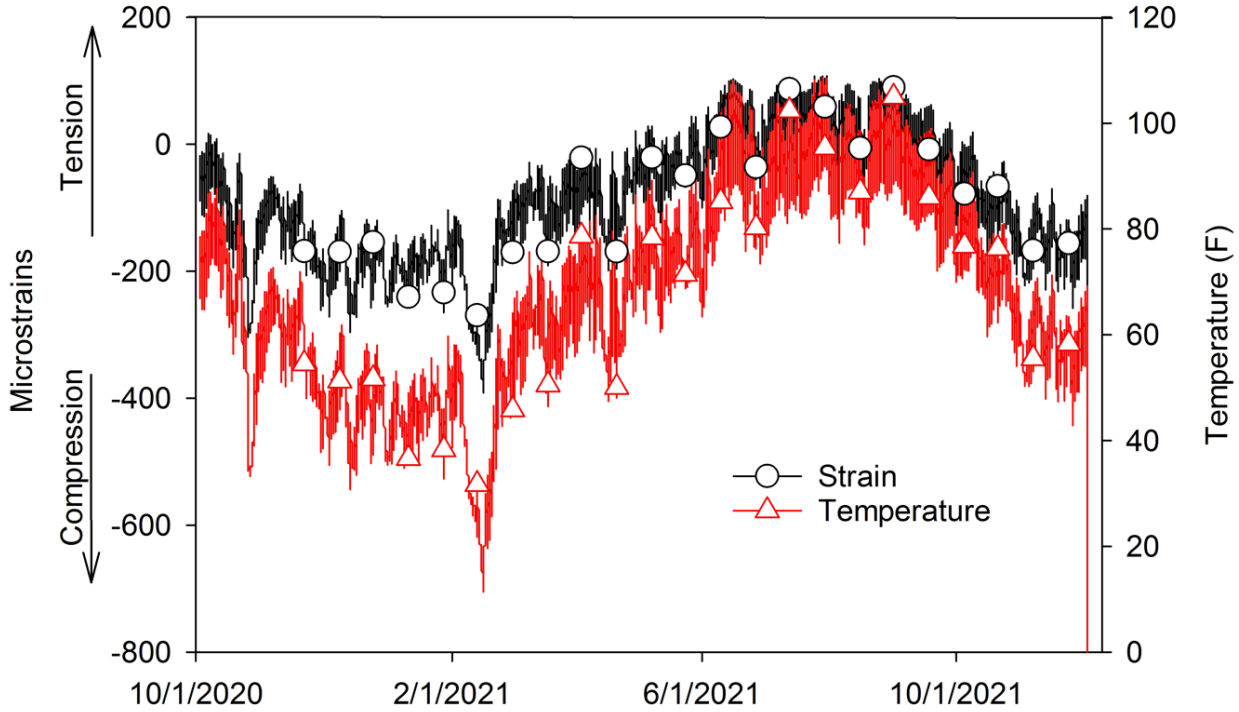

Figure 57. 19th Street over I-35 concrete strain:

West approach roadway north lane

The same general trend was observed for all the strain gauges. As the temperature increases the strain also increases indicating that the new approach roadway panel is experiencing more tension as it is expanding into the pressure relief joints. The magnitude of strain recorded in the east approach roadway panel was larger than what was recorded on the west side of the bridge.

Crackmeters

The recorded data from the crackmeters is shown in Figure 58 – Figure 65. The data logger on the east side of the bridge malfunctioned from October 5, 2021 through November 2, 2021.

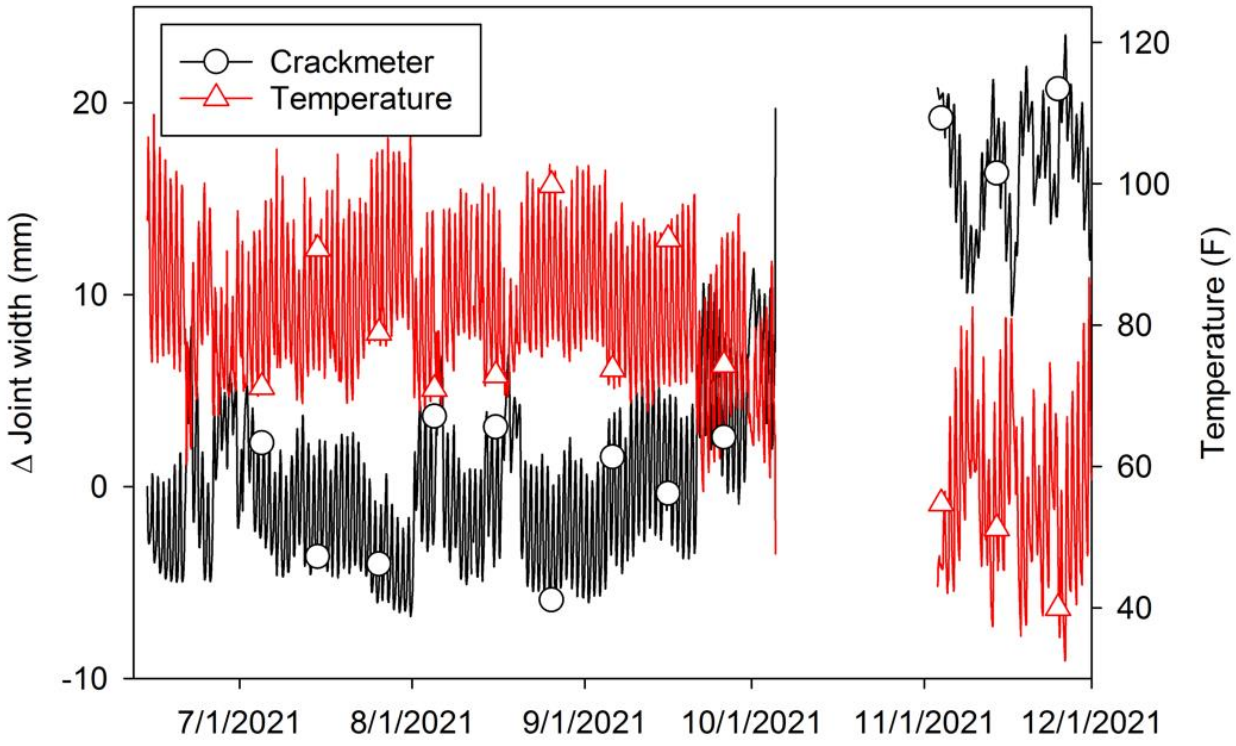

Figure 58. 19th Street over I-35 pressure relief joint width: East approach south non-doweled joint

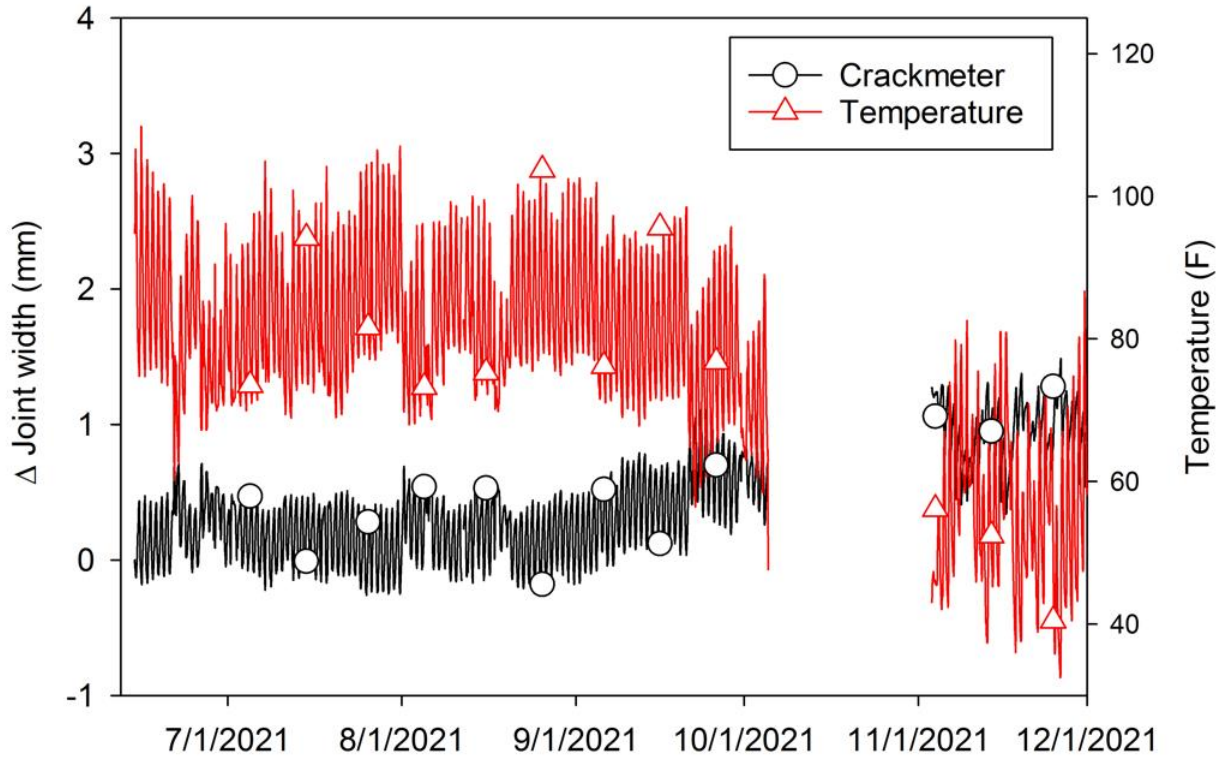

Figure 59. 19th Street over I-35 pressure relief joint width: East approach south doweled joint

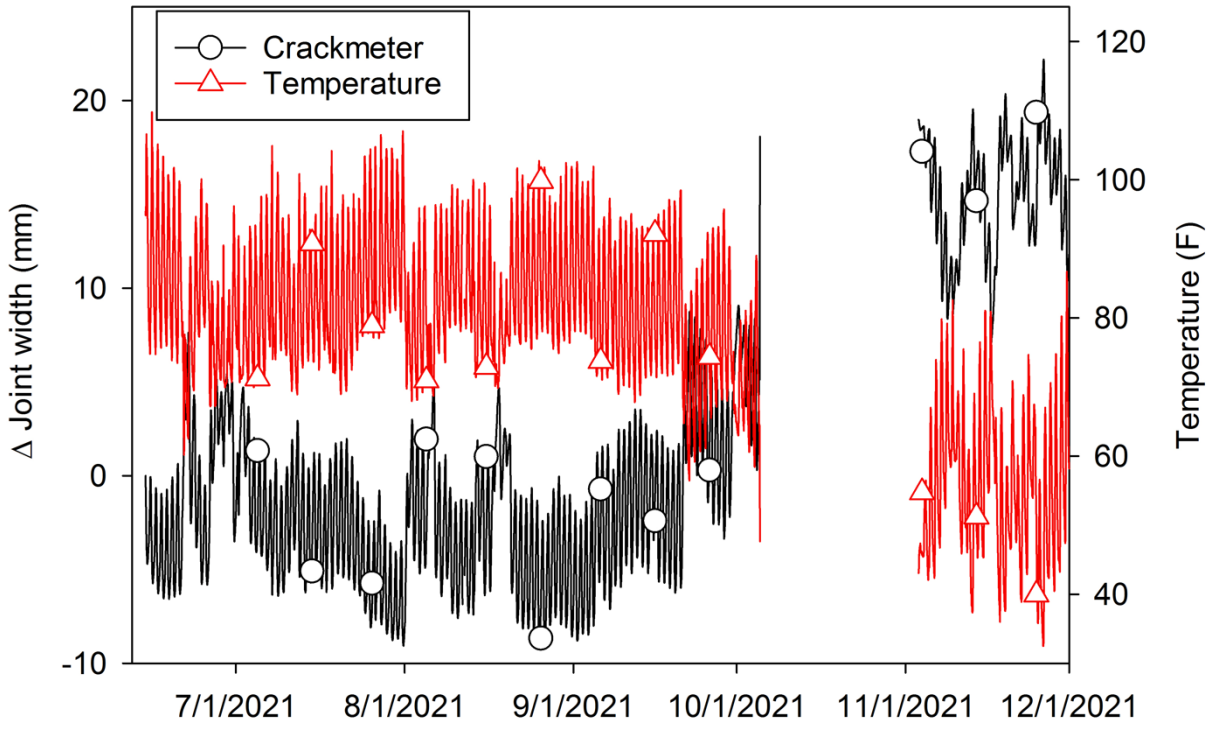

Figure 60. 19th Street over I-35 pressure relief joint width: East approach north non-doweled joint

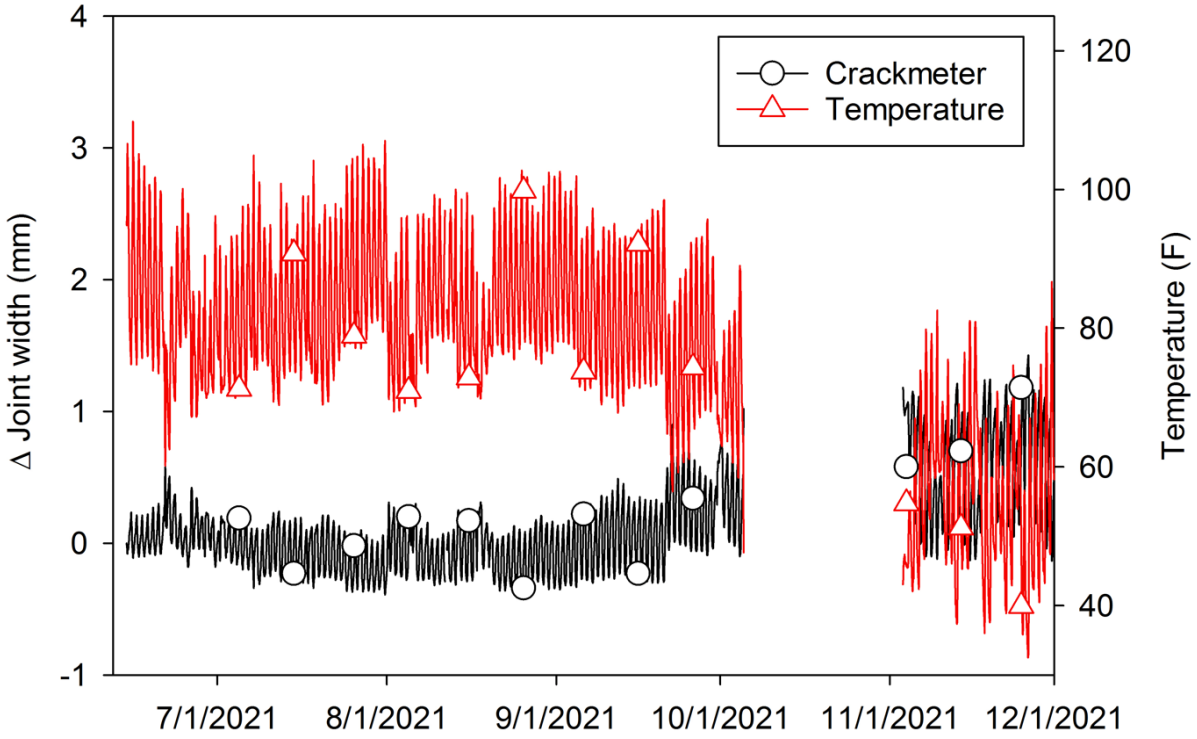

Figure 61. 19th Street over I-35 pressure relief joint width: East approach north doweled joint

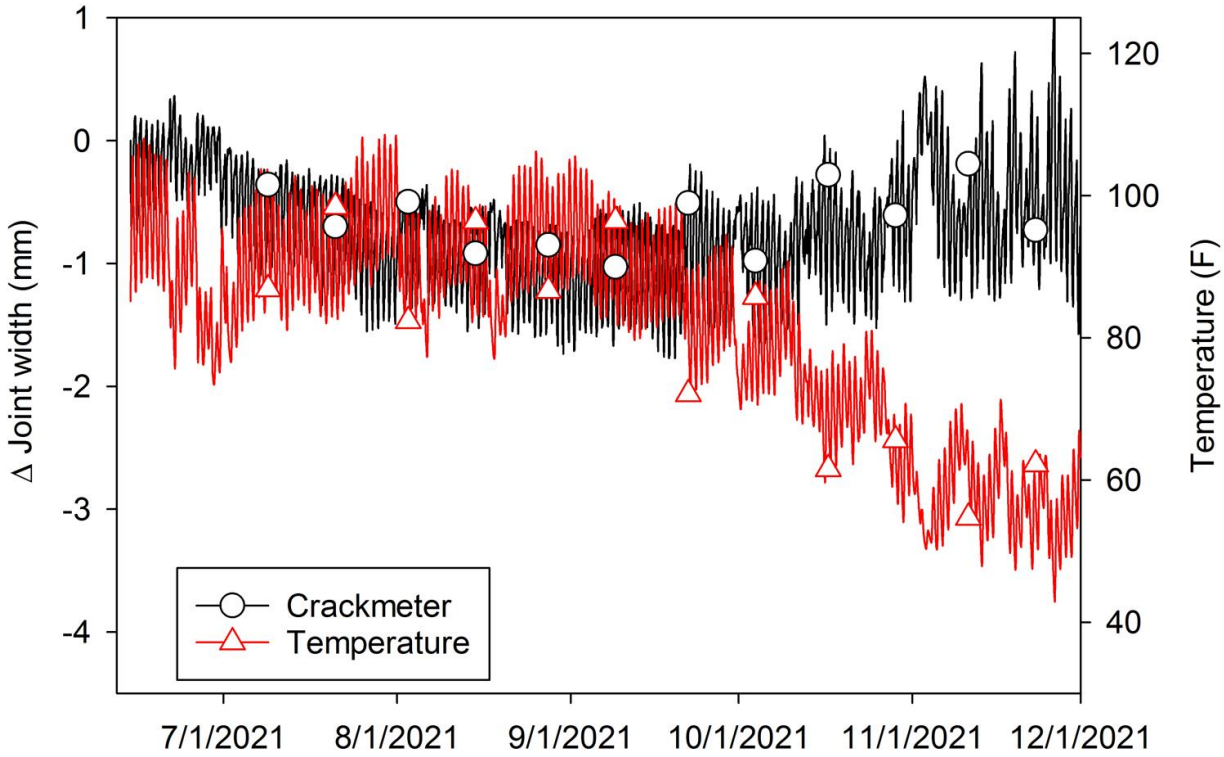

Figure 62. 19th Street over I-35 pressure relief joint width: West approach south non-doweled joint

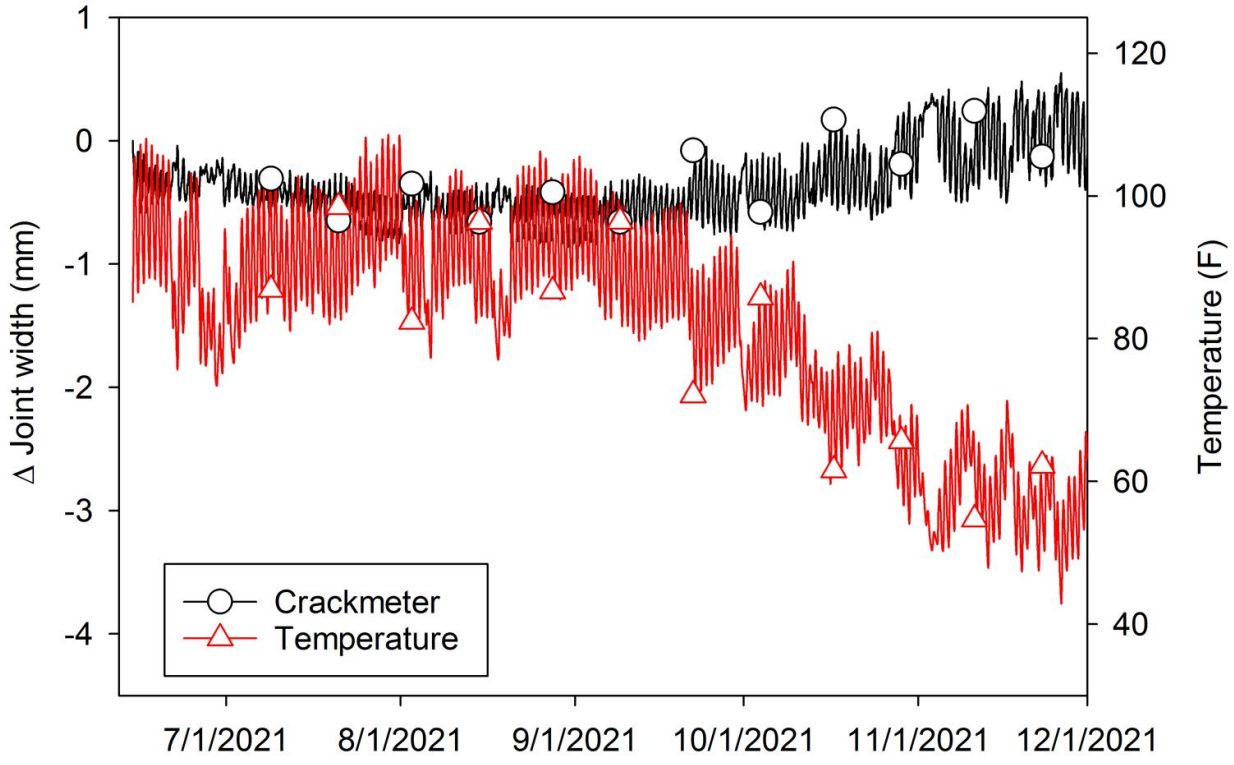

Figure 63. 19th Street over I-35 pressure relief joint width: West approach south doweled joint

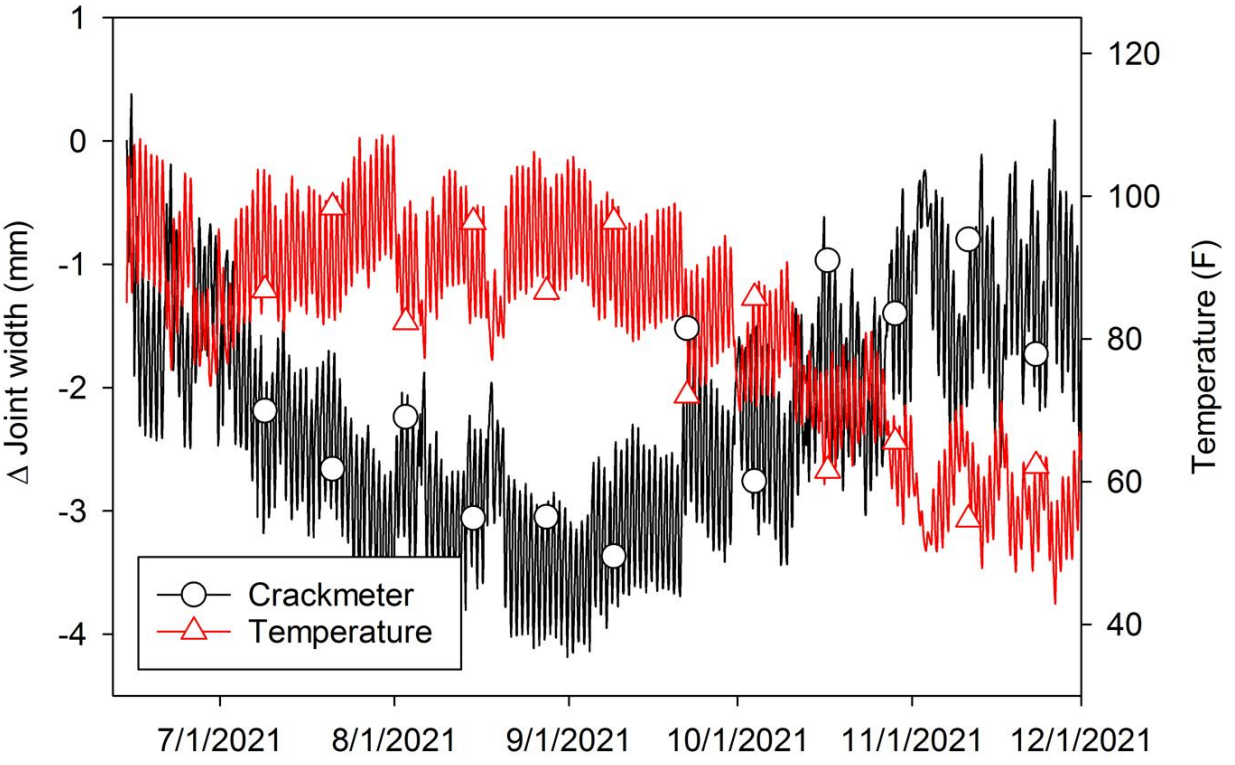

Figure 64. 19th Street over I-35 pressure relief joint width: West approach north non-doweled joint

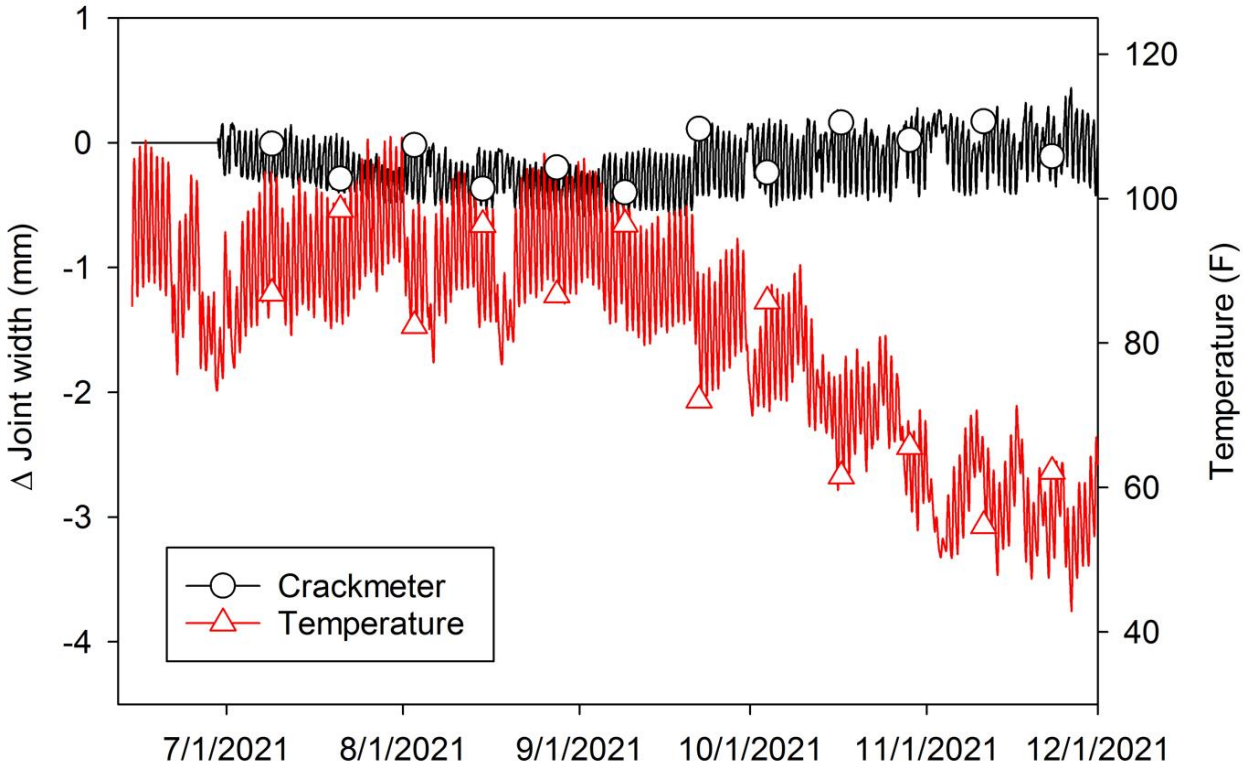

Figure 65. 19th Street over I-35 pressure relief joint width: West approach north doweled joint

The non-doweled pressure relief joints experienced much more movement than the doweled pressure relief joints during the monitoring period. The joints on the east side of the bridge experienced more movement than the west side. This is most notable from the non-doweled joints. The non-doweled joints on the east side experienced about 20 to 25 mm of movement while the west side non-doweled joints only experienced 2 to 4 mm of movement. The daily variations are also greater for the non-doweled joints on both sides of the bridge. The joints appear to be functioning correctly and responding to daily and seasonal temperature changes effectively.

4.4 Joint Replacements Using Ultra-High Performance Concrete

Two bridge retrofit projects in Oklahoma have included ultra-high performance concrete (UHPC) for joints and have been monitored by the OU research team. The first

was a demonstration project involving replacement of an expansion joint header on the SH-3E bridge over the N. Canadian River in Pottawatomie Co. (NBI No. 19276) completed in 2017 and was originally monitored as part of another ODOT sponsored project (SPR 2276) and is described in (Floyd et al. 2021a) with some of that discussion repeated here. The second included replacement of connections of precast concrete girders made continuous for live load on the U.S. 183/412 bridge over Wolf Creek in Fort Supply in Woodward County (NBI No. 21124) completed in 2019 and monitored as part of SPR 2284 (Floyd et al. 2021b). These two projects provide insight into potential behavior of UHPC as an expansion joint header and as a replacement of damaged continuity connections.

4.4.1 SH-3E Bridge Over the N. Canadian River

This project consisted of a partial replacement of the areas immediately adjacent to a portion of one of the expansion joints (headers) on the SH-3E bridge over the N. Canadian River in Pottawatomie Co. (NBI No. 19276), part of ODOT Division 3. The bridge was repaired specifically as a demonstration for UHPC, even though the replacement was not part of the ODOT's 8-Year Construction Work Plan, using funding from the ODOT sponsored research project and labor provided by the Division 3 maintenance crew and OU research team. Lafarge Ductal® was contracted for rental of their mixers appropriate for this project, providing the required quantity of materials, and providing on-site support. Approximately 12 feet of a single expansion joint over the westernmost pier was removed and replaced by Division 3 personnel and the OU research team using the commercially available UHPC material Ductal® for the joint headers. Photographs of the bridge and joint before replacement are shown in Figure 66. Corrosion damage was visible at most piers in the end diaphragms, underside of the

slab, beam ends, or pier caps, providing an indication of the need for joint replacement. Deterioration near the candidate joint is visible in the picture of the underside of the deck overhang shown in Figure 67.

Figure 66. SH-3 bridge over N. Canadian River (left) and expansion joint to be replaced (right)

Figure 67. Underside of the SH-3 bridge over N. Canadian River at the candidate joint showing concrete deterioration

The original plan consisted of replacing the joint utilizing the unusually wide shoulders on the two-lane bridge to replace the joint in sections with limited disruption of traffic. The scope of the replacement was adjusted after the first casting day due to slow strength gain of the material in the cold weather. The OU research team provided support to the Division 3 crew related to mixing, placing, curing, and testing the UHPC. Approximately 1 foot of concrete was removed from either side of the existing joint depending on the condition of the concrete and as much of the reinforcement was left in place as possible. It was decided that a partial depth replacement was sufficient near the expansion joint due to the condition of the concrete which aided in constructability and reduced the time required to form the joint. The final joint detail used for construction is shown in Figure 68. The top of the joint was formed over to finish the joint ¼ in. higher than the surrounding concrete to allow for grinding and a chimney was used for placement to ensure positive flow of the UHPC. A vent hole was included on the opposite end of the joint. Heat curing was applied using materials and recommendations provided by the OU research team and was intended to continue until the compressive strength as determined by cylinder breaks reached 14,000 psi. When the appropriate compressive strength was achieved, the joint as ground smooth with the bridge deck, and the expansion joint fill material was placed. Manhattan Road & Bridge agreed to provide assistance in grinding the planned joint. Vibrating wire strain gauges with internal thermistors were installed before concrete placement by the OU research team to monitor the joint performance and collect a temperature history to relate to compressive strength. Data loggers were placed on the parapet wall to ensure the equipment would be protected.

Concerns with differential shrinkage were addressed by ensuring properly roughened and dampened surfaces of the existing concrete and exposing the top rebar

mat. The deterioration shown in Figure 67 was not disturbed as part of the proposed half depth repair. This additional repair was considered outside the scope of the UHPC implementation. The majority of the work on the joint replacement was completed in December 2017.

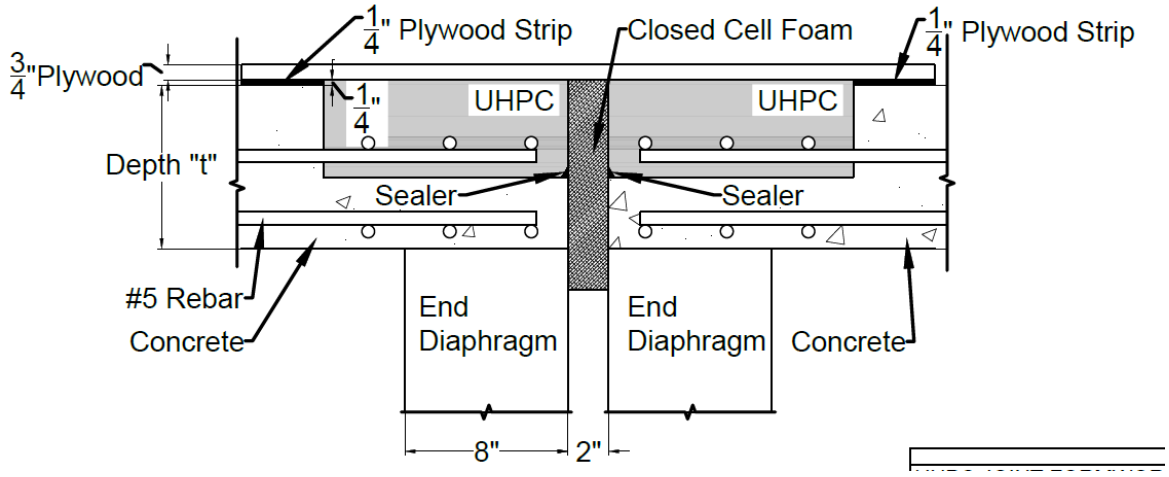

Figure 68. Details of the UHPC expansion joint headers including formwork

All required UHPC materials and equipment were transported to the ODOT Tecumseh maintenance yard and then to the bridge site by the OU research team. Two high shear mixers rented from Lafarge were used on the project. Figure 69 shows the mixers in place at the bridge site and wired to the generator used for power on site. Traffic control was put in place by the ODOT Division 3 maintenance crew on December 11 and the joint section was removed by the ODOT Division 3 maintenance crew on December 11. Concrete was removed to approximately 2 inches below the top rebar mat, for a total depth of approximately 6 inches which varied due to the roughness of the remaining concrete. Approximately 12 inches of concrete was removed on either side of the joint in the direction parallel to the roadway as shown in Figure 68. During concrete removal the remains of an older steel finger expansion joint were discovered, and the crew did their best to work around this material. A decision was made to

encapsulate the remainder of the older joint. Existing rebar was kept in place and cleaned by sand blasting and a single No. 5 rebar (not epoxy coated) was placed parallel to the joint on each side. The concrete surface was roughened during removal and was sand blasted clean. Figure 70 shows the joint after concrete removal and other preparations, except for placement of the top form. All exposed concrete surfaces were wetted to a damp, surface dry condition immediately before the top form was placed.

Figure 69. High shear mixers used for mixing UHPC

Figure 70. Joint after removal of existing concrete and before placement of the top form

Two 6-inch Geokon vibrating wire strain gauges were placed in the joint header on the west side, one with its axis oriented perpendicular to the roadway (parallel to the joint) and one oriented parallel to the roadway (perpendicular to the joint). The gauge perpendicular to the roadway was located 83 inches from the face of the parapet and 4 inches from the face of the joint. The gauge parallel to the roadway was located 88 inches from the face of the parapet and 7 inches from the joint face. The gauges are shown in Figure 71. Both gauges were connected to a Geokon datalogger placed in a steel box attached to the back side of the bridge parapet.

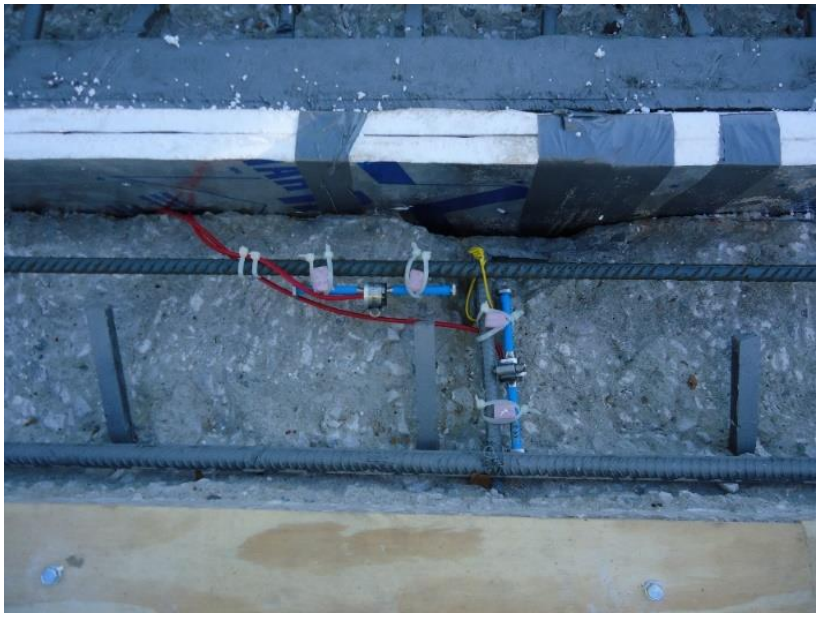

Figure 71. Strain gages within the joint header

Formwork for the joint opening consisted of sheets of Styrofoam stacked to create the proper opening width. Strips of ¼ inch plywood were attached to the bridge deck on either side of the joint and a top form consisting of sheets of ¾ inch plywood placed on top of the ¼ inch plywood sheets was attached to the concrete deck using screw anchors. The formwork was intended to create a concrete surface ¼ inch above the existing bridge deck to allow for grinding of the top surface to final grade. The top form had two holes cut on either side of the joint, one approximately 2/3 of the pour length from the parapet intended to be the fill hole and one at the parapet acting as a vent hole.

Raw materials were separated into the amount required for separate 5 ft^3 batches and staged on a flatbed trailer backed up to the concrete mixers. The Lafarge representative on site directed the mixing operations with the OU research team responsible for mixing and placement. The mixing procedure consisted of mixing all dry ingredients for approximately 7 minutes followed by adding the required water and chemical admixtures slowly. Steel fibers were added after approximately 20 minutes of

mixing. The UHPC was discharged after approximately 35 minutes of mixing and the next batch was started immediately. The UHPC was transported from the mixers to the joint using four wheeled plastic carts and placed into a funnel in the fill hole using shovels. The east joint header was filled approximately 2/3 full with the first batch, the west side header was filled with the second batch to ensure equal pressure on both sides of the joint formwork, and the third batch was used to top off both sides. The material was allowed to flow from the fill hole to the vent hole and the joint was considered full when material was observed coming out of the vent hole. The Lafarge representative adjusted the water content of the mixture due to the cold weather conditions (30° to 40° F ambient temperature), adding slightly less water than the standard proportion.

The joint was covered with insulating blankets with the top form still in place and heat lamps were put in place to facilitate heat curing at 3:30 pm, approximately 2.5 hours after completion of the pour. The Geokon datalogger did not function properly due to a bad set of batteries, so manual measurements of the vibrating wire strain gages and associated temperatures were taken for the first 10.5 hours after the start of heat curing. The datalogger batteries were replaced and the gages were hooked to this apparatus at 2:00 am on December 13. Throughout heat curing, the internal concrete temperature slowly increased (shown in Figure 72), but the same 80° to 95° C measured in the lab for a similar joint detail were never observed. Measured temperatures were consistently higher than the ambient temperature, which reached freezing during the night. The heat lamps were turned off at 6:00 am and cylinders were taken back to Fears Structural Engineering Lab for testing. Cylinders were tested at an age of approximately 20 hours including 15 hours of attempted heat curing. Compressive strength test results are presented in Table 1.

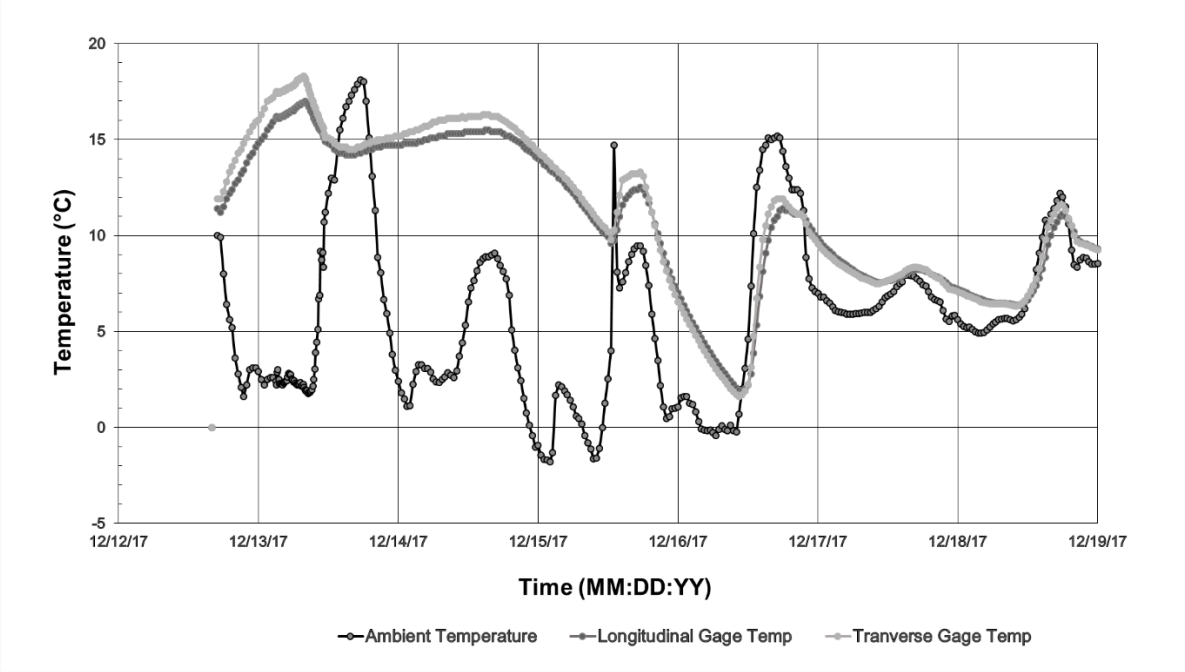

Figure 72. UHPC temperature over the first week after casting

Table 1. UHPC compressive strength for SH-3E joint

Age (days)	Compressive Strength (psi)
0.83 (20 hr)*	3580
3*	11,110
4	13,280
7*	15,600
14	20,900
28	22,430

Note: *indicates only two cylinders were tested

The compressive strength measured at 20 hours was well below the targeted value of 14,000 psi. Based on the low early age compressive strength and concerns about the time required to achieve strength necessary to reopen the roadway to service, the Division 3 Engineer made the decision to halt the joint replacement after the first section. Traffic control was kept in place to protect the UHPC joint for 3 days at which time the compressive strength was in excess of 11,000 psi, which was still less than the targeted 14,000 psi. However, the location of the joint on the shoulder of the roadway

limits the amount of loading it would receive. The low ambient temperatures at the time of casting were primarily to blame for the slow strength gain.

The UHPC used for the joint was cast ¼ inch above the intended finished grade to allow for grinding of the portion containing a high concentration of air bubbles that tends to collect at the top of the material. Manhattan Road & Bridge agreed to provide grinding services in conjunction with another project in the area. Grinding was conducted on December 20, 2017 by a subcontractor to Manhattan, with two representatives of Manhattan present at the time of grinding. The UHPC had a compressive strength of approximately 15,500 psi at the time of grinding, and the machinery operator indicated no problems grinding the material. Photos before and after grinding are shown in Figure 73. The difference in elevation between the two bridge sections did create a problem in grinding the UHPC on both sides of the joint to the same elevation. A decision was made by the research team and ODOT maintenance engineers to match the grade of the higher section to avoid any damage to the bridge deck. The dimensions of the grinding equipment also did not allow for grinding immediately adjacent to the parapet. The difference in ground surfaces can be seen in Figure 73 and the entire section after grinding is shown in Figure 74.

Figure 73. UHPC joint before (left) and after (right) grinding

Figure 74. Entire Joint after grinding

A representative of SSI Highway Products and the Division 3 bridge maintenance crew installed a precompressed EMSEAL BEJS (bridge expansion joint system) joint fill on March 30, 2018. Figure 75 shows placement of the sealant material after each header had been coated with epoxy. Figure 76 shows the end of a section of sealant where a bead of epoxy was applied to connect the next section. Since the original joint opening was wider than the planned 2 inch opening, the new joint headers were formed to produce an opening with a step down from a 2 inch width to a 3 inch width approximately 2 inches from the top of the joint. This prevented the joint material from being installed with the appropriate recess from the top of the joint. It was determined that this should not be a major issue since most of the replacement is on the shoulder area of the bridge but was noted for future installations. The completed joint sealant material is shown in Figure 77.

Figure 75. Installation of BEJS material by SSI Highway Products personnel

Figure 76. End of BEJS stick prepared for splicing

Figure 77. UHPC joint headers on SH-3E bridge immediately after BEJS material was placed

Detailed photographs were taken of the joint immediately after formwork removal and grinding to provide a baseline for a visual assessment of joint performance. Visits were made to the SH-3E bridge periodically until September 2021 to take photos of the joint and monitor progress of any cracks. The vibrating wire strain gages were only monitored for the first few months to measure temperature at early ages and to ensure proper performance of the joint. No cracking was observed between the UHPC header and the pre-existing bridge deck. Minor cracking transverse to the joint headers was observed in one of the first visits to the joint spaced along the length of the joint at 6 inch to 12 inch Spacing. The crack widths were very small, but crack width was not measured and only one appeared to widen substantially over time. These hairline cracks are identified by black arrows in Figure 78. Some surface rusting of the steel fibers was also observed and is shown in Figure 79. Any exposed fibers broke away

from the matrix, but no deterioration of the UHPC material around these locations was observed. Figure 80 shows photos of the joint over time. It is apparent from these photos that other than being covered with grit and gravel the joint is in very similar condition to when it was placed after almost 4 years of exposure. In September 2021 some cracking and spalling was observed on the SW corner of the joint where the header elevation is higher than the west deck section. Throughout the monitoring period the adjacent elastomeric nosing and poured silicone joint showed visible deterioration.

Strain gage data collected over the first seven months after placement shown in Figure 81 indicate that the UHPC showed limited shrinkage in the direction restrained by the deck concrete and more shrinkage in the direction transverse to the joint where one edge was unrestrained. In both cases the measured shrinkage was less than what would be expected for a free condition. The header material appeared to act together with the bridge deck relative to movement caused by changes in ambient temperature.

Figure 78. UHPC joint headers on SH-3E bridge before joint sealant was placed and showing hairline cracks

Figure 79. UHPC joint headers on SH-3E bridge before joint sealant was placed and showing surface rusting of the exposed steel fibers

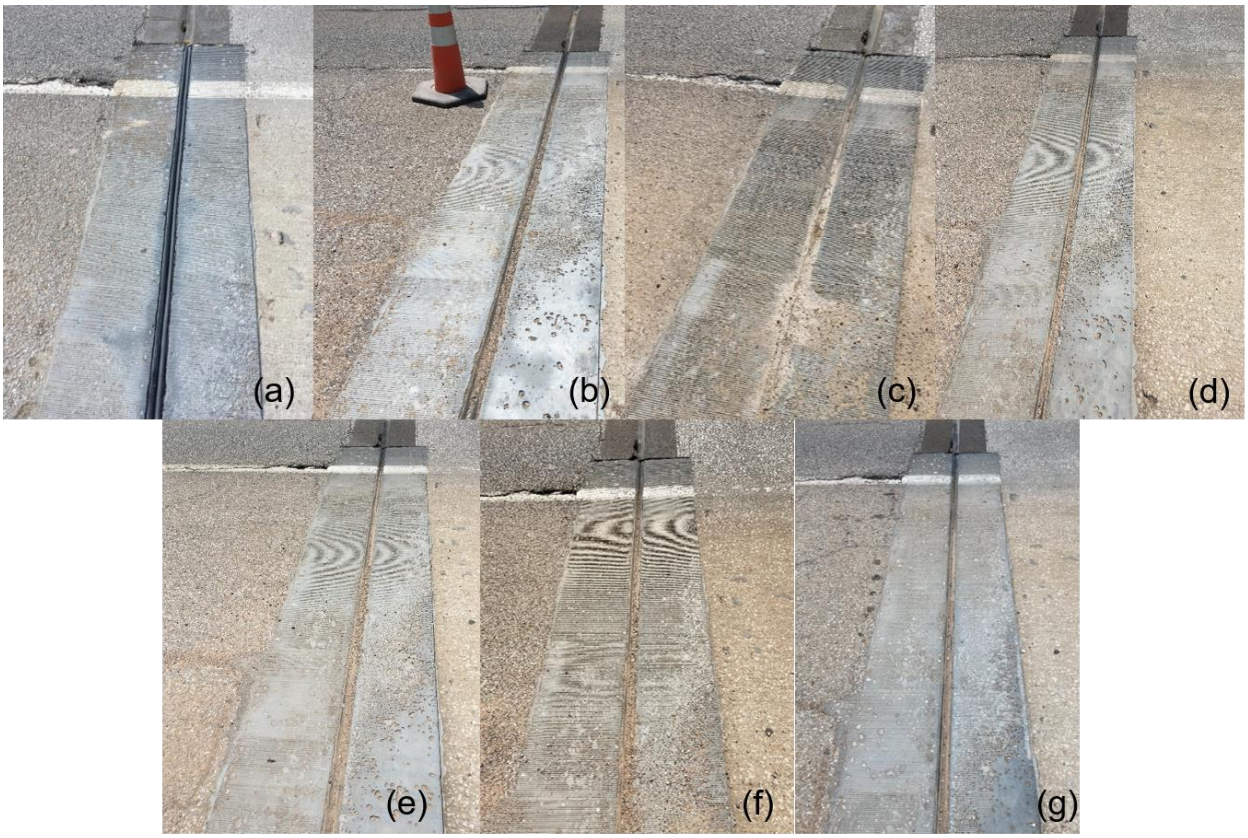

Figure 80. Photos of the UHPC joint on the SH-3E bridge over the North Canadian River (a) immediately after BEJS placement, on March 29, 2018 3 months after casting, (b) 7 months after casting, (c) 14 months after casting, (d) 21 months after casting, (e) 29 months after casting, (f) 33 months after casting, and (g) 45 months after casting

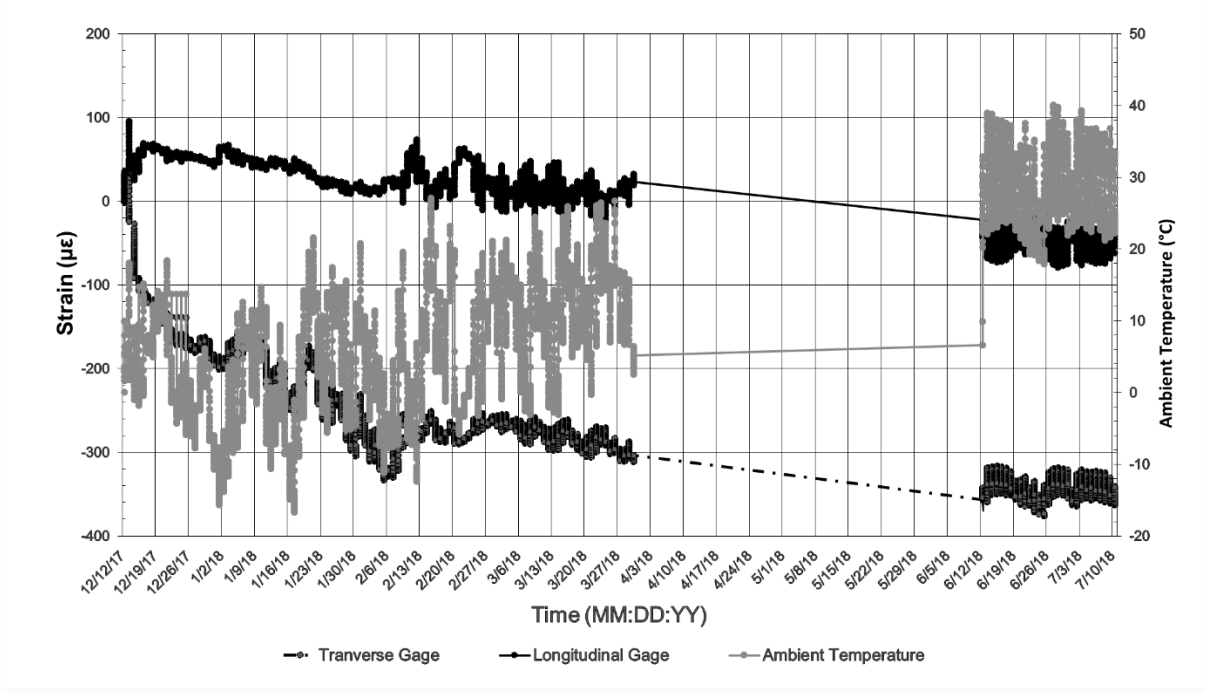

Figure 81. Strain measured in the UHPC material for approximately seven months after placement

4.4.2 U.S. 183/412 over Wolf Creek in Woodward County

The U.S. 183/412 bridge over Wolf Creek in Fort Supply in Woodward County (NBI No.: 21124) was selected for continuity connection repairs using UHPC. It was considered to be representative of a number of in-service bridges in Oklahoma that were designed using simply supported precast, prestressed concrete girders made continuous for live load with approximately 10 inch thick individual continuity joints connecting the two girder ends from each span. These joints were typically connected to the base of the girders using up-turned prestressing strands and mild steel bars and were cast simultaneously with the deck such that the deck reinforcement served as the negative moment reinforcement. Creep and shrinkage strain in the precast concrete girders over time combined with restraint of the system caused positive moments at the continuity joint locations. For many bridges, these moments were large enough to cause

cracking at the base of the continuity connections such as that shown for the Wolf Creek bridge in Figure 82. All continuity connections were demolished from the Wolf Creek bridge and replaced with a proprietary UHPC material. Load tests were conducted before and after retrofit of the bridge to evaluate the effectiveness of the repair at restoring continuity.

Figure 82. Example of positive moment cracking in a continuity joint of the U.S. 183/412 bridge over Wolf Creek

The Wolf Creek bridge was constructed in 1985 and carries U.S. 183/412 and crosses over Wolf Creek in Fort Supply, OK. A plan view and a cross-section of the bridge are shown in Figure 83 and Figure 84. Each of the five spans consists of five AASHTO Type IV girders spanning approximately 85 feet at a 9.75 feet spacing and a 9.25 inch thick deck. Spans one and five are simply supported, while spans two through four are connected at piers 2 and 3 with continuity joints. There are a total of ten continuity joints which only connect the individual girders and do not connect the adjacent five girders across the width of the bridge as a diaphragm. Damage similar to

that shown in Figure 82 was seen in all ten joints in the bridge. The bridge load rating had therefore been reduced assuming loss of continuity.

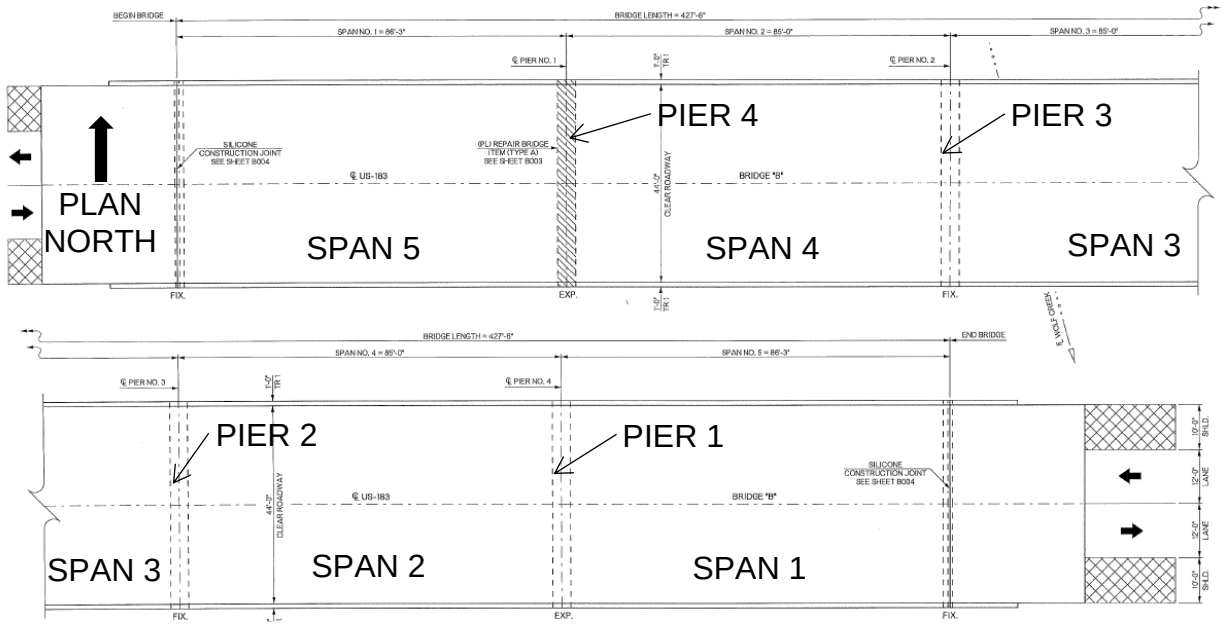

Figure 83. Plan view of U.S. 183/412 over Wolf Creek bridge

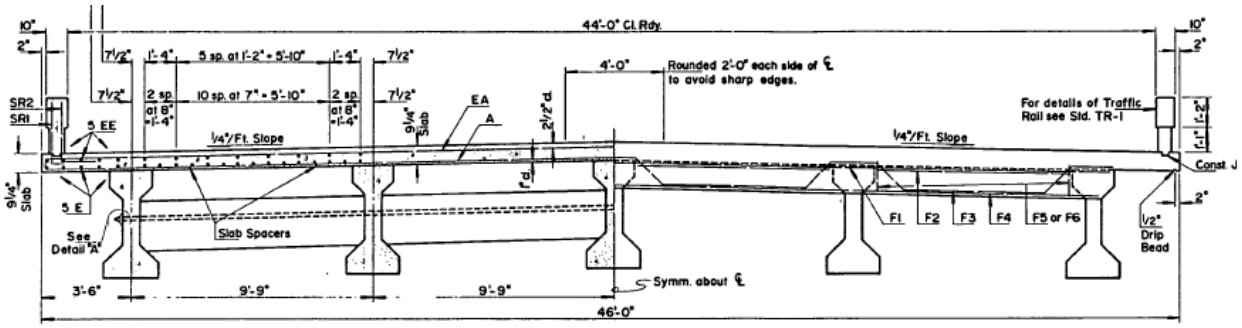

Figure 84. Cross-section view of U.S. 183/412 over Wolf Creek bridge

The original details used for the joint construction are shown in Figure 85. To construct the joint, the girders were placed on the pier cap with their ends 10 inches apart. Six prestressing strands at the bottom of the girder extended a length of 3 feet past the girder ends and were bent at a 90° angle approximately 6 inches from the girder face. At the top of the joint, six No. 4 Grade 60 reinforcing bars that were bent to a 90° angle were placed at the top of the joint with the 18 inch leg tied to the bottom deck bars and the 32 inch leg extending down into the joint. Six straight 18 inch long

bars were placed perpendicular to the girder span with two at the top and bottom and two in the middle. The joint was formed to be the same width as the top flange of the girder with that width extending down until it intersected the bottom flange, then the joint was formed to match the contour of the bottom flange.

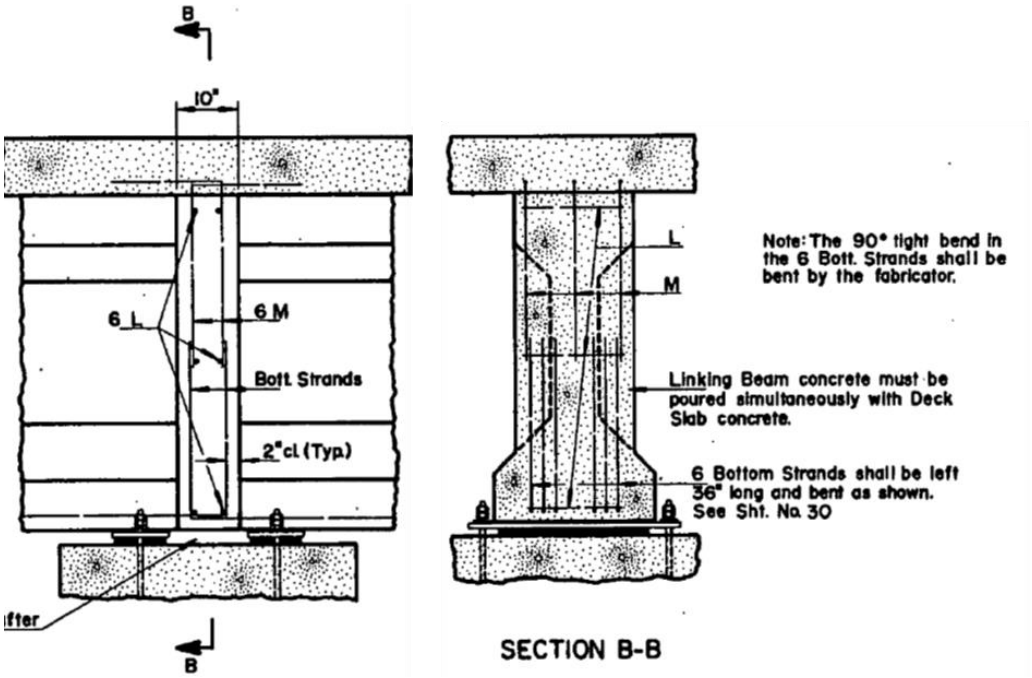

Figure 85. U.S. 183/412 over Wolf Creek continuity joint details from original drawings

4.4.3.1 Load Test Procedure

Displacement measurements were taken at the center of span 4 on all five girders during controlled load tests conducted before and after repair to assess the continuity of the spans at each girder location. The primary measurement method involved using Craftsman® Laser Distance Measurers, and secondary measurements were taken using plumb bobs hung from each girder and with a surveying level. Additional detail on the load testing measurement methods is available in Floyd et al. (2021b) and (Looney et al. 2021). An overall view of the measurement setup is shown in Figure 86.

Figure 86. Laser measurer and plumb bob setup (left), clamp on the girder bottom (middle), and method used for measurement with the plumb bob (right)

The girders were numbered with girder 1 being on the south side of the deck and girder 5 being on the north side of the deck. The bridge was loaded using two dump trucks filled with approximately 12 yd^3 of 3/8 in. crushed stone. The trucks were measured to ensure that the center of the truck's wheelbase was placed at the center of the span under consideration for each load stage. Table 2 shows the dimensions and weights of the trucks. Note that Truck 2 was the same truck for both tests.

Table 2. Truck Information

Truck	Truck 1 Pre-Repair	Truck 2 Pre-Repair	Truck 1 Post-Repair	Truck 2 Post-Repair
ID	86-5048	86-4891	86-5114	86-4891
Weight (lb)	50780	51060	55260	55880

Initial measurements were taken prior to truck placement as a starting point for the bridge. Flaggers were used to reduce traffic to one lane through the duration of the load test. Traffic was restricted to the north lane and the loaded trucks placed in the south lane throughout testing. Care was taken to ensure deflection readings were taken when no additional truck traffic was on the bridge along with the loaded dump trucks.

During the load stages when both trucks were on the same span simultaneously, traffic was halted completely, and a truck was placed in each of the traffic lanes for the measurement. The trucks were staged at various locations on the bridge simultaneously to assess the level of continuity provided by the joint before and after repair. The truck locations at each load stage are shown in Figure 87. At each load stage, the trucks were stopped on the designated span such that the center axle was located at the midspan of the girders and a measurement was taken using each method. The initial measurement was then subtracted from each loaded measurement to obtain deflection. The trucks at Load Stage 6 are shown in Figure 88.

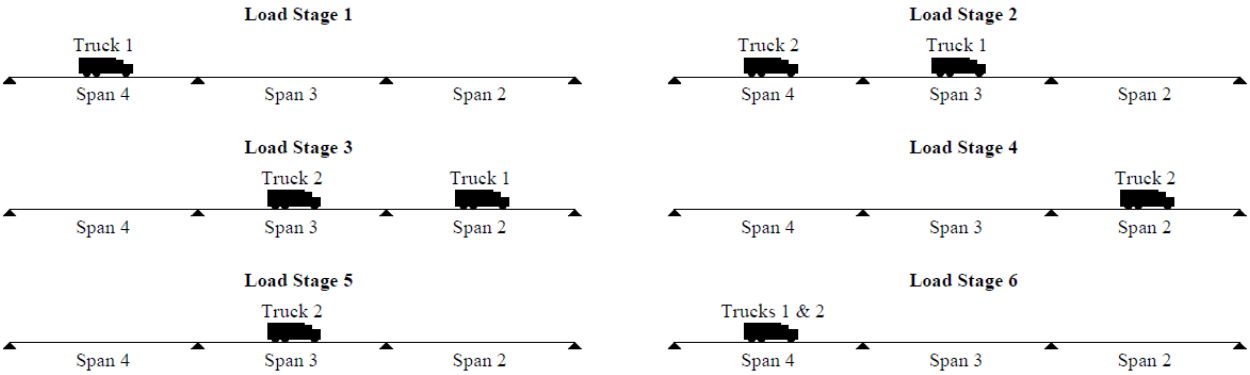

Figure 87. Truck locations for each load stage

Figure 88. Trucks located for Load Stage 6

The post-repair load test was conducted approximately one year after the joints were cast. The same measurement methods and load stages were employed on the second load test for direct comparison of test results. In addition, the two embedded strain gauges were used to collect strain data throughout testing.

4.4.3.2 Continuity Joint Instrumentation and Repair

After the existing continuity joints were completely demolished and before the UHPC was placed, researchers embedded a foil strain gauge and a vibrating wire strain gauge in the center and south exterior joints located at pier 3. Additional detail on gage placement is provided in Floyd et al. (2021b) and Looney et al. (2021), but the final gauge placement is shown in Figure 89.

Figure 89. Strain gauge placement in the joint

The proprietary UHPC product, Ductal®, was chosen for use in the continuity joints. Placement of the UHPC for the continuity connections was done in three pours on November 6, 8, and 20, 2019. At least one representative from the OU research

team was on site to observe each pour and a representative from LafargeHolcim was present on site during all pours to direct mixing of the Ductal® UHPC, run fresh property tests, and cast compressive strength cylinder specimens. Bagged Ductal® premix was delivered to the site along with the associated steel fibers and high range water reducer and all materials were kept in a large storage container. The contractor provided the mixing water. All UHPC materials were heated to the temperatures specified on the plans using portable heaters placed at the opening of the storage container. Mixing water was warmed with a portable water tank heater. Water and steel fibers were weighed for each batch using a portable scale. The material was mixed in 750 lb batches (approximately 4.7 ft^3) using a high shear pan mixer rented from LafargeHolcim (Figure 90) that was placed on span 3 between the two continuity connection locations (piers 2 and 3). A backup mixer was also on site in case any problems were encountered with the first mixer.

Figure 90. High shear pan mixer in place on the bridge deck (left) and placement of UHPC materials in the mixer (right)

Since this project was the first time the contractor used UHPC, a test batch was conducted in cooperation with the Ductal® representative to familiarize the contractor with the mixing procedure, quality control testing, and workability. The trial batch was successfully completed with a 69° F temperature and 8 inch flow, and six compressive strength cylinders were cast.

The inside of the forms and the beam ends were prewetted using a garden sprayer placed through the pour holes. UHPC was poured into the continuity joints through 2.5 inch. holes cored through the top of the bridge deck centered on the joints. Since a minimum sacrificial 3/8 inch pour height was required above the top of the deck, a 1.5 inch tall piece of lumber with the same size hole was attached to the bridge deck to provide the additional height to the pour. The pour holes are shown in Figure 91. Initially the material was placed into the fill holes in the deck using a steel funnel as shown in Figure 92 but was eventually poured directly into the pour holes from the plastic five-gallon buckets used to transport the material from the mixer.

Figure 91. Pour holes for UHPC joints on the Wolf Creek bridge

Figure 92. Placement of UHPC into fill hole in the bridge deck

The joints were replaced in two stages to allow for traffic in one lane while the contractor worked on the other half of the bridge. Mobile traffic lights placed at each end of the bridge were used to automatically control traffic. The first stage of replacement was on four joints on the north side of the deck (two on pier 2 and two on pier 3) on November 6, 2019. Immediately after the test batch, a full batch was mixed to start pouring into the continuity joint forms. However, after filling approximately half of the first joint, the forms began to leak around the edges. The leak appeared to be caused by hydrostatic pressure that UHPC creates due to its tremendous flowability. Each joint was more than 5 feet tall which resulted in significant pressure on the bottom of the formwork. The contractor was unable to stop the leak, so the forms were removed, the joint was cleaned out, and the formwork replaced for a second attempt. Even though the material had been in the forms for over an hour, it flowed out of the continuity joint

formwork, off of the pier cap, and formed a puddle on the ground (Figure 93). Compressed air and a pressure washer were used immediately to clean the remaining material out of the joint. The forms were rebuilt and braces were wedged between the forms to force the forms against the girders and brace against lateral movement to reduce the chance of leaking. For the exterior girder the braces were supported by lumber directly attached to the deck soffit and to the girder bottom flange. The braced forms are shown in Figure 94.

Figure 93. UHPC from failed formwork

During the second attempt at pouring the four north joints, the foam board used to support the bottom of the form compressed under the weight of the UHPC as it was poured into two separate joints, which caused the joints to leak through the bottom seam. The contractor was able to wedge the bottom form into place quickly so very little material was lost. The remaining joints on the north pour were then filled without any additional issues. Wood bases were used in lieu of foam board for the second stage of six joints on the south half of the deck to ensure this issue did not occur again. Once the

UHPC reached at least 14,000 psi, the traffic lane was switched to allow the contractor to work on the remaining six continuity joints.

Figure 94. Final joint forms after adding bracing

The continuity connections on the southwest side of the bridge were cast on November 20, 2019 from a total of 9 full batches (750 lb each) and one-half batch. It began to rain during the next to last batch of UHPC, but the mixer was covered, the pour holes covered between placement, and no detrimental effects were observed. One form wall failed during the pour due to failure of a concrete anchor, but the contractor was able to reinstall the formwork for the affected joint while filling the other joints. Also, small leaks were observed on several joints at the form seams where it appeared the sealant used did not completely seal the seam. These leaks did not create a large loss of material and stopped soon after starting, likely due to blockages caused by the fibers.

Another issue that occurred during placement was constant settlement of the UHPC in the joints after the initial top-off of the forms. The material was poured into a 2.5 inch hole and the top flange of the girder was 20 inches wide, which left a 90° change in geometry along the bottom of the bridge deck. As the UHPC filling the joint reached the bottom of the bridge deck, air was trapped in the corners of the forms. Due

to its viscosity and slow setting time, the entrapped air took several hours to be released through the fill hole. This delay in air release caused the top of the pour to slowly settle after form top-off, leaving the top surface as much 8 inches below the top of deck in several joints. However, no joint settled below the bottom of the bridge deck, so each continuity joint was filled completely. A completed UHPC continuity joint is shown in Figure 95. Once the wood was removed from around the pour holes on the bridge deck, the contractor manually dug out the voided surface at the top of the UHPC pour then used Rapid Set® Concrete Mix to fill the holes to the top of the deck.

Figure 95. Completed UHPC continuity joint after form removal

4.4.3.3 UHPC Joint Construction Data

Eighteen compression test cylinders were cast for the first UHPC pour and shipped to the ODOT Materials Division for testing after being allowed to cure for three days. Testing was planned for 4, 7, 14, and 28 days along with six cylinders to be

provided to the OU research team for companion testing. At the time of the four-day tests it was discovered that the ODOT materials division cylinder grinder was not capable of grinding 3 inch by 6 inch cylinders. The 4-day cylinders were tested with only sawcutting used for end preparation resulting in a compressive strength of 10,010 psi, less than the required 14,000 psi. The cylinders were then transported to Fears Lab for grinding on day 5. The OU research team ground the remaining cylinders and returned them to ODOT Materials Division for testing. The OU research team tested a comparison cylinder at 5 days of age that achieved a compressive strength of 16,140 psi. Results of all compressive strength tests are shown in Table 3. The average 28-day compressive strength of the UHPC used for all of the joint pours was over 24,000 psi, and no individual test was below 21,700 psi. All joint material was able to reach the strength required for resumption of traffic and form removal after five days with no heat curing. The heat gain and ambient temperatures measured using the vibrating wire strain gages are shown plotted in Figure 96. The UHPC placement including the instrumented joints began at approximately 8:00 a.m. There is a slight increase in temperature upon initial curing, but the curing temperatures remained relatively low. This could be due to the colder ambient temperatures, as well as the tendency for UHPC to cure at a slower rate due to the high dosage of high range water reducing admixture (Floyd et al. 2020; Russell et al. 2013).

Table 3. Compressive strength test results for the UHPC used on Wolf Creek bridge

Concrete Age (days)	Casting 2, November 8, 2019 Tested at ODOT Lab (psi)	Casting 2, November 8, 2019 Tested OU (psi)	Casting 3, November 20, 2019 Tested at OU (psi)
3	NA	NA	11,100
4	10,010	NA	NA
5	NA	16,140	15,750
7	16,500	18,070	18,800
14	20,640	NA	19,780
28	24,110	NA	25,340

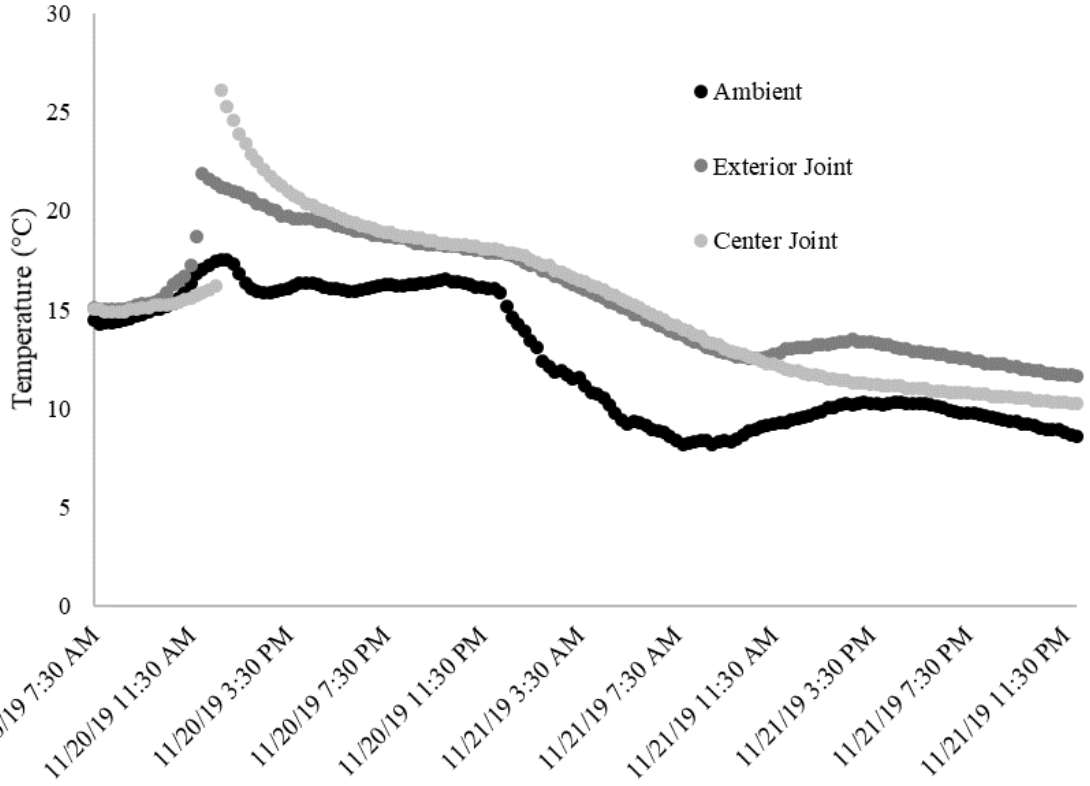

Figure 96. UHPC heat evolution for center and exterior joint on pier 3

4.4.3.4 Load Test Results

The midspan deflections obtained for span 4 using the laser distance measurers are shown in Figure 97. This Figure shows a comparison of results from each load stage before and after continuity joint replacement.

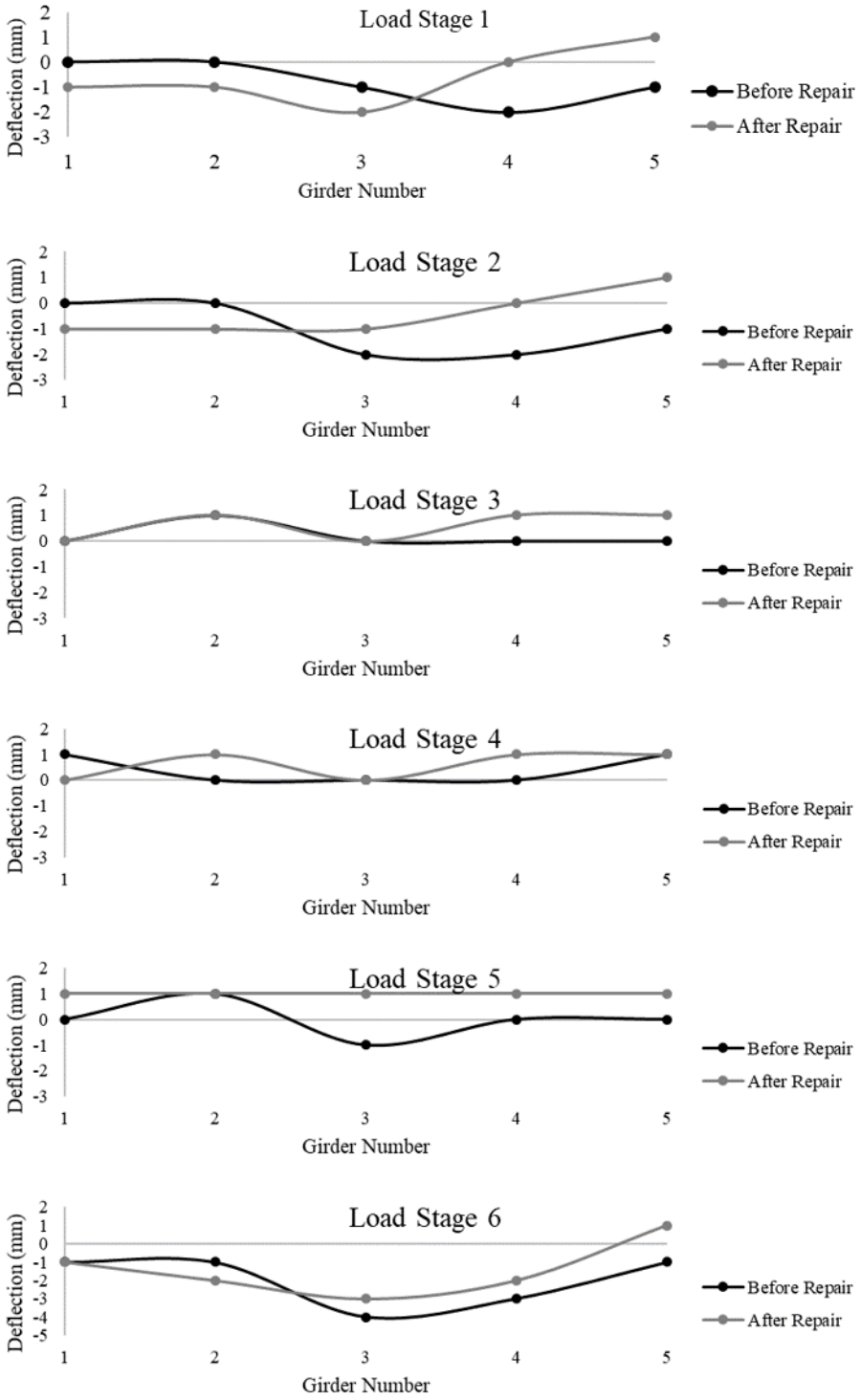

Figure 97. Span 4 midspan deflections during each of the six load stages

Due to the stiffness of the bridge, all measured deflections were very small. The largest deflection was observed on load stage 6 of the pre-repair load test, when both trucks were centered on span 4. Results from load stages 1 through 4 do not appear to

show a clear change in behavior due to joint repair. However, there does appear to be a change in behavior for load stages 5 and 6. There is a clear upward deflection measured for load stage 5 post-repair, which is the expected behavior of a continuous beam when loaded on the adjacent span. Also, there was generally less deflection measured in load stage 6 after the repair, which could indicate load sharing across the repaired joint, creating continuous behavior.

Since the measured deflections were so small, hand calculations were completed to verify the test results and are outlined in Floyd et al (2021) and Looney et al. (2021). When comparing the calculated values to the measured deflections, it appears that the original continuity joint was damaged enough to significantly reduce the level of continuity it provided. Furthermore, the measurements and calculations appear to show that the UHPC joints result in the girder system behaving as a continuous system.

The data collected from the embedded foil strain gauges are shown in Figure 98. Since one lane was left open to traffic during load stages 1 through 5, there was additional measured strain even after final truck placement, which is apparent in the spikes during the load stages. The spikes did not occur during load stage 6, since traffic was completely halted while a truck was placed in each lane. The strain values between spikes were averaged for each load stage to remove the effect of the local traffic and isolate the strain caused only by the trucks. In addition to the foil gauges, measurements from the vibrating wire strain gauges were manually collected at discrete points during each load stage. The average foil gauge and vibrating wire gauge readings are shown in Figure 99.

The same general trend was observed for each type of gauge and both sets of gauge readings tend to show continuous behavior. The two highest strains were recorded at load stages 2 and 6, which are the truck locations expected to produce the

highest moment transfer across the measured joint at pier 3. Also, at load stage 4, a positive moment is recorded by both gauges. This is also expected behavior at pier 3 when a truck is placed at the last span of a continuous three-span system. In all exterior joint readings, the foil gauge measurement was higher than the vibrating wire gauge. This was expected since the foil gauge was placed closer to the extreme edge of the cross-section. However, in all but one reading for the center joint the foil gauge reading was lower than the vibrating wire strain reading. Nevertheless, the data collected from each set of gauges display the same continuous behavior throughout the test providing evidence that the UHPC repair restored continuity for this bridge.

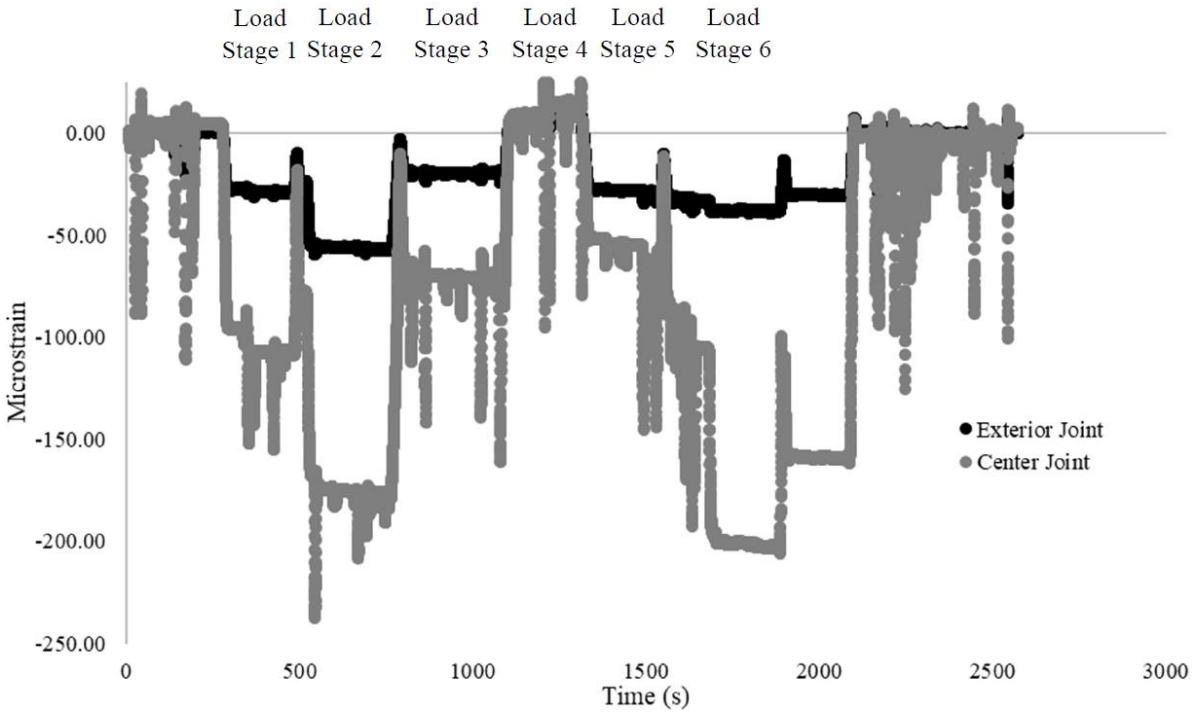

Figure 98. Foil strain gauge data for post-repair load test

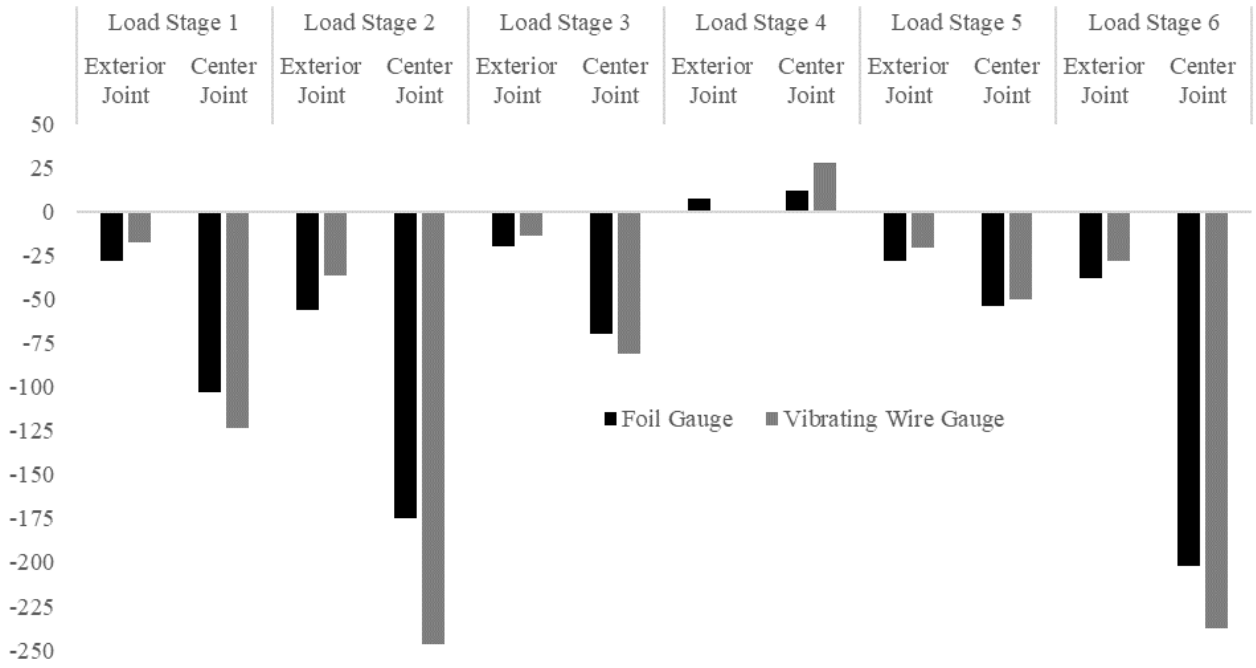

Figure 99. Collected average strain gauge readings

4.5 Tall Embankments on Soft Soils

The SH-3 bridges over the Burlington Northern Santa Fe (BNSF) railroad are located on the southern edge of Ada, Oklahoma. The five span twin bridges were built in 1980 and are oriented east to west. The span lengths are 53.27 ft – 72 ft – 72 ft – 72 ft – 72.27 ft from west to east. An aerial view of the bridges is shown in Figure 100.

Figure 100. SH-3 over BNSF Railroad; aerial overview

The bridges have experienced several problems related to interactions with the approach embankment. The distress was noted on inspection reports three years after the bridge was constructed. The distress included closed expansion joints, tilted roller bearings, and beams pushing against the abutment backwalls. The concrete slope wall had also buckled. It was hypothesized that the distress was the result of the approach embankment moving laterally towards the bridges. The lateral movement caused the expansion joints to close. Following this thermal movements damaged various bridge components. Photographs showing some of the distress are shown in Figure 101. This

bridge was initially monitored as part of SP&R 2228. During SP&R 2228 it was established that the most likely cause of the distress was approach embankment lateral movement. The bridge was further inspected as part of this project. Numerical modeling of the embankment and abutment was also completed as part of this current project.

Figure 101. SH-3 over BNSF: Bridge distress (a) closed expansion joint, (b) buckled slope wall, (c) cracked backwall, (d) sheared anchor bolt

4.5.1 Site Investigation

A geotechnical site investigation was carried out on March 11, 2020. The purpose of the site investigation was to gather soil samples and log borings to characterize the site stratigraphy and soils. Representative soils were tested to characterize the soil in the numerical modeling phase of the investigation. Three soil borings were drilled at the site. One boring (B-1) was located in the west embankment center median and two borings (B-2 & B-3) were located in the center median of the east embankment. The approximate locations of the borings are shown in Figure 102. The boring termination depths were 38.5 ft, 71.5 ft, and 63.5 ft for borings B-1, B-2, and B-3, respectively. The borings were extended to the top of bedrock. Bedrock was identified by SPT refusal. That is if for 50 blows the SPT did not advance 6 inches. SPT refusal was encountered in the embankment fill material as well. However, the borings were continued since it was known that the refusal at that location was not indicative of bedrock. The embankment fill materials encountered included an assortment of clay, sandstone, and sandy shale. The strength of the foundation soils varied considerably due to the presence of sandstone and shale that was used as part of the fill material. The foundation or native soils consisted of lean clay with cobbles. The bedrock encountered at the site was sandstone and limestone.

The borings were drilled using a CME 75 all-terrain mounted drill rig, with the drilling services provided by Drilling Services of Oklahoma. Wet rotary drilling methods were used to advance the borings. Sampling of the soil was completed using the SPT (ASTM-D1586 2011) with a split spoon sampler and 3 inch outer diameter thin wall tube sampling (ASTM-D1587 2008). Boring logs from the site investigation showing the in-

situ testing that was conducted as well as the results of index tests completed on the samples can be found in Appendix C.

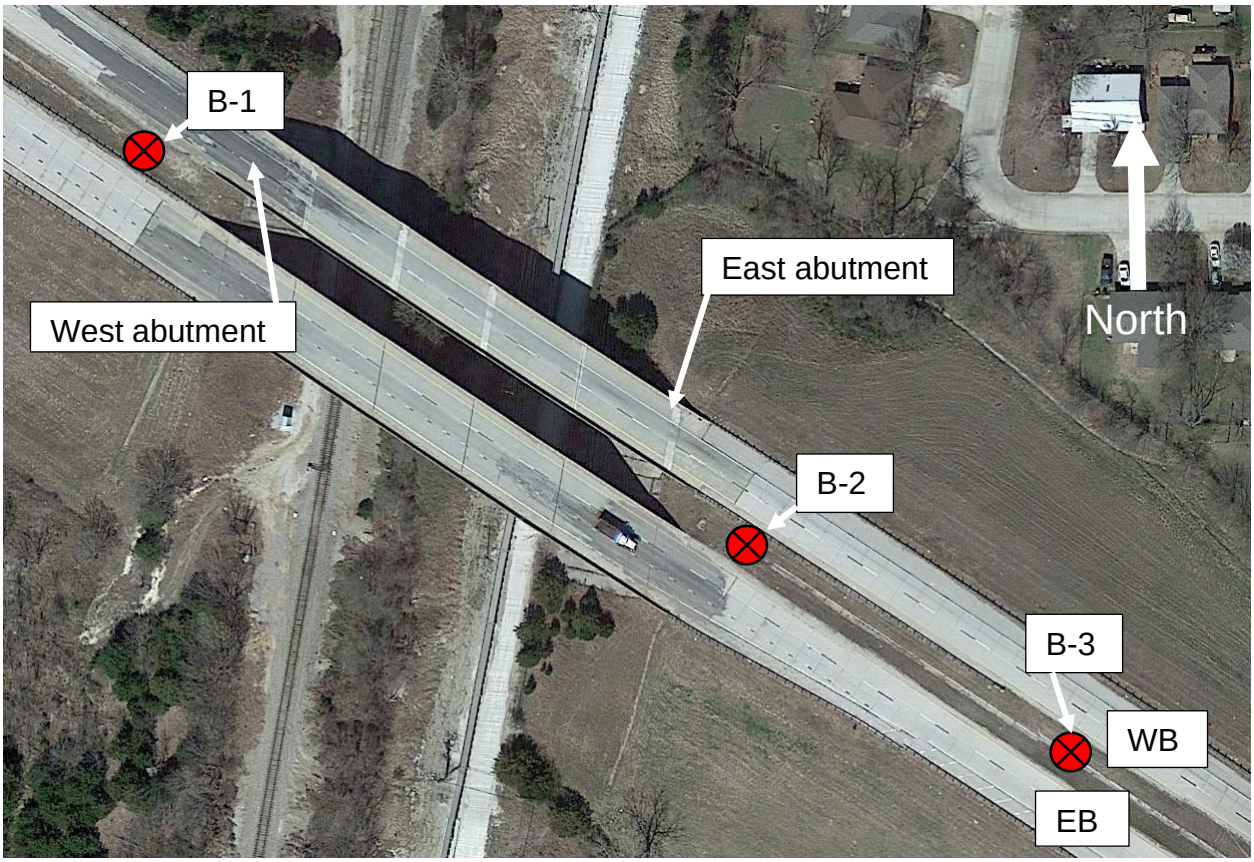

Figure 102. SH-3 over BNSF: Boring locations

The collected samples were tested at the University of Oklahoma following the site investigation. The lab testing included the following:

- Moisture content tests (ASTM-D2216 1998) for all collected samples
- Atterberg limits tests (ASTM-D4318 2005) for select samples
- Finer than 75 µm sieve by washing tests (ASTM-D1140 2017) for select samples
- One-dimensional consolidation tests (ASTM D2435 2010) for select undisturbed samples
- Consolidated undrained triaxial tests (ASTM-D4767 2011) for select undisturbed samples

Results from the moisture content, Atterberg limits, and washed sieve tests are included on the boring logs in Appendix C. Results from the one-dimensional consolidation and triaxial tests are included in Appendix D. Most of the triaxial testing completed were in compression, but one sample was tested in extension as well. The tests were necessary to calibrate the soil model used during the numerical modeling phase of the investigation.

4.5.2 Numerical Analysis

The SH-3 over BNSF Railroad bridge abutment and embankments were modeled using the finite element method. The numerical analyses were used to better understand the behavior of tall embankments founded on soft soils. For these analyses, the finite element software PLAXIS 2D (PLAXIS 2020) was used. These analyses assumed plane strain conditions. These analyses were fully coupled. Fully coupled analysis calculates the pore water pressures and soil deformation simultaneously. Fully coupled analysis is the most realistic analysis offered in PLAXIS 2D.

An important factor in any finite element analysis is the selection of the soil constitutive model, also known as the material model. Soil is a highly non-linear time dependent material. Due to this complex behavior a single generalized model does not exist for all soils. Rather soil models are tailored to a specific category of soil or loading conditions (Whittle and Kavvadas 1994). For the behavior observed at SH-3 over BNSF Railroad a model capable of modeling lightly overconsolidated soils accurately was needed. One such model is the bounding surface plasticity model developed by Dafalias and Herrmann (1986). An added advantage of using this model is the authors' familiarity with the model. The model is not available in PLAXIS 2D. Therefore, the model had to be implemented within PLAXIS 2D. The implementation was verified using

the legacy finite element program SAC-2 (Herrmann and Mish 1983) and a single element program, EVALK (Kaliakin and Herrmann 1991). A brief description of the soil model follows.

4.5.2.1 Bounding Surface Plasticity Model; Dafalias and Herrmann (1986)

The Bounding Surface model was developed within the framework of critical state soil mechanics. One of the major advantages of the model is that it allows for plastic deformation within the bounding surface during loading. Including plastic deformation within the bounding surface allows for more realistic prediction capabilities. During unloading the behavior is elastic but plastic deformation is allowed once reloading begins.

The bounding surface for the model is composed of three parts, two ellipses and a hyperbola. A schematic of the model in stress invariant space is shown in Figure 103.

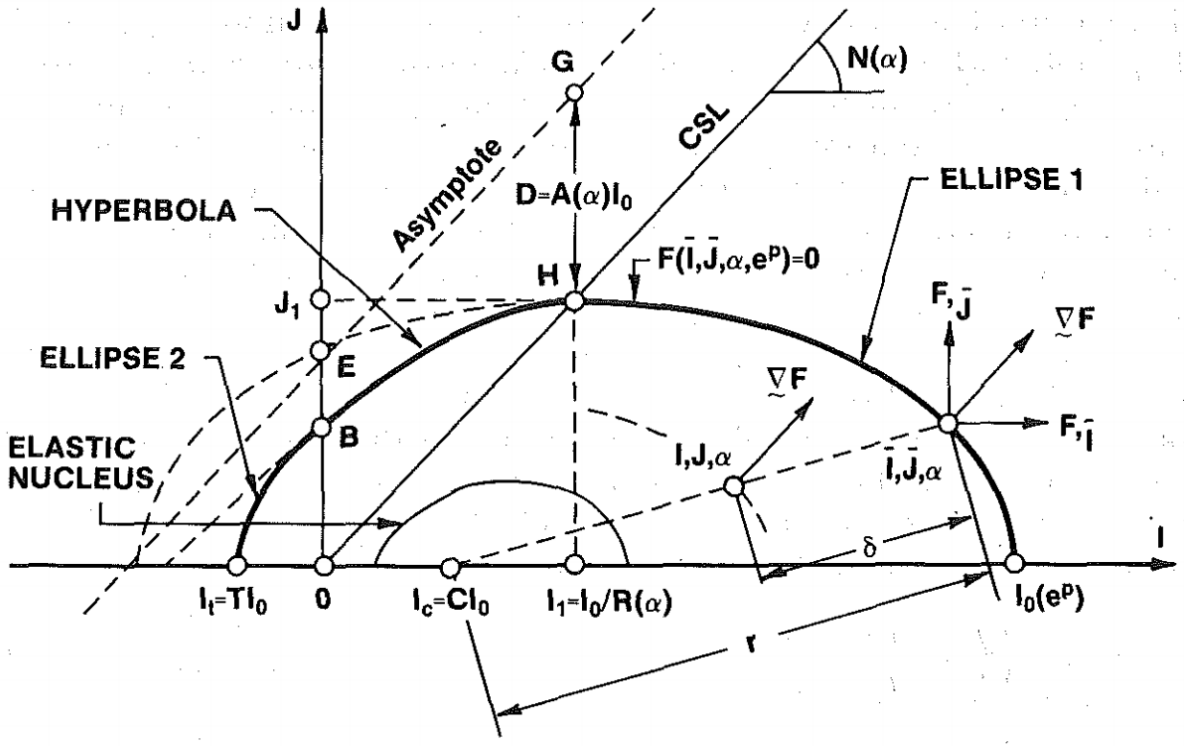

Figure 103. Schematic illustration of bounding surface model, from Dafalias and Herrmann (1986)

The bounding surface is a function of the current stress state, expressed in terms of invariants, as mapped onto the bounding surface, denoted by $\bar{I}$ and $\bar{J}$, the lode angle α and the plastic void ratio e^p. The bar over I and J represent the image of the current stress state projected onto the surface. The image point is determined using a simple radial rule: a straight line connecting the current stress state (I, J) and the project center (I_c) is extended to the bounding surface. The amount of plastic strain is related to the distance between the current stress state and the bounding surface, denoted as δ. As the magnitude of δ decreases the amount of plastic strain increases. The initial size of the bounding surface, I_0, is based on the initial vertical and horizontal stresses as well as the over consolidation ratio. For a full description of the model see Dafalias and Herrmann (1986).

4.5.2.2 Model Parameters

The bounding surface model has a well-established calibration procedure. This procedure is presented by Kaliakin et al. (1987). The calibration involved determining the traditional model parameters (λ, κ, M_c, M_e, and ν) from the results of one-dimensional consolidation tests and undrained triaxial compression and extension tests. The remaining parameters were determined using curve fitting techniques. This was accomplished by systematically varying the parameters and comparing the resultant graphs. The adopted soil parameters and parameter definitions are shown in Table 4.

Table 4. Adopted Soil Parameters

Property	Soft Clay	Stiff Clay	Embankment
Traditional model parameters			
Slope of isotropic consolidation line in e – ln p' plot, λ	0.076	0.056	0.06
Slope of elastic rebound line in e – ln p' plot, κ	0.026	0.02	0.01
Slope of critical state line in q – p' space (compression), M_c	1.25	0.95	1.0
Slope of critical state line in q – p' space (extension), M_e	1.0	0.77	1.0
Poisson's ratio, ν	0.2	0.2	0.3
Bounding surface configuration parameters			
Value of parameter defining ellipse 1 in compression, R_c	1.5	1.6	2.0
Value of parameter defining ellipse 1 in extension, R_e	1.65	1.6	2.0
Value of parameter defining hyperbolic portion in compression, A_c	0.07	0.125	0.2
Value of parameter defining hyperbolic portion in extension, A_e	0.077	0.125	0.2
Value of parameter defining ellipse 2 (purely tensile zone), T	0.1	0.1	0.1
Projection center parameter, C	0.6	0.6	0.5
Elastic zone parameter, S	1.2	1.0	1.75
Hardening Parameters			
Positive material constant, m	0.02	0.02	0.02
Shape hardening parameter in triaxial compression, h_c	20	40	50
Shape hardening parameter in triaxial extension, h_e	20	40	50
Shape hardening parameter for states near I axis, h_2	20	10	50

Note: e, void ratio; p' and q, stress state variables in triaxial space, where $p' = (\sigma'_1 + 2\sigma'_3)/3$, $q = \sigma'_1 - \sigma'_3$, and σ'_1 and σ'_3 are the principle effective stresses.

The overconsolidation ratio (OCR) of the foundation soil prior to the embankment construction is not known. However, based on the qualitative description from the original bridge plans the top layer of soil is described as soft so an OCR of 1.2 was adopted. The bottom layer of soil is described as stiff so an OCR of 5.2 was adopted.

The bridge piles were characterized as a linear elastic material. According to the bridge plans the piles used to support the abutment are standard HP 10x42 piles. The bridge abutment was characterized as a linear elastic rigid plate. The plates were connected to the tops of the piles with a fixed connection. The values used to characterize the bridge piles and abutment are shown in Table 5 and 6, respectively. Note that the analysis parameters were selected using SI units. This causes their Imperial counterparts to not be very rounded numbers. The analyses parameters converted to Imperial units are shown in the tables. Since the analyses were all plane strain the distance between piles is indicated by the spacing parameter. The program updates the stiffness of the pile-soil zone based on the out of plane spacing of the piles. The bridge abutment is supported by either a straight or battered pile every 6.5 feet. The only way to capture the alternating straight and battered piles was to place them together in the same plane and change the spacing to 13 feet.

Table 5. Parameter Values for Abutment Piles

Properties	Values
Modulus of elasticity, E (ksf)	417,708
Unit weight, γ (pcf)	360
Area, A (in^2)	12.38
Moment of inertia, I (in^4)	208.8
Spacing, S (ft)	13

Table 6. Parameter Values for Abutment Plates

Properties	Values
Normal stiffness, EA (k/ft)	1,370,435
Flexural rigidity, EI (k-ft/ft)	1,231,728
Equivalent thickness, D (ft)	3.28
Weight, W (lb/ft/ft)	1713
Poisson's ration, ν	0.15

4.5.2.3 Finite Element Model

The bridge embankments were modeled individually (Figure 104). The embankments are approximately 215 feet apart when measured at the toe of the embankment. Through preliminary analysis this distance was determined to be large enough that one embankment would not influence the other. Modeling the embankments separately allows a finer mesh to be created. PLAXIS 2D uses an automatic mesh generator that is impacted by the project dimensions. In general, as the project dimensions increase the element sizes also increase.

The horizontal boundary opposite the abutment was set approximately 330 feet away from the embankment crest. This distance was determined to be far enough away to negate any influence from the boundary. Horizontal displacements were set to zero on the left and right boundaries. Horizontal and vertical displacements were set to zero along the bottom boundary. The groundwater table was placed at the base of the embankment. The water table is expected to fluctuate with the season, however standing water has been observed at the foot of the embankment during some of site visits.

The soil was modeled using six-node triangular elements. The bridge piles were modeled using one-dimensional beam elements with three degrees of freedom per node, two translational and one rotational. The mesh used for the east embankment contained 769 elements and 1742 nodes. The mesh for the west embankment contained 603 elements and 1400 nodes.

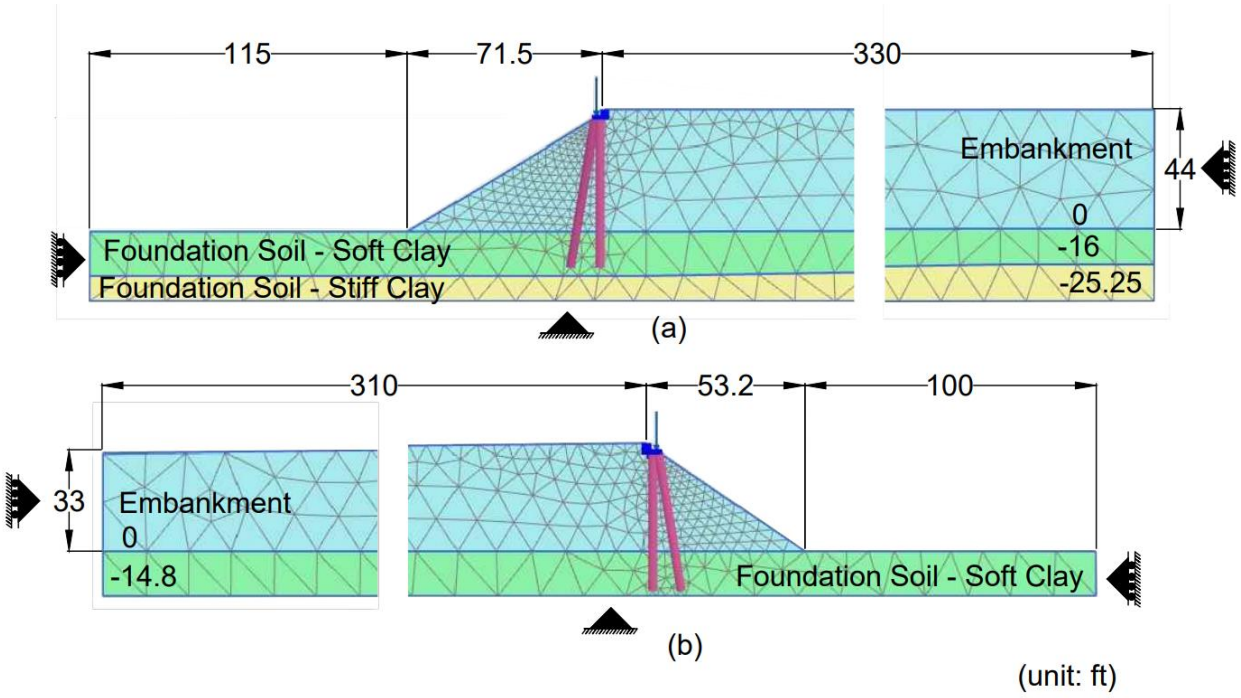

Figure 104. SH-3 over BNSF Railroad: Finite element mesh
(a) east embankment, (b) west embankment

4.5.2.4 Simulation Results

With respect to the current project, the main simulation results of interest are the lateral and vertical deformation of the embankments. The settlement as measured from the bridge seat with respect to time is shown in Figure 105. The lateral displacement as measured from the bridge seat is shown in Figure 106. The time on the horizontal axis represents the time post construction. Any construction movements were reset during the analysis. This was done so that the model would be representative of a completed embankment in the field.

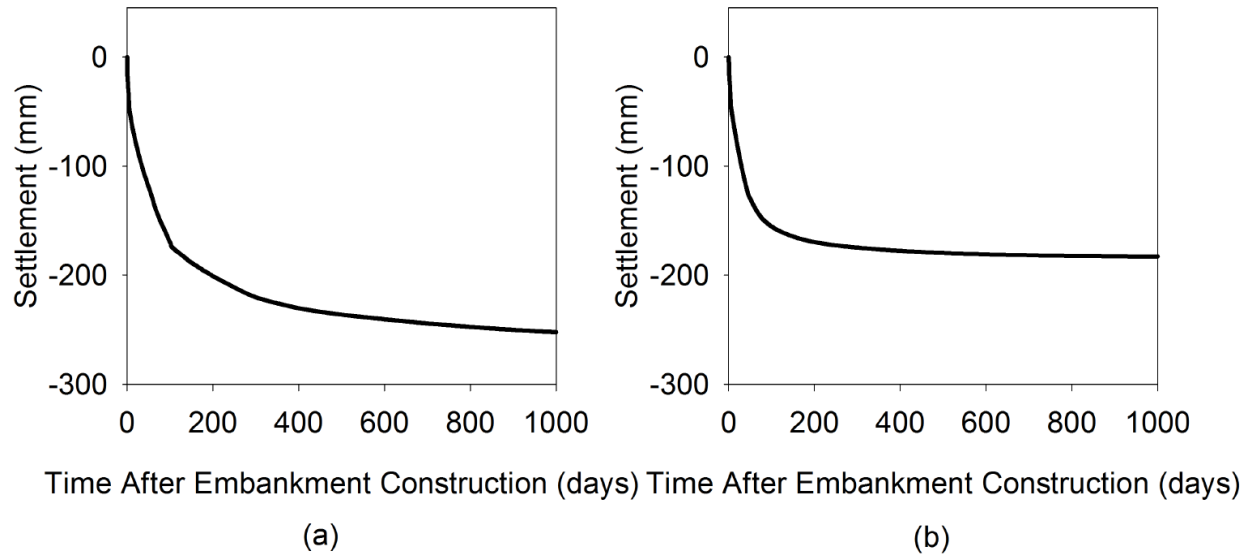

Figure 105. SH-3 over BNSF Railway: simulated settlement
(a) east embankment, (b) west embankment

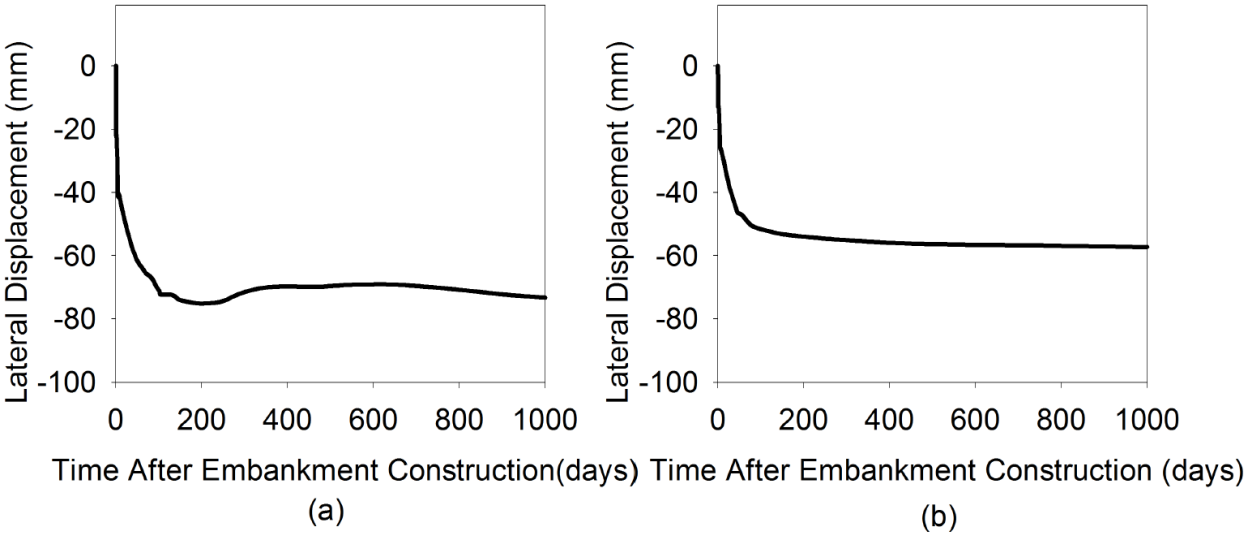

Figure 106. SH-3 over BNSF Railway: simulated lateral displacement
(a) east embankment, (b) west embankment

The settlement isochrones at the end of the analysis are shown in Figure 107 and Figure 108 for the east and west embankment, respectively. The maximum settlement is located around the sloped portion of the embankment. Most of the settlement occurs in the upper soft layer of the foundation soils.

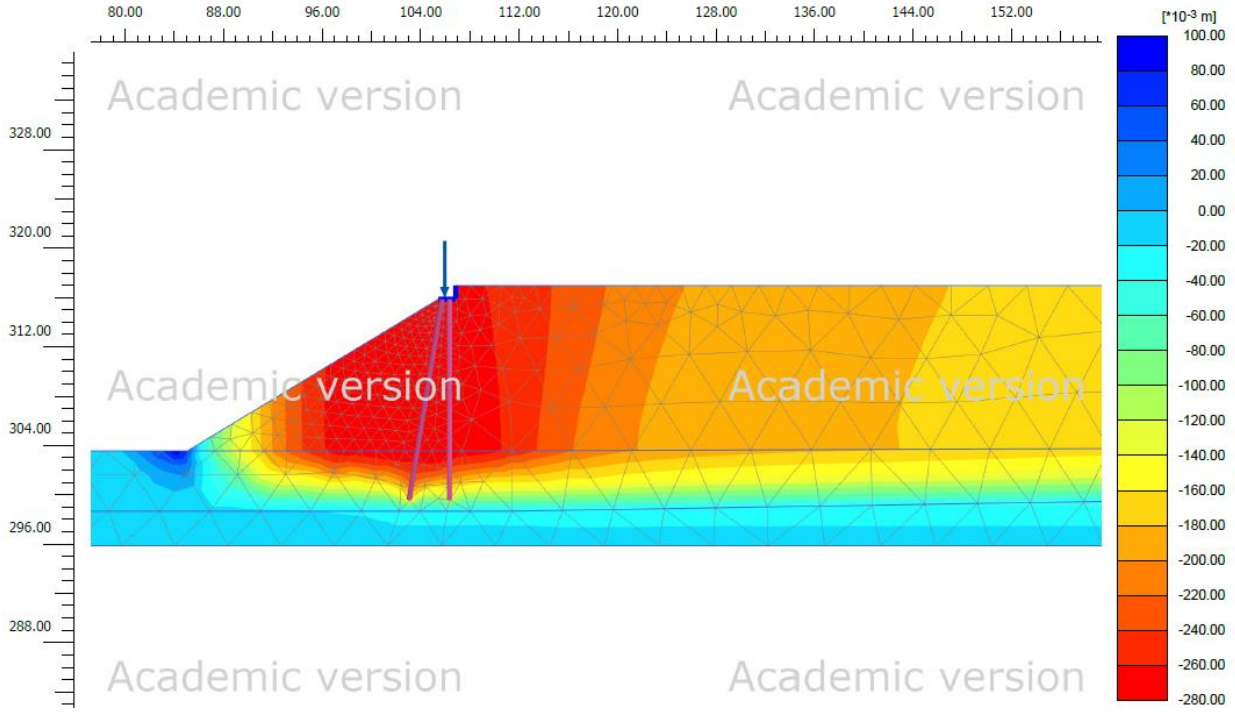

Figure 107. SH-3 over BNSF Railroad: Settlement isochrones – east embankment

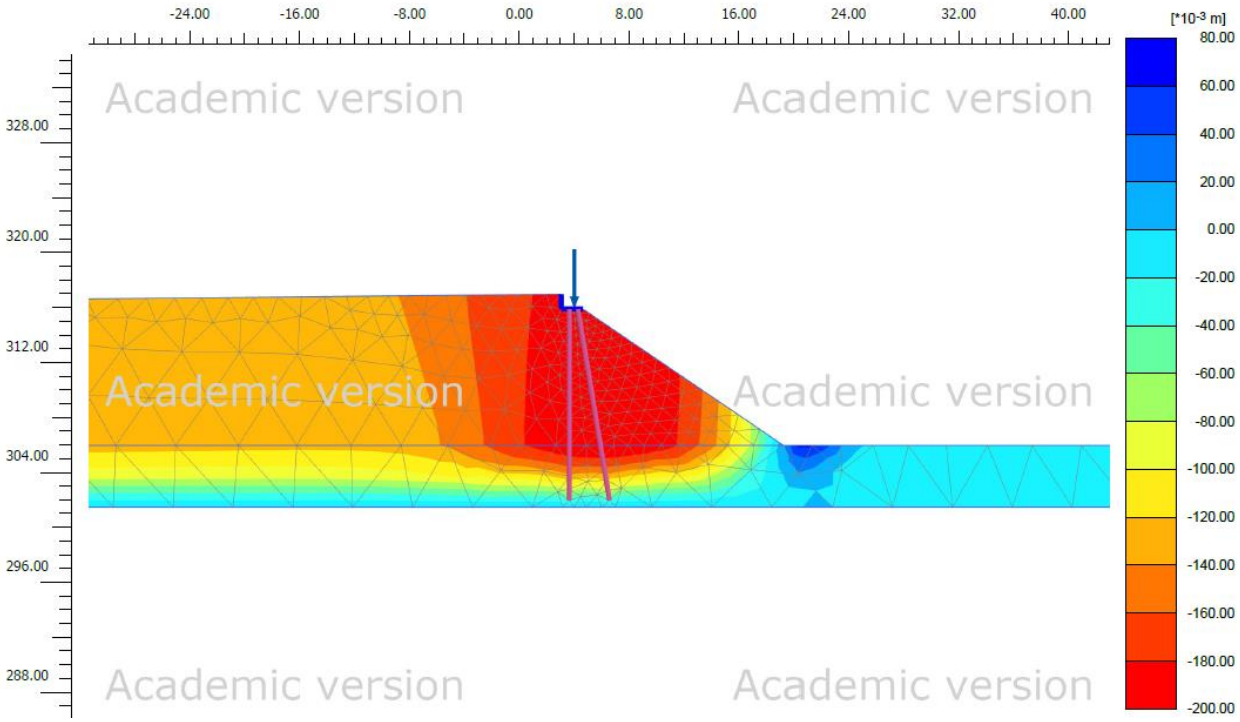

Figure 108. SH-3 over BNSF Railroad: Settlement isochrones – west embankment

The lateral deformation isochrones at the end of the analysis are shown in Figure 109 and Figure 110 for the east and west embankments, respectively. In both embankments the maximum lateral deformation occurs at the toe of the embankment. The deformation isochrones show that the sloped end of the embankment is essentially carried by the movement in the soft clay layer. The piles were terminated in the soft clay layer according to the as built plans. The piles were likely terminated right on top of the bottom stiff clay layer. This causes the piles and abutment to also be carried along with the embankment. A pinning effect may be realized if the piles are driven into the hard stratum. This lateral movement is suspected to have played a key role in initially closing the bridge expansion joints.

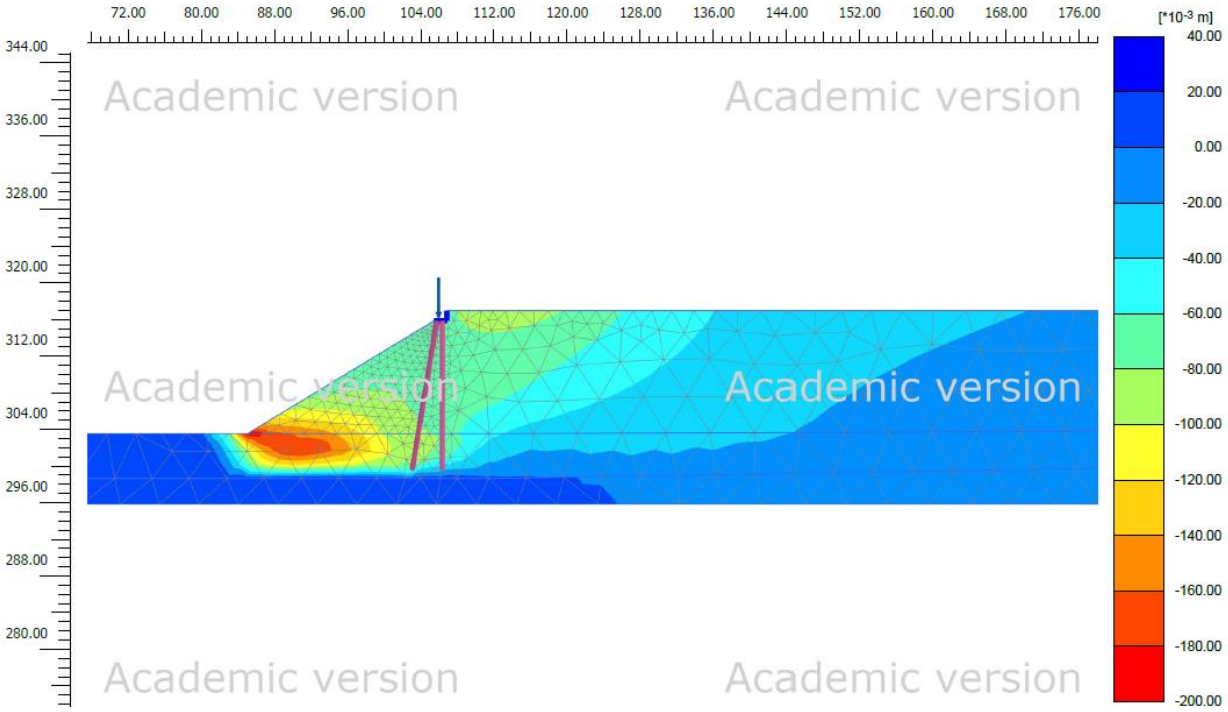

Figure 109. SH-3 over BNSF Railroad: Lateral deformation isochrones – east embankment

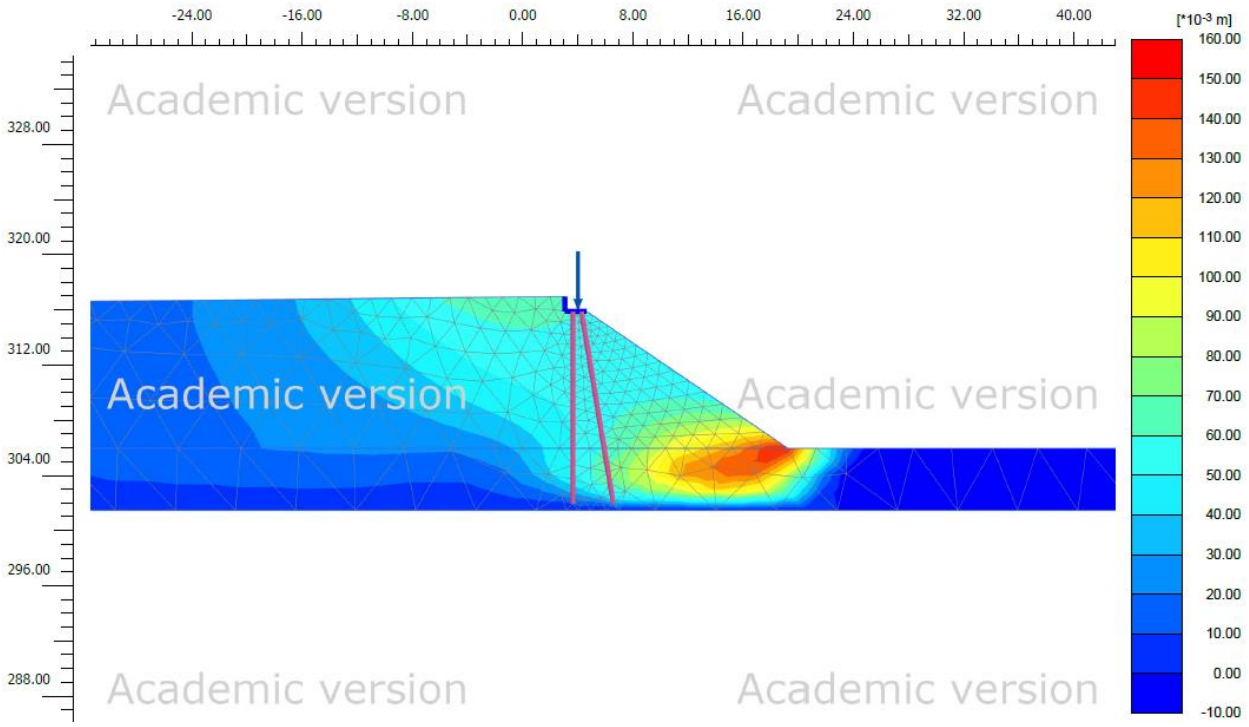

Figure 110. SH-3 over BNSF Railroad: lateral deformation isochrones – west embankment

4.6 Observations of Oklahoma Bridge Drainage Systems

In a previous study conducted by the University of Oklahoma (Miller et al. 2013), 58 bridge approaches were surveilled to study issues related to bridge approach settlement. It was observed that nearly all of the bridges had issues related to drainage. These included lack of surface seals between slabs or between the approach slab and wing walls, which was observed at 84% of the bridges. Cracks in approach slabs that also permitted ingress of water to areas below the approach pavements were observed at about 43% of the bridges. Additionally, 10% of the bridges had blocked outlet drains coming from the backfill drainage system and 7% of the bridges had surface drainage channels that were impaired. Concrete drainage channels were observed to have collapsed into voids created by undermining.

Other common problems observed at the 58 bridge approaches examined were voids caused by undermining of abutments and approach slabs. Approximately 21% of the bridges visited had visible voids under the approach slabs. Figure 111 shows a void under an approach slab observed at the bridge on SH6 over Sadler Creek and another at SH59A over Big Creek. These voids may form in part from settlement of underlying soil, but once created are a preferential flow path for water and erosion. Note also that not all approach slabs allow for direct visual observation of voids so the 21% number could be higher.

Figure 111. Void beneath approach slab and possible path for water flow (black arrow) at bridge over Sadler Creek (left photo), and another under the approach slab at SH59A over Big Creek (right photo)

At 29% of the 58 bridges, erosion under the abutments could be observed, although again the percentage could be greater because sometimes the bottom of the abutment was obscured, such as by rip rap. Examples of the type of erosion observed are shown in Figure 112. As noted, the erosion can become quite severe once it begins. Also note the exposed piling in these photos.

Figure 112. Erosion observed under abutment at Bridge B on US177 over the Salt Fork River (left photo) and at the bridge on SH152 over Willow Creek (right photo)

To get a better understanding of the cause of erosion under the abutment, the backfill drainage detail for bridges exhibiting this problem were examined. Figure 113 through Figure 115 show details for three bridge abutment drainage systems associated with erosion under the abutments. While each of these designs have some differences relative to the backfill type and abutment style, they all have a similar underdrain placement at the base of abutment. It is believed that this placement represents an inherent design flaw in these drainage systems, as will be discussed subsequently.

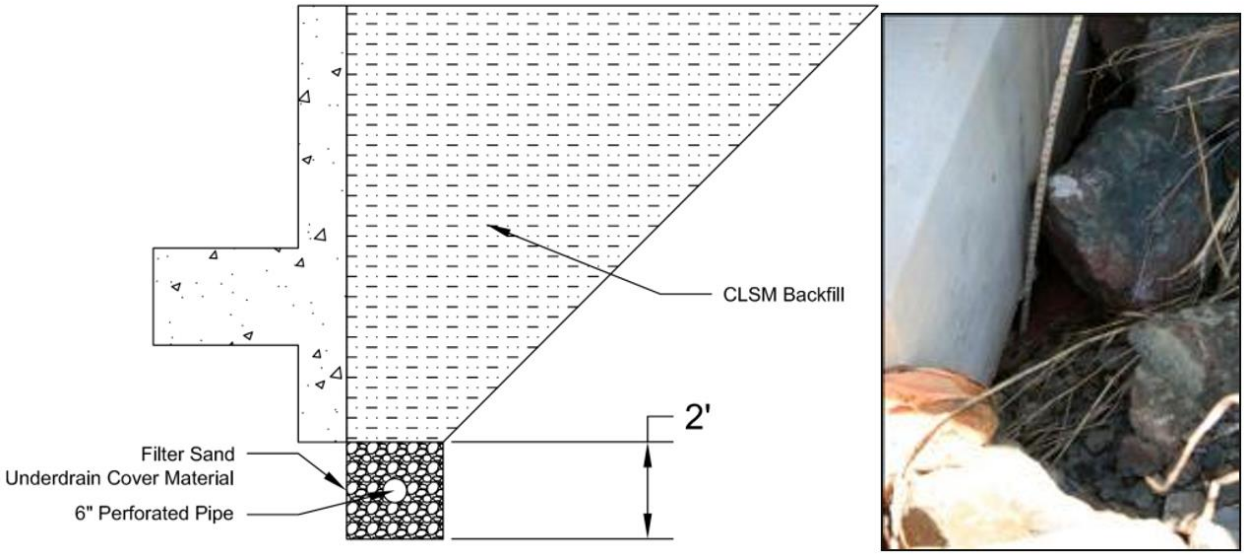

Figure 113. Underdrain design, after ODOT Proposed Plan for S.H. 3W over Big Creek

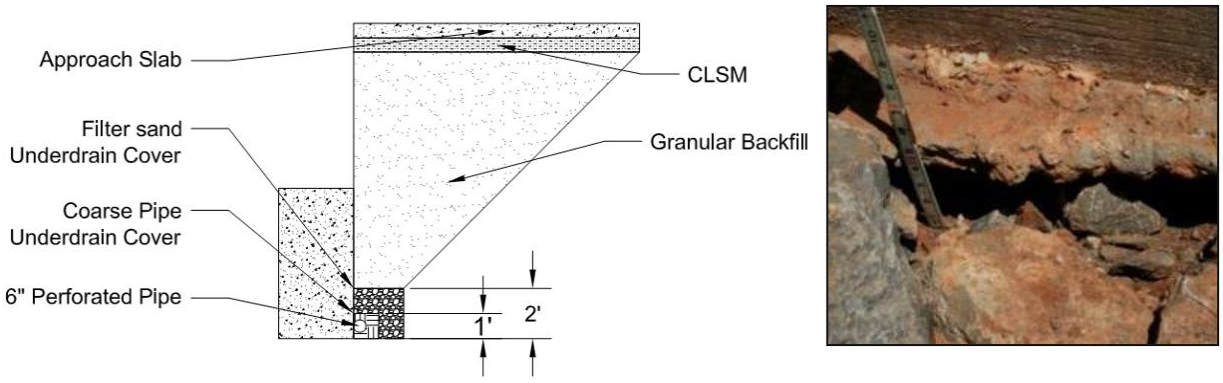

Figure 114. Underdrain Design, after ODOT Proposed Plan for S.H. 6 over West Elk Creek

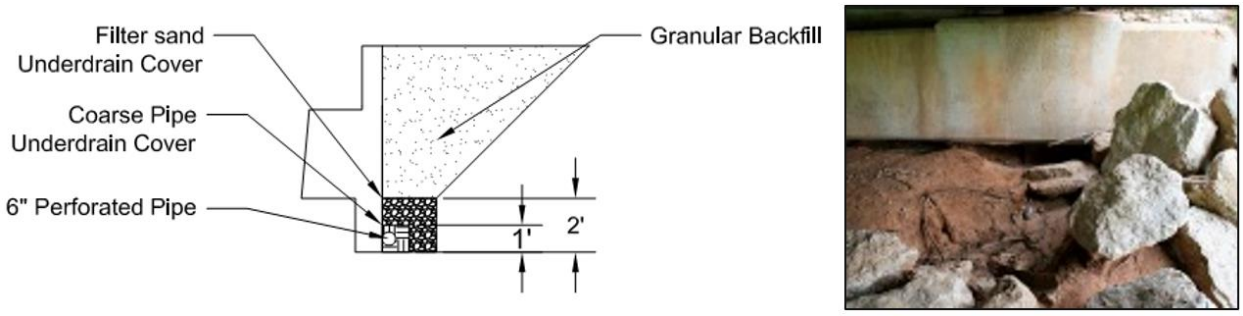

Figure 115. Underdrain Design, after ODOT Proposed Plan US 177 over Salt Fork, Bridge A

As a comparison, two examples of drainage designs that appear to prevent erosion under the abutment were also examined as shown in Figure 116 and Figure 117. While these details are different, what they both have in commons is a water barrier that prevents water from flowing from the drainage system under the abutment. In Figure 116 a neoprene sheet extends under the underdrain and is bonded to the abutment, whereas in Figure 117 the abutment footing acts as a water barrier.

In comparison, it is seen that the details associated with erosion under the abutment in Figure 113 through Figure 115 do not include a measure to prevent water flowing from the underdrain under the abutment. This essentially leads to a short circuit of water from the underdrain under the abutment leading to erosion. The concept is illustrated in Figure 118. The problem is due to differential settlement between the embankment soil and abutment. The abutment is pile supported and not expected to settle much; however, all embankment soils will settle under their own self-weight and from compression of the underlying foundation materials. Even if this settlement is small, it only takes a very small gap to create a short circuit. To prevent this short circuit, a water barrier needs to be included in the design of these drainage systems, such as that suggested by Miller et al. (2013) as shown in Figure 119 and Figure 120 for granular backfill. A similar approach could be used with CLSM backfill.

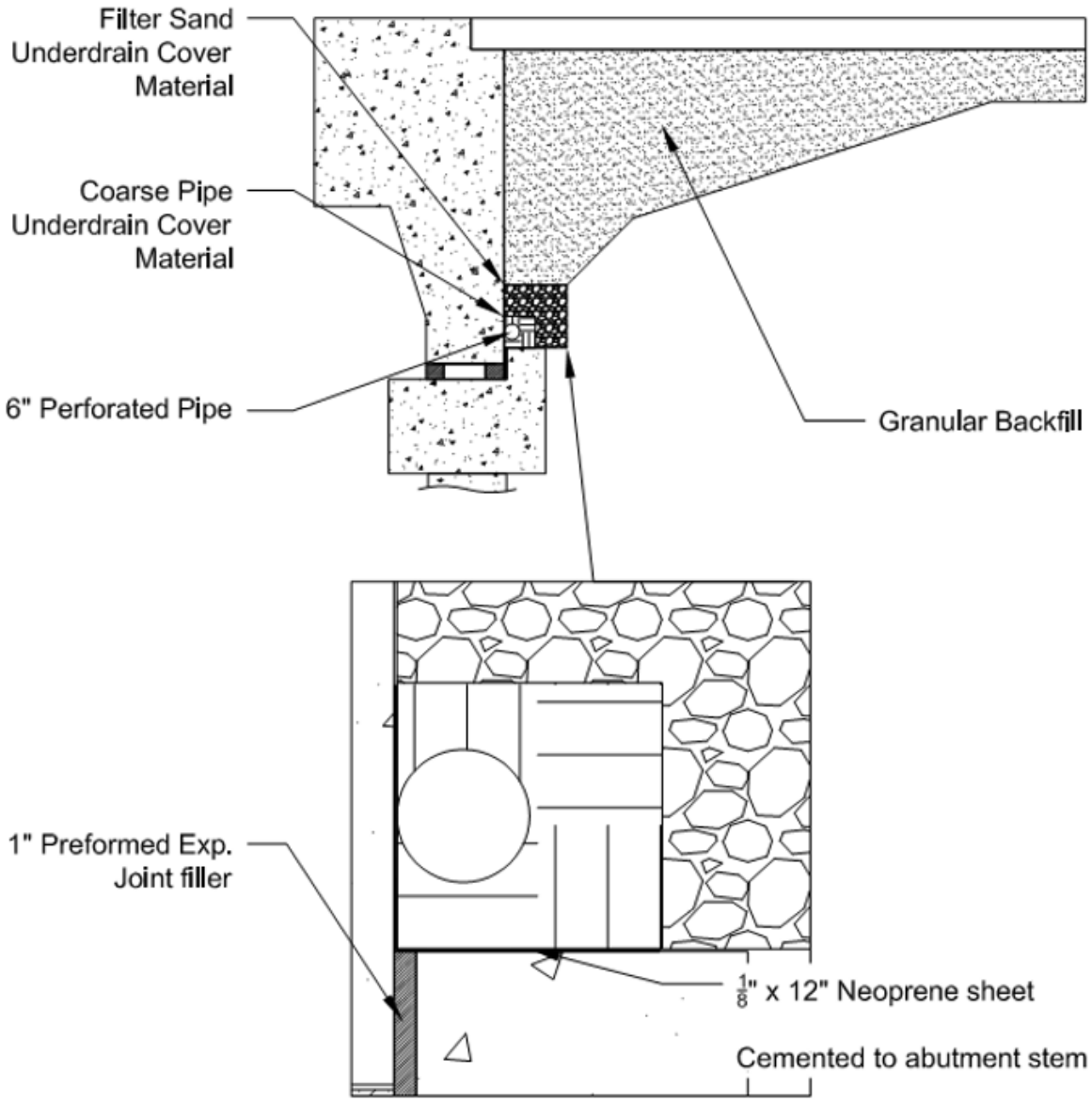

Figure 116. Underdrain Design, After ODOT Proposed Plan for Shields Boulevard over I-35

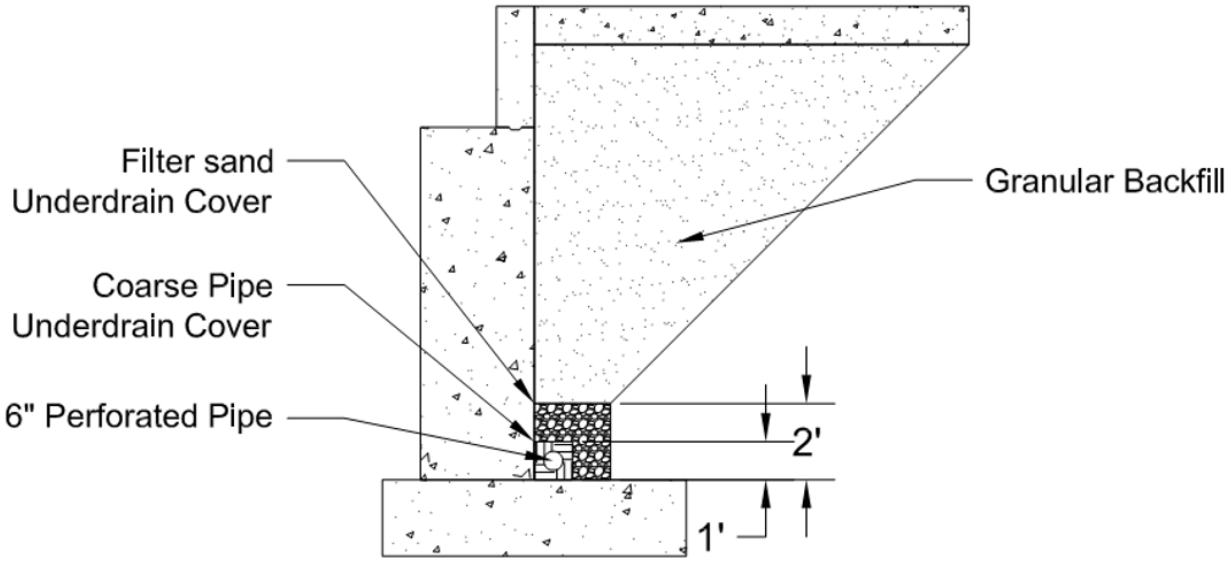

Figure 117. Underdrain Design, After ODOT Proposed Plan for Tecumseh Road over I-35

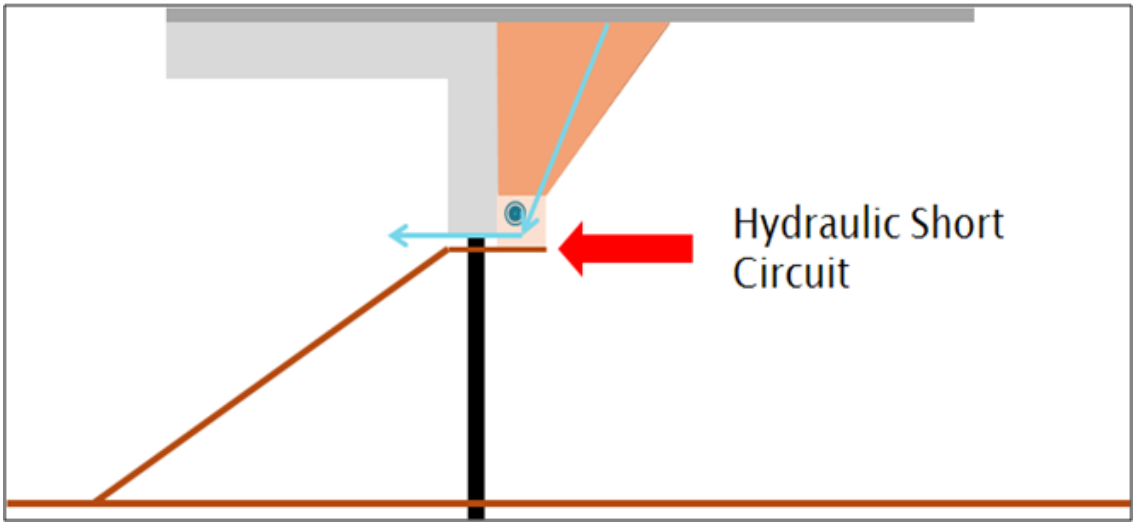

Figure 118. Schematic Cross-Section View of Hydraulic Short Circuit that Can Develop in the Abutment Drainage System (from Miller et al. 2013)

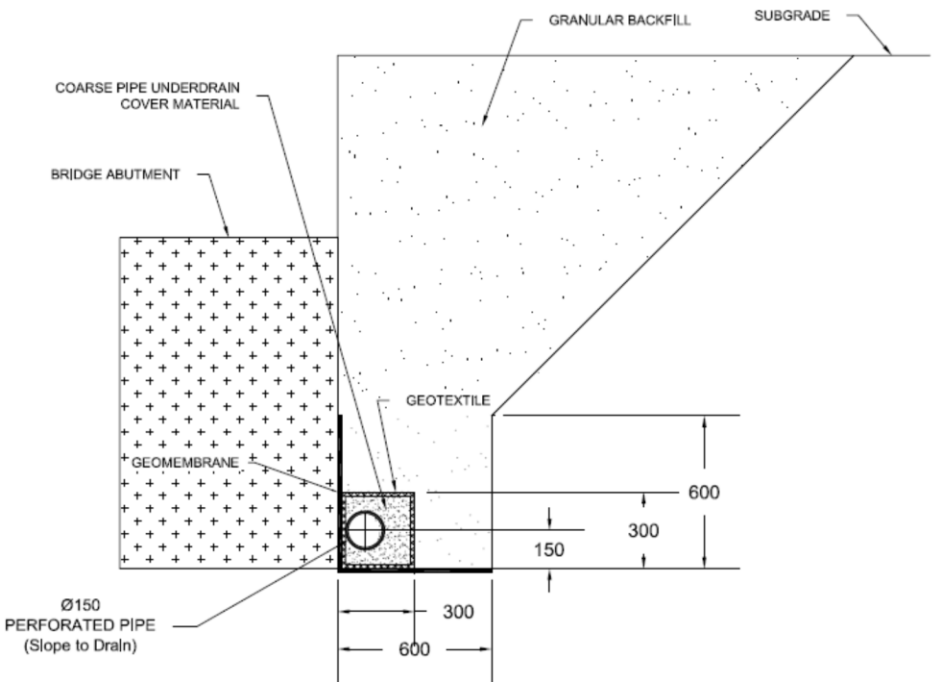

Figure 119. Proposed Abutment Backfill Drainage System with Geomembrane and Geotextile Filter (units in mm: 300 mm≈12 inches) (from Miller et al. 2013)

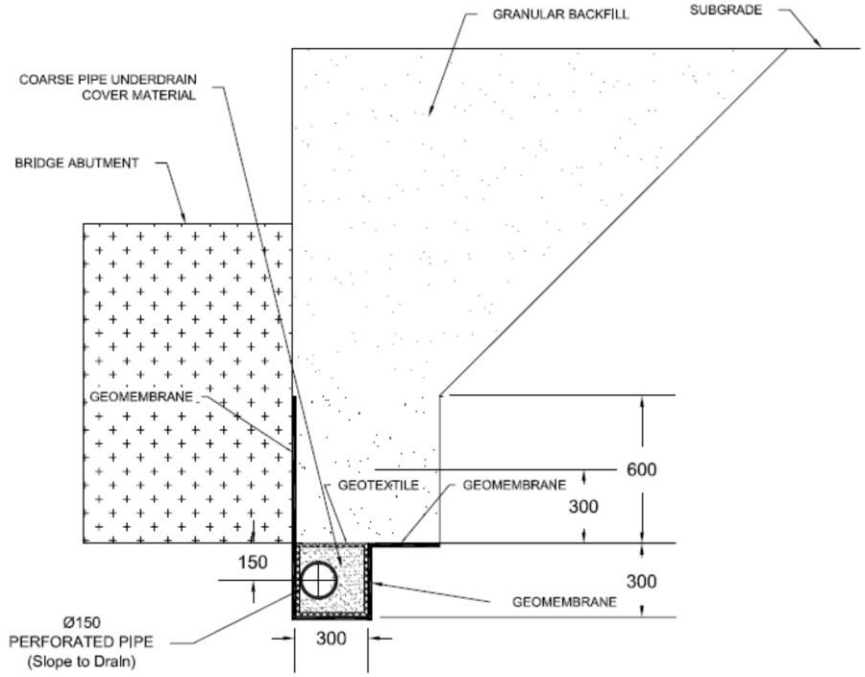

Figure 120. Proposed Abutment Backfill Drainage System, Depressed with Geomembrane and Geotextile Filter (units in mm: 300 mm≈12 inches) (from Miller et al. 2013)

Some other issues associated with drainage systems were observed during the study by Miller et al. (2013). At the bridge on Shields Blvd. over I-35 soil was observed flowing from the underdrain outlet as shown in Figure 121, which could indicate improper filtration of fines in the undrain. It is important to provide a proper filter between the embankment soil, granular backfill and coarse underdrain cover material. This is especially important if the coarse underdrain material is in contact with embankment soil or a much finer granular backfill. Improved filtration could be achieved by including geotextiles in the filter design, for example as shown in Figure 119 and Figure 120.

Figure 121. Soil flowing out of underdrain outlet.

Another problem that causes unwanted erosion is placement of the underdrain outlets. When underdrain outlets are placed near the top of the slope wall, the water exiting these drains can enter joints or cracks in the slope wall and flow along the margins of the slope wall causing severe erosion and undermining as shown in Figure 122.

Figure 122. Water flowing from underdrain outlets onto slope wall, Tecumseh Rd. over I-35. (note large void under slope wall)

Finally, as mentioned previously, at several locations observed during the study by Miller et al. (2013) the underdrain outlets were blocked or partially blocked by soil and vegetation. Water backing up into the underdrain system can force the water to exit through other locations, such as under the abutment leading to unwanted erosion.

As discussed in this section, there are several issues associated with drainage systems being used in Oklahoma bridge systems. However, most of these issues can be easily addressed through some simple modifications in the design of the drainage systems. These are discussed in the section on recommended practices. One of the suggested modifications to design was implemented on a trial basis not long after the 2013 study and will be discussed in that section as well.

5.0 Recommended Practices

This section presents the recommended practices. The section is divided into general, conventional bridge, integral bridge, and conventional to jointless bridge conversion recommendations. The recommendations are based on the surveyed literature, bridge monitoring, and combined experiences of the authors.

5.1 General Recommendations for Design and Construction

Recommendations regarding pressure relief joints, drainage systems, tall approach embankments on soft soils, abutment backfill, joint retrofits, and wing walls are included in this section.

5.1.1 Pressure Relief Joints

It is recommended that pressure relief joints be included for all new bridges with concrete approach pavement. Based on the monitoring results for 19th Street over I-35 in Moore, it appears that more movement occurs when the load transfer is established with a sleeper slab as opposed to dowels. Therefore, with new construction sleeper slabs should be used to ensure free thermal movement of the bridge and approach roadway if proper load transfer can be achieved. In many scenarios one pressure relief joint at each end of the bridge may not be sufficient. In these situations, a series of joints should be used. The Michigan DOT has developed a standard for pressure relief joint spacing that can be adopted. The standard is summarized in Section 2.3 of this report. The standard is shown in Figure 123. According to the standard multiple pressure relief joints should be used when long stretches of rigid pavement approach a bridge.

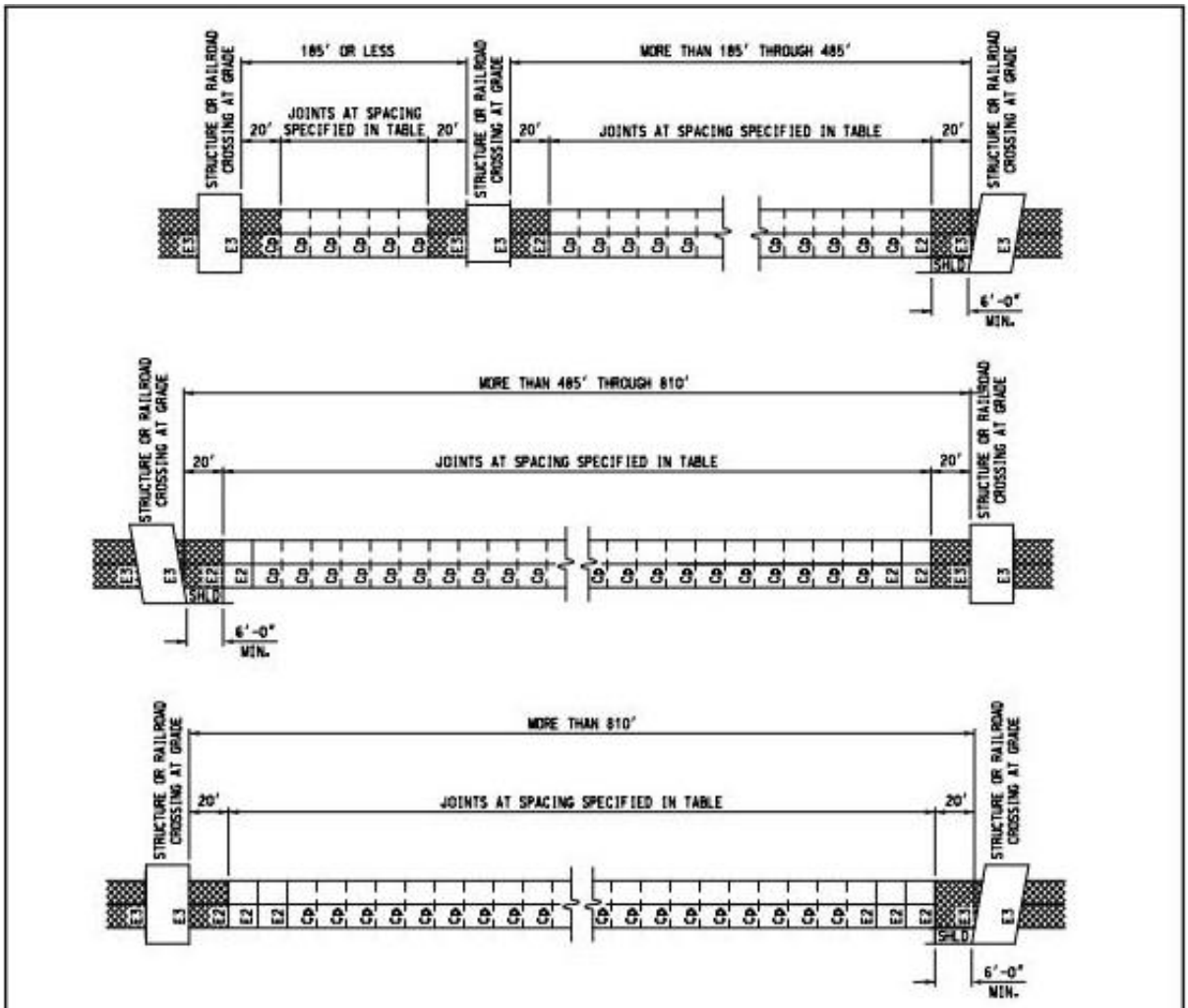

PLAN VIEW SHOWING TRANSVERSE JOINT LOCATIONS

NOTE:
SEE SHEET 2 FOR DETAIL OF JOINT SPACING WITH INTEGRAL / SEMI-INTEGRAL ABUTMENTS AND SLEEPER SLAB.

JOINT LEGEND
ACCORDING TO STANDARD PLAN R-39-SERIES

(E2) 1" TRANSVERSE EXPANSION JOINT WITH LOAD TRANSFER ASSEMBLY
(E3) 1" TRANSVERSE EXPANSION JOINT WITHOUT LOAD TRANSFER ASSEMBLY
(Cp) TRANSVERSE CONTRACTION JOINT
REINFORCED CONCRETE PAVEMENT ADJACENT TO BRIDGE REFERENCE LINE OR SLEEPER SLAB

JOINTED PLAIN CONCRETE PAVEMENT	
PAVEMENT THICKNESS	JOINT SPACING
6½" TO 8¾"	12'
9" TO 11¾"	14'
12" OR MORE	16'

MDOT
PREPARED BY DESIGN DIVISION
DRAWN BY: B.L.T.
CHECKED BY: M.K.P.

DEPARTMENT DIRECTOR
Kirk T. Steudle
APPROVED BY: DIRECTOR, BUREAU OF FIELD SERVICES
APPROVED BY: DIRECTOR, BUREAU OF HIGHWAY DEVELOPMENT

MICHIGAN DEPARTMENT OF TRANSPORTATION
BUREAU OF HIGHWAY DEVELOPMENT STANDARD PLAN FOR

LOCATION OF TRANSVERSE JOINTS IN PLAIN CONCRETE PAVEMENT

1-25-2013	2-8-2012	R-43-I	SHEET 1 OF 2
F.H.W.A. APPROVAL	PLAN DATE		

Figure 123. Michigan DOT pressure relief joint spacing standard drawing (from MDOT)

The pressure relief joints monitored during this project were retrofits to an existing bridge. The joints included a full depth 12-inch asphalt joint, a 4-inch BEJS foam joint, and a series of two 2-inch BEJS foam joints. Based on the results of the monitoring it appears that the asphalt joint did not fully mitigate the risk of pavement shoving, see Section 4.1.3. The asphalt joint may have slowed down the shoving when compared with no joint at all. ODOT has had success in the past using asphalt joints, it is not known why this particular joint did not stop the pavement from shoving into the approach slab. The remaining two joints (BEJS) have performed well so far. The drawback of the BEJS joints is the continued maintenance and durability of the joint.

The BEJS joints do require load transfer. During this project this was accomplished using dowels and a sleeper slab. The sleeper slab appears to be more effective at allowing the slab to move freely. When a sleeper slab is not present at the location of a proposed pressure relief joint one can be added. One of the survey participants outlined a method to add a sleeper slab below the proposed joint location. Essentially a section of the concrete pavement is removed and a sleeper slab is installed at the desired location. The pavement section is replaced leaving a 4-inch gap for a pressure relief joint. The new pavement section is tied to the existing pavement using tie bars or dowel bars. Louisiana DOT has this process as one of their standard drawings. The standard is shown in Figure 124. A pressure relief joint retrofit such as this would ensure the dowel bars are not keeping the pavement from moving freely. This type of retrofit would require the road to be closed for a longer period of time since the sleeper slab would need to be poured and gain strength before the pavement is replaced.

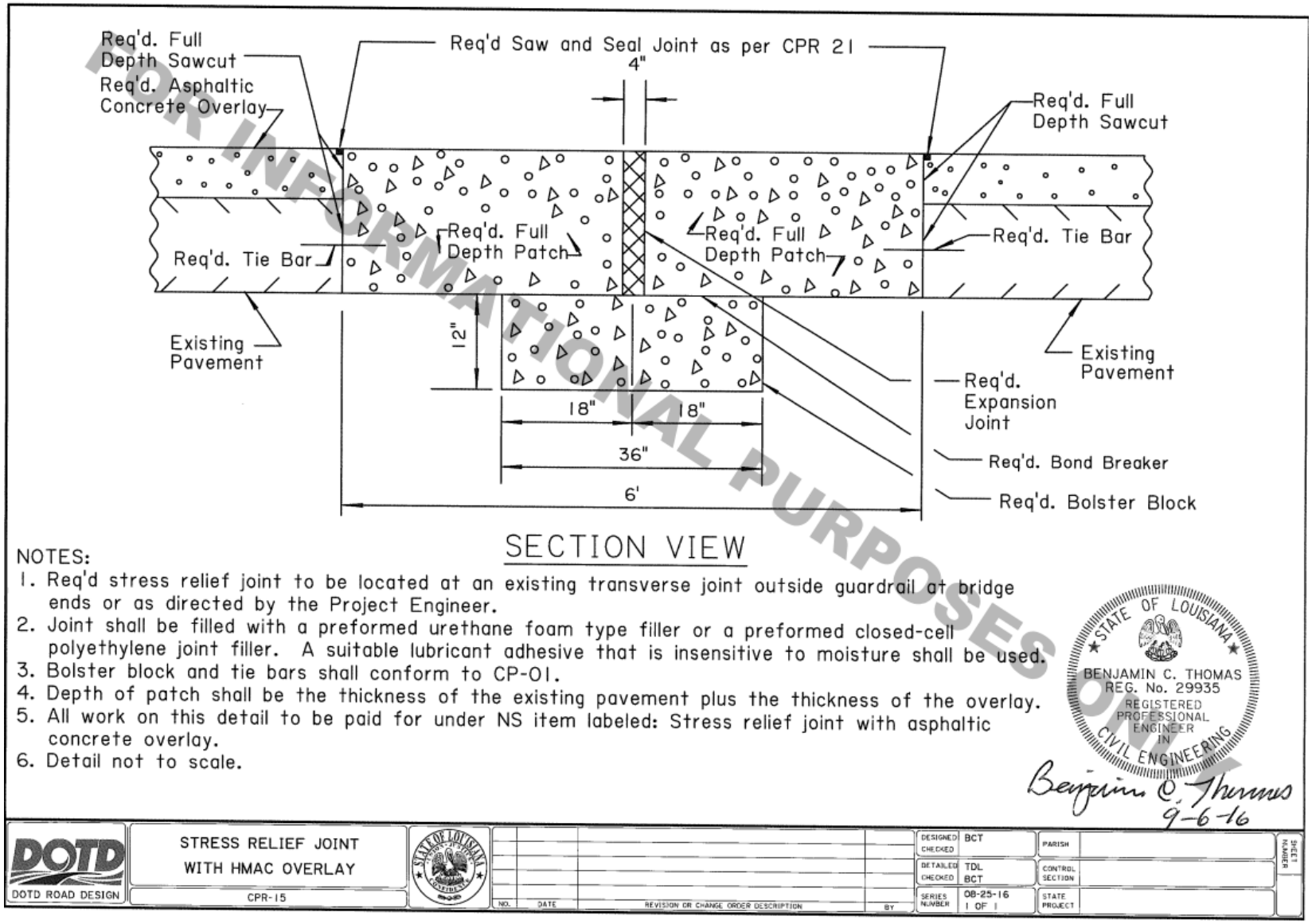

Figure 124. Louisiana DOTD pressure relief joint retrofit standard (from Louisiana DOTD)

A rigorous maintenance routine will be necessary to ensure longevity of the pressure relief joints. The pressure relief joints should at a minimum be cleaned during the late spring or early summer before the pavement starts to undergo thermal expansion. Ideally the joints should be cleaned routinely throughout the summer when the threat of pavement shoving on the approach slab is the greatest.

5.1.2 Tall Approach Embankments on Soft Soil

Numerical analysis is not needed for every tall embankment. However, a check or flag should be established to determine if advanced analysis is needed. A method to check the embankment movement is proposed. The SH-3 over BNSF Railroad Bridges are used to illustrate how to check an embankment for the possibility of excessive movement and estimate what that movement could be. The vertical deformation or settlement of an embankment can be estimated using one-dimensional consolidation tests and analytical equations. The current available methods to estimate settlement have been found to be sufficiently accurate (for example Tavenas et al. 1979). The lateral displacement generally requires the use of finite element methods to estimate accurately. However, several analytical methods have been proposed to relate lateral displacement to the soil strength and one-dimensional settlement. The methods generally equate the undrained shear strength (S_u) of the foundation soil to the embankment load or relate the lateral displacement to the estimated settlement. The Federal Highway Administration (FHWA) includes an equation to determine if lateral deformation and possibly abutment tilting will occur in the publication *Design and Construction of Driven Pile Foundations – Volume 1* (Hannigan et al. 2016). The equation is shown below.

$$\gamma_f h_f > 3S_u \quad (1)$$

γ_f = unit weight of fill

h_f = height of fill

S_u = undrained shear strength of soft cohesive soil

Equation (1) can only be used to determine if lateral displacement of the embankment will be possible or problematic. The FHWA publication also presents a relationship to estimate the magnitude of lateral displacement based on the amount of settlement. The relationship is shown below.

$$S_h = 0.25S_v \quad (2)$$

S_h = horizontal abutment movement (inches)

S_v = vertical fill settlement (inches)

The undrained shear strength of the SH-3 foundation soils prior to the embankment construction has been back calculated to be approximately 4.4 psi. Using this undrained shear strength, 120 pcf for the unit weight of fill, and Equation (1) both embankments, east and west sides, would be expected to experience lateral deformation. The settlement has been calculated using the results of the one-dimensional consolidation tests included in Appendix D.1. The settlement was estimated to be approximately 1.8 feet for the east embankment and 1.5 feet for the west embankment. The estimated settlement is the total settlement, this value could have been mitigated through construction staging allowing the embankment to settle prior to construction. Using the analytically estimated settlement values and Equation (2) the estimated lateral movement of the embankment is approximately 0.45 feet and 0.38 feet for the east and west sides, respectively.

The analytically estimated settlement and lateral displacement were larger than what was calculated numerically. The method outlined above could be used as a flag

during the analysis phase of embankments on soft soils. When the lateral movement is deemed a problem using Equation (1) and/or excessive using Equation (2) advanced analysis should be considered. If excessive deformation is expected the consolidation process can be sped up using preloading and/or wick drains. Another option would be to monitor the embankment and let it settle before construction of the bridge and roadway.

The potential for excessive settlement or lateral deformation of the embankment should be clearly stated within the bridge plans and communicated to the contractor. The field inspector should be made aware that remedial measures such as a settling or resting time for the embankment are necessary.

The settlement of the embankment itself is often overlooked. There is an assumption that when the soil is compacted to at least 95% maximum dry density and ±2% optimum moisture content that the compacted soil settlement will be negligible. This is not always true. It will be an issue when embankments are tall. The settlement of the embankment fill material should also be evaluated. The borrow soil should be compacted to at least 95% maximum dry density and ±2% optimum moisture content and one-dimensional consolidation testing (ASTM D2435 2010) should be completed on the fill material. The settlement of the embankment material can then be calculated using analytical equations. The magnitude of embankment settlement should be added to the magnitude of estimated foundation soil settlement. If the settlement is considered excessive mitigation techniques such as preloading or allowing the embankment to settle prior to construction the bridge should be considered.

5.1.3 Drainage Systems

Based on the background information described in Section 4.6, several recommendations are provided to improve the performance of the bridge drainage systems.

Abutment Backfill Drainage

Abutment backfill is either granular, typically clean sand, or CLSM. It is recommended that the coarse underdrain be wrapped in a geotextile filter compatible with the filter requirements of the material surrounding the drain, which could be granular backfill or embankment soil depending on the design. There is uncertainty regarding the impact of CLSM on the filtration performance of the geotextile; however, it is expected that geotextile will minimize the intrusion of CLSM into the coarse underdrain and maintain some functionality. For CLSM, due to the uncertainty regarding its impact on the geotextile, it would be beneficial to cover the geotextile with a layer of sand to provide some protection and additional filtration. In lieu of a geotextile, a properly designed graded granular filter could be used.

A water barrier should be placed between the abutment and embankment soils to prevent short circuiting of water from the underdrain through the space between the bottom of the abutment and underlying embankment soils (Figure 118). Some possible details for such a water barrier are shown in Figure 119 and Figure 120. Alternatively, a layer of low permeability clay could be used to create a water barrier, such as shown in Figure 3, which depicts a detail developed by the Kansas DOT.

ODOT incorporated some of the suggested details for underdrains into the Single Point Urban Interchange (SPUI) Main Street bridge over I-35 in Norman, including a water barrier between the drainage system, abutment and underlying soil as shown in Figure 125. Based on a recent visual inspection of this site, this system appears to be

functioning well since its installation in 2013. It is expected that the use of a water barrier will be even more advantageous for typical stub abutments that do not have a footing and where the bottom of the abutment is higher on the embankment.

Drainage outlets

Drainage outlets should be positioned where the potential for erosion is minimized. Placing drainage outlets near the top of the slope wall or high on the approach embankment should be avoided. Outlets should be surrounded with erosion resistant materials where needed, and they should be inspected and maintained on an annual basis to ensure they are not blocked and are functioning properly.

Surface drainage

Surface drainage should be designed to handle expected flows and should divert water away from the bridge system. Concrete lined drainage channels can become undermined due to water flowing under and along the channel, rendering them ineffective. Such channels should be supported on erosion resistant materials, such as coarse gravel, with a proper filter between the gravel and underlying subgrade soil. Alternative channel linings such as geosynthetic lined and vegetated channels or channels with flexible armor, such as surge stone over a proper filter layer may prove more effective in the long term. It is recommended to explore other alternatives to the concrete lined channel where appropriate.

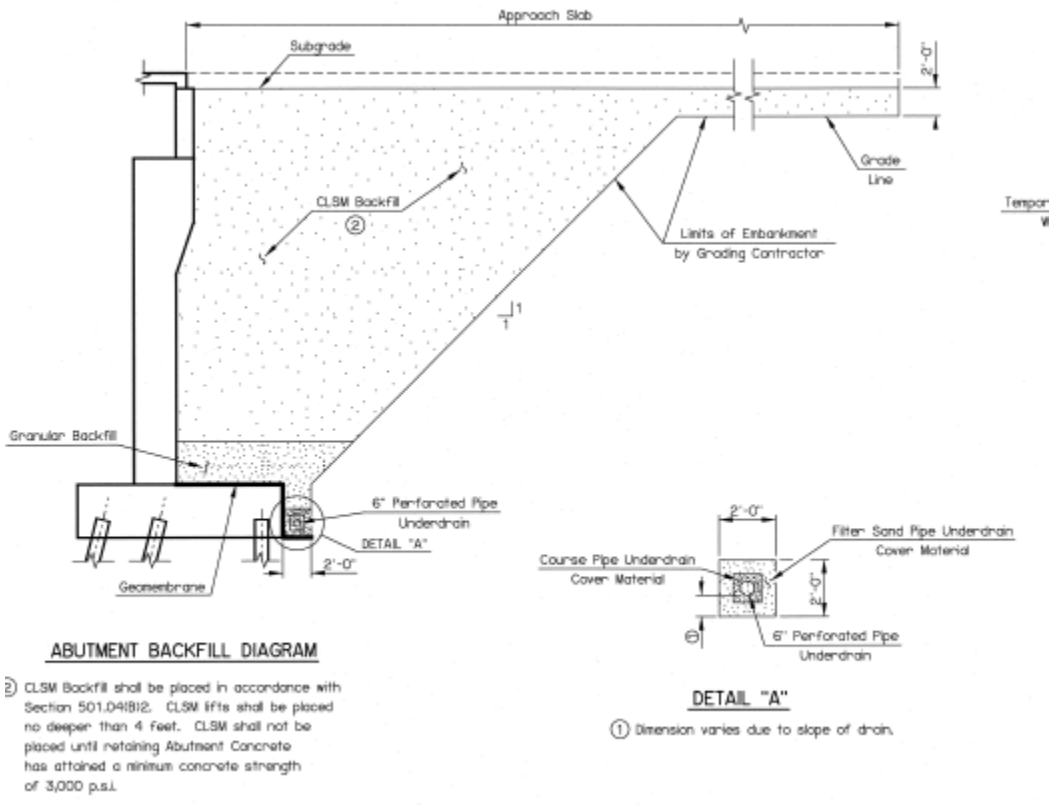

Figure 125. Backfill drainage system for SPUI bridge on Main Street over I-35 in Norman

5.1.4 Abutment Backfill

ODOT currently uses CLSM as abutment backfill material on the majority of newly constructed bridges. CLSM does not need to be compacted making it an attractive option for backfill material. However, since CLSM is placed as a fluid there are large fluid pressures exerted on the backwall and wingwalls of the bridge abutment. To resist some of this fluid pressure and the thrust from CLSM placement on conventional, or jointed, bridges, construction staging restrictions have been implemented. The restrictions state that the superstructure must be in place before the CLSM can be placed. The resistance provided by the superstructure will help resist the fluid and thrust pressure from the CLSM.

The construction staging results in the backfill cavity being left exposed for many weeks or months in between construction of the abutment and placement of the backfill. During this time rain can soak the soil and pond in the cavity. Solar radiation can dry the soil out beyond the accepted specifications. The backfill drainage system can fill in with debris and soil. Care should be taken to make sure the soil does not get over wetted or over dried. The drainage system should also be inspected prior to backfilling to ensure it is free from blockages.

There is an interest in using LDCC as an alternative to CLSM as abutment backfill. LDCC has the added advantage of being lightweight when compared to CLSM or granular backfill. The density of LDCC could allow for taller lifts to be poured. LDCC would also decrease the fluid pressure placed on the abutment backwall and wingwalls during placement. Research on LDCC is still relatively new with respect to use as abutment backfill. However, research from Rollins et al. (2019) found that LDCC developed less passive pressure than CLSM on abutment backwalls when the backwall was displaced. They found the developed passive pressure to be closer to that of granular backfill for LDCC. The lower passive pressure is another desirable trait of LDCC especially as it relates to integral abutment backfill. Although some state DOT's have adopted LDCC as an option for abutment backfill, its use is not widespread. The use of LDCC as abutment backfill needs to be explored further through research or as a pilot study.

5.1.5 Wingwalls

For conventional, or jointed, bridges the standard wingwall design includes an additional pile foundation at the open end of the wingwall. The pile is oriented in weak axis bending relative to the abutment backwall. That is, it will provide more resistance

perpendicular to the roadway than it will parallel to the roadway. When wingwalls are very tall special consideration is needed. In these situations, the wingwall is acting as a large cantilever wall supported on the pile foundations. This is despite the connection with the abutment backwall. When the wingwall is non-standard analysis should be conducted on the wall-pile system incorporating the effects of the soil. This type of analysis could conservatively be done in the commercial software LPILE (Ensoft 2019). The analysis would be conservative since the tie-in with the abutment backwall could not be incorporated into the design. The effects of the backfill and backfill placement should be considered in the analysis. The backfill placement will be especially important when CLSM is used for abutment backfill material. Depending on the results of the analysis additional supporting piles may be warranted.

5.1.6 Joint Retrofits

Several different possibilities for retrofit of existing bridge deck expansion joints and connections of precast concrete girders for live load continuity were investigated as part of this project. Retrofit of expansion joints includes both the rehabilitation of existing expansion joints and elimination of some of the expansion joints to create a continuous deck over the intermediate pier without creating live load continuity for the bridge girders. Methods examined by the research team in this project and in previous work sponsored by ODOT include conventional concrete (Muraleetharan et al. 2018), UHPC expansion joint headers (Floyd et al. 2021a), full-depth and half-depth UHPC connections to create a continuous deck between spans (Floyd et al. 2021a), and UHPC connections for live load continuity of the bridge girders (Floyd et al. 2021a,b).

5.1.6.1 Expansion Joint Rehabilitation

Deteriorating expansion joints can lead to leaking of the joints, offsets between adjacent slabs negatively impacting rider comfort, and damage to vehicles if steel armoring used for the joint edges comes loose and enters the roadway. These joints can be retrofitted using conventional concrete to return the joint to near its original state as was done on the SH 3 Bridge over BNSF Railroad in Ada, OK (Figure 126). The development length requirements to connect the conventional concrete joint repair into the existing slab require several feet of the existing deck to be removed for the full depth as shown in (Figure 126). This method also does not necessarily improve the future performance of the joint, only restores it to near original condition. The same is true for simple repair methods such as elastomeric or rapid setting concrete nosing materials that can be used for fast repairs.

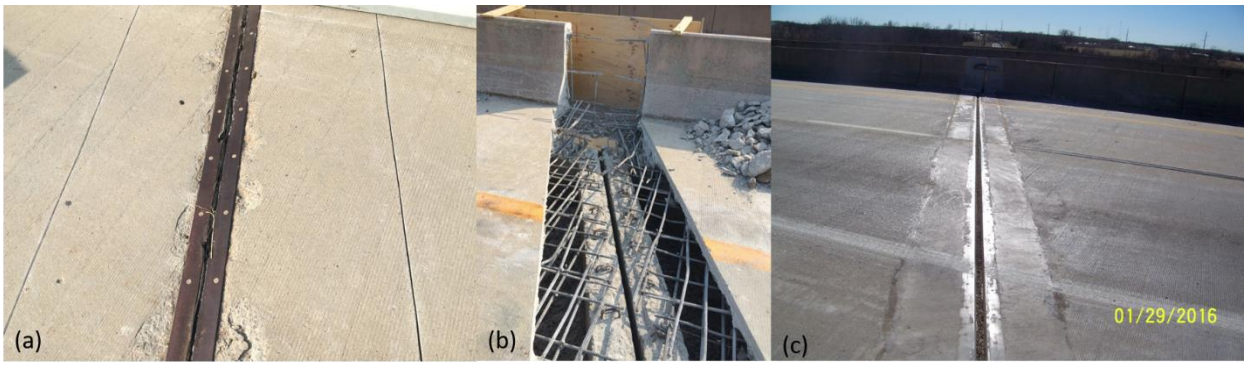

Figure 126. Retrofit of bridge deck expansion joint using conventional concrete (a) before retrofit, (b) after demolition, and (c) after retrofit completion

UHPC joint headers can reduce the amount of concrete that must be removed for retrofit of an expansion joint since the required development length of reinforcement in UHPC (approximately $8d_b$) is significantly less than in conventional concrete and UHPC strongly bonds to conventional concrete substrate. The demonstration joint header described in Section 4.4.1 was done with 12 inches of concrete removed on each side

of the joint, but work in the laboratory (Floyd et al. 2021a) indicates that this distance could be reduced to 6 inches – 8 inches. UHPC expansion joint headers also can be half-depth or less and do not need steel armoring due to the high impact resistance of UHPC. They can be ground to grade at multiple points during the life of the joint to reduce the effects of expansion joints on rider comfort if the deck slabs shift over time. UHPC is nearly impermeable, has high freeze thaw resistance, and resists corrosion in the reinforcement (Floyd et al. 2021b). These items working together have the potential to extend the overall life of the joint as supported by four years of monitoring of the one demonstration joint in Oklahoma. The detail shown in Figure 127 is recommended for future uses of UHPC expansion joint headers in Oklahoma with the distance into the slab to be determined by the engineer. It is recommended that the top rebar mat should be engaged in the repair with a UHPC cover depth of $3d_b$ below the reinforcement and a bar embedment of at least $8d_b$ based on the recommendations of (Graybeal 2014). If the distance below the reinforcement is between $2d_b$ and $3d_b$ the required embedment should be increased to $10d_b$ (Graybeal 2014). It is recommended that the depth below the bars should not be less than 0.5 inch.

The EMSEAL BEJS joint system has been shown to be successful when used with UHPC joint headers as it is easily applied to a vertical surface and since it is precompressed may exhibit less tendency to pull away from the header material. It is possible that other joint systems could be used successfully, but the details would need to be modified to account for the attachment of the joint material to the headers.

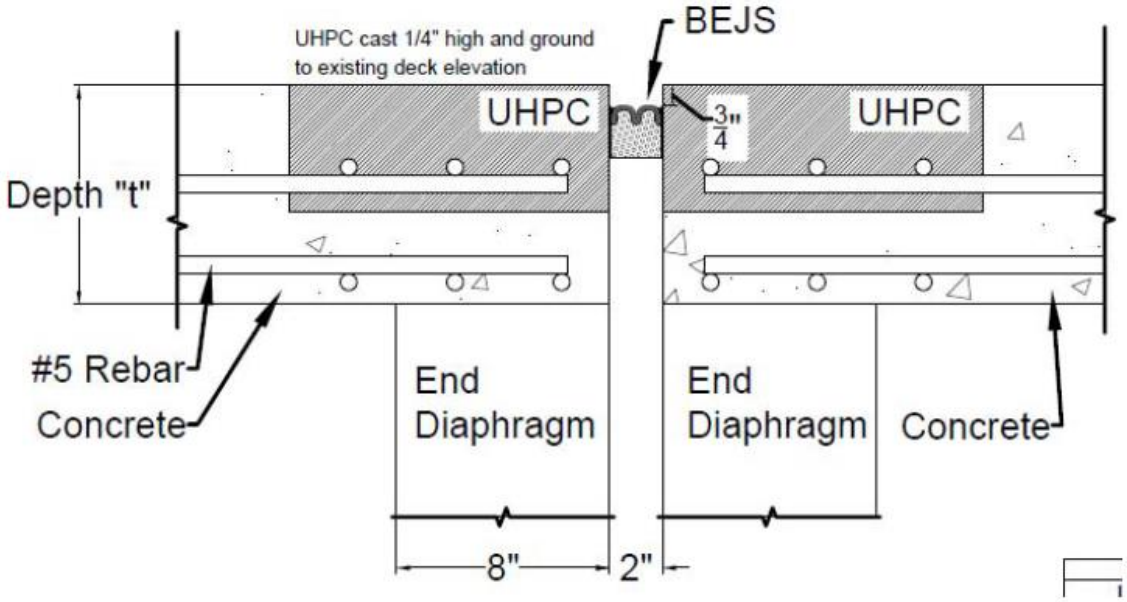

Figure 127. Recommended general detail for UHPC expansion joint headers

5.1.6.2 Expansion Joint Removal

Removal of some expansion joints in a given bridge can be a solution to reduce the number of possible pathways for water to reach the superstructure and substructure elements and required maintenance. It should be noted that consideration should still be made for thermal movements of the structure, such as moving expansion joints to the end of the bridge. Potential options for joint removal include making the slab continuous over the pier with construction joints, link slabs to maintain simple span behavior, or making the girders and slab continuous over the pier. Both conventional concrete and UHPC can be used for these purposes, but as with the expansion joint retrofits the improved reinforcement development capability and high durability of UHPC provides definite advantages. Flexural testing of full-depth and half-depth UHPC retrofits examined as part of previous research (Floyd et al. 2021a) and shown in Figure 128, indicated that the UHPC connections provided strength greater than the monolithic slab with only a 12 to 14 inch total width of the connection. However, if used for removing an expansion joint where unrestrained simple span behavior was originally expected, the

added stiffness in the slab may result in cracking at the interface between the UHPC and deck concrete or in the deck slab.

Figure 128. Full-depth (left) and half-depth (right) UHPC connections intended for removal of expansion joints in bridge deck slabs

Conventional concrete or UHPC link slabs provide similar deck continuity, but with a reduced stiffness and debonded length that allows rotation at the level of the slab to maintain the expected simple span behavior (Caner and Zia 1998). Proper stiffness of the link slab is a critical consideration for design as one that is too stiff can lead to cracking in the deck slab (Seibert et al. 2019) or link slab (Karim and Shafei 2021). Design of link slabs in general is detailed in Caner and Zia (1998) and for UHPC in Scarlata (2017). Figure 129 shows a typical detail for UHPC link slab retrofit utilized by the New York DOT for steel girders, but a similar detail can be used for concrete girders. These link slabs can also be utilized for full deck replacement or new construction as shown in Figure 130 and Figure 131 using either conventional concrete or UHPC. Link slabs are an appealing option because they maintain expected behavior of simple span beams and are less likely to have wide cracks resulting in high durability. However, the type of bearings used at piers where link slabs are used can affect

performance of the link slab (Gergess and Douaihy 2020) and if the bearings must also be replaced the difficulty of a retrofit will increase substantially.

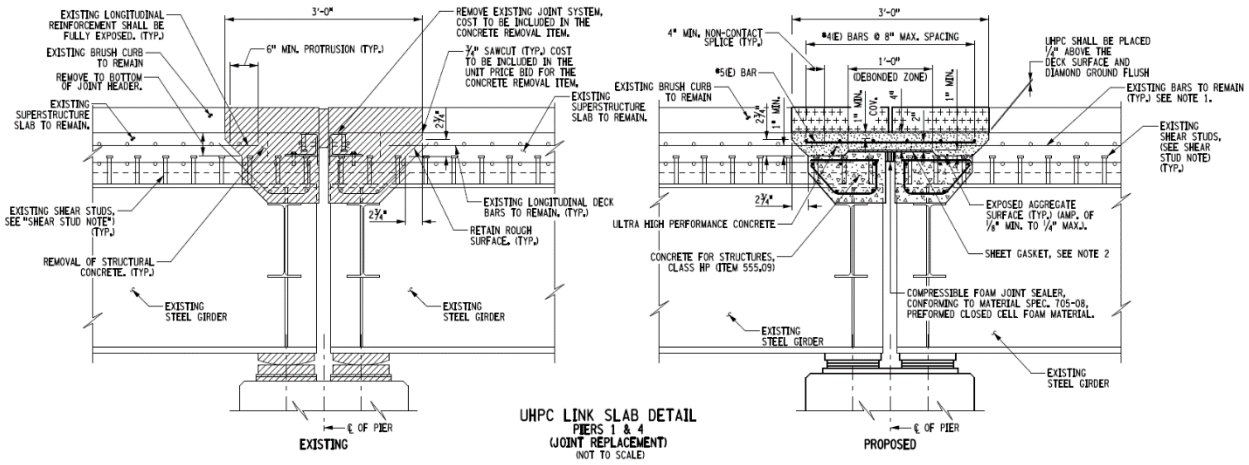

Figure 129. Typical detail for retrofit of an existing expansion joint using a UHPC link slab (NYSDOT)

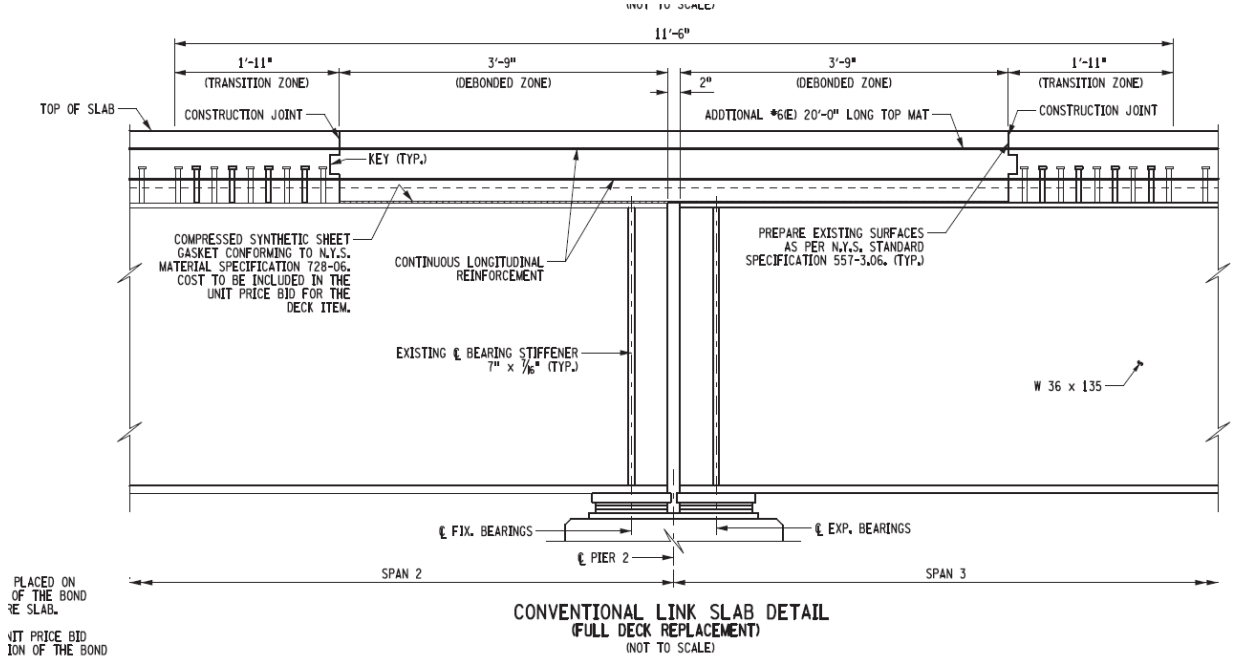

Figure 130. Conventional concrete link slab detail for full-depth deck replacement (NYSDOT)

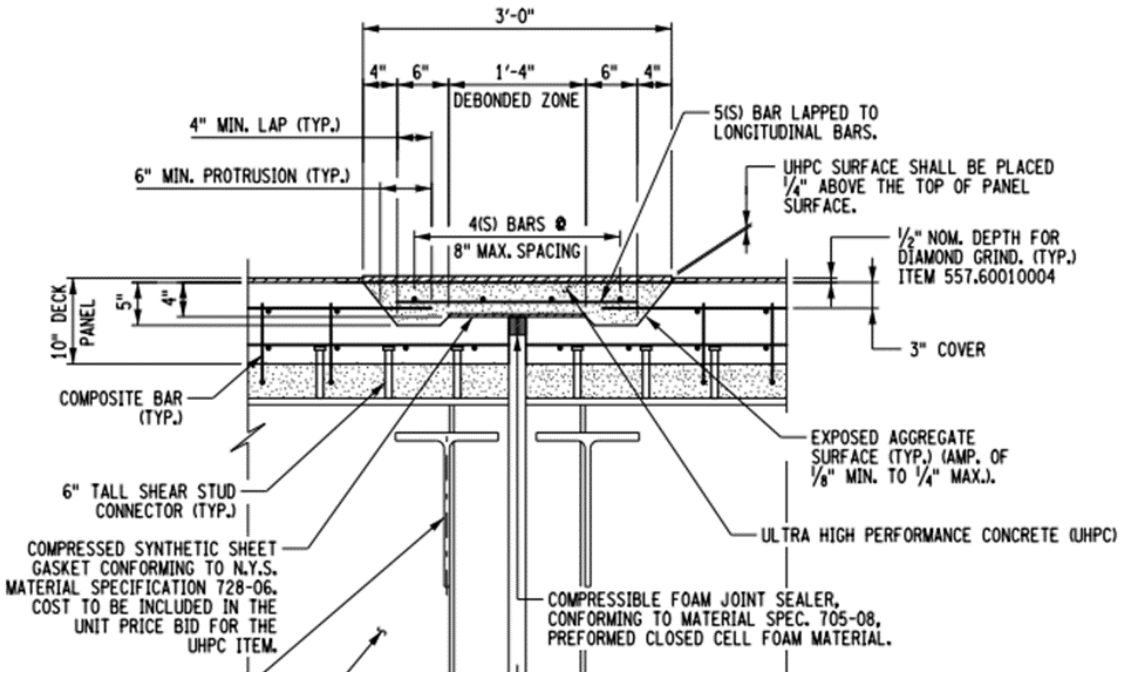

Figure 131 UHPC link slab detail for new construction (NYSDOT)

5.1.6.3 UHPC Connections of Precast Girders for Live Load Continuity

As described in Section 4.4.3, connections of precast girders made continuous for live load tend to exhibit cracking from moments that develop due restrained creep and shrinkage in the girders. UHPC has been shown to be effective for replacement of these connections and restoring live load continuity using the existing joint reinforcement. UHPC has the benefit of high tensile strength to resist additional potential cracking, even though most restraint moments should have dissipated by the time of a retrofit. The short required development lengths can help compensate for some damage to the in-place reinforcing steel required to anchor the connection. UHPC also benefits from a higher modulus of elasticity than regular concrete. The modulus of elasticity ranges from 5,000 to 7,500 ksi and can be estimated using the following relationship proposed by the FHWA (Graybeal 2006):

$$E_c = 1460 * \sqrt{f'^c} \quad (3)$$

E_c = modulus of elasticity

f'_c = UHPC compressive strength (ksi)

Previous research at OU (Floyd et al 2021a) indicated that UHPC could be used to create a retrofit connection to make existing simply supported girders continuous for live load by encapsulating a portion of the end of the girders and placing the positive moment reinforcement required to resist 1.2 times the cracking moment (AASHTO 2017) in the encapsulating UHPC block outside of the girder. Straight bars and studs embedded in the girder ends were used to transfer the loads and reinforcement in the deck was used for the required negative moment capacity. The retrofit connection tested in the laboratory exhibited similar performance to a similar new construction detail designed using AASHTO (2017). Careful consideration of the additional stiffness of the connection on the existing girder design is necessary to ensure proper performance of the girder relative to moment and shear induced by the new support condition. Additional work is needed to determine design modifications that can be made to incorporate the superior properties of UHPC in continuity connection design.

5.2 Conventional Bridges

Bridge structures are subjected to a variety of loads – including traffic and environmental loads – that result in movement of the bridge elements. Addressing thermal expansion and contraction is critical to extending the service life of a bridge and reducing the effects of secondary stresses (Azizinamini et al. 2013). In conventional bridges, expansion and contraction of the structure is accommodated through movable (expansion) joints placed at prescribed locations within the bridge deck, typically at the superstructure/abutment interface and at the piers. The performance of these joints is one of the most important factors affecting the deterioration of bridge elements. Joints

that leak will allow road salts and other chemicals to penetrate below the deck, resulting in a variety of maintenance and deterioration problems.

The components of an overall strategy for successful expansion joint design, installation, and performance consist of the following:

- Identify appropriate selection and design methodologies for the different types of expansion joints – compressed seal, poured sealant, asphaltic plug, sheet seal, sliding plate, strip seal, or modular joints.
- Consider life-cycle costs in selecting a durable expansion joint type.
- Specify best practices for construction of the type of expansion joint selected.
- Develop an effective maintenance plan that includes periodic cleaning and repairs.

The critical characteristics of a successful expansion joint consist of the following:

- Accommodate the required thermal expansion and contraction of the bridge.
- Accommodate movement of the bridge elements caused by traffic-induced loads.
- Provide a smooth ride.
- Prevent the creation of hazards and safety issues.
- Accommodate snow removal equipment.
- Prevent leaking of moisture and other chemicals to elements of the superstructure below.
- Require minimal maintenance.

Skewed and curved bridges require additional considerations for effective expansion joint design and installation. The joint design must consider both lateral and longitudinal movement based on the geometry of the deck and the design of bearings and keeper assemblies. Bridges with excessive skew or curvature may require a thermal expansion analysis of the deck to determine the direction of thermal movements relative to the bridge joint configuration.

Another concern for jointed bridges is the unrestrained expansion of the approach pavements, which can result in complete closure of the movable deck joints and significant compressive stresses within the bridge superstructure and approach slabs (Burke 2009). The result is often damage to the approach slabs, bridge seats, abutments, and piers. An effective method for combating this problem is the installation of pressure relief joints between the approach pavement and the approach slab; pressure relief joints must be sized to accommodate pavement pressure (due to potential failure of pavement contraction joints) as well as thermal movements of the bridge superstructure.

5.3 Integral Abutment Bridges

Integral abutment bridges developed to overcome the detrimental effects that movable deck joints have had on the long-term durability and integrity of bridge superstructure and substructure components (Burke 2009; Kunin and Alampalli 2000; Oesterle et al. 1999). Movable deck joints often fail over time, allowing roadway drainage (often containing de-icing chemicals and other contaminates) to flow over beam ends, bearings, bridge seats, piers, and abutments, resulting in corrosion and deterioration. Over time, this deterioration results in costly repairs to these bridge elements or, sometimes, the need for a complete bridge replacement.

Conversely, many bridges with movable deck joints end up with their joints completely closed and significant levels of compressive stresses within the bridge superstructure and approach slabs (Burke 2009). This phenomenon is due to the unchecked growth of pavement sections leading up to the bridges. As the pavement sections contract during low temperature cycles, pavement contraction joints open and can become filled with compression-resistant roadway debris. When the temperatures rise, the filled joints become ineffective, and the pavement sections begin to act as one long, monolithic element. The expansion of these pavement sections exerts significant forces on the bridge, often completely closing the movable deck joints and causing damage to the approach slabs, bridge seats, abutments, and piers.

Integral abutment bridges consist of either single-span or continuous multiple-span superstructures constructed without movable transverse deck joints (Burke 2009; Oesterle et al. 1999). Connection to the abutment is often achieved by encasing the beam ends, as shown in Figure 132, while connection to the piers can be achieved either with movable bearings supported by rigid piers or flexible piers constructed integrally with the superstructure. To reduce soil pressures and restraint, stub-type abutments supported on a single row of piles are often used, as shown in Figure 132, although taller abutments are not uncommon.

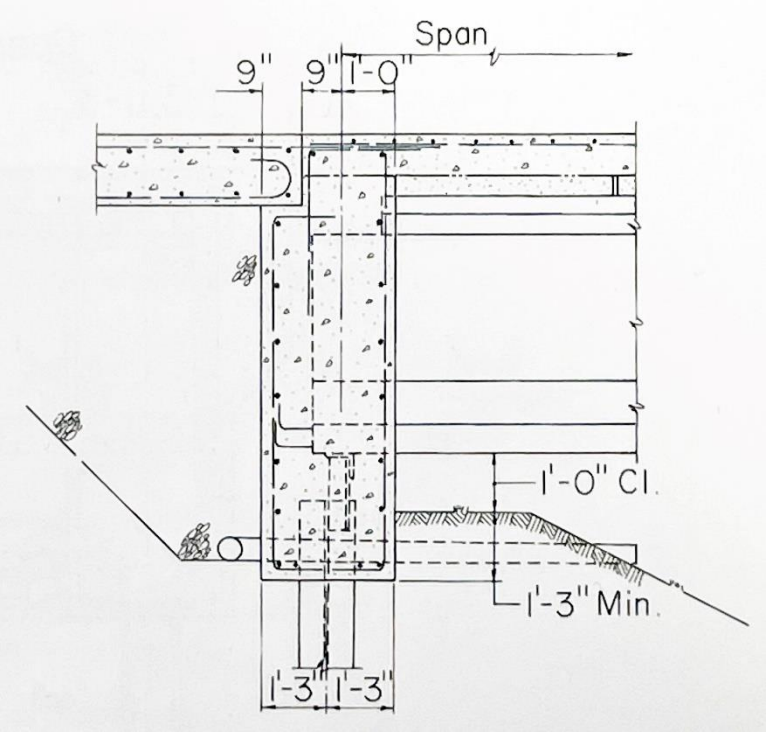

Figure 132. Integral Stub-Type Abutment Detail (Burke 2009)

A review of bridge design standards and state DOT guidelines indicates some variations in the details for integral abutment bridges, but common themes do begin to emerge. In general, successful integral abutment bridges have been constructed within the following guidelines or best practices:

- Limit bridge lengths to a maximum of 300 feet.
- Limit bridge skews to a maximum of 30° and bridge curvatures to a maximum of 5°.
- Provide stub-type abutments supported by a single row of vertical piles oriented for weak axis bending; H-piles are recommended although drilled shafts may be used for bridges up to 165 feet in length.
- Provide minimum pile lengths of 10 feet, although longer, more flexible piles will improve foundation performance.
- Design abutment for full passive earth pressures.

- Provide adequate continuity reinforcement between the abutments and the superstructure.
- Provide in-line wingwalls cantilevered from the abutment stem with a maximum length of 14 feet; longer wingwalls should be detached from the abutment, supported on their own independent foundation, and installed with a flexible joint between the abutment/wingwall interface.
- Provide continuous construction for multiple-span superstructures, preferably through both deck and girder continuity joints at the piers; alternatively, continuity may be achieved at pier locations using link slabs in the deck with discontinuous girders supported on movable (flexible) bearings.
- Provide approach slabs over the full width of the bridge and tied to the abutments with diagonal ties (to act as a hinge) to accommodate potential settlement of the far end.
- Provide pressure relief joints between the approach pavement and the approach slab; pressure relief joints must be sized to accommodate pavement pressure (due to potential failure of pavement contraction joints) as well as thermal movements of the bridge superstructure.

A refined analysis is recommended for all integral abutment bridges that exceed these guidelines and best practices. For this refined analysis, a three-dimensional finite element model is recommended in order to determine the maximum loads acting on the piles, abutment stem, backwall, and superstructure. This model should include the effects of skew, curvature, soil-structure interaction including ratcheting, thermal movements, dead and live loads, and roadway grade.

The ODOT Interstate-44 Bridge over Medicine Bluff Creek in Comanche County, Oklahoma, is an example of an integral abutment bridge that falls within these recommended guidelines and best practices and that has performed very well over its 14 years of life. Recent inspections rated the superstructure in excellent condition, the substructure in very good condition, and the deck in satisfactory condition. Issues that have arisen include joint sealant failure in the sawed construction joint between the approach slab and abutment, hairline transverse cracking in the deck, and voids beneath the approach slabs.

Design features for the bridge, shown in Figure 133, include the following:

- Overall length of 210 feet.
- Precast/prestressed concrete girders with spans of 60 ft. – 90 ft. – 60 ft.
- Skew angle of 10°.
- Stub-type abutments supported by a single row of vertical H-piles oriented for weak axis bending.
- Minimum pile length of 25 feet.
- In-line wingwalls cantilevered from the abutment stem
- Link slabs at pier locations with discontinuous girders supported on movable (flexible) bearings over rigid piers (drilled shafts).
- Approach slabs over full width of bridge and tied to the abutments.

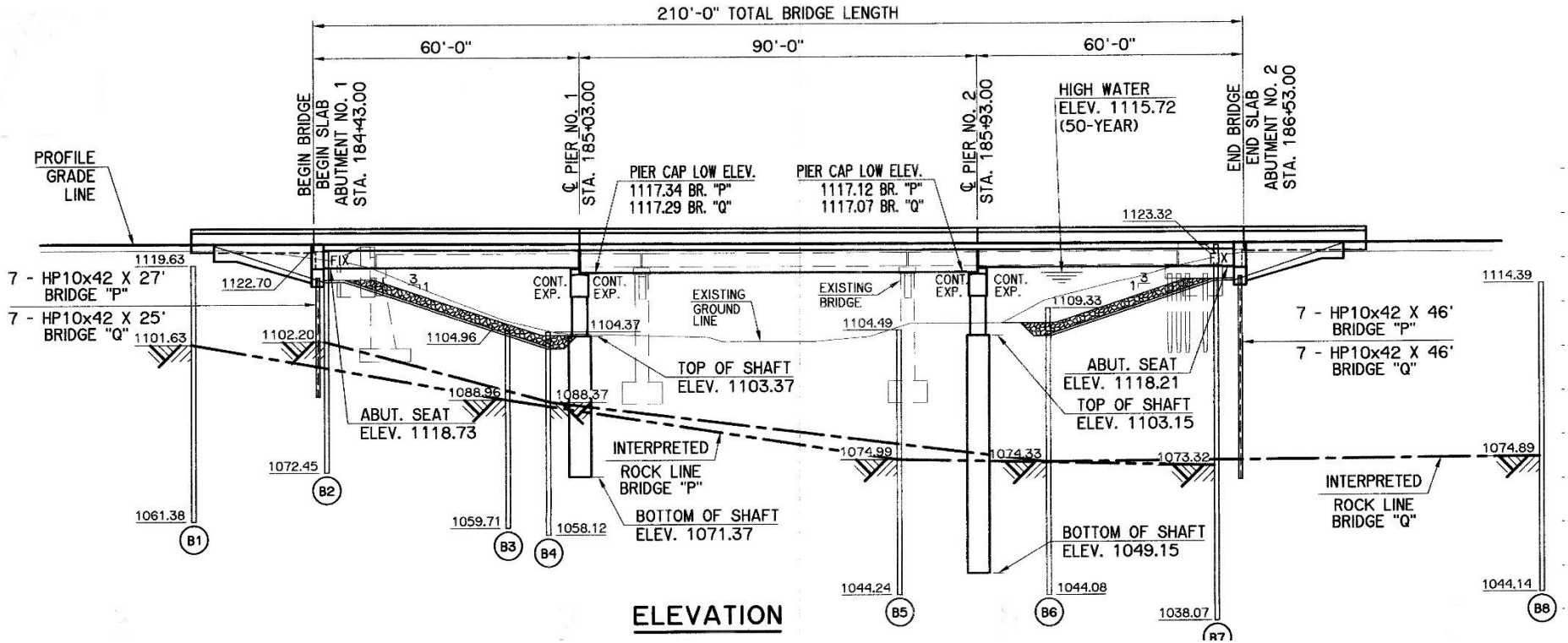

Figure 133. I-44 Bridge Over Medicine Bluff Creek (ODOT 2008)

5.4 Semi-Integral Abutment Bridges

As with Integral abutment bridges, semi-integral abutment bridges developed to overcome the detrimental effects experienced by bridges containing movable deck joints – deterioration of the deck joints over time (resulting in contamination of the bridge superstructure and substructure) or closure of the deck joints and excessive pressures exerted on the bridge due to unrestrained expansion of the approach pavements. The other reason that semi-integral abutment bridges developed was to address locations where the site characteristics precluded the use of a flexible abutment foundation, most often due to the presence of bedrock relatively near the surface.

Semi-integral abutment bridges consist of either single-span or continuous multiple-span superstructures constructed without movable transverse deck joints (Burke 2009; Oesterle et al. 1999). Connection to the abutment is often achieved by encasing the beam ends and providing a sliding joint between the upper (movable) portion of the abutment and the lower (fixed) portion of the abutment, as shown in Figure 134. Connection to the piers can be achieved either with movable bearings supported by rigid piers or flexible piers constructed integrally with the superstructure. To reduce soil pressures and restraint, the height of the upper (movable) portion of the abutment is limited to as small as practically achievable.

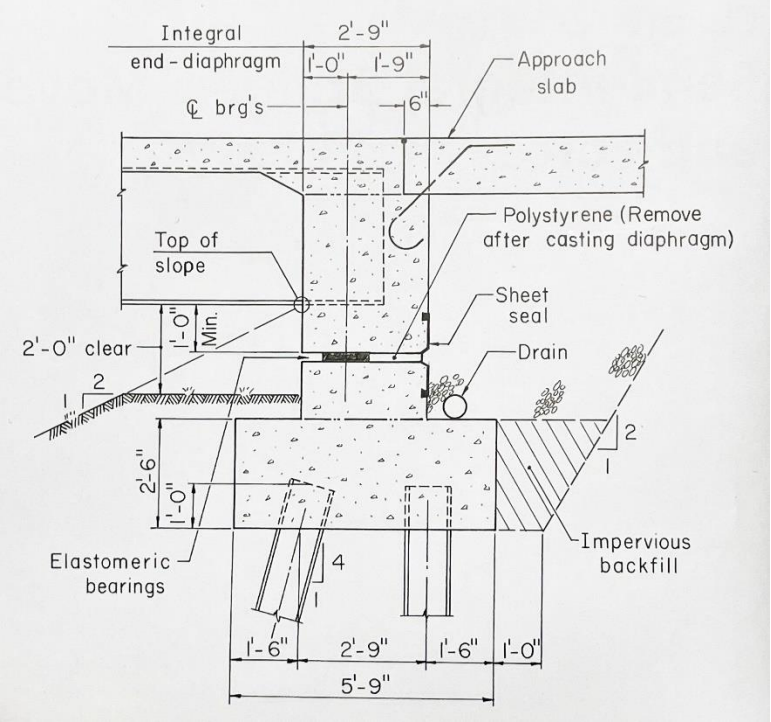

Figure 134. Semi-Integral Abutment Detail (Burke 2009)

A review of bridge design standards and state DOT guidelines indicate some variations in the details for semi-integral abutment bridges, but common themes do begin to emerge. In general, successful semi-integral abutment bridges have been constructed within the following guidelines or best practices:

- Limit bridge lengths to a maximum of 300 feet.
- Limit bridge skews to a maximum of 30°.
- Avoid curved girder bridges or limit applications to very slight curvatures, on the order of no more than 2°.
- Limit the height of the upper (movable) portion of the abutment to as small as practically achievable.
- Provide corrosion-resistant elastomeric bearings for the bridge seat joint and very durable elastomeric joint seals.

- Provide guide bearings for skewed bridges greater than 10° and all curved bridges to prevent rotation of the bridge in the horizontal plane.
- Provide independent wingwalls from the upper (movable) portion of the abutment, including a vertical, flexible joint at the interface.
- Design the upper (movable) portion of the abutment for full passive earth pressures.
- Provide adequate continuity reinforcement between the upper (movable) portion of the abutment and the superstructure.
- Provide continuous construction for multiple-span superstructures, preferably through both deck and girder continuity joints at the piers; alternatively, continuity may be achieved at pier locations using link slabs in the deck with discontinuous girders supported on movable (flexible) bearings.
- Provide approach slabs over the full width of the bridge and tied to the abutments with diagonal ties (to act as a hinge) to accommodate potential settlement of the far end.
- Provide pressure relief joints between the approach pavement and the approach slab; pressure relief joints must be sized to accommodate pavement growth (due to potential failure of pavement contraction joints) as well as thermal movements of the bridge superstructure.

A refined analysis is recommended for all semi-integral abutment bridges that exceed these guidelines and best practices. For this refined analysis, a three-dimensional finite element model is recommended in order to determine the maximum loads acting on the upper (movable) portion of the abutment, backwall, guide bearings,

and superstructure. This model should include the effects of skew, curvature, soil-structure interaction including ratcheting, thermal movements, dead and live loads, and roadway grade.

5.5 Bridge Retrofit – Integral and Semi-Integral Conversions

Poor performance of existing conventional bridges containing movable deck joints has led numerous State DOTs to convert these bridges to integral or semi-integral structures instead of performing repeated repairs over their lifetime (Burke 2009; Oesterle et al. 1999). Movable deck joints often deteriorate over time, allowing roadway drainage (often containing de-icing chemicals and other contaminates) to flow over beam ends, bearings, bridge seats, piers, and abutments, resulting in severe corrosion and deterioration if left unchecked. Conversely, unrestrained expansion of the approach pavements can lead to complete closure of the deck joints and excessive pressures on the bridge structure, leading to severe damage to the approach slabs, bridge seats, abutments, and piers. Conversion to an integral or semi-integral bridge type eliminates both problems and offers improved long-term performance as well as decreased maintenance costs.

The choice between either an integral or semi-integral conversion is largely a function of the existing abutment. Abutments founded on a single row of flexible piles (e.g., vertical H piles at least 10 feet in length) lend themselves to integral abutment conversions, while fixed abutments (e.g., multiple rows of piles including battered piles) lend themselves to semi-integral abutment conversions. An integral abutment conversion typically involves removing the joint between the abutment backwall and bridge deck and encasing the beam end as part of a new upper portion of the abutment, as shown in Figure 135. A semi-integral abutment conversion typically involves

separating the existing abutment into an upper (movable) portion and a lower (fixed) portion, with a sliding joint between the two, as shown in Figure 136. The semi-integral conversion also includes the removal of the joint between the abutment backwall and bridge deck and encasing of the beam ends in the upper (movable) portion of the new abutment.

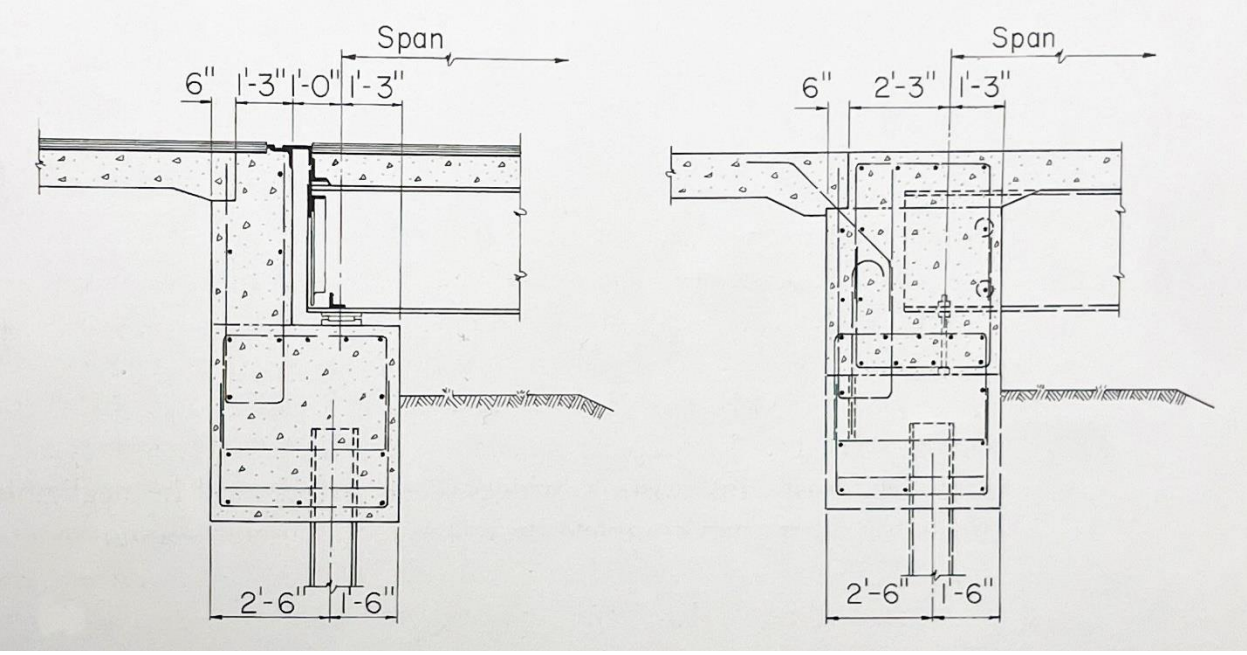

Figure 135 Integral Abutment Conversion: Before (l) and After (r) (Burke 2009)

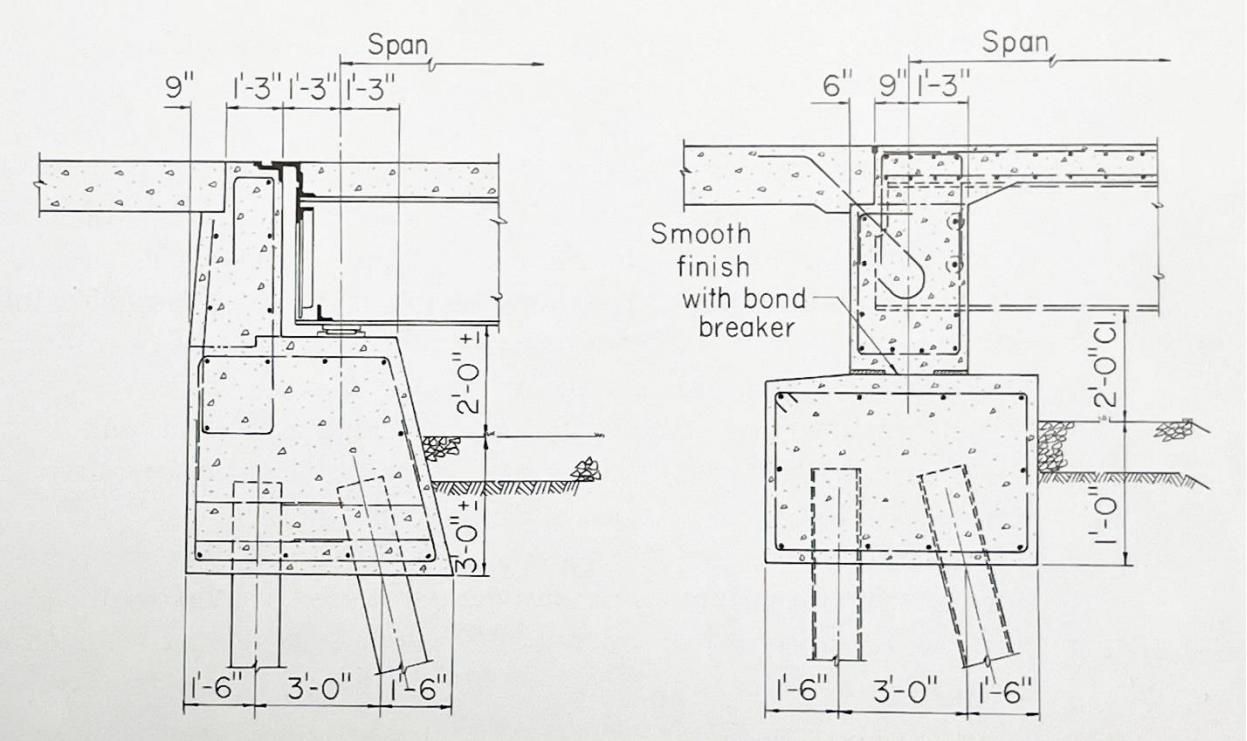

Figure 136. Semi-Integral Abutment Conversion: Before (l) and After (r) (Burke 2009)

Both conversion types also include removal of any movable deck joints at the pier locations, resulting in a continuous superstructure. At pier locations where it does not already exist, some conversions include providing continuity in both the deck and girders, while others only include providing continuity in the deck in the form of link slabs. However, where link slabs are used, it is important to install movable bearings at the beam ends if they do not already exist. The movable bearings are necessary to transfer the point of rotation from the bearings to the centerline of the link slab for optimum performance (Thorkildsen 2020).

Conversions should be limited to existing conventional bridges that meet the parameters for new integral and semi-integral abutment bridges discussed in Sections 5.3 and 5.4, respectively. Bridges outside of these limitations may still perform much

better after an integral or semi-integral conversion but may also experience some detrimental side effects as a result of their conversion.

The ODOT I-44 Bridge over Southwest 15th Street in Oklahoma City, Oklahoma, is an example of a conversion from a jointed to a jointless bridge, although not a typical integral or semi-integral conversion. Constructed in 1975 and shown in Figure 137, the original structure – two identical skewed, two-span, continuous, steel plate girder bridges with overall lengths of 152 feet – contained expansion joints and roller bearings at the abutments. Over time, the skewed bridges started to rotate in plan and push the girder ends off of the roller bearings. This phenomenon was most likely the result of complete closure of the deck expansion joints due to unrestrained expansion of the approach pavement. Once the joints were closed, thermal expansion of the bridge resulted in lateral translation of the girder ends due to the skew, pushing the beams off of the bearings.

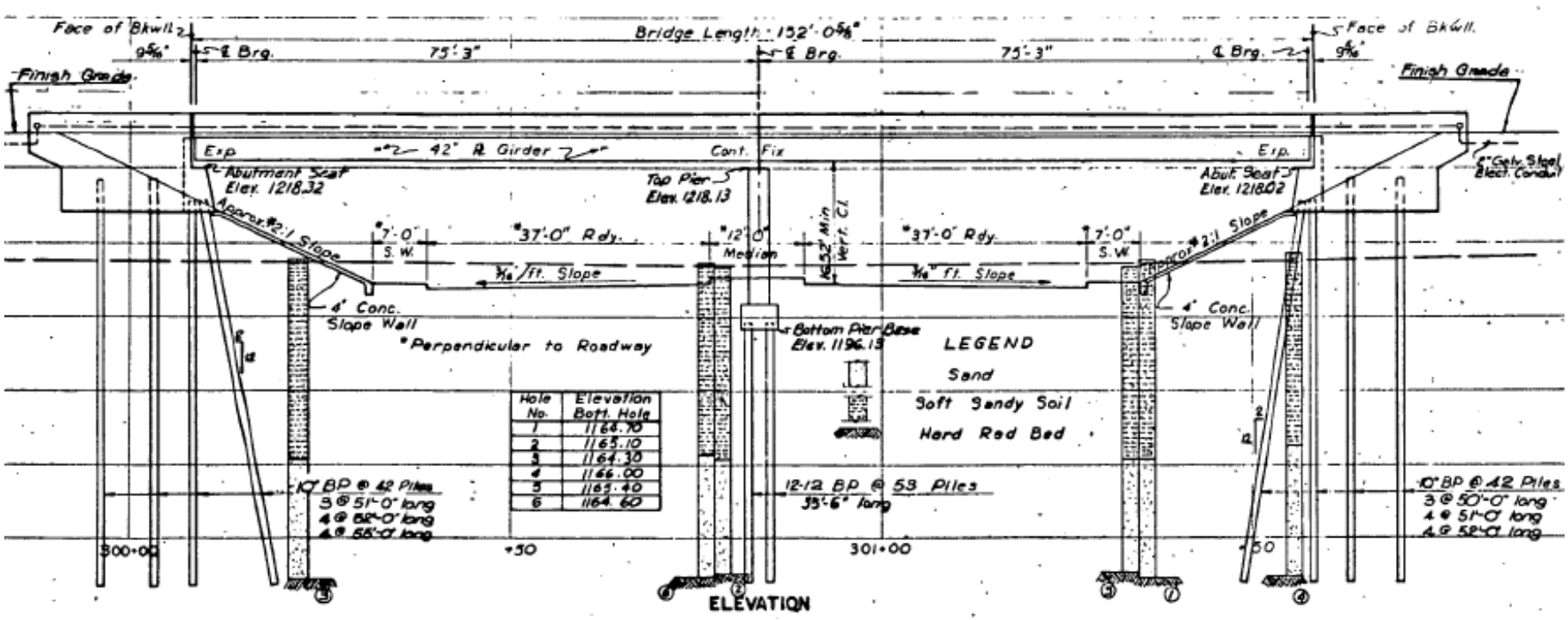

Figure 137. I-44 Bridge Over Southwest 15th Street, Oklahoma City, Oklahoma (ODOT 1975)

The conversion involved encasing the beam ends and bearings in concrete doweled into the existing abutment backwall and removal of the deck expansion joints at the abutments. No other modifications were made to the abutments, which were of a fixed type due to multiple rows of piles, including battered piles. As such, this conversion does not fall under either a traditional integral abutment conversion or a semi-integral abutment conversion. Integral abutment conversions require flexible abutments, and semi-integral conversions require installation of a sliding joint between the upper (movable) portion and the lower (fixed) portion of the abutment. However, the bridge has performed very well since the conversion. Recent inspections rated the superstructure in satisfactory condition, the substructure in fair condition, and the deck in fair condition. Issues that have arisen include deterioration of the asphalt overlay at the abutment and pier deck construction joints and leakage onto the superstructure below, moderate spalling in the concrete bridge railings near the abutments likely due to the skew, and large cracks in the concrete approach slabs.

Design features of the original bridge construction include the following:

- Companion bridges with overall lengths of 152 feet.
- Continuous, two-span, steel plate girders with spans of 75 ft.– 75 ft.
- Skew angle of 15°.
- Fixed abutments supported by multiple rows of H-piles including battered piles.
- In-line wingwalls attached to the abutment stem and supported on H-piles.
- Deck expansion joints at the abutments.
- Approach slabs over full width of bridge and tied to the abutments.

6.0 Conclusions and Recommendations

As discussed in the previous chapters, many problems experienced by bridges are caused by designing and constructing bridges and adjacent roadways as separate elements. Designing, constructing, and maintaining bridges and adjacent roadways as systems can lead to elimination of problems such as bridge expansion joints closing and costly repairs associated with these problems. Several recommendations for designing, constructing, and maintaining these systems are summarized in Chapter 5. Some key aspects of these recommendations are given below:

a) When bridges have concrete approach pavements, it is critical to provide a pressure relief joint at the approach slab/approach pavement interface and additional pressure relief joints on the approach pavement depending on the length of the pavement. A 4 inch BEJS type compressed foam joint supported on a sleeper slab is a good choice for the pressure relief joint at the approach slab/approach pavement interface. A sleeper slab with a bond breaker allows the pavement sections to move more freely than dowels. For new construction a sleeper slab with a bond breaker should be used under pressure relief joints. A standard from Louisiana DOT (Figure 124) describes a method to add a sleeper slab during retrofit. When feasible a sleeper slab retrofit should be used. However, adding a sleeper slab during the retrofit may require the road to be closed for an unacceptable amount of time. If the addition of a sleeper slab is not feasible during retrofit, dowels with caps should be used to provide load transfer across the joint. Adequate load transfer is necessary to avoid premature failure of the pavement adjacent to the pressure relief joint. It is also critical to maintain all the pressure relief

joints for the longevity of the joints as well as the bridges. Additional details can be found in Section 5.1.1.

b) When an approach embankment to a bridge is built on soft soil, and especially for taller embankments, it is essential to investigate the lateral deformation potential of this embankment and take appropriate remedial measures to ensure that the lateral deformation of the embankment is minimized before constructing the bridge. The threshold for investigating the lateral deformation potential of bridge embankments is dependent on the strength of the foundation soil. If the unit weight of fill (γ_f) multiplied by the height of fill (h_f) exceeds 3 times the foundation soil's undrained shear strength (S_u), the potential for lateral deformation should be analyzed. As part of this analysis, vertical settlement should also be estimated. Additional details can be found in Section 5.1.2.

c) Approach slab settlement is a common occurrence. In addition to the potential for lateral spreading, vertical settlement of approach embankments should be analyzed and addressed during the design stage as needed, particularly for tall embankments and when the underlying foundation materials are compressible.

d) Improper drainage around bridges leads to many problems. One critical aspect of drainage around bridges is to provide a water barrier between the abutment and embankment soils to prevent short circuiting of water from the underdrain through the space between the bottom of the abutment and underlying embankment soils. Additional details can be found in Section 5.1.3.

e) Low Density Cellular Concrete (LDCC) appears to be an attractive abutment backfill material and should be explored further.

f) For the design of tall wingwalls in conventional bridges, advanced soil-structure interaction analyses are necessary. Additional details are provided in Section 5.1.5.

g) Ultra-High Performance Concrete (UHPC) is an effective choice for longevity of bridge joint repairs and replacements and for replacement of girder live load continuity connections. Additional details are provided in Section 5.1.6.

h) For conventional (jointed) bridges, design, construction, and maintenance of expansion joints on the deck is one of the critical items. Skewed and curved bridges require additional considerations for effective expansion joint design and installation. Additional details can be found in Section 5.2.

i) Integral and semi-integral abutment bridges provide attractive alternatives to conventional bridges by eliminating the deck expansion joints and the problems associated with these joints. Integral and semi-integral bridges can be successfully designed, constructed, and maintained, if length, skew, and curvatures can be limited. If these limitations have to be exceeded, refined analyses, including soil-structure interaction analyses, are necessary. Additional details can be found in Sections 5.3 and 5.4.

j) If a conventional bridge is being retrofitted as an integral or a semi-integral bridge by eliminating deck joints, special consideration should be given to the existing abutment foundation. If the existing abutment foundation is a fixed type (e.g., multiple rows of piles including battered piles), then a semi-integral abutment conversion with an upper (movable) portion and a lower (fixed)

portion, with a sliding joint between the two is the best option. Additional details can be found in Section 5.5.

7.0 Acknowledgements

ODOT's Assistant Bridge Engineer for Maintenance, Mr. Walt Peters, provided valuable insight and support throughout this project. His support is gratefully acknowledged.

References

AASHTO. 2017. *LRFD Specifications for Highway Bridges, 8th Edition*. Washington, DC: AASHTO.

ASTM-D1140. 2017. “Standard Test Methods for Amount of Material in Soils Finer Than the No . 200 (75-μm).” *ASTM International, West Conshohocken, PA.*

ASTM-D1586. 2011. “Standard Test Method for Standard Penetration Test (SPT) and Split-Barrel Sampling of Soils.” *ASTM Standard Test Method*, D1586-11, 1–9.

ASTM-D1587. 2008. “Standard Practice for Thin-Walled Tube Sampling of Soils for Geotechnical Purposes.” *ASTM Standard Practice*, D1587-08(Reapproved 2007), 1–4.

ASTM-D2216. 1998. “Standard Test Method for Laboratory Determination of Water (Moisture) Content of Soil and Rock by Mass.” *ASTM International*, (January), 1–5.

ASTM-D3441. 2016. “Standard Test Method for Mechanical Cone Penetration Tests of Soil.” *ASTM International, West Conshohocken, PA, United States*, (July 2016), 1–8.

ASTM-D4318. 2005. “Standard Test Methods for Liquid Limit, Plastic Limit, and Plasticity Index of Soils.” *Report*, 04(March 2010), 1–14.

ASTM-D4767. 2011. “Standard Test Method for Consolidated Undrained Triaxial Compression Test for Cohesive Soils.” *ASTM International, West Conshohocken*, 11(Reapproved), 1–14.

ASTM D2435. 2010. “Standard Test Methods for One-Dimensional Consolidation Properties of Soils Using This standard is for EDUCATIONAL USE ONLY .” *Annual Book of ASTM Standards*, i(Reapproved), 1–10.

Azizinamini, A., Power, E. H., Myers, G. F., Ozyildirim, H. C., Kline, E. S., Whitmore, D.

W., and Mertz, D. R. 2013. *Design guide for bridges for service life*.

Balakumaran, S. S. G., O'Neill, K., Springer, T. C., and Matteo, A. 2018. *Elastomeric Concrete Plug Joints: A New Durable Bridge Expansion Joint Design*. *Transportation Research Record: Journal of the Transportation Research Board*.

Burke, M. 2009. *Integral and Semi-integral Bridges*. John Wiley & Sons.

Cai, C. S., Shi, X. M., Voyiadjis, G. Z., and Zhang, Z. J. 2005. "Structural Performance of Bridge Approach Slabs under Given Embankment Settlement." *Journal of Bridge Engineering*, 10(4), 482–489.

Caner, A., and Zia, P. 1998. "Behavior and design of link slabs for jointless bridge decks." *PCI Journal*, 43(3), 68–78.

Colorado DOT. 2021. *Bridge Design Manual*. Denver, CO.

Dafalias, Y. F., and Herrmann, L. R. 1986. "Bounding Surface Plasticity. II: Application to Isotropic Cohesive Soils." *Journal of Engineering Mechanics*, 112(12), 1263–1291.

EMSEAL. 2021. *EMSEAL Bridge Expansion Joint Product Data Sheet*.

Enright, M., and Frangopol, D. 2000. "Survey and Evaluation of Damaged Concrete Bridges." *Journal of Bridge Engineering*, 5(1), 31–38.

Ensoft. 2019. *LPILE v2019 user's manual: a program for the analyses of deep foundaitons under lateral loading*. Austin, TX.

Florida DOT. 2021. *Design Manual*. Tallahassee, FL.

Floyd, R. W., Volz, J. S., Funderburg, C. K., Mcdaniel, A. S., Looney, T., Choate, J., Roswurm, S., Casey, C., Coleman, R., Leggs, M., Serey, K., and Chea, V. 2021a. *Evaluation of Ultra-High Performance Concrete for Use in Bridge Connections and Repair*. Oklahoma Departemtn of Transportation, Oklahoma City, OK.

Floyd, R. W., Volz, J. S., Looney, T., Mesigh, M., Ahmadi, M., Roswurm, S., Huynh, P.,

and Manwarren, M. 2021b. *Evaluation of Ultra-High Performance Concrete, Fiber Reinforced Self-Consolidating Concrete, and MALP Concrete for Prestressed Girder Repair*. Oklahoma Departemtn of Transportation, Oklahoma City, OK.

Floyd, R. W., Volz, J. S., Zaman, M., Dyachkova, Y., Roswurm, S., Choate, J., Looney, T., and Walker, C. 2020. *Development of Non-Proprietary UHPC Mix*. *Quarterly Progress Report OU-2016-2-1, ABC-UTC*, Florida International University, Miami, FL.

Geokon. 2017. *Micro-1000 Datalogger*. Lebanon, NH.

Geokon. 2019. *Concrete Embedment Strain Gauges Data Sheet*.

Geokon. 2020. *Vibrating Wire Displacement Transducers*. Lebanon, NH.

Gergess, A. N., and Douaihy, E. Z. 2020. "Effects of Elastomeric Bearing Stiffness on the Structural Behavior of Bonded Link-Slabs." *Transportation Research Record*, SAGE Publications Sage CA: Los Angeles, CA, 2674(4), 428–443.

Graybeal, B. A. 2006. *Material property characterization of ultra-high performance concrete*. United States. Federal Highway Administration. Office of Infrastructure ….

Graybeal, B. A. 2014. *Design and Construction of Field-Cast UHPC Connections: TECHNOTE*. *Fhwa-Hrt-14-084*.

Hannigan, P. J., Rausche, F., Likins, G. E., Robinson, B. R., and Becker, M. L. 2016. *Design and Construction of Driven Pile Foundations Workshop Manual - Volume I*. United States Federal Highway Administration.

Harbuck, D. I. 1993. "Lightweight foamed concrete fill." *Transportation Research Record*, (1422), 21–28.

Herrmann, L. R., and Mish, K. D. 1983. *User's Manual for SAC-2. A Two-Dimensional Nonlinear, Time Dependent Soil Analysis Code Using the Bounding Surface*

Plasticity Model. California Univ. Davis.

Horvath, J. S. 2005. “Integral-abutment bridges: geotechnical problems and solutions using geosynthetics and ground improvement.” *2005 FHWA Conference: Integral Abutment and Jointless Bridges*.

Kaliakin, V. N., Dafalias, Y. F., and Herrmann, L. R. 1987. “Time dependent bounding surface model for isotropic cohesive soils: notes for a short course.” *Second International Conference on Constitutive Laws for Engineering Materials: THEORY and APPLICATION, Tucson, Arizona*.

Kaliakin, V. N., and Herrmann, L. R. 1991. *Guidelines for implementing the elastoplastic-viscoplastic bounding surface model*. *Technical Rep., Department of Civil Engineering, Univ. of California, Davis, Calif*.

Karim, R., and Shafei, B. 2021. “Performance of fiber-reinforced concrete link slabs with embedded steel and GFRP rebars.” *Engineering Structures*, Elsevier Ltd, 229(December 2020), 111590.

Kunin, J., and Alampalli, S. 2000. “Integral Abutment Bridges: Current Practice in United States and Canada.” *Journal of Performance of Constructed Facilities*, 14(3), 104–111.

Loewen, E. B., Baril, M., and Eric, R. 2012. “Chief Peguis Trail Extension - Rothesay St. Overpass rapid design & construction of an integral abutment bridge with MSE walls & cellular concrete backfill.” *2012 TAC Conference and Exhibition - Transportation: Innovations and Opportunities, TAC/ATC 2012*, 1–19.

Looney, T., Volz, J., and Floyd, R. 2021. “Behavior of a 3-Span Continuous Bridge Before and After Continuity Joint Replacement Using Ultra-High-Performance Concrete.” *Journal of Performance of Constructed Facilities*, 35(6), 04021087.

Mekkawy, M. M., White, D. J., Suleiman, M. T., and Sritharan, S. 2005. “Simple Design

Alternatives to Improve Drainage and Reduce Erosion at Bridge Abutments.” *2005 Mid-Continent Transportation Research Symposium*.

Miller, G. A., Osborne, C., Hatami, K., and Cerato, A. B. 2013. *Applied Approach Slab Settlement Research , Design / Construction*.

Minnesota DOT. 2021. *LRFD Bridge Design Manual*. Oakdale, MN.

Muraleetharan, K. K., Miller, G. A., Floyd, R., Zhang, B., Taghavi, A., Bounds, T. D., and Bright, Z. 2018. *Overturning Forces at Bridge Abutments and the Interaction of Horizontal Forces from Adjacent Roadways*. No. FHWA-OK-17-03. Oklahoma Department of Transportation, 2018.

Muraleetharan, K. K., Miller, G. A., Kirupakaran, K., Krier, D., and Hanlon, B. 2012. *Soil-Structure Interaction Studies for Understanding the Behavior of Integral Abutment Bridges*. Oklahoma City, OK.

New York State DOT. 2021. *Bridge Manual*. Albany, New York.

Oesterle, R., Tabatabia, H., Refai, T., Volz, J., and Scanlon, A. 1999. *Jointless and Integral Abutment Bridges: Volume III - Summary Report*. Washington, D.C.

PLAXIS. 2020. “PLAXIS 2D.”

Purvis, R. L., and Burke, M. P. 2003. *Bridge Deck Performance*. Transportation Research Board, Washington, D.C.

Rhode Island DOT. 2018. *Standard Specifications for Road and Bridge Construction*. Providence, RI.

Rollins, K., Wagstaff, K., and Black, R. 2019. “Passive Force-Deflection Curves for Controlled Low-Strength Material (CLSM) and Lightweight Cellular Concrete (LCC).” *Geo-Congress 2019*, 119–126.

Russell, H. G., Graybeal, B. A., and Russell, H. G. 2013. *Ultra-high performance concrete: A state-of-the-art report for the bridge community.* United States. Federal

Highway Administration. Office of Infrastructure ….

Scarlata, J. 2017. *UHPC Link Slab Design*. NYDOT.

Seibert, P. J., Perry, V. H., and Corvez, D. 2019. “Performance Evaluation of Field Cast UHPC Connections for Precast Bridge Elements.” 1–11.

Sherafati, A., and Azizinamini, A. 2015. “Flexible Pile Head in Jointless Bridges: Experimental Investigation.” *Journal of Bridge Engineering*, 20(4), 1–12.

Tavenas, F., Mieussens, C., and Bourges, F. 1979. “Lateral displacements in clay foundations under embankments.” *Canadian Geotechnical Journal*, 16(3), 532–550.

Thorkildsen, E. T. 2020. “Case Study: Eliminating Bridge Joints with Link Slabs-An Overview of State Practices.” United States. Federal Highway Administration.

Tiwari, B., Wykoff, J., and Villegas, D. 2020. *State of the Practice Use of Lightweight Cellular Concrete (LCC) Materials in Geotechnical Applications*. California Nevada Cement Association.

Whittle, A. J., and Kavvadas, M. J. 1994. “Formulation of MIT-E3 constitutive model for overconsolidated clays.” *Journal of Geotechnical Engineering*, 120(1), 173–198.

Appendix A – State Dot Standard Plans Referenced

Alabama DOT (2021). Standard Drawings. Alabama Department of Transportation, Montgomery.https://alletting.dot.state.al.us/Docs/Standard_Drawings/StdSpecialDrawingsEnglish2021.htm

Arizona DOT (2021). Standard Detail Drawings. Arizona Department of Transportation, Phoenix. https://azdot.gov/business/engineering-and-construction/bridge/bridge-design-services/structure-detail-drawings

Arkansas DOT (2021). Standard Bridge Drawings. Arkansas Department of Transportation, Little Rock. https://www.ardot.gov/divisions/bridge/list-of-standard-drawings/

Colorado DOT (2019). Structural Worksheets. Colorado Department of Transportation, Denver. https://www.codot.gov/library/bridge/bridge-manuals/design-standards/structural-worksheets-pdfs

Connecticut DOT (2009). Standard Drawings. Connecticut Department of Transportation, Newington. https://portal.ct.gov/DOT/Office-of-Engineering/CTDOT-CONTRACT-DRAWING-STANDARDS

Florida DOT (2021). Standard Plans for Road and Bridge Construction. Florida Department of Transportation, Tallahassee. https://www.fdot.gov/design/standardplans/default.shtm

Iowa DOT (2020). Bridge Standards. Iowa Department of Transportation, Ames. https://iowadot.gov/bridge/bridge-and-culvert-standards/bridge-standards

Kansas DOT (2021). Standard Drawings. Kansas Department of Transportation, Topeka. https://kart.ksdot.org/StandardDrawings/StandardDetail.aspx

Louisiana DOTD (2021). Standard Plans and Special Details. Louisiana Department of Transportation and Development, Baton Rouge. http://wwwsp.dotd.la.gov/Inside_LaDOTD/Divisions/Engineering/Standard_Plans/Pages/default.aspx

Michigan DOT (2020). Standard Plans. Michigan Department of Transportation, Lansing. https://mdotjboss.state.mi.us/stdplan/standardPlansIndex.htm

Minnesota DOT (2021). Standard Plans. Minnesota Department of Transportation, St. Paul. https://standardplans.dot.state.mn.us/

New York State DOT (2019). Drawings. New York State Department of Transportation, Albany. https://www.dot.ny.gov/main/business-center/engineering/cadd-info/drawings/standard-sheets-us

North Carolina DOT (2018). Standard Drawings. North Carolina Department of Transportation, Raleigh. https://connect.ncdot.gov/resources/Specifications/Pages/2018-Roadway-Standard-Drawings.aspx

Oklahoma DOT (2016). Bridge Design Standards and Specifications. Oklahoma Department of Transportation, Oklahoma City. https://www.odot.org/bridge/2009-sb/brd_std_2009-lrfd-sb-index.php

Pennsylvania DOT (2021). Standards for Bridge Construction. Pennsylvania Department of Transportation, Harrisburg. https://www.penndot.gov/ProjectAndPrograms/Bridges/Pages/Plans,-Standards-and-Specifications.aspx

Rhode Island DOT (2015). Bridge Design Standard Details. Rhode Island Department of Transportation, Providence. http://www.dot.ri.gov/business/contractorsandconsultants.php

South Carolina DOT (2021). Standard Drawings. South Carolina Department of Transportation, Columbia. https://falcon.scdot.org/falconwebv4/default.aspx?cmd=logon&hiddenLogon=1

Tennessee DOT (2020). Standard Structures Drawings. Tennessee Department of Transportation, Nashville. https://www.tn.gov/content/tn/tdot/structures-/standard-structures-drawings.html

Texas DOT (2021). Bridge Standards. Texas Department of Transportation, Austin. https://www.dot.state.tx.us/insdtdot/orgchart/cmd/cserve/standard/bridge-e.htm

Appendix B – Bridge Systems Survey

Thank you for participating in this research survey. We will be compiling all survey responses and publishing an anonymized summary on the Oklahoma Department of Transportation website. Please indicate whether you would like to be notified when the results are published:

The survey will take approximately 20 minutes to complete. You may exit and return to complete the survey using the same device if needed. Unfinished surveys will be automatically submitted after 2 weeks.

The survey is divided into 5 parts:
1) Bridge approach roadway and longitudinal forces due to excessive pavement pressure,
2) Tall embankment performance,
3) Conventional bridges with expansion joints,
4) Integral and semi-integral bridges,
5) Abutment backfill material.

Q.1 Please enter the following, responses will be kept anonymous.

- ○ Name: _____
- ○ Organization: _____
- ○ Position/Job Title: _____
- ○ Mailing Address: _____
- ○ Email Address: _____

The following set of questions pertain to:
Bridge Approach Roadway and Excessive Pavement Pressure

Q.2 Does your state install expansion joints, or pavement pressure relief joints, in new approach pavements leading up to bridges?

Q.3 Pertaining to pavement pressure relief joints:

- ○ What are the standard procedures?

_____

- ○ What is the standard joint width?

_____

- ○ What is the standard joint spacing?

_____

Excessive pavement pressure on bridges often shows up as:
*Excessive pavement cracking
*Shoving on the bridge (causes tilted bearings, sheared anchor bolts, etc.)
*U cracking or spalling of the backwall (see example photo below)
*Pavement pop outs

Q.4 Does your state have problems with excessive pavement pressure on bridges?

- ○ Yes, at numerous locations
- ○ Yes, at a few locations
- ○ Not sure
- ○ No

Q.5 Does your state retrofit or repair pavement pressure problems as described above with pavement pressure relief joints in approach pavements?

Q.6 Pertaining to retrofit and repair of pavement pressure problems with relief joints:

- ○ What is the standard repair procedure?

_____

- ○ What is the standard joint width?

_____

- ○ If a series of joints is used, what is the standard joint spacing?

_____

The following set of questions pertain to:
Tall Embankment Performance

Q.7 Have you noticed performance problems with your bridges when the approach embankments are tall?

Q.8 At what height would an embankment be considered tall?

_____

Q.9 Please describe the performance problems noticed with tall embankments.

_____

The following set of questions pertain to:
Conventional Bridges

Q.10 Approximately what percentage of bridges in your state are constructed as conventional bridges with expansion joints?

Q.11 What percentage of conventional bridges fall into the following performance categories.
Good : _____
Fair : _____
Poor : _____
Severe : _____

Q.12 List any common performance problems in your state with conventional bridges? If there are multiple problems, please list them from most problematic to least problematic.

_____

The following set of questions pertain to:
Integral and Semi-Integral Bridges

Q.13 Does your state allow the construction of integral or semi-integral bridges?

Q.14 Approximately what percentage of bridge in your state are constructed as integral or semi-integral bridges?
Integral Bridges : _____
Semi-Integral Bridges : _____

Q.15 What percentage of **integral bridges** fall into the following performance categories.
Good : _____
Fair : _____
Poor : _____
Severe : _____
Not Applicable : _____

Q.16 What percentage of **semi-integral bridges** fall into the following performance categories.
Good : _____
Fair : _____
Poor : _____
Severe : _____
Not Applicable : _____

Q.17 List any common performance problems in your state with integral or semi-integral bridges? If there are multiple problems, please list them from most problematic to least problematic.

○ Problems noted with Integral Bridges

_____

○ Problems noted with Semi-Integral Bridges

_____

Q.18 Does your state place any restrictions on the length of integral or semi-integral bridges?

Q.19 What is the length restrictions in your state?

- ○ Integral Bridges _____
- ○ Semi-Integral Bridges

_____

Q.20 Does your state allow skewed integral or semi-integral bridges?

Q.21 Are there limits placed on the amount of skew allowed for integral or semi-integral bridges? If so, what is the limit?

- ○ Integral Bridges _____
- ○ Semi-Integral Bridges

_____

Q.22 Does your state allow curved integral or semi-integral bridges?

Q.23 Are there limits placed on the amount of curvature for integral bridges? If so, what is the limit?

- ○ Integral Bridges _____
- ○ Semi-Integral Bridges

_____

Q.24 What percentage of **Integral Bridges** utilize precast/prestress girders and what percentage utilized steel girders?
precast/prestressted: _____
steel: _____

Q.25 What percentage of Semi-Integral Bridges utilize precast/prestress girders and what percentage utilized steel girders?
precast/prestressed: _____
steel: _____

Q.26 Are there any specific substructure details specific to integral or semi-integral bridges in your state (e.g., weak axis pile orientation, joints between abutment and wing walls)?

- ○ Integral Bridges _____
- ○ Semi-Integral Bridges _____

Q.27 Are there any special superstructure details specific to integral or semi-integral bridges in your state (e.g., additional reinforcement in pier continuity joints, specific deck pour sequence)?

- ○ Integral Bridges _____
- ○ Semi-Integral Bridges _____

Q.28 Does your state retrofit conventional bridges to integral or semi-integral bridges?

Q.29 How would you rate the performance of conventional bridges retrofitted to integral or semi-integral bridges?

- ○ Excellent
- ○ Good
- ○ Average
- ○ Poor
- ○ Terrible

Q.30 Please add any additional comments below regarding the performance of conventional bridges that have been retrofitted to integral or semi-integral bridges.

_____

The following set of questions pertain to:
Bridge Abutment Backfill Material

Q.31 What type of backfill material does your state typically use for conventional, integral, and semi-integral bridges? Select all that apply.

	Conventional Bridges	Integral Bridges	Semi-Integral Bridges
Granular Backfill	○	○	○
Controlled Low Strength Material (CLSM)/ Flowable Fill	○	○	○
Low Density Cellular Concrete (foamed Concrete)	○	○	○
other	○	○	○

Q.32 Has your state used low density cellular concrete backfill (also known as foamed concrete)?

Q.33 How would you rate the performance of low-density cellular concrete backfill?

- ○ Excellent
- ○ Good
- ○ Average
- ○ Poor
- ○ Terrible

Q.34 Please add any additional comments on the use of low density cellular concrete backfill.

_____

Q.35 May we contact you to follow up on your responses if more information is sought?

Appendix C – SH-3 over BNSF Boring Logs

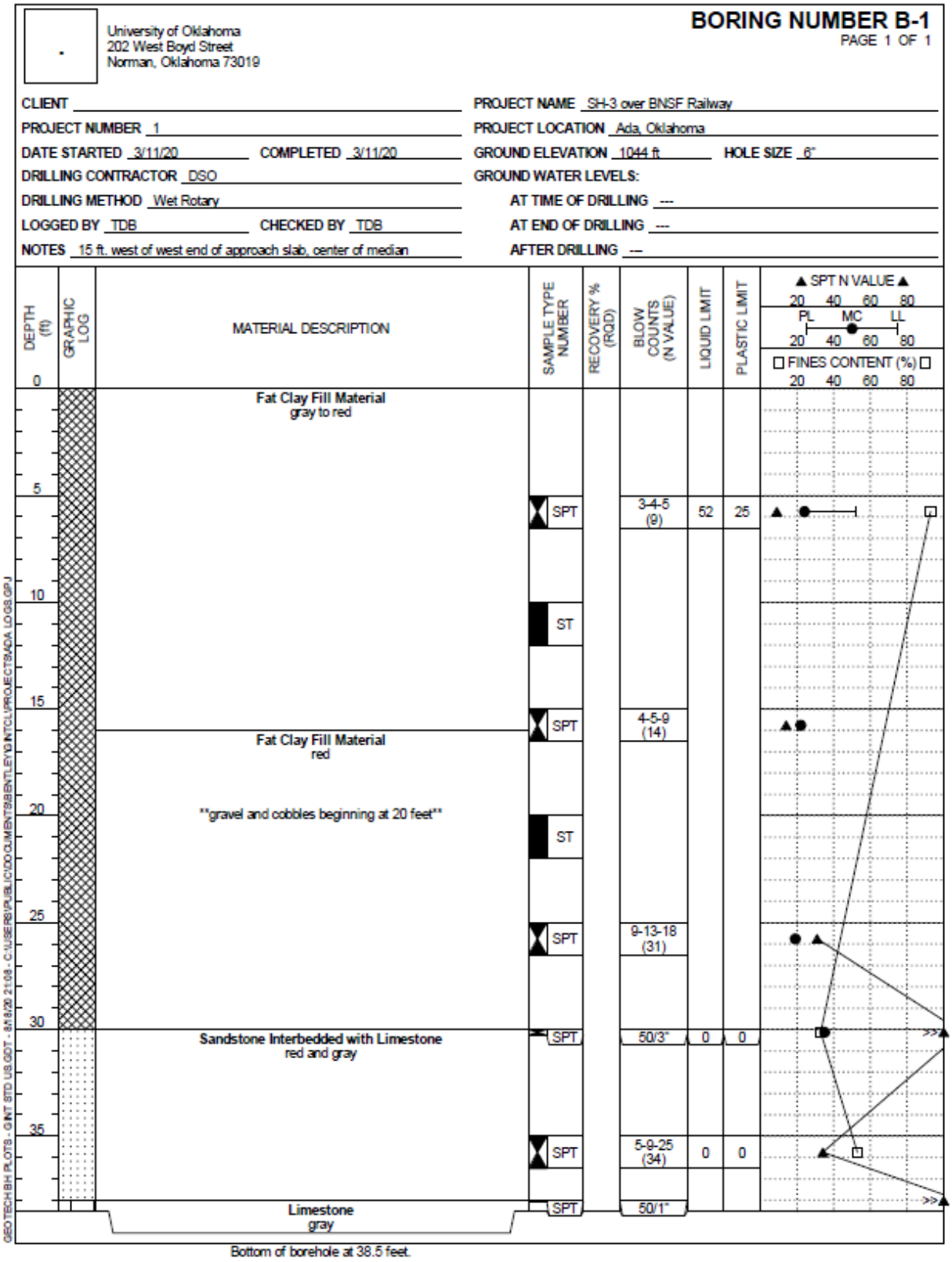

University of Oklahoma
202 West Boyd Street
Norman, Oklahoma 73019

BORING NUMBER B-2

CLIENT

PROJECT NAME SH-3 over BNSF Railway

PROJECT NUMBER 1

PROJECT LOCATION Ada, Oklahoma

DATE STARTED 3/11/20 COMPLETED 3/11/20

GROUND ELEVATION 1042 ft HOLE SIZE 6"

DRILLING CONTRACTOR DSO

GROUND WATER LEVELS:

DRILLING METHOD Wet Rotary

AT TIME OF DRILLING ---

LOGGED BY TDB CHECKED BY TDB

AT END OF DRILLING ---

NOTES 10 ft. east of east approach slab, center median

AFTER DRILLING ---

DEPTH (ft)	GRAPHIC LOG	MATERIAL DESCRIPTION	SAMPLE TYPE NUMBER	RECOVERY % (RQD)	BLOW COUNTS (N VALUE)	LIQUID LIMIT	PLASTIC LIMIT	▲ SPT N VALUE ▲ 20 40 60 80 / PL MC LL 20 40 60 80 / □ FINES CONTENT (%) □ 20 40 60 80
0								
5		**Lean Clay Fill Material** greenish brown to reddish brown	SPT		4-9-10 (19)			
10			ST					
15			SPT		5-5-8 (13)			
20		**Sandy Shale Fill Material** gray to black	SPT		34-13-14 (27)			
25			SPT		3-35-49 (84)			
30			SPT		19-50/6"	58	42	>>
35		**Silty Sandstone Fill Material** black to red	SPT		20-33-50/4"	0	0	>>
40								

(Continued Next Page)

GEOTECH BH PLOTS - GINT STD US.GDT - 8/18/20 21:08 - C:\USERS\PUBLIC\DOCUMENTS\BENTLEY\GINTCL\PROJECT\BACA LOGS.GPJ

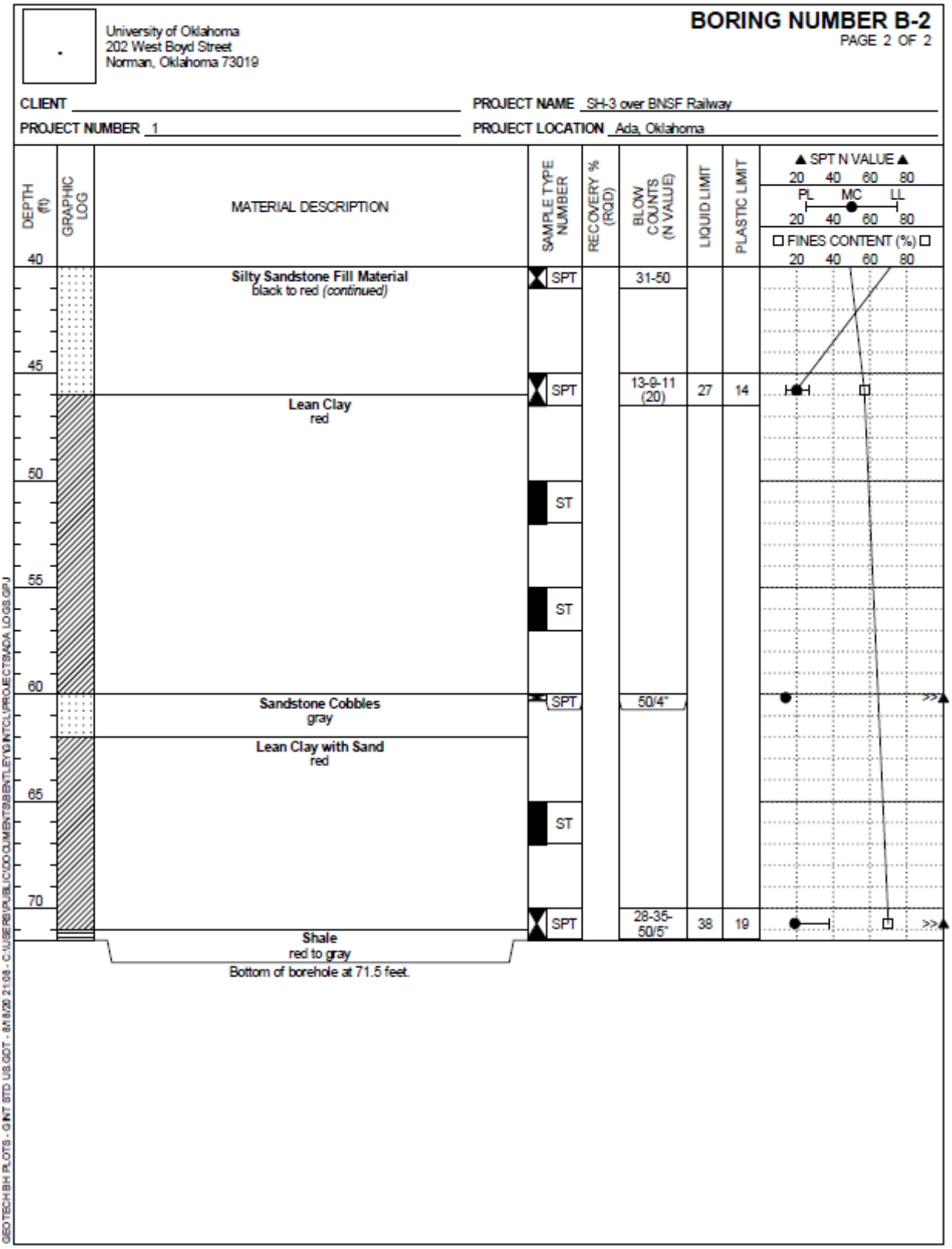
University of Oklahoma
202 West Boyd Street
Norman, Oklahoma 73019
BORING NUMBER B-2
PAGE 2 OF 2
CLIENT
PROJECT NAME SH-3 over BNSF Railway
PROJECT NUMBER 1
PROJECT LOCATION Ada, Oklahoma
DEPTH (ft)
GRAPHIC LOG
MATERIAL DESCRIPTION
SAMPLE TYPE NUMBER
RECOVERY % (RQD)
BLOW COUNTS (N VALUE)
LIQUID LIMIT
PLASTIC LIMIT
▲ SPT N VALUE ▲
20 40 60 80
PL MC LL
20 40 60 80
☐ FINES CONTENT (%) ☐
20 40 60 80
40
45
50
55
60
65
70
Silty Sandstone Fill Material
black to red (continued)
SPT
31-50
SPT
13-9-11 (20)
27
14
Lean Clay
red
ST
ST
Sandstone Cobbles
gray
SPT
50/4"
>>
Lean Clay with Sand
red
ST
Shale
red to gray
SPT
28-35-50/5"
38
19
>>
Bottom of borehole at 71.5 feet.
GEOTECH BH PLOTS - GINT STD US.GDT - 8/18/20 21:08 - C:\USERS\PUBLIC\DOCUMENTS\BENTLEY\GINT\CLI\PROJECTS\ADA LOGS.GPJ

University of Oklahoma
202 West Boyd Street
Norman, Oklahoma 73019

BORING NUMBER B-3

CLIENT

PROJECT NAME SH-3 over BNSF Railway

PROJECT NUMBER 1

PROJECT LOCATION Ada, Oklahoma

DATE STARTED 3/11/20 COMPLETED 3/11/20

GROUND ELEVATION 1031 ft HOLE SIZE 6"

DRILLING CONTRACTOR DSO

GROUND WATER LEVELS:

DRILLING METHOD Wet Rotary

AT TIME OF DRILLING ---

LOGGED BY TDB CHECKED BY TDB

AT END OF DRILLING ---

NOTES 250 ft. eat of east approach slab, center median

AFTER DRILLING ---

DEPTH (ft)	GRAPHIC LOG	MATERIAL DESCRIPTION	SAMPLE TYPE NUMBER	RECOVERY % (RQD)	BLOW COUNTS (N VALUE)	LIQUID LIMIT	PLASTIC LIMIT
0							
5		**Lean Clay Fill Material** **"Shale and Sandstone Cobbles Mixed in Fill Material"** greenish gray	SPT		5-7-13 (20)		
10		**Silty Sand Fill Material** **"Shale and Sandstone Cobbles Mixed in Fill Material"** greenish gray	SPT		20-40-43 (83)	0	0
15		**Lean Clay Fill Material** **"Shale and Sandstone Cobbles Mixed in Fill Material"** greenish gray	SPT		9-22-25 (47)		
20		**Clayey Sand and Gravel Fill Material** Black to red to gray **"Strong Organic Odor"**	SPT		17-21-16 (37)	42	30
25			SPT		27-39-50/5"	0	0
30			SPT		50/3"		
35		**Lean Clay** greenish brown to red to dark brown	SPT		4-10-11 (21)		
40							

▲ SPT N VALUE ▲
20 40 60 80
PL MC LL
20 40 60 80
☐ FINES CONTENT (%) ☐
20 40 60 80

(Continued Next Page)

University of Oklahoma
202 West Boyd Street
Norman, Oklahoma 73019

BORING NUMBER B-3

CLIENT _____ PROJECT NAME SH-3 over BNSF Railway

PROJECT NUMBER 1 PROJECT LOCATION Ada, Oklahoma

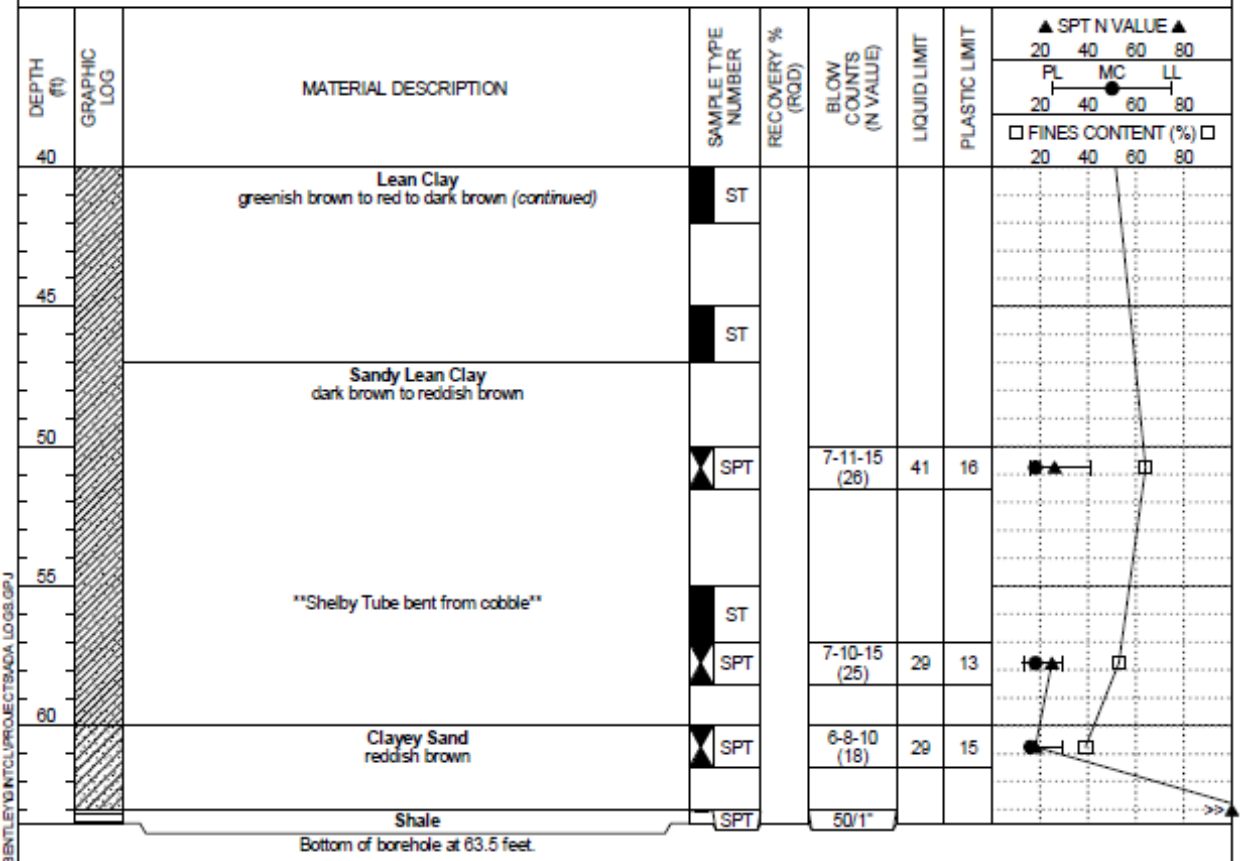

Appendix D – SH-3 over BNSF Lab Test Results

D.1 One Dimensional Consolidation Results

CONSOLIDATION TEST REPORT

ASTM D2435

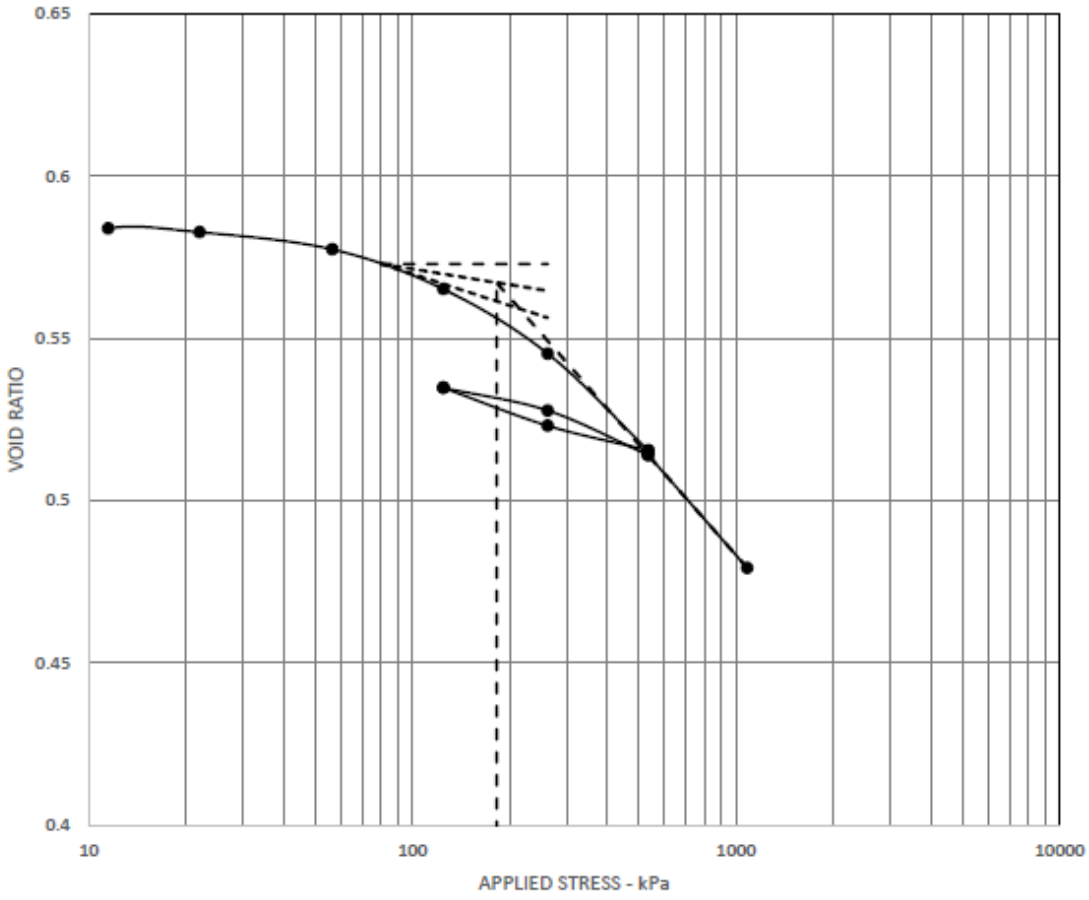

C_c	C_r	e_0	Pc (kPa)	OCR
0.113	0.04	0.573	182	2.8

Sample and Test Data				Project Information
Sample Location:	B-1	3.4	Meters	
Description:	lean clay			Client:
Assumed Specific Gravity = 2.7				Project #:
				Sample Type: Undisturbed
Initial Mc (%)	17.4	Final Mc (%)	16.2	Date Sampled:
dia. (in)	2.495			
Saturation (%)	81.85			
Dry Density (pcf):	107			Technician: TDB

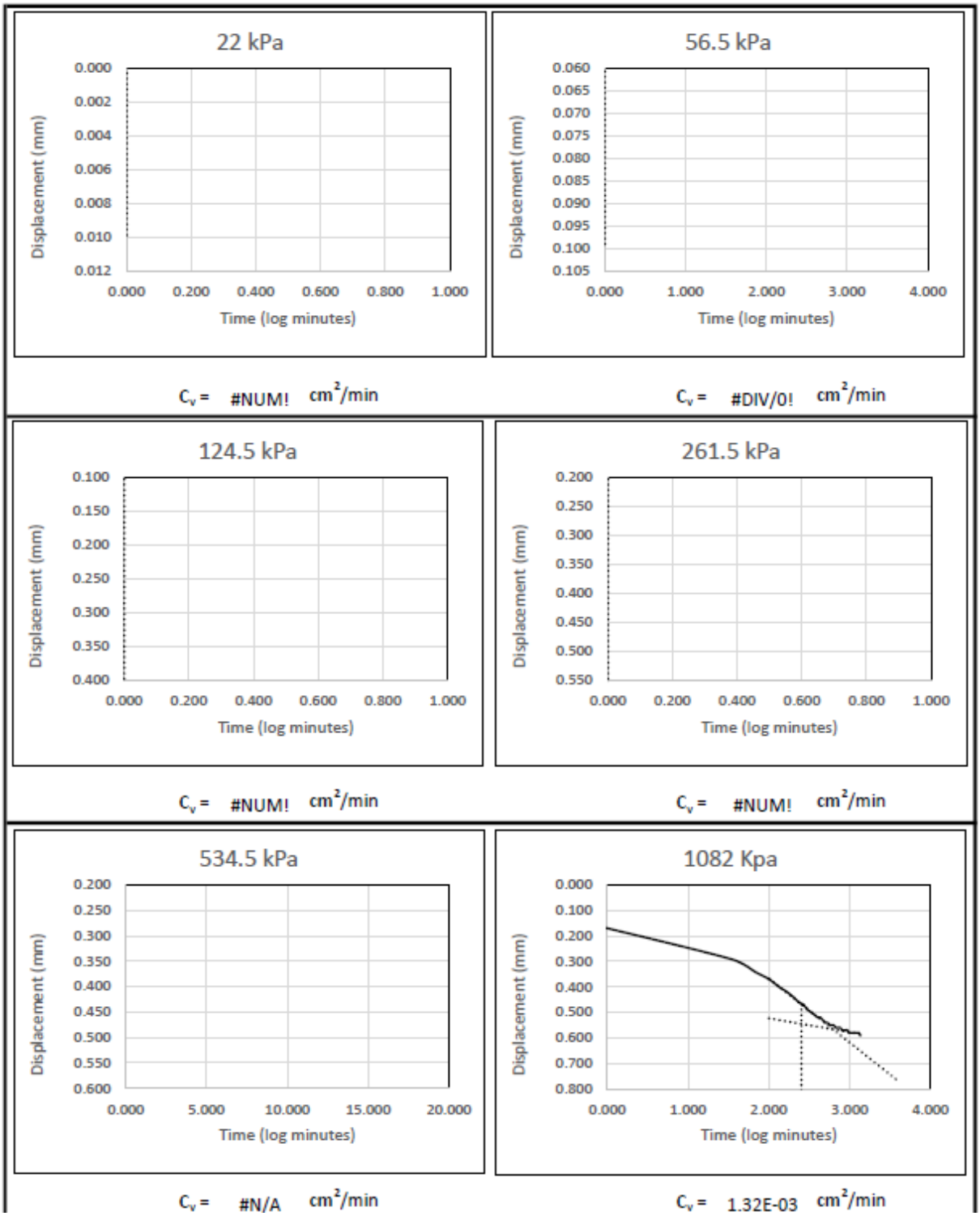

C_v = #NUM! cm^2/min

C_v = #DIV/0! cm^2/min

C_v = #NUM! cm^2/min

C_v = #NUM! cm^2/min

C_v = #N/A cm^2/min

C_v = 1.32E-03 cm^2/min

CONSOLIDATION TEST REPORT

ASTM D2435

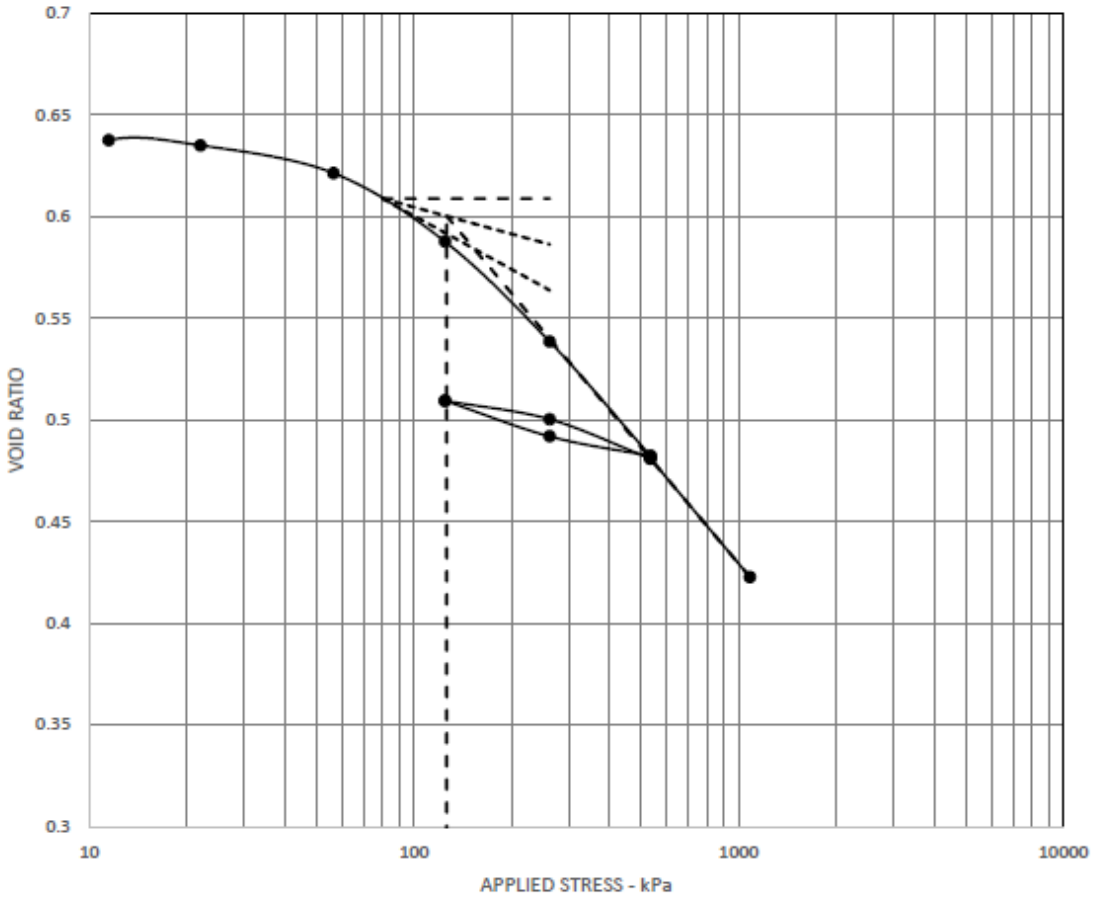

C_c	C_r	e_0	Pc (kPa)	OCR
0.19	0.11	0.616	126	1

Sample and Test Data				Project Information
Sample Location:	B-1	6.5	Meters	
Description:	lean clay			**Client:**
Assumed Specific Gravity = 2.7				**Project #:**
				Sample Type: Undisturbed
Initial Mc (%)	20.3	Final Mc (%)	18.5	**Date Sampled:**
dia. (in)	2.5			
Saturation (%)	88.93			
Dry Density (pcf):	104.2			**Technician: TDB**

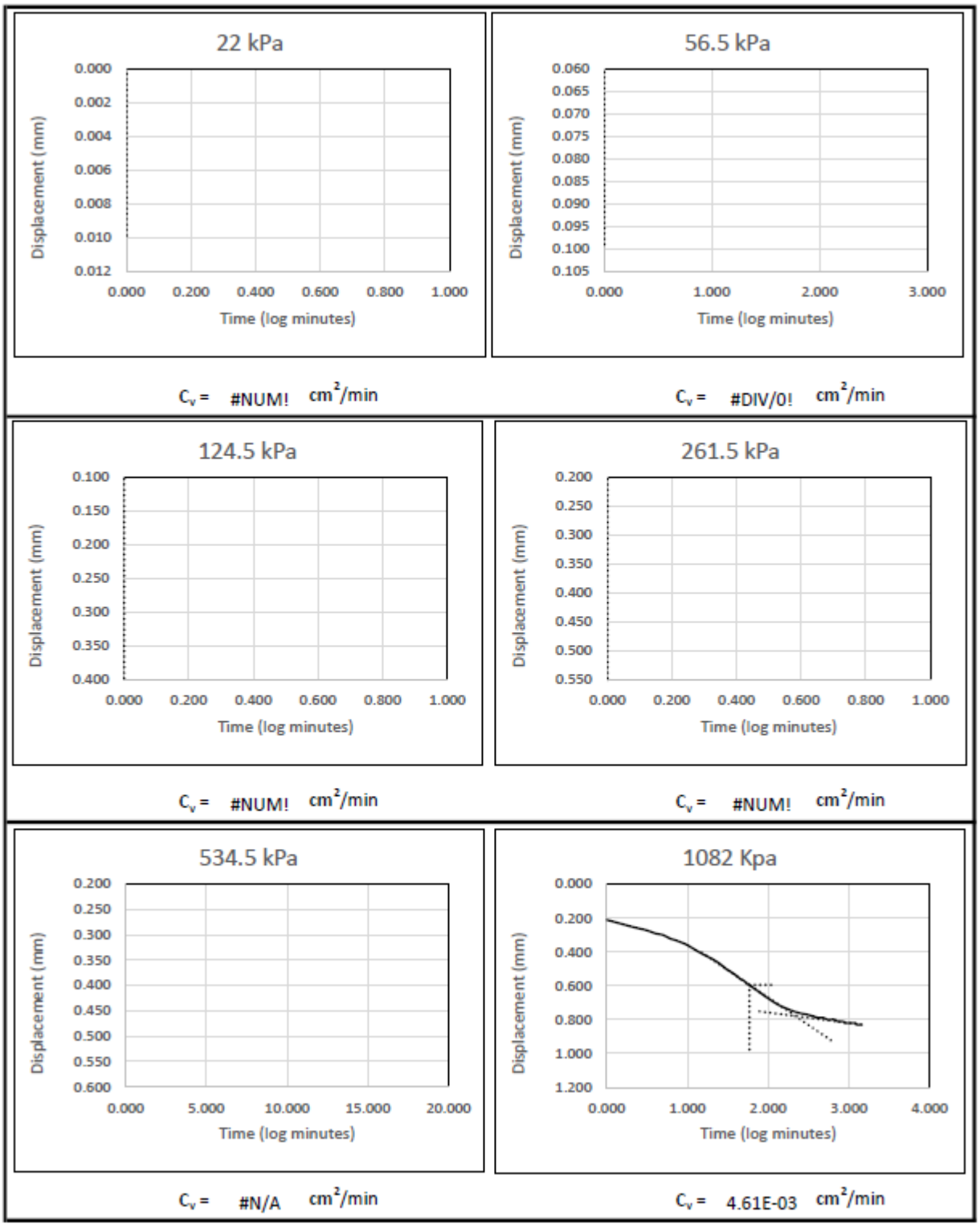

C_v = #NUM! cm^2/min

C_v = #DIV/0! cm^2/min

C_v = #NUM! cm^2/min

C_v = #NUM! cm^2/min

C_v = #N/A cm^2/min

C_v = 4.61E-03 cm^2/min

CONSOLIDATION TEST REPORT

ASTM D2435

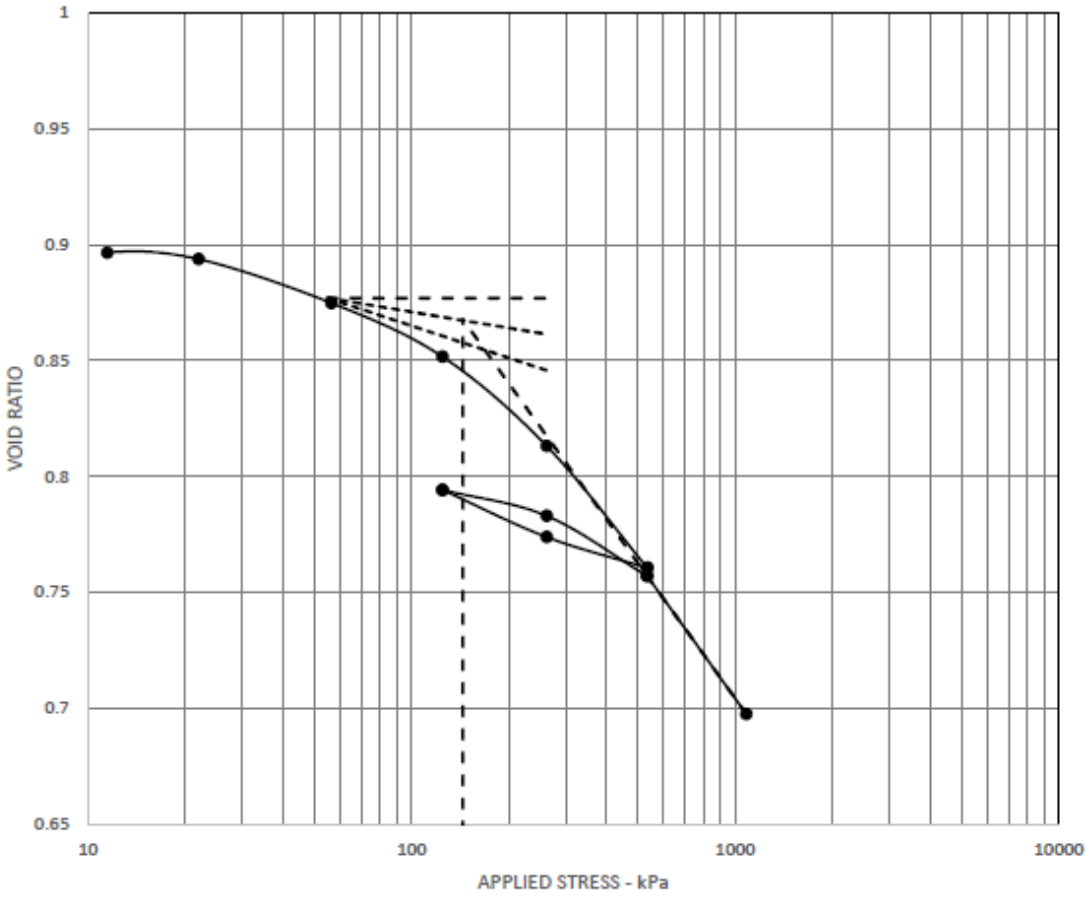

C_c	C_r	e_0	Pc (kPa)	OCR
0.194	0.071	0.887	144	2.3

Sample and Test Data				Project Information
Sample Location:	B-2	3.2	Meters	
Description:	lean clay			**Client:**
Assumed Specific Gravity = 2.7				**Project #:**
				Sample Type: Undisturbed
Initial Mc (%)	25.3	Final Mc (%)	21.6	**Date Sampled:**
dia. (in)	2.5			
Saturation (%)	76.97			
Dry Density (pcf):	89.3			**Technician: TDB**

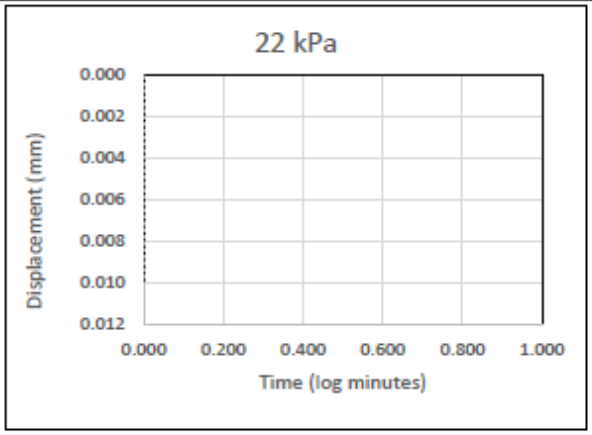

C_v = #NUM! cm^2/min

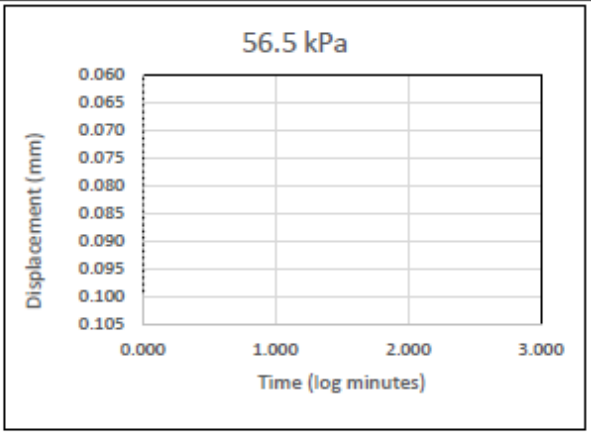

C_v = #DIV/0! cm^2/min

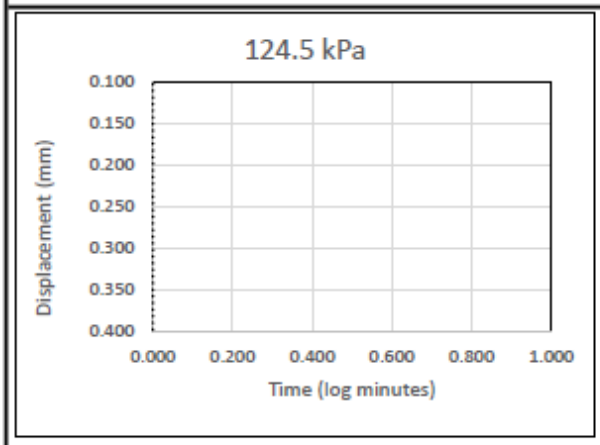

C_v = #NUM! cm^2/min

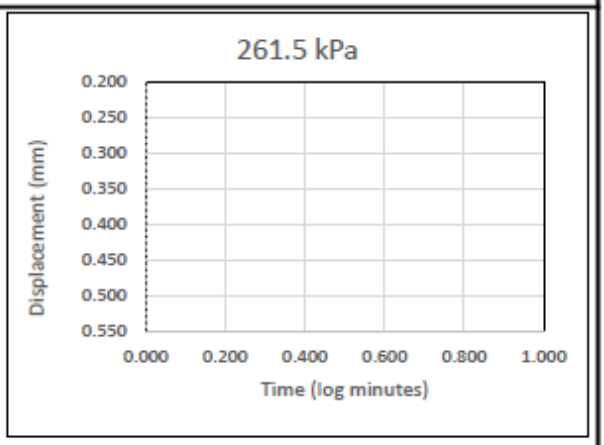

C_v = #NUM! cm^2/min

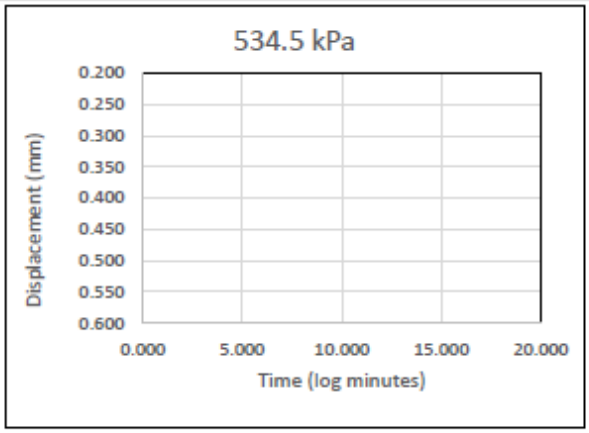

C_v = #N/A cm^2/min

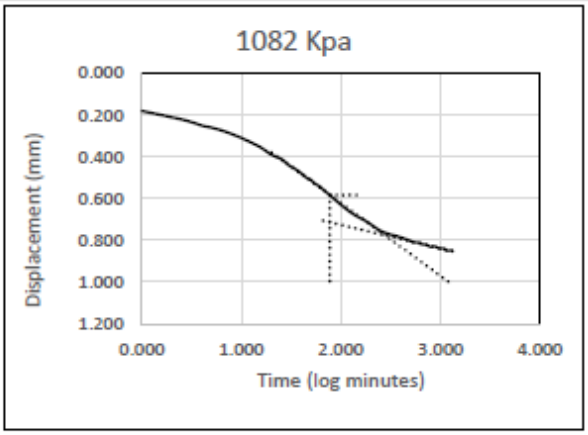

C_v = 4.06E-03 cm^2/min

CONSOLIDATION TEST REPORT

ASTM D2435

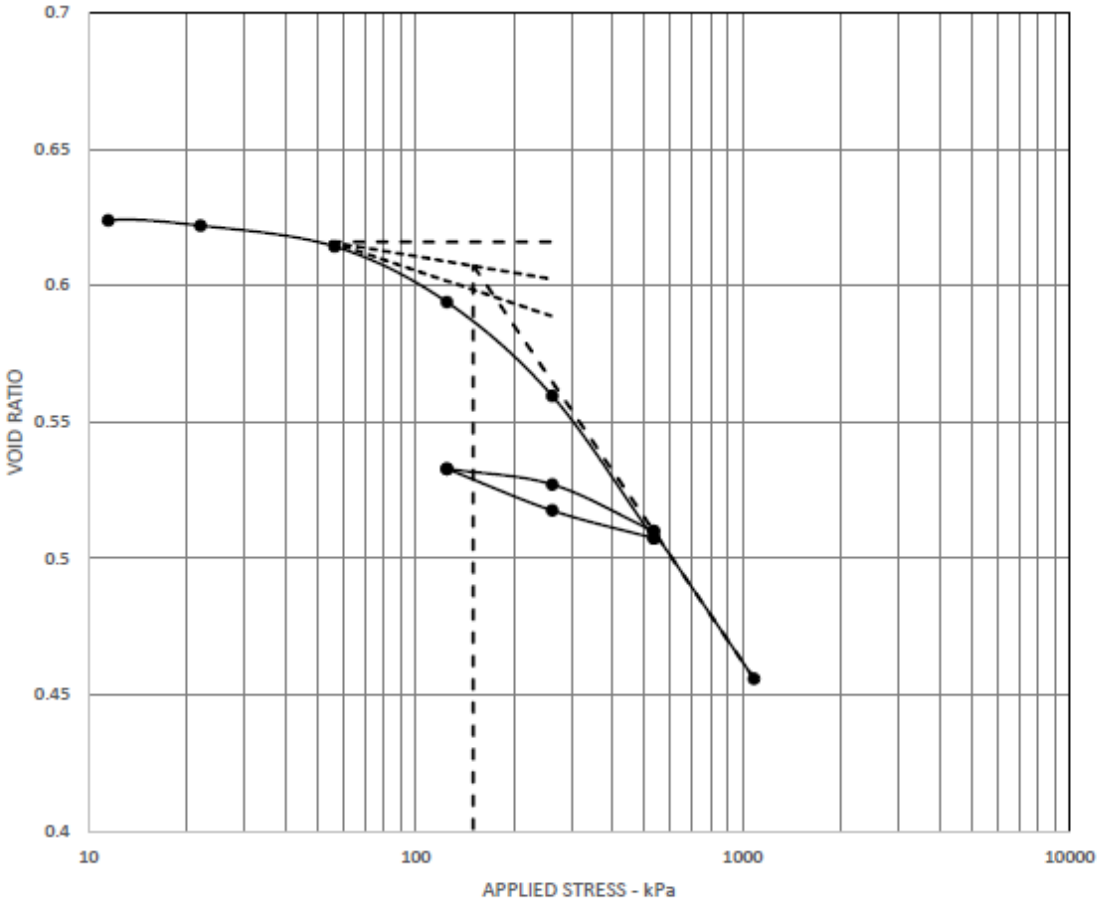

C_c	C_r	e_0	Pc (kPa)	OCR
0.176	0.062	0.616	150	0.4

Sample and Test Data				Project Information
Sample Location:	B-2	16.9	Meters	
Description:	lean clay			Client:
Assumed Specific Gravity = 2.7				Project #:
				Sample Type: Undisturbed
Initial Mc (%)	21	Final Mc (%)	19.1	Date Sampled:
dia. (in)	2.5			
Saturation (%)	91.9			
Dry Density (pcf):	104.2			Technician: TDB

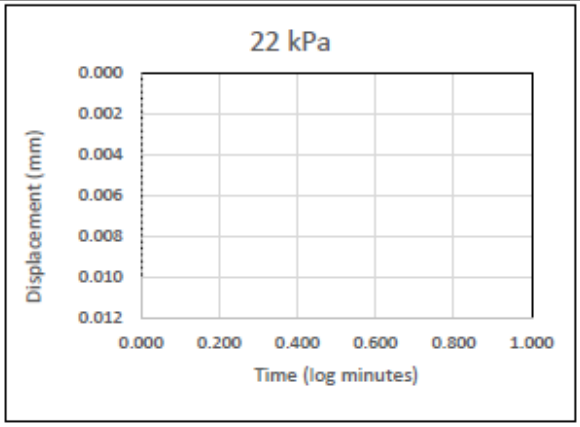

C_v = #NUM! cm^2/min

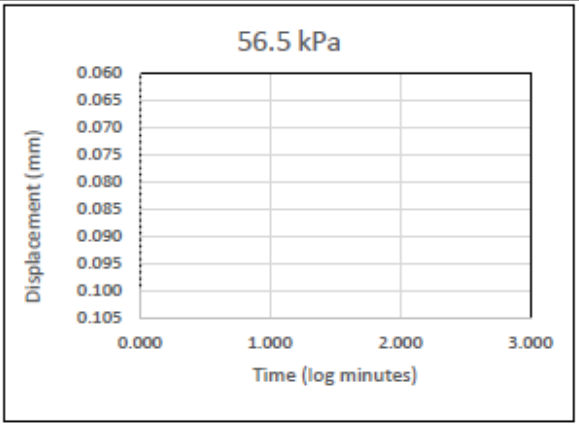

C_v = #DIV/0! cm^2/min

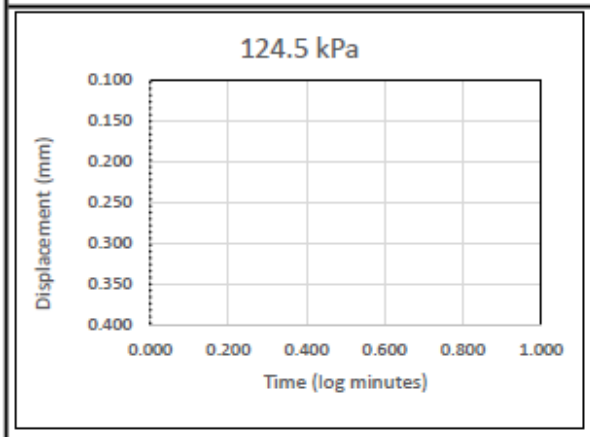

C_v = #NUM! cm^2/min

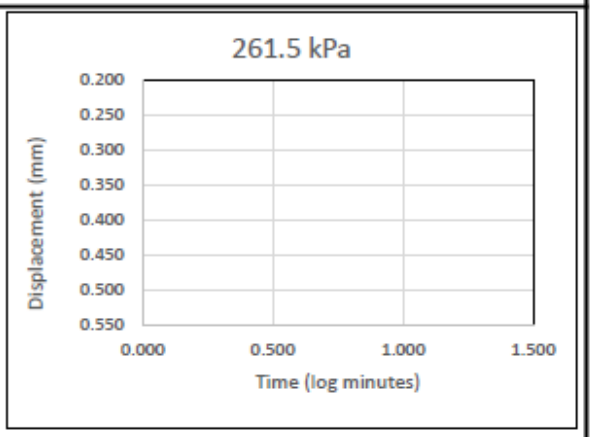

C_v = 4.44E-01 cm^2/min

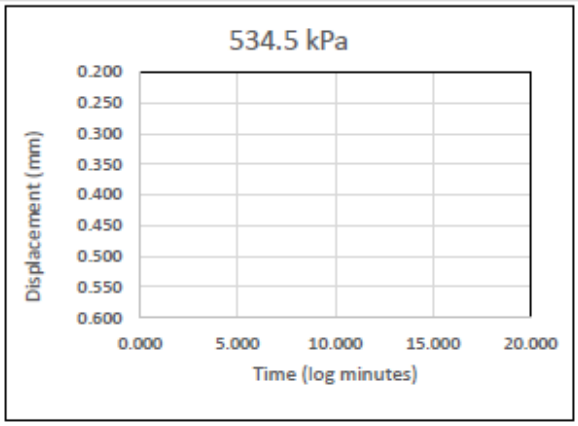

C_v = #N/A cm^2/min

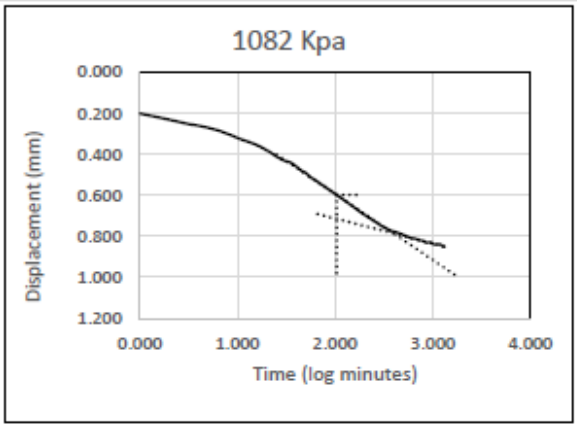

C_v = 2.69E-03 cm^2/min

CONSOLIDATION TEST REPORT

ASTM D2435

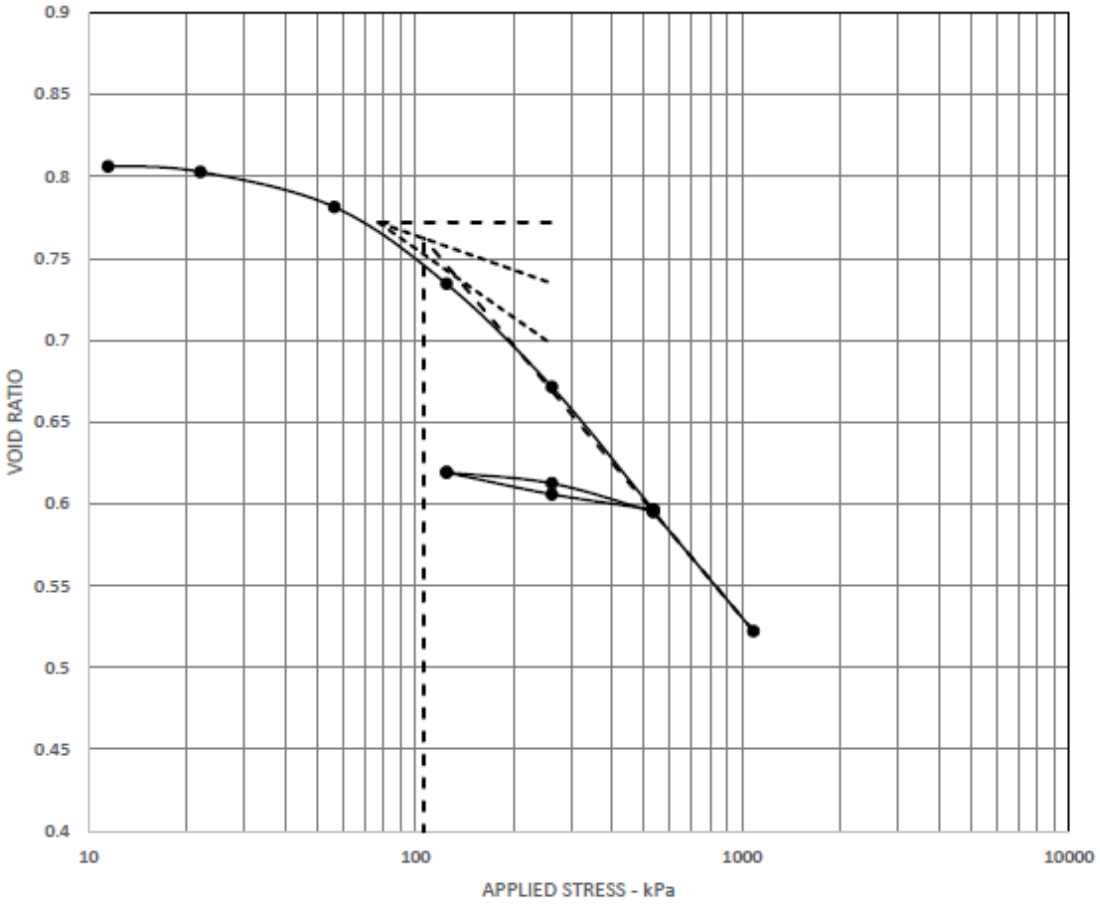

C_c	C_r	e_0	Pc (kPa)	OCR
0.238	0.179	0.802	106	0.3

Sample and Test Data				Project Information
Sample Location:	B-2	17	Meters	
Description:	lean clay			**Client:**
Assumed Specific Gravity = 2.7				**Project #:**
				Sample Type: Undisturbed
Initial Mc (%)	23.6	Final Mc (%)	17	**Date Sampled:**
dia. (in)	2.495			
Saturation (%)	79.37			
Dry Density (pcf):	93.4			**Technician: TDB**

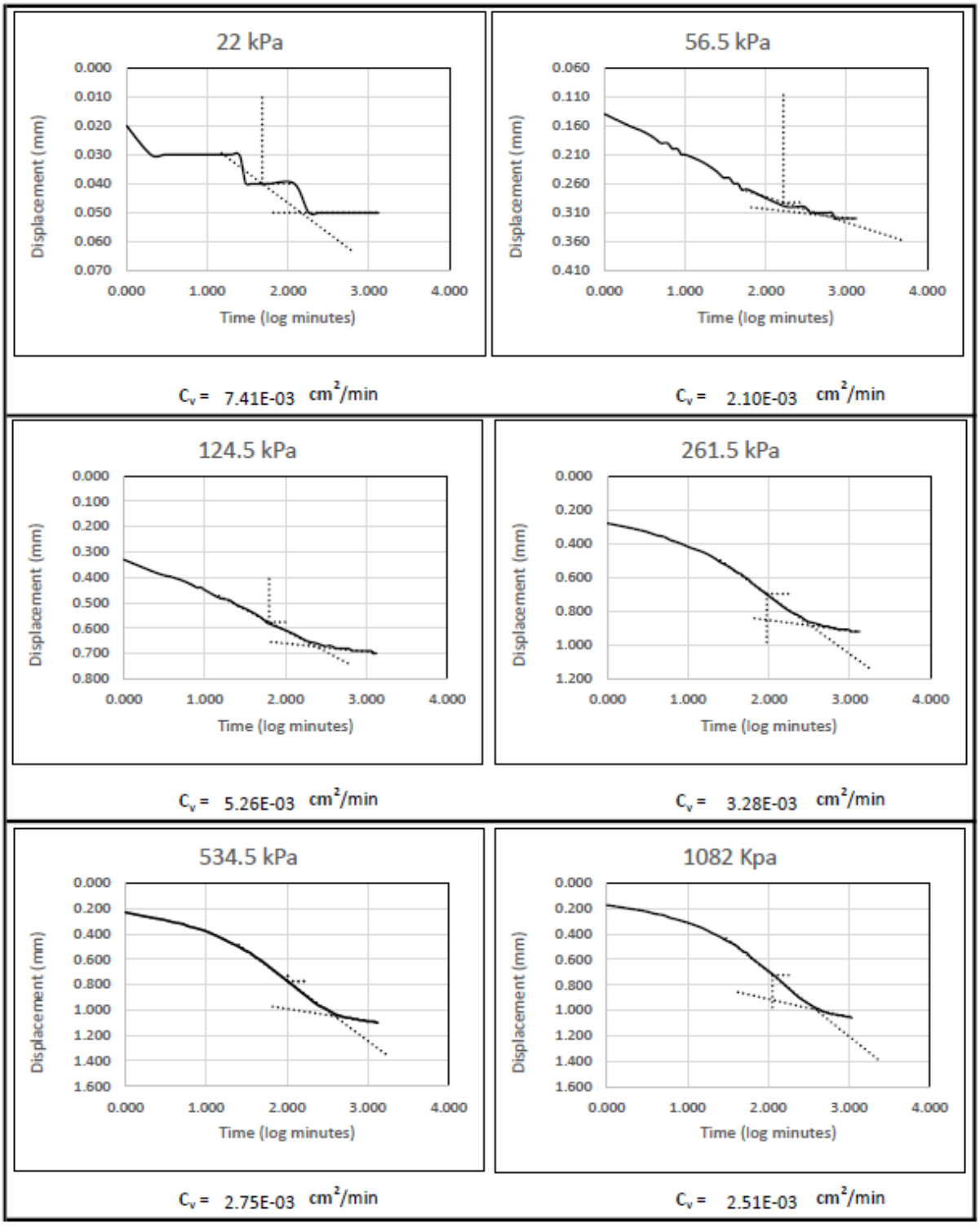
22 kPa
Displacement (mm)
0.000
0.010
0.020
0.030
0.040
0.050
0.060
0.070
0.000
1.000
2.000
3.000
4.000
Time (log minutes)
C_v = 7.41E-03 cm^2/min
56.5 kPa
Displacement (mm)
0.060
0.110
0.160
0.210
0.260
0.310
0.360
0.410
0.000
1.000
2.000
3.000
4.000
Time (log minutes)
C_v = 2.10E-03 cm^2/min
124.5 kPa
Displacement (mm)
0.000
0.100
0.200
0.300
0.400
0.500
0.600
0.700
0.800
0.000
1.000
2.000
3.000
4.000
Time (log minutes)
C_v = 5.26E-03 cm^2/min
261.5 kPa
Displacement (mm)
0.000
0.200
0.400
0.600
0.800
1.000
1.200
0.000
1.000
2.000
3.000
4.000
Time (log minutes)
C_v = 3.28E-03 cm^2/min
534.5 kPa
Displacement (mm)
0.000
0.200
0.400
0.600
0.800
1.000
1.200
1.400
1.600
0.000
1.000
2.000
3.000
4.000
Time (log minutes)
C_v = 2.75E-03 cm^2/min
1082 Kpa
Displacement (mm)
0.000
0.200
0.400
0.600
0.800
1.000
1.200
1.400
1.600
0.000
1.000
2.000
3.000
4.000
Time (log minutes)
C_v = 2.51E-03 cm^2/min

CONSOLIDATION TEST REPORT

ASTM D2435

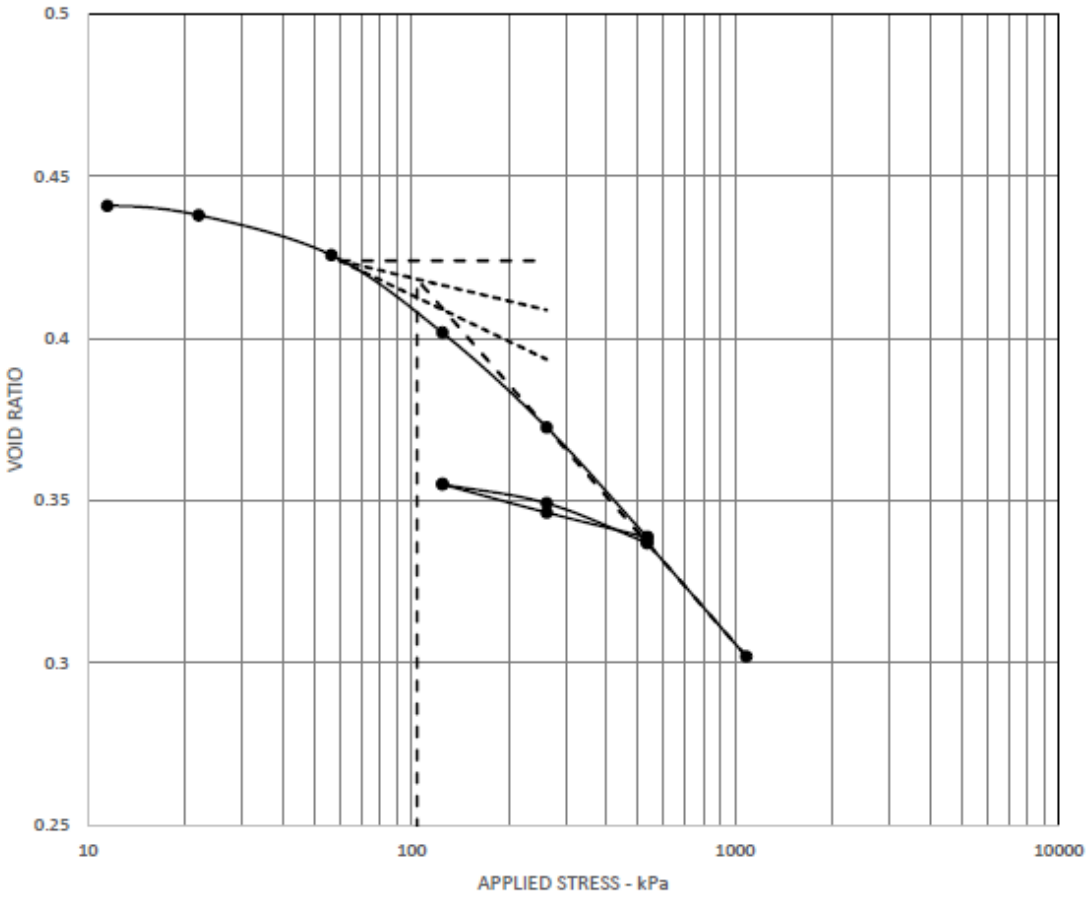

C_c	C_r	e_0	Pc (kPa)	OCR
0.114	0.07	0.438	104	0.4

Sample and Test Data				Project Information
Sample Location:	B-3	12.3	Meters	
Description:	lean clay			**Client:**
Assumed Specific Gravity = 2.7				**Project #:**
				Sample Type: Undisturbed
Initial Mc (%)	16.4	Final Mc (%)	14.9	**Date Sampled:**
dia. (in)	2.5			
Saturation (%)	100.95			
Dry Density (pcf):	117.1			**Technician: TDB**

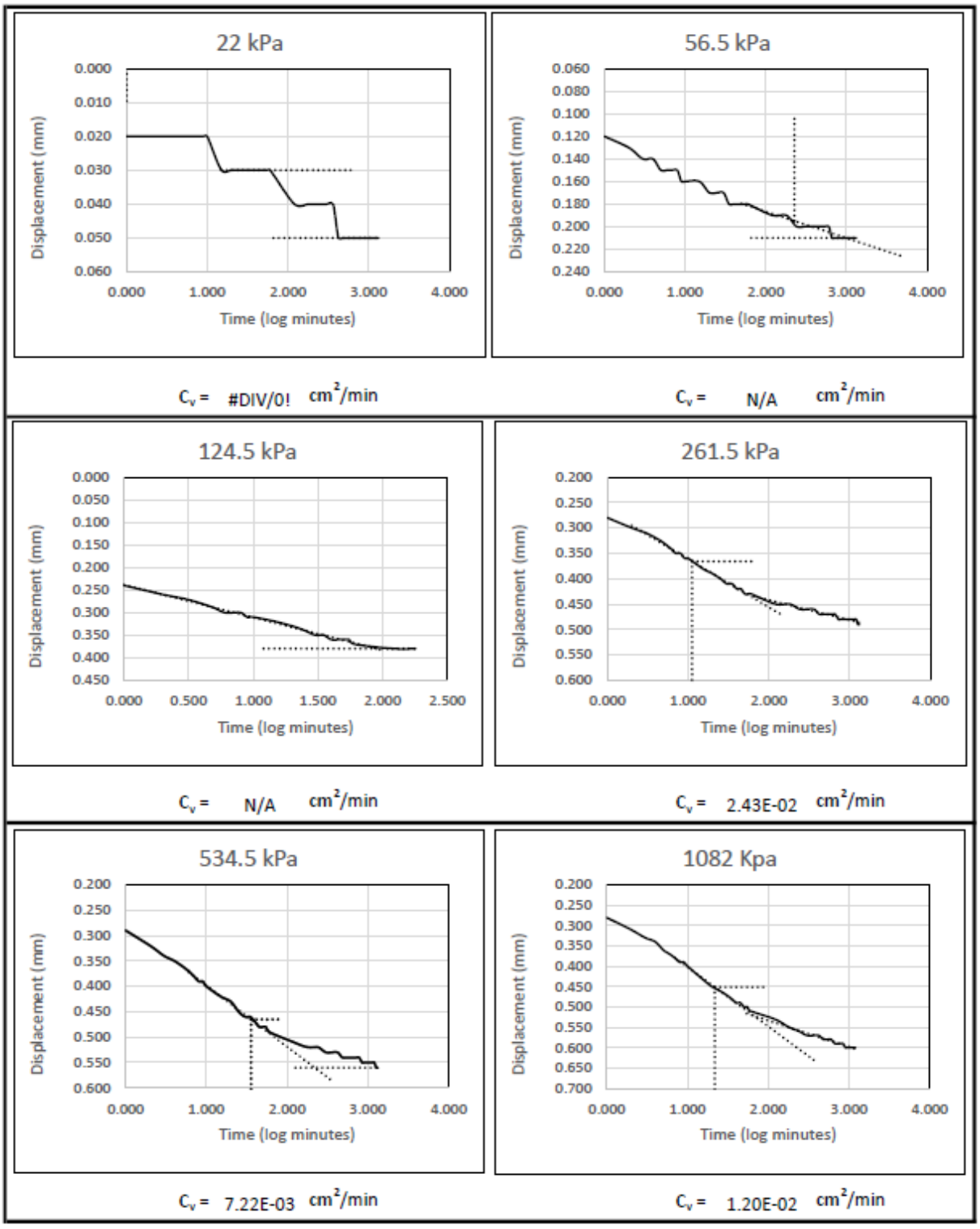
22 kPa
Displacement (mm)
0.000
0.010
0.020
0.030
0.040
0.050
0.060
0.000
1.000
2.000
3.000
4.000
Time (log minutes)
C_v = #DIV/0! cm^2/min
56.5 kPa
Displacement (mm)
0.060
0.080
0.100
0.120
0.140
0.160
0.180
0.200
0.220
0.240
0.000
1.000
2.000
3.000
4.000
Time (log minutes)
C_v = N/A cm^2/min
124.5 kPa
Displacement (mm)
0.000
0.050
0.100
0.150
0.200
0.250
0.300
0.350
0.400
0.450
0.000
0.500
1.000
1.500
2.000
2.500
Time (log minutes)
C_v = N/A cm^2/min
261.5 kPa
Displacement (mm)
0.200
0.250
0.300
0.350
0.400
0.450
0.500
0.550
0.600
0.000
1.000
2.000
3.000
4.000
Time (log minutes)
C_v = 2.43E-02 cm^2/min
534.5 kPa
Displacement (mm)
0.200
0.250
0.300
0.350
0.400
0.450
0.500
0.550
0.600
0.000
1.000
2.000
3.000
4.000
Time (log minutes)
C_v = 7.22E-03 cm^2/min
1082 Kpa
Displacement (mm)
0.200
0.250
0.300
0.350
0.400
0.450
0.500
0.550
0.600
0.650
0.700
0.000
1.000
2.000
3.000
4.000
Time (log minutes)
C_v = 1.20E-02 cm^2/min

CONSOLIDATION TEST REPORT

ASTM D2435

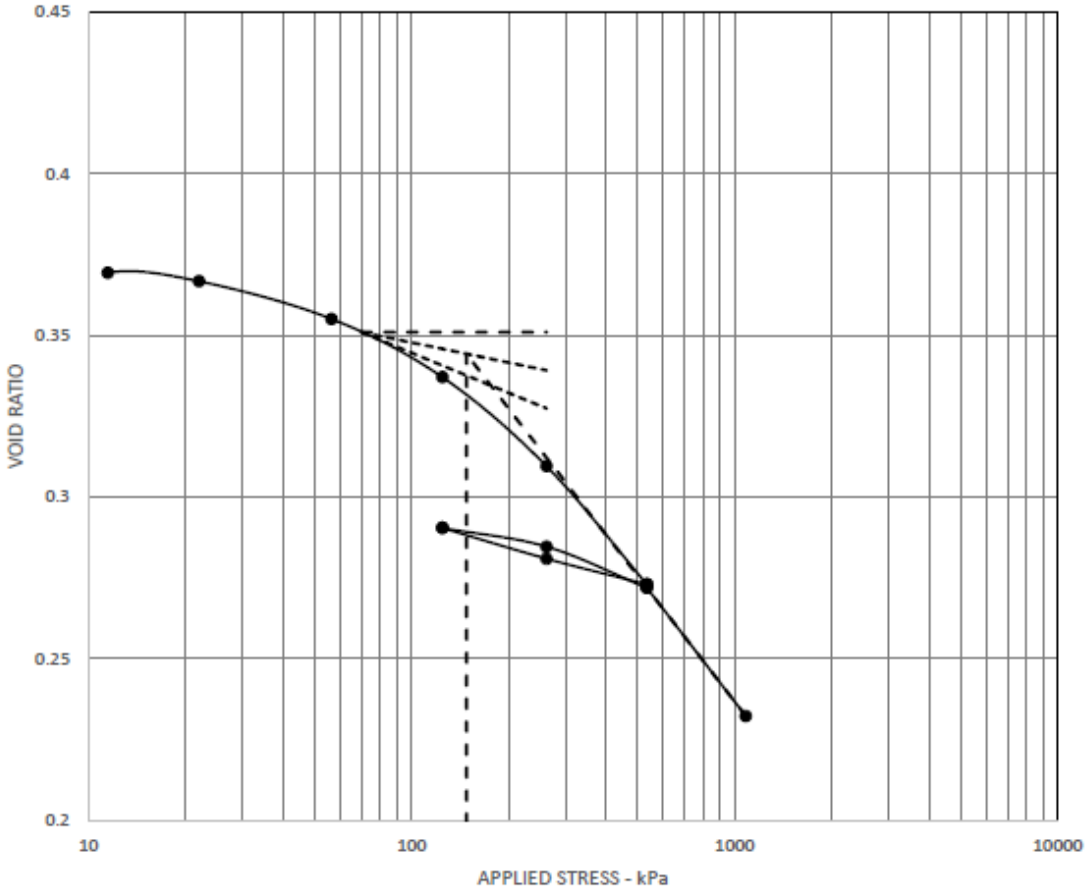

C_c	C_r	e_0	Pc (kPa)	OCR
0.129	0.055	0.358	148	0.5

Sample and Test Data				Project Information
Sample Location:	B-3	14.2	Meters	
Description:	lean clay			Client:
Assumed Specific Gravity = 2.7				Project #:
				Sample Type: Undisturbed
Initial Mc (%)	3.7	Final Mc (%)	16.9	Date Sampled:
dia. (in)	2.495			
Saturation (%)	27.84			
Dry Density (pcf):	124			Technician: TDB

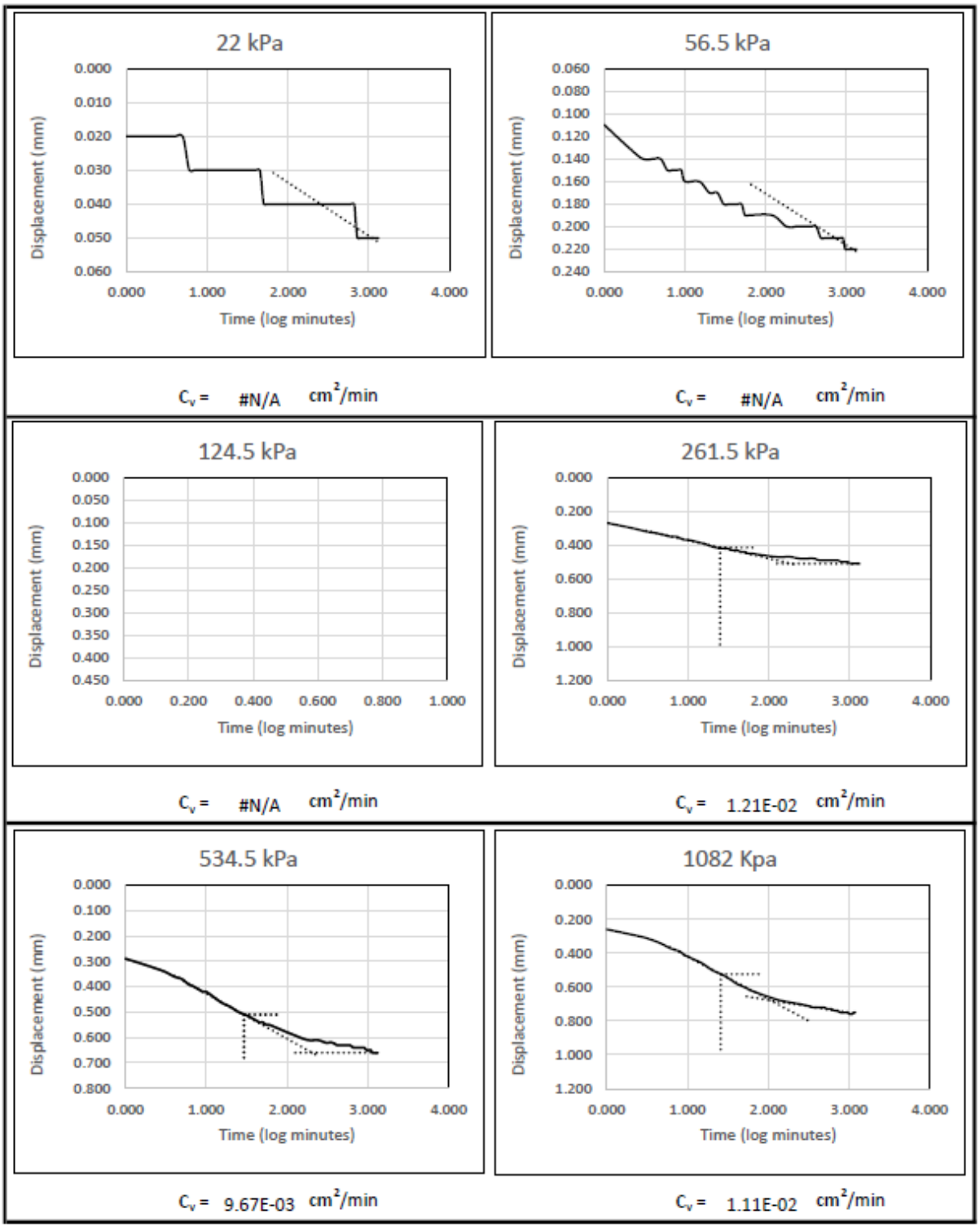
22 kPa
Displacement (mm)
0.000
0.010
0.020
0.030
0.040
0.050
0.060
0.000
1.000
2.000
3.000
4.000
Time (log minutes)
C_v = #N/A cm²/min
56.5 kPa
Displacement (mm)
0.060
0.080
0.100
0.120
0.140
0.160
0.180
0.200
0.220
0.240
0.000
1.000
2.000
3.000
4.000
Time (log minutes)
C_v = #N/A cm²/min
124.5 kPa
Displacement (mm)
0.000
0.050
0.100
0.150
0.200
0.250
0.300
0.350
0.400
0.450
0.000
0.200
0.400
0.600
0.800
1.000
Time (log minutes)
C_v = #N/A cm²/min
261.5 kPa
Displacement (mm)
0.000
0.200
0.400
0.600
0.800
1.000
1.200
0.000
1.000
2.000
3.000
4.000
Time (log minutes)
C_v = 1.21E-02 cm²/min
534.5 kPa
Displacement (mm)
0.000
0.100
0.200
0.300
0.400
0.500
0.600
0.700
0.800
0.000
1.000
2.000
3.000
4.000
Time (log minutes)
C_v = 9.67E-03 cm²/min
1082 Kpa
Displacement (mm)
0.000
0.200
0.400
0.600
0.800
1.000
1.200
0.000
1.000
2.000
3.000
4.000
Time (log minutes)
C_v = 1.11E-02 cm²/min

D.2 Triaxial Compression Results

TRIAXIAL SHEAR TEST REPORT

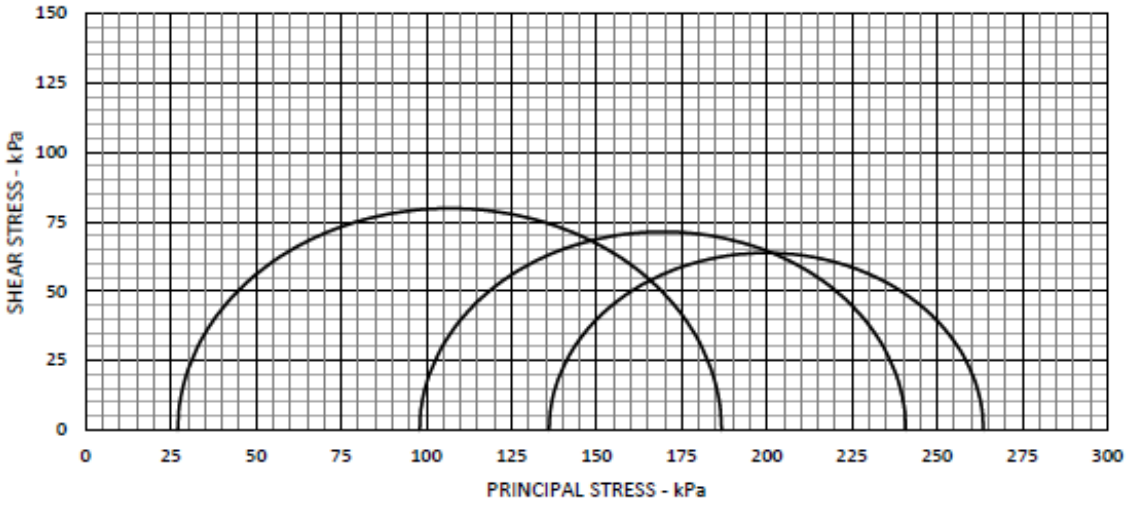

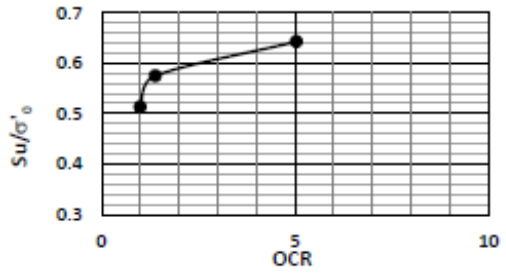

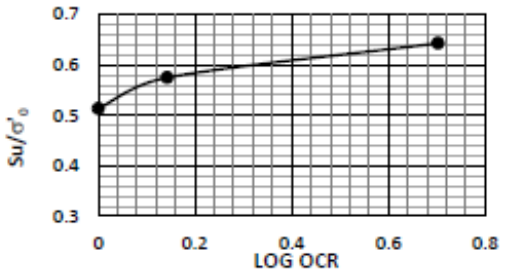

EFFECTIVE STRESS PARAMETERS	c' =	kPa	ϕ' =	deg.

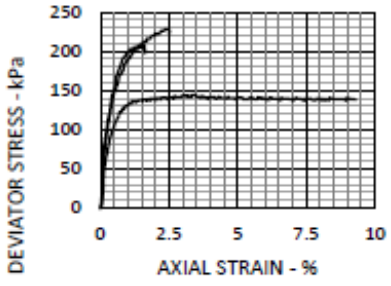

SAMPLE NO.	1	2	3
Initial Moisture Content - %	0.19	0.19	0.19
Final Moisture Content - %	0.23	0.23	0.23
Dry Density - kN/m^3	16.45	16.45	16.45
Diameter - mm	73.16	73.16	73.16
Height - mm	146.00	146.00	146.00
Effect. Cell Pressure - kPa	136	98	27
Strain Rate - mm/min	0.02	0.02	0.02
σ_1' at Failure - kPa	263.545	240.761	186.6575
σ_3' at Failure - kPa	136	98	27

TEST METHOD:	Consolidated Undrained
SAMPLE TYPE:	Undisturbed
DESCRIPTION:	Reddish Brown Lean Clay
BORING:	B-1
DEPTH:	21' 5" to 21' 11"

PROJECT INFORMATION

PROJECT:	SH 3 over BNSF
LOCATION:	Ada, Oklahoma
DATE:	7/15/2020
COMMENT:	Multistage test, loaded to NC condition and then unloaded to mimic overconsolidated soil
TESTED BY:	Tommy D. Bounds, PE

SAMPLE 1

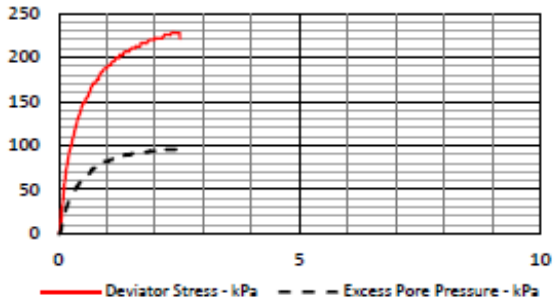

SAMPLE 2

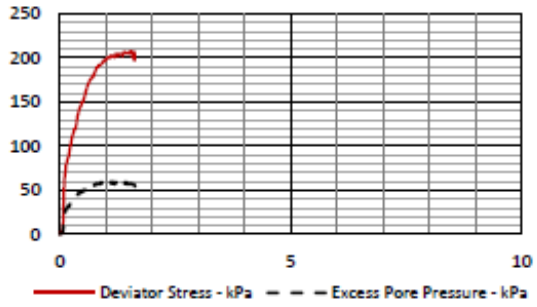

SAMPLE 3

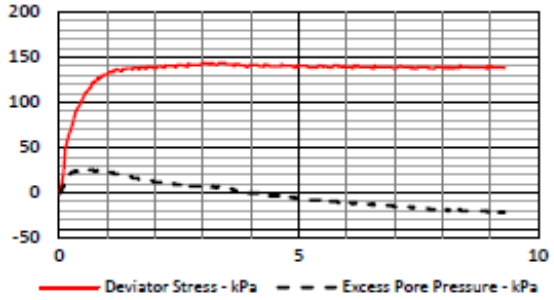

NOTE:

p' and q calculated based on Cambridge definition under triaxial stress conditions

$$p' = \frac{(\sigma_1' + 2\sigma_3')}{3}$$

$$q = (\sigma_1 - \sigma_3)$$

p'-q Diagram

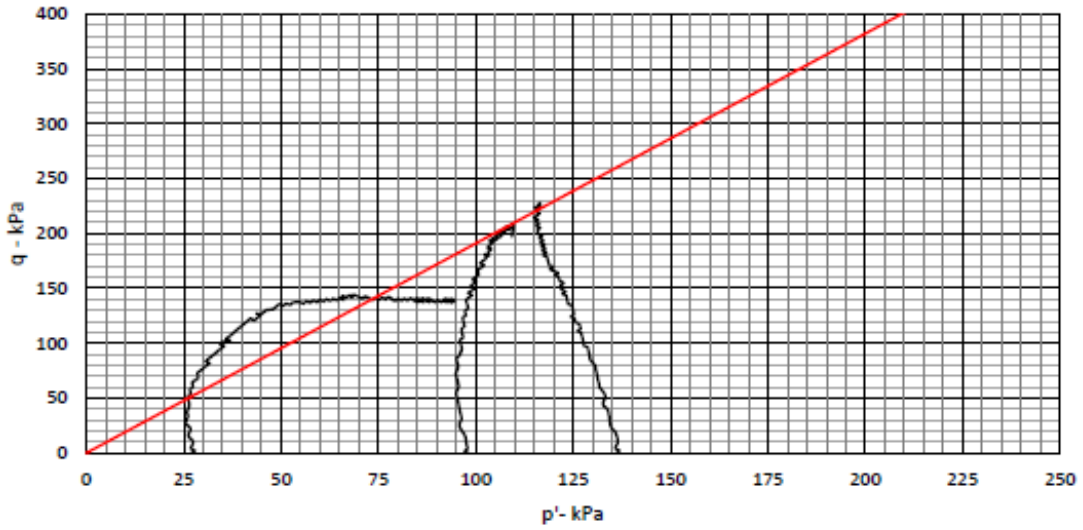

PROJECT:	SH 3 over BNSF	BORING:	B-1
LOCATION:	Ada, Oklahoma	DEPTH:	21' 5" to 21' 11"
DATE:	7/15/2020	TESTED BY:	Tommy D. Bounds, PE

TRIAXIAL SHEAR TEST REPORT

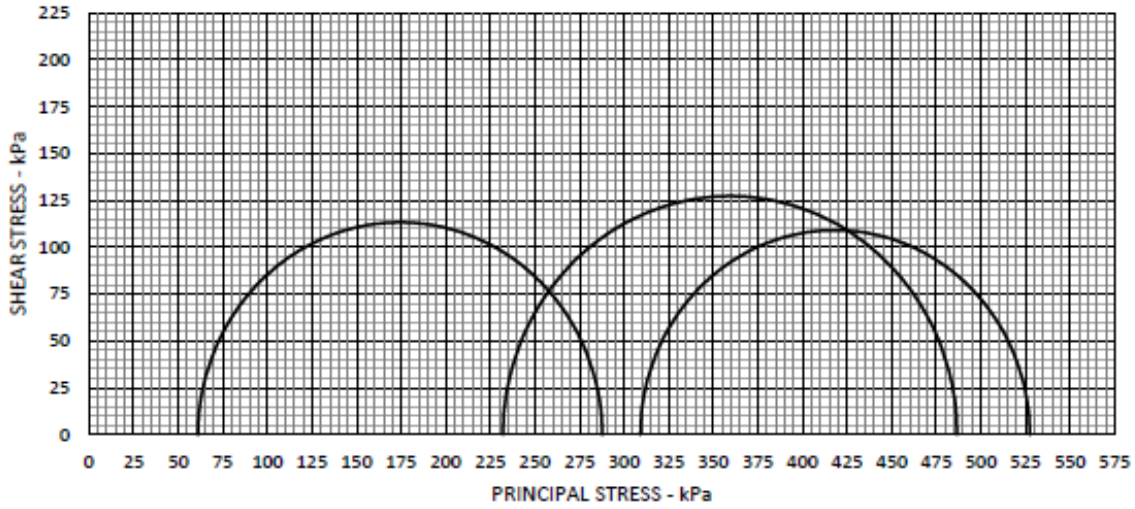

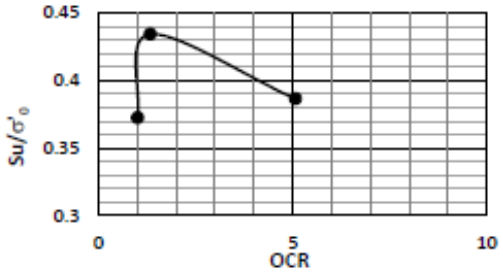

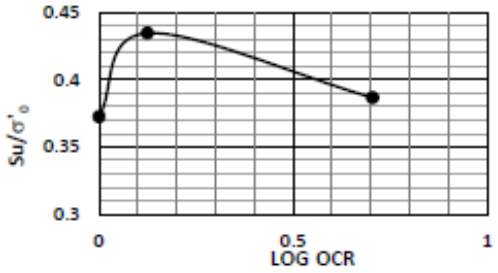

EFFECTIVE STRESS PARAMETERS	c' =	kPa	ϕ' =	deg.

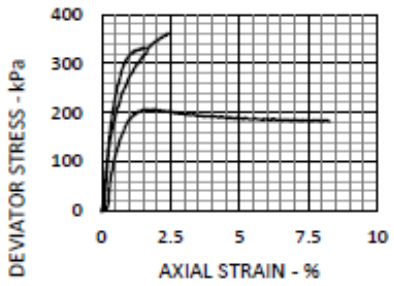

SAMPLE NO.	1	2	3
Initial Moisture Content - %	0.19	0.19	0.19
Final Moisture Content - %	0.22	0.22	0.22
Dry Density - kN/m^3	16.05	16.05	16.05
Diameter - mm	73.91	73.91	73.91
Height - mm	145.90	145.90	145.90
Effect. Cell Pressure - kPa	309	232	61
Strain Rate - mm/min	0.02	0.02	0.02
σ_1' at Failure - kPa	527.3034	486.5765	287.6001
σ_3' at Failure - kPa	309	232	61

TEST METHOD:	Consolidated Undrained
SAMPLE TYPE:	Undisturbed
DESCRIPTION:	Reddish Brown Lean Clay
BORING:	B-2
DEPTH:	50'-10" to 51'-4"

PROJECT INFORMATION

PROJECT:	SH 3 over BNSF
LOCATION:	Ada, Oklahoma
DATE:	7/15/2020
COMMENT:	Multistage test, loaded to NC condition and then unloaded to mimic overconsolidated soil
TESTED BY:	Tommy D. Bounds, PE

SAMPLE 1

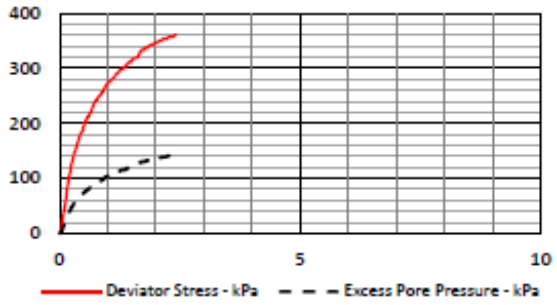

SAMPLE 2

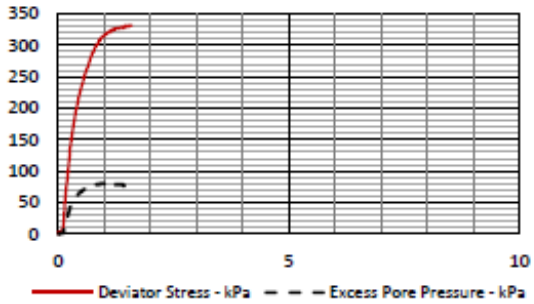

SAMPLE 3

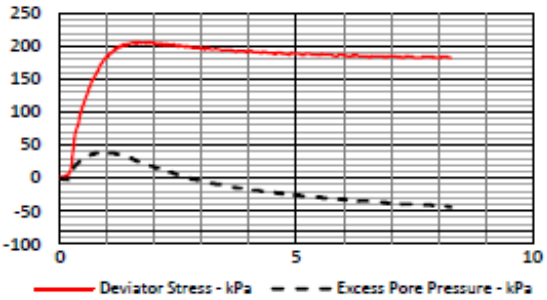

NOTE:

p' and q calculated based on Cambridge definition for triaxial stress conditions

$$p' = \frac{(\sigma_1' + 2\sigma_3')}{3}$$

$$q = (\sigma_1 - \sigma_3)$$

p'-q Diagram

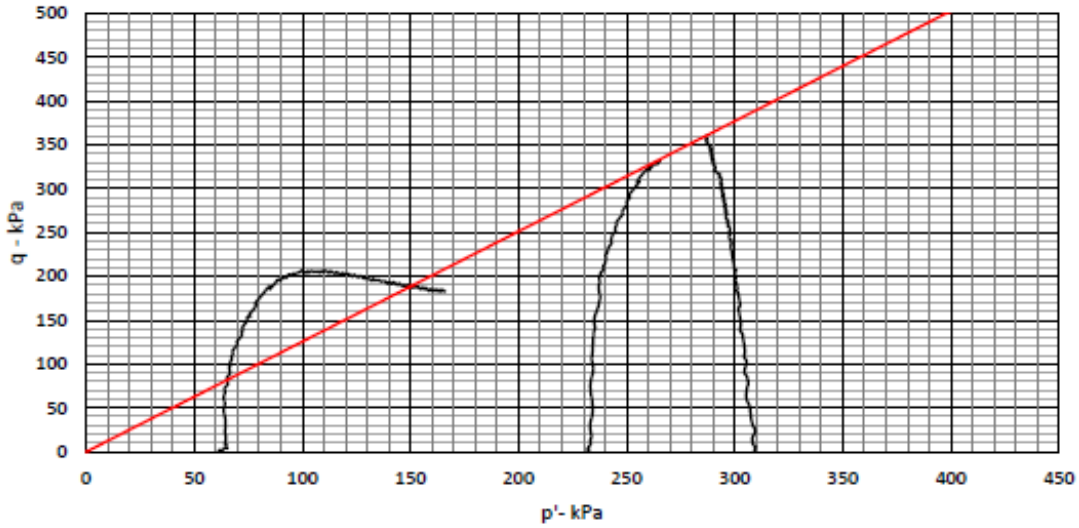

PROJECT:	SH 3 over BNSF	BORING:	B-2
LOCATION:	Ada, Oklahoma	DEPTH:	50'-10" to 51'-4"
DATE:	7/15/2020	TESTED BY:	Tommy D. Bounds, PE

TRIAXIAL SHEAR TEST REPORT

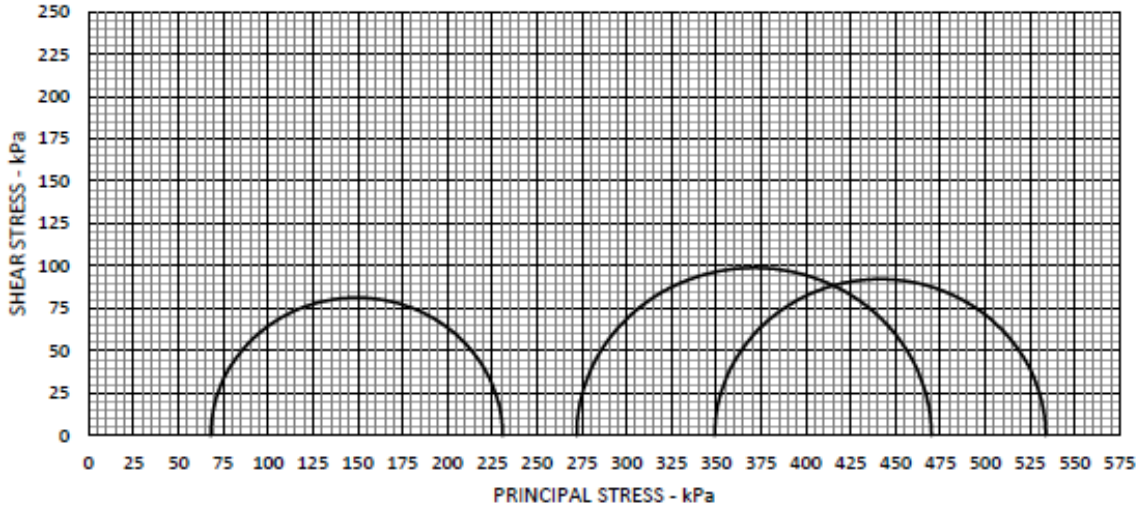

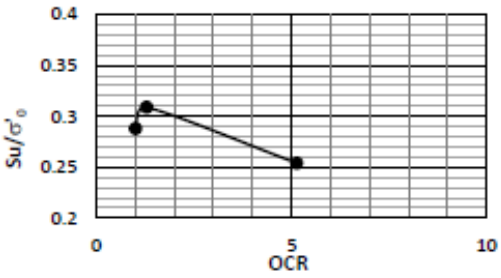

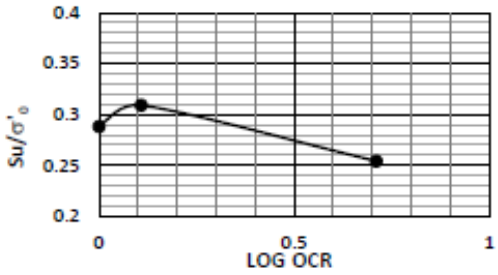

EFFECTIVE STRESS PARAMETERS | c' = kPa | ϕ' = deg.

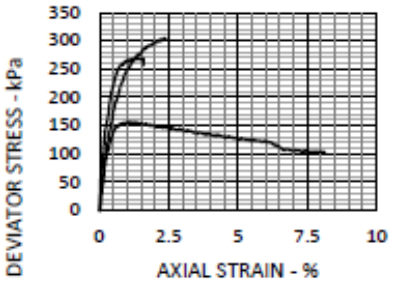

SAMPLE NO.	1	2	3
Initial Moisture Content - %	#DIV/0!	#DIV/0!	#DIV/0!
Final Moisture Content - %	0.21	0.21	0.21
Dry Density - kN/m^3	#DIV/0!	#DIV/0!	#DIV/0!
Diameter - mm	72.92	72.92	72.92
Height - mm	145.16	145.16	145.16
Effect. Cell Pressure - kPa	349	272	68
Strain Rate - mm/min	0.02	0.02	0.02
σ_1' at Failure - kPa	533.6142	469.9335	230.7747
σ_3' at Failure - kPa	349	272	68

TEST METHOD:	Consolidated Undrained
SAMPLE TYPE:	Undisturbed
DESCRIPTION:	Reddish Brown Lean Clay
BORING:	B-2
DEPTH:	55'-8" to 56'-2"

PROJECT INFORMATION

PROJECT:	SH 3 over BNSF
LOCATION:	Ada, Oklahoma
DATE:	7/15/2020
COMMENT:	Multistage test, loaded to NC condition and then unloaded to mimic overconsolidated soil
TESTED BY:	Tommy D. Bounds, PE

SAMPLE 1

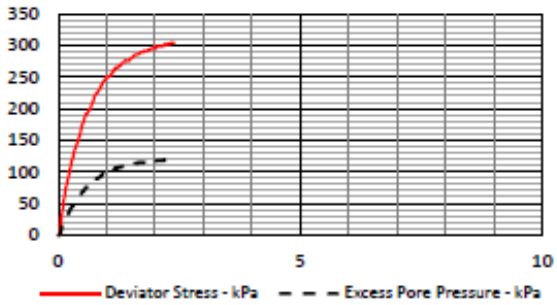

SAMPLE 2

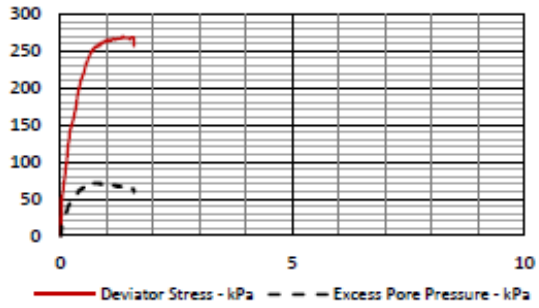

SAMPLE 3

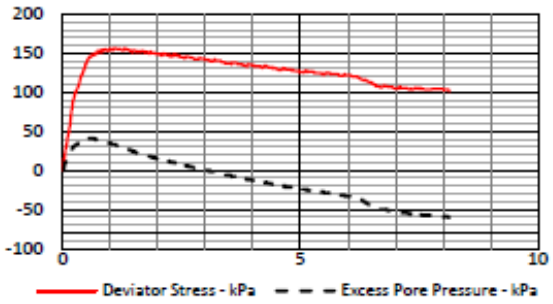

NOTE:

p' and q calculated based on Cambridge definition under triaxial stress conditions

$$p' = \frac{(\sigma_1' + 2\sigma_3')}{3}$$

$$q = (\sigma_1 - \sigma_3)$$

p'-q Diagram

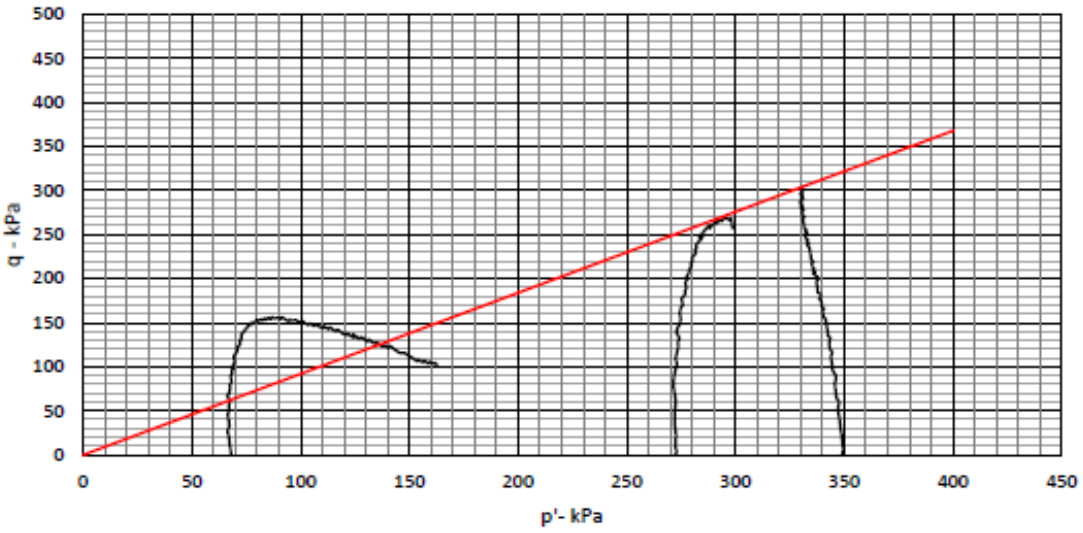

PROJECT:	SH 3 over BNSF	BORING:	B-2
LOCATION:	Ada, Oklahoma	DEPTH:	55'-8" to 56'-2"
DATE:	7/15/2020	TESTED BY:	Tommy D. Bounds, PE

TRIAXIAL SHEAR TEST REPORT

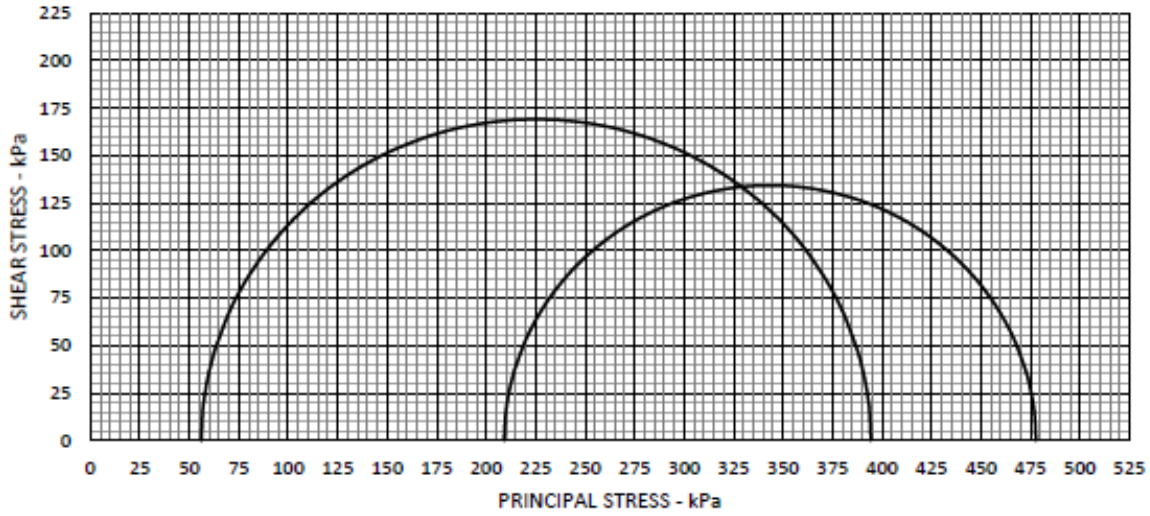

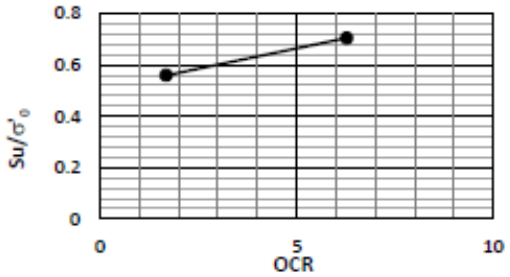

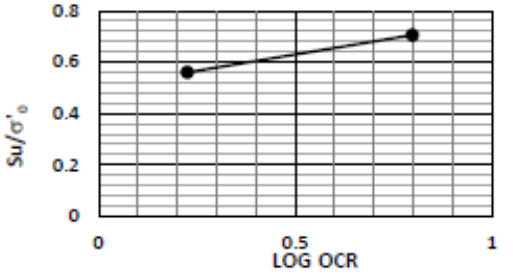

EFFECTIVE STRESS PARAMETERS | c' = kPa | φ' = deg.

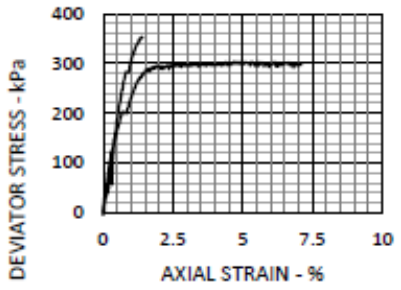

SAMPLE NO.	1	2	3
Initial Moisture Content - %	0.17	0.17	0.17
Final Moisture Content - %	0.16	0.16	0.16
Dry Density - kN/m^3	17.94	17.94	17.94
Diameter - mm	71.69	71.69	71.69
Height - mm	147.17	147.17	147.17
Effect. Cell Pressure - kPa		209	56
Strain Rate - mm/min		0.02	0.02
σ_1' at Failure - kPa		477.718	394.3418
σ_3' at Failure - kPa		209	56

TEST METHOD:	Consolidated Undrained
SAMPLE TYPE:	Undisturbed
DESCRIPTION:	Reddish Brown Lean Clay
BORING:	B-3
DEPTH:	41'-6" to 42'-0"

PROJECT INFORMATION

PROJECT:	SH 3 over BNSF
LOCATION:	Ada, Oklahoma
DATE:	7/15/2020
COMMENT:	Issue with loading during Normally Consolidated Sample
TESTED BY:	Tommy D. Bounds, PE

SAMPLE 1

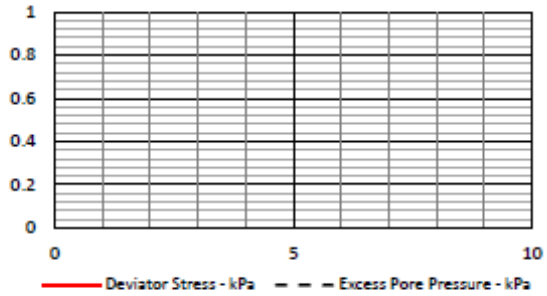

SAMPLE 2

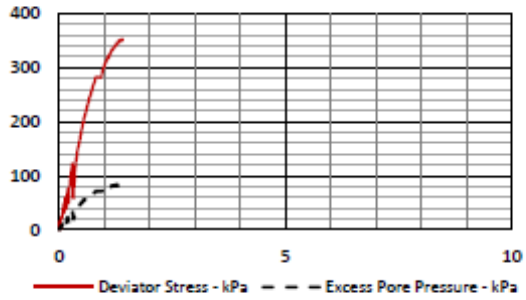

SAMPLE 3

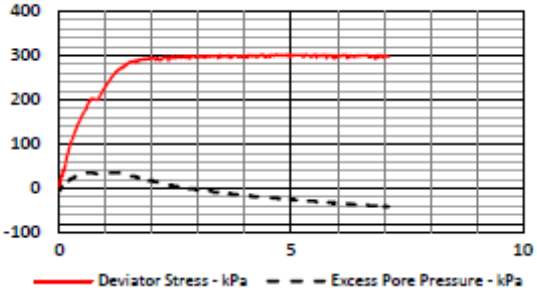

NOTE:

p' and q calculated based on Cambridge definition for triaxial stress conditions

$$p' = \frac{(\sigma_1' + 2\sigma_3')}{3}$$

$$q = (\sigma_1 - \sigma_3)$$

p'-q Diagram

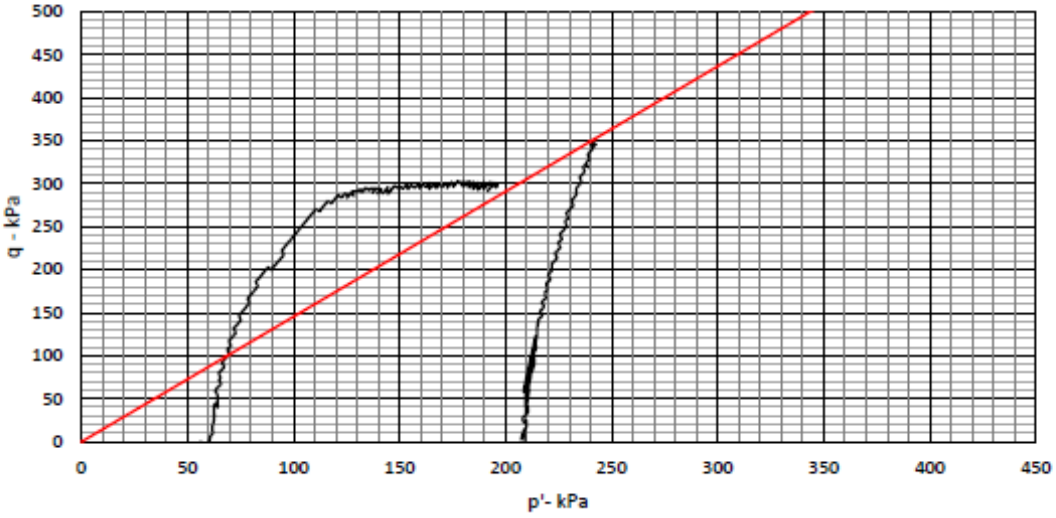

PROJECT:	SH 3 over BNSF	BORING:	B-3
LOCATION:	Ada, Oklahoma	DEPTH:	41'-6" to 42'-0"
DATE:	7/15/2020	TESTED BY:	Tommy D. Bounds, PE

TRIAXIAL SHEAR TEST REPORT

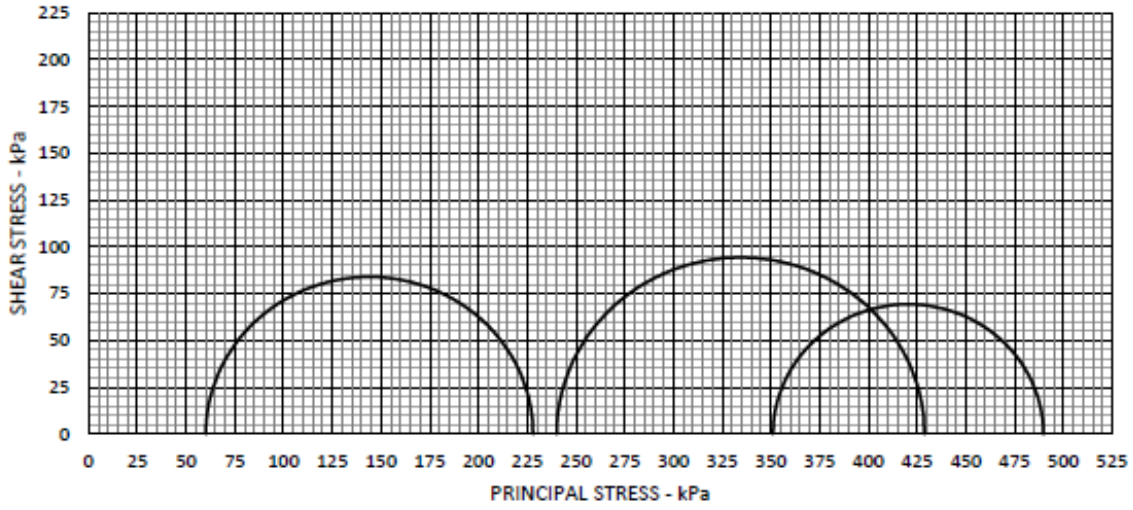

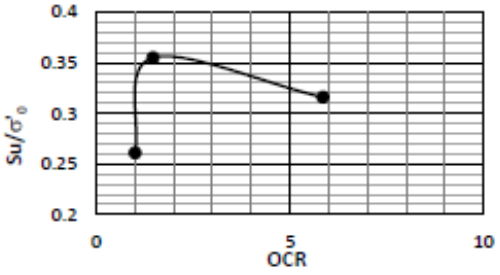

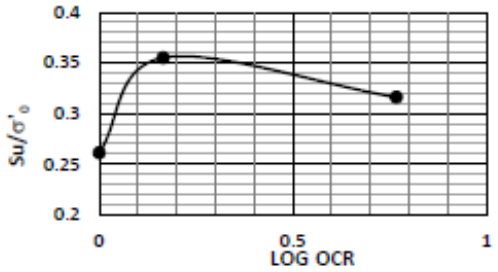

EFFECTIVE STRESS PARAMETERS | c' = kPa | ϕ' = deg.

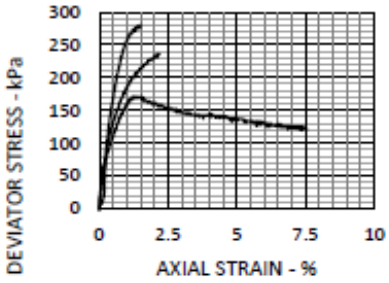

SAMPLE NO.	1	2	3
Initial Moisture Content - %	0.18	0.18	0.18
Final Moisture Content - %	0.17	0.17	0.17
Dry Density - kN/m^3	17.57	17.57	17.57
Diameter - mm	71.53	71.53	71.53
Height - mm	143.89	143.89	143.89
Effect. Cell Pressure - kPa	351	240	60
Strain Rate - mm/min	0.02	0.02	0.02
σ_1' at Failure - kPa	489.729	428.7107	227.9381
σ_3' at Failure - kPa	351	240	60

TEST METHOD:	Consolidated Undrained
SAMPLE TYPE:	Undisturbed
DESCRIPTION:	Reddish Brown Lean Clay
BORING:	B-3
DEPTH:	46'-0" to 46'-6"

PROJECT INFORMATION

PROJECT:	SH 3 over BNSF
LOCATION:	Ada, Oklahoma
DATE:	7/15/2020
COMMENT:	Multistage test, loaded to NC condition and then unloaded to mimic overconsolidated soil
TESTED BY:	Tommy D. Bounds, PE

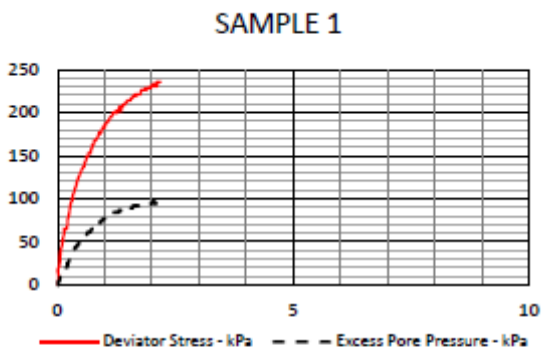

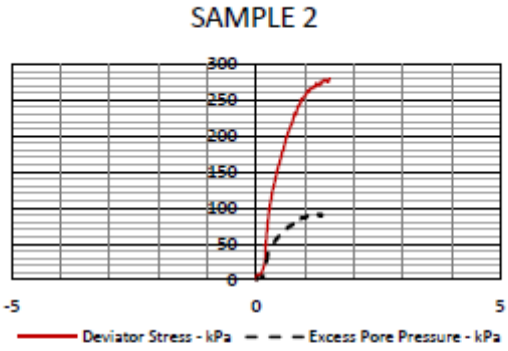

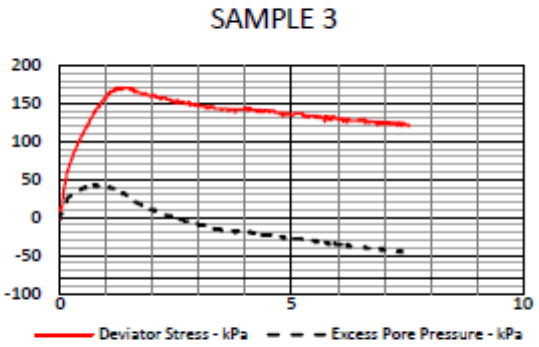

NOTE:

p' and q calculated based on Cambridge definition for triaxial stress conditions

$$p' = \frac{(\sigma_1' + 2\sigma_3')}{3}$$

$$q = (\sigma_1 - \sigma_3)$$

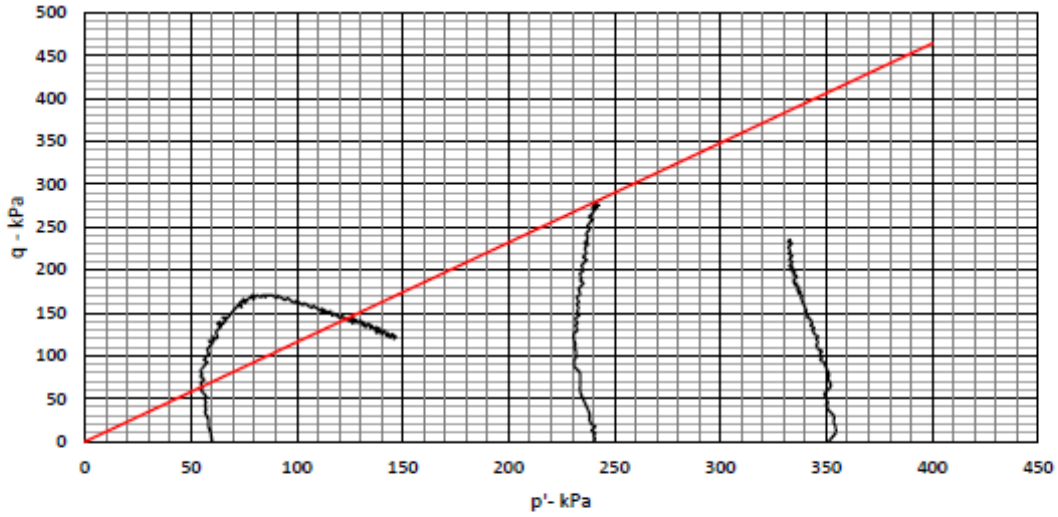

PROJECT:	SH 3 over BNSF	BORING:	B-3
LOCATION:	Ada, Oklahoma	DEPTH:	46'-0" to 46'-6"
DATE:	7/15/2020	TESTED BY:	Tommy D. Bounds, PE

D.3 Triaxial Extension Results

TRIAXIAL SHEAR TEST REPORT

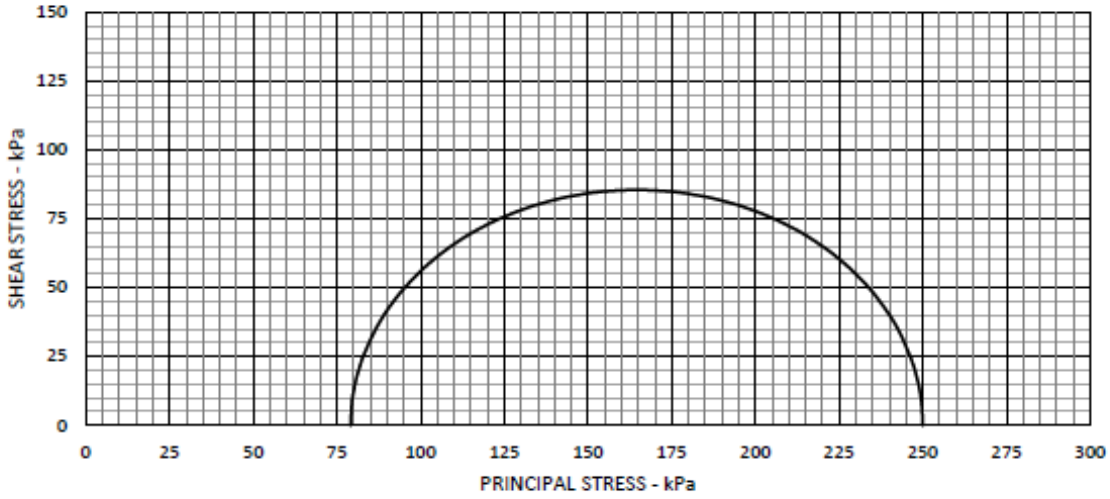

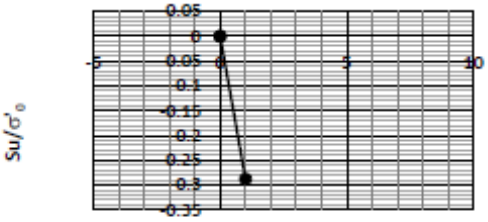

OCR

LOG OCR

EFFECTIVE STRESS PARAMETERS | c' = kPa | ϕ' = deg.

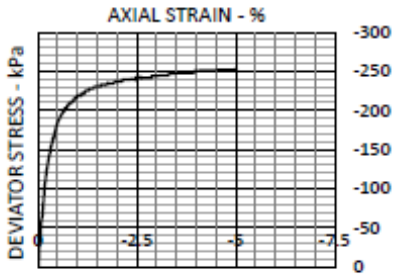

SAMPLE NO.	1	2	3
Initial Moisture Content - %	0.22		
Final Moisture Content - %	0.21		
Dry Density - kN/m^3	15.76		
Diameter - mm	72.88		
Height - mm	145.42		
Effect. Cell Pressure - kPa	250		
Strain Rate - mm/min	0.02		
σ_1' at Failure - kPa	79.03658		
σ_3' at Failure - kPa	250		

TEST METHOD:	Consolidated Undrained
SAMPLE TYPE:	Undisturbed
DESCRIPTION:	Reddish Brown Lean Clay
BORING:	B-2
DEPTH:	51'-6" to 52'-0"

PROJECT INFORMATION

PROJECT:	SH 3 over BNSF
LOCATION:	Ada, Oklahoma
DATE:	8/26/2020
COMMENT:	Multistage test, loaded to NC condition and then unloaded to mimic overconsolidated soil
TESTED BY:	Tommy D. Bounds, PE